Investigations of some Material Properties for Structural Analysis of LECA Masonry

by

Tore Kvande

Thesis for the degree of doktor ingeniør

Norwegian University of Science and Technology
Faculty of Civil and Environmental Engineering
Department of Building and Construction Engineering

March 2001

Advisors:
Professor Jan Vincent Thue, Inst. for bygg- og anleggsteknikk – NTNU
Professor Tore Haavaldsen, Inst. for bygg- og anleggsteknikk – NTNU

Adjudication Committee:
Professor Jan Vincent Thue, Inst. for bygg- og anleggsteknikk – NTNU, Administrator
Professor ir. D.R.W. Martens, Technische Universiteit Eindhoven, The Netherlands
Researcher, siv.ing. Alf M. Waldum, Norges byggforskningsinstitutt
Professor II, dr.ing. Svein Willy Danielsen, Inst. for geologi og bergteknikk - NTNU

Doktoravhandling 2001:9
ISBN 82-7984-170-9
ISSN 0809-103X

Preface

The work presented in this report is submitted as a Doctoral Thesis at the Norwegian University of Science and Technology, Department of Building and Construction Engineering. The work is a part of the research program "Load-bearing Masonry 1997-2000" co-ordinated by Mur-Sentret (Norwegian Institute for Masonry Research and Information).

Initially, a motivating factor for the choice of research work was the observed general lack of rules for movement-joint design of masonry. Even though there are few studies on crack damage in LECA masonry, it is commonly known that restrained shrinkage is one of the major causes of such damage in LECA masonry.

Today, the availability of numerical tools makes it possible to develop more reliable rules for movement-joint design. However, there is a lack of experimental data on LECA masonry from which the material/model parameters can be determined and later used in accurate numerical modelling.

In this doctoral study, a number of material properties applicable for numerical modelling of LECA masonry have been studied. The results from the different tests of material properties were adapted to generic material models available in DIANA by Høiseth at Marintek Department of Structural Engineering. DIANA (DIsplacement ANAlyzer) is a general finite element software environment, which is applicable for structural analysis of masonry. The models allow for analysis of masonry structures with random geometry, boundary conditions and loading. The analysis may cover complete deformation processes, from elastic behaviour via cracking to global failure.

An important investigation is described in the last enclosed appendix (Appendix 8), where the shrinkage and crack behaviour of a LECA masonry wall restrained at the foundation is studied. The intention at the beginning of this doctoral study was to evaluate the quality of the adapted calculation models in DIANA by comparing numerical results with observations of the full-scale laboratory experiments. The numerical work carried out by Høiseth on this particular problem is not included in this thesis. The observations of the full-scale laboratory experiments are, however, documented by this thesis, and a comparison with numerical analysis will hopefully be carried out sometime in the future.

An important part of the experimental work of this doctoral study has been carried out at Technische Universiteit Eindhoven, the Netherlands. By close collaboration with TNO Building and Construction, they together hold a leading position in development of combined numerical and experimental research tools for masonry structures. DIANA is developed at TNO Building and Construction.

The funds for the doctoral study, provided by The Research Council of Norway and Norsk Leca (presently Optiroc), are highly appreciated. Hopefully, the supporters will find the work useful as a basis for and further product development of LECA masonry products and structures.

Finally, I want to express my gratitude to everyone who has made it possible for me to carry out the work. In particular, I want to thank Kalle Høiseth for his enthusiasm and fruitful co-operation and Rob van der Pluijm for his positive attitude, many important corrections and for making my experimental program feasible.

Thanks also go to:

- Noralf Bakken for invaluable help with all the practical stuff in the lab,
- Einar Bergheim for important support and discussions,

- Finn E. Madsø for initiating the doctoral study,
- Oddvar Hyrve for his positiveness,
- Jan Vincent Thue for being the administrator,
- Tore Haavaldsen for his many important corrections and discussions,
- Alf M. Waldum for teaching me masonry,
- Terje Jacobsen for taking care,

- Lars Myhre for advice and many important corrections,
- Trond Husby for his kind assistance with computer stuff,

- Rune Sæther and the capable staff of the factory at Norsk Leca Lillestrøm,
- the Masonry Group with Gabi Bertram, Ad Th. Vermeltfoort and Dirk Martens at Technische Universiteit Eindhoven (TUE) for a warm reception and inspiration during my almost nine month long stay at the university,
- the competent staff of the Pieter van Musschenbroek Laboratory at TUE, in particular Martien Ceelen and Cor Naninck, for their support in carrying out parts of my experimental work,

- and finally to Geir O. Olsen and Thorbjørn Conradi for support in carrying out parts of my experimental program during their student projects.

To my dearest Mari and Siri: Gla' i dokk!

November 2000

Tore Kvande

Abstract

Masonry made from Light Expanded Clay Aggregate (LECA) concrete blocks is by far the most popular manufactured masonry in Norway. LECA is a lightweight aggregate (LWA).

The main objective of this study is to expand the knowledge about the material properties of LECA masonry to enable more accurate structural analysis and design of such masonry. The thesis comprises largely of experimental studies on the material behaviour of LECA masonry. Due to the relatively limited knowledge on the material properties of LECA masonry compared to that of concrete, a wide range of properties of LECA masonry has been studied in this thesis.

Because restrained shrinkage cracking is a major cause of damage to LECA masonry, mapping the behaviour of masonry with obstructed shrinkage is selected as an example. To be able to determine the deformation process of restrained LECA masonry, an identification of material properties of particular interest has been carried out. The identification was based on a restrained shrinkage cracking example. A summary of the material properties studied in this thesis work is given in Table 1. For comparison, design values of Eurocode 6 are also included in Table 1.

By determining a relatively wide range of important material properties, this thesis study has been largely instrumental in expanding the knowledge about the material behaviour of LECA masonry. While also the composition and the properties of the raw materials of the LECA blocks are documented, the study may form an important basis for further structural analysis of performance and further product development of such masonry.

Even though a restrain shrinkage example was taken as a basis for the identification of interesting material properties, the experimentally obtained properties is relevant also for application of other structural problems. The validity of the properties is, however, limited to the LECA block quality "3/770" only.

In order to pave the way for finite element analysis and design of LECA masonry structures, experimental determination of relevant material/model parameters were carried out in this thesis study. A micro-modelling can be restricted to account for the quasi-brittle material behaviour of the LECA and the average in-situ properties of the applied mortar. By applying generic material models in DIANA, the current tests of LECA masonry subjected to uniaxial tension and compression/shear, this approach gave satisfactory results (see Høiseth and Kvande (2000) and Høiseth (2000b)).

Although the average stiffness and strength of mortar is usually somewhat higher than for the LECA units, a macro-modelling based on the LECA block properties should in general give sufficiently accurate results in global analysis of real structures. It must however be emphasised that the open perpend joint of LECA masonry makes the compound behaviour highly anisotropic. This anomaly represents discontinuity planes, which may be accounted for by interface elements representing predefined discrete cracks.

Table 1:
Summary of material properties experimentally obtained in this thesis work

Material property	Symbol [1]	Obtained value of LECA masonry in this thesis work	Design value of Eurocode 6 [2]	Unit
Compressive stress-strain relationship	f_c	2.7	-	N/mm²
	E_c	4 100	2 300	N/mm²
	ε_{cn}	0.66	-	mm/m
	ε_{c1}	0.92	2	mm/m
	ε_{cu}	1.8	3.5	mm/m
Poisson's ratio	ν	0.2	-	-
Final shrinkage value	ε_{sh}	30 % RH: -0.65 50 % RH: -0.55 85 % RH: -0.40	-0.4	mm/m
Creep coefficient	ϕ_∞	1.7 – 8.0	2.0	-
Coefficient of thermal expansion	α_T	$6.7 – 7.4 \cdot 10^{-6}$ dependent of moisture content	$10 \cdot 10^{-6}$	1/K
Tensile stress-deformation relationship	f_t^u	0.5	-	N/mm²
	f_t^j	0.25	-	N/mm²
	E_o^u	3 000	-	N/mm²
	E_o^j	1 300	-	N/mm²
	G_{fI}^u	0.030	-	N/mm
	G_{fI}^j	0.011	-	N/mm
		Support Hordijk-softening		
Shear stress-deformation relationship	τ_u	σ_c = 0.06 N/mm²: 0.88	-	N/mm²
		σ_c = 0.15 N/mm²: 0.93	-	N/mm²
		σ_c = 0.23 N/mm²: 0.97	-	N/mm²
	G_o	σ_c = 0.06 N/mm²: 1 500	-	N/mm²
		σ_c = 0.15 N/mm²: 1 500	-	N/mm²
		σ_c = 0.23 N/mm²: 1 500	-	N/mm²
	G_{fII}	σ_c = 0.06 N/mm²: 0.092	-	N/mm
		σ_c = 0.15 N/mm²: 0.137	-	N/mm
		σ_c = 0.23 N/mm²: 0.138	-	N/mm
	μ	0.88	-	-
		Support partly exponential cohesion-softening and dilatancy softening		

[1] See list of symbols for explanations.
[2] Due to general application only design values from the European Prestandard for design of masonry structures is included in the table.

By adopting the experimental results of this study in generic material models available in general FEM-packages like DIANA, the models should generally permit analysis of structures with random geometry, boundary conditions and loading. Such analyses will cover the complete deformation process, from elastic behaviour via cracking to global failure. The full-scale testing of restrained shrinkage carried out in this study, should serve as suitable verification case for global analysis of LECA masonry.

Summary of appendixes

A Brief Presentation of Norwegian LECA Masonry, Appendix 1, gives an introduction of the type of masonry focused on in this thesis. Information about the process of manufacturing of LECA blocks as well as typical material properties of the masonry is included. Together with favourable material properties, individual attention to customers and skilled marketing, the result is a masonry concept with large market share and a good reputation in Norway today.

The Influence of Curing Conditions on Shrinkage and Compressive Strength of Masonry Units of LWA Concrete, Appendix 2, studies the effect of different curing regimes on shrinkage and compressive strength of LECA blocks. To reduce the risk of crack development, it is important that the mason uses relatively dry units when making the masonry. On the other hand, one can argue that too early drying of blocks reduces the final strength of the blocks. To study the effects, masonry units from the same production batch were exposed to five different climate conditions during the first month after arriving from the production line. The different curing conditions in this case, did not significantly influence neither the total drying shrinkage nor the compressive strength. It is concluded that to reduce the risk of cracking of masonry made of LECA blocks, it may be recommended to dry the blocks as early as possible after leaving the curing chamber.

Determination of Creep and Shrinkage in LECA Masonry, Appendix 3, describes an experimental determination of the behaviour of LECA masonry subjected to creep and shrinkage. Knowledge of masonry deformation due to creep and shrinkage is important for the assessment of crack resistance. The main purpose of the investigation was to establish final creep coefficients and final shrinkage values for LECA masonry. Creep due to both compression and tension load was studied.

Creep and shrinkage deformations were found to be larger than the elastic ones. Hence, it emphasises the importance of taking creep and shrinkage into account in the design of masonry structures.

The obtained final compression creep coefficient was found to be a somewhat lower than the design value of Eurocode 6 for LWA masonry. A lower design value of final shrinkage than that given in Eurocede 6 should be used according to the established final shrinkage in this test program. Obtained tensile creep coefficients in the high stress area was larger than expected. A relatively large widening of the open perpend joint is also recorded

Tensile Creep Behaviour of LWA Masonry, Appendix 4, gives a study of the creep behaviour of LECA masonry loaded in tension in the longitudinal direction of the masonry. Normally such masonry is made without mortar in the perpend joints. When the masonry is exposed to restrained shrinkage, an unclear tensile stress distribution may appear because of the open joints. Instead of using "ordinary" creep tests under compression, the specimens were loaded with constant uni-axial tensile stress in the longitudinal direction of the masonry. The tensile stress distribution close to the open joints was especially focused on. Due to ESPI measurements, a relatively large widening of the open perpend joint are explainable by the stress distribution in the specimens. The obtained creep coefficient for the highest stressed area is considerable high.

Deformation Ccontrolled Tensile Tests on LECA Masonry, Appendix 5, gives an overview of deformation controlled tensile tests carried out on LECA blocks as well as on small specimens of LECA masonry. The main purpose of the test was to establish the behaviour of

LECA masonry in uni-axial tension. The obtained behaviour may be applied for numerical modelling of tensile cracking of LECA masonry. Values for tensile strength, modulus of elasticity and mode I fracture energy for LECA blocks and bond has been established. A close relationship with the experimental softening due to tension, i.e. the post peak behaviour, was obtained with Hordijk-softening for both LECA block and mortar joint.

Constitutive Properties of Lightweight Concrete Masonry, Appendix 6, deals with the uni-axial stress-strain relationship of LECA blocks and masonry. The purpose of the study was to demonstrate the capability to reproduce experimental observations by numerical simulations. In the numerical simulations, the mechanical behaviour was represented by a smeared crack model with a non-linear softening diagram. The obtained relationship between load and deformation, as well as the crack-pattern and crack-propagation was in good agreement with the experiments. Concerning the stress/deformation relationship, the smeared crack models dependency of the crackband-width has been demonstrated. The study has shown the significance of shear retention in crack-planes even under uni-axial conditions

Deformation Controlled Combined Compression and Shear Tests on LECA Masonry, Appendix 7, gives an overview of deformation-controlled combined compression and shear tests carried out on LECA masonry. The main purpose of the test was to establish the behaviour of LECA masonry subjected to combined compression and shear actions. The obtained behaviour may be applied for numerical modelling of shear cracking of bed joints in LECA masonry. The results include mean values for shear strength, shear stiffness, mode II fracture energy and dry friction coefficient. The results support partly the validity of exponential cohesion-softening and dilatancy softening of the bond interface to describe the post peak behaviour.

Behaviour of LECA Masonry under Restrained Shrinkage, Appendix 8, gives the shrinkage behaviour of LECA masonry restrained to the bottom by a foundation. To control the effect of shrinkage reinforcement, the investigation contains five restrained LECA walls with different amount of reinforcement. In comparison, two walls made on "ideal" sliding layers and three single LECA blocks were tested. Even though no cracking of LECA blocks were observed during the test period, the test results indicate that the amount and placement of the shrinkage reinforcement influence the magnitude of the horizontal shrinkage. Smallest horizontal shrinkage was obtained on the wall with most reinforcement ($A_s/A_M \approx 0.67$ ‰). The effect of the reinforcement seems, however, to be limited. Due to insignificant difference between vertical shrinkage of the restrained walls and the shrinkage of the other specimens, design values for shrinkage may be derived from tests of single untreated LECA blocks.

Symbols

A	area	[mm²]
A_{cs}	component cross-section	[mm²]
CV	coefficient of variation	[%]
E	modulus of elasticity	[N/mm²]
	E_c compression, secant at $^1/_3 \cdot f_c$ for masonry and $0.4 \cdot f_c$ for concrete	
	E_o tension, tangent of first linear part	
	E_u tension, secant at ultimate stress	
F_n	normal force	[N]
F_s	shear force	[N]
F_u	normal force at failure	[N]
G	shear modulus	[N/mm²]
	G_o tangent of first linear part	
	G_u secant at ultimate stress	
G_{fI}	mode I fracture energy, associated with tensile cracking	[N/mm]
$G_{fI;theory}$	estimated total G_{fI} based on measurement and Hordijk (1992)	[N/mm]
G_{fII}	mode II fracture energy, associated with shear failure	[N/mm]
Ø	diameter of reinforcement	[mm]
c	cohesion	[N/mm²]
c_1, c_2	dimensionless constants	[-]
c_o	initial cohesion or shear bond strength	[N/mm²]
c_r	residual cohesion	[N/mm²]
e	eccentricity	[mm]
f_c	compressive strength	[N/mm²]
f_{cd}	design value of compressive strength, f_{ck}/γ_C	[N/mm²]
f_{ck}	characteristic value of compressive strength	[N/mm²]
f_{cu}	compressive strength	[N/mm²]
f_k	characteristic compressive strength of masonry	[N/mm²]
f_s	shear bond strength	[N/mm²]
f_t	tensile strength	[N/mm²]
f_{tb}	tensile bond strength	[N/mm²]
f_{tk}	characteristic tensile strength of reinforcing steel	[N/mm²]
f_{tu}	(arbitrary) ultimate value of the tensile strength	[N/mm²]
h	height	[mm]
r	roughness distance over which $\Delta\tan\psi$ reduces to zero	[mm]
t	thickness	[mm]
t_o	age at loading	[day]
t_{ef}	effective thickness or notional size	[mm]
u	normal deformation of specimen over gauge length	[mm]
u_{cs}	perimeter of area exposed to drying	[mm]
u_{pl}	plastic normal displacement	[mm]
v	shear deformation of specimen over gauge length	[mm]
v_{pl}	plastic shear displacement	[mm]
v_{nonlin}	softening distance	[mm]

w	crack width	[mm]
w_c	crack width at which no stresses are transferred any more	[mm]
w_{last}	last measured crack width	[mm]
α	reduction factor for long term effects on the compressive strength	[-]
α_T	coefficient of thermal expansion	[1/K]
δ	factor allowing for height and width of specimens	[-]
ε	strain	[-]
ε_c	compressive strain	[-]
ε_{c1}	strain at ultimate compressive stress	[-]
ε_{cn}	nominal compressive strain, given by and f_s and E_c	[-]
ε_{cu}	ultimate compressive strain	[-]
ε_{cr}	creep strain	[-]
ε_{el}	elastic strain	[-]
ε_{total}	total strain in specimen	[-]
ε_{sh}	shrinkage strain	[-]
$\varepsilon_{sh\infty}$	final shrinkage strain	[-]
ϕ	creep coefficient	[-]
ϕ_∞	final creep coefficient	[-]
γ_C	partial safety factor for concrete	[-]
φ	angle of internal friction	[°]
μ	dry friction coefficient	[-]
ρ	dry density	[kg/m³]
ρ_r	ageing coefficient for relaxation	[-]
σ	normal stress	[N/mm²]
σ_c	compressive stress	[N/mm²]
σ_{fr}	normal stress when τ_{fr}	[N/mm²]
σ_{last}	last measured stress in descending branch	[N/mm²]
τ	shear stress	[N/mm²]
τ_u	shear bond strength	[N/mm²]
τ_{fr}	friction at shear stress	[N/mm²]
ν	Poisson's ratio	[-]
ψ	angle of dilatancy	[°]
ψ_r	relaxation coefficient	[-]

Superscripts

C	of concrete
c	in compression
j	of (mortar) joint including the interface joint/unit
j+u	of joint + masonry unit within measuring length
M	of masonry
m	of mortar
u	of masonry unit
s	of reinforcement

Abbreviations

CEM	cement
LAC	lightweight aggregate concrete with open structure
L/CEM	air lime and cement
LECA	lightweight expanded clay aggregate
LWA	lightweight aggregate
LWAC	lightweight aggregate concrete
NWC	normalweight concrete
RH	relative humidity

Contents

APPENDIXES

Reading guide for appendixes

Appendix 1
Kvande, T.
A Brief Presentation of Norwegian LECA Masonry.
Unpublished.

Appendix 2
Kvande, T. and Conradi, T.
The Influence of Curing Conditions on Shrinkage and Compressive Strength of Masonry Units of LWA Concrete.
Submitted for publication in Masonry International, November 2000.

Appendix 3
Kvande, T.
Determination of Creep and Shrinkage in LECA Masonry.
Report N 8330-9, Norwegian Building Research Institute, Trondheim 2001.

Appendix 4
Kvande, T., Vermeltfoort, A.T., Pluijm, R. van der and Høiseth, K.V.
Tensile Creep Behaviour of LWA Masonry.
Submitted for publication in Masonry International, November 2000.

Appendix 5
Kvande, T.
Deformation Controlled Tensile Tests on LECA Masonry,
Report N 8330-6, Norwegian Building Research Institute, Trondheim 2001.

Appendix 6
Høiseth, K.V. and Kvande, T.
Constitutive Properties of Lightweight Concrete Masonry,
12th International Brick and Block Masonry Conference, Madrid 2000.

Appendix 7
Kvande, T.
Deformation Controlled Combined Compression and Shear Tests on LECA Masonry,
Report N 8330-7, Norwegian Building Research Institute, Trondheim 2001.

Appendix 8
Kvande, T. and Høiseth, K.V.
Behaviour of LECA Masonry under Restrained Shrinkage.
Submitted for publication in Masonry International, January 2001.

CHAPTER 1

1. INTRODUCTION

1.1 Background

1.1.1 Position of LECA masonry in Norway

Masonry made from Light Expanded Clay Aggregate (LECA) concrete blocks is by far the most popular manufactured masonry in Norway. LECA is a lightweight aggregate (LWA), see definition of LWA in prEN 1520:1999. Dry loose bulk density of Norwegian LECA for manufacturing of concrete blocks is about 250-350 kg/m³, while typical dry net density of LECA blocks are between 600 and 1300 kg/m³. For other applications dry loose bulk density of LECA between 200-900 kg/m³ may be produced.

LECA masonry blocks have been produced in Norway for more than 40 years. During the last years, 1.0 – 2.0 million m² walls of LECA masonry have been produced annually in the country. Production of LECA blocks represents approximately 80 % of the total Norwegian masonry market. According to the production volume, as much as 80 million m² wall may be built of LECA masonry in Norway. Compared with other countries the position of LECA masonry in Norway is rather unique.

Today, there is only one producer of both LECA and LECA blocks in Norway. Imported LECA blocks cover about 15 % of the LECA masonry market. However, the toughest competition comes from alternative construction materials such as concrete, steel and wood as well as other types of masonry.

Initially, LECA masonry was mainly used for basement walls in private dwellings. Special blocks for outer walls above ground, fire resistant walls, sound insulating walls etc. were later developed. Positioning the product assortment at a relatively high level of technology and know-how has given the LECA concept supremacy in the Norwegian market. In order to maintain this position, increasing efforts have been made in recent years to secure more business from professional contractors and architects. The focus on professional contractors will probably enlarge the market for LECA masonry in buildings with longer and higher façades and in constructions with complicated geometry.

1.1.2 Research needs

Restrained shrinkage cracking of masonry walls is one of the major causes of damage in masonry (Jong 1992, Madsø 1997). Despite this, movement-joint design in masonry remains very much an art, guided by rule-of-thumb. The introduction of a thermally insulated unit

(sandwich unit) in the early 1980s emphasised the problem of restrained shrinkage cracking of LECA masonry (Waldum et al. 1993a, Waldum 1998). In accordance with Haugen (2000), more shrinkage cracking of LECA masonry has been registered in Norway compared with Denmark, Finland and Sweden. It should, however, be noted that the record do not take in account the variations of amount of LECA masonry made in each country.

Due to the risk of restrained shrinkage cracking, the use of LECA masonry in longer and higher façades and in constructions with more complicated geometry than traditionally, will demand careful attention and more optimal structural utilisation of the masonry. To establish reliable models for e.g. movement-joint design, a thorough knowledge of masonry deformation due to creep and shrinkage as well as crack resistance and development is required.

Despite the position of LECA masonry in the Norwegian market, the material properties of the masonry is not very well documented. The information gathered focusing on LECA (Kvande 1998) mainly revealed investigations into fire resistance and high strength concrete. Very few studies of the behaviour of LECA masonry during its “daily life” have been found for masonry of similar qualities as the Norwegian LECA masonry.

Concerning lightweight aggregate concrete (LWAC) in general, the knowledge about its material properties is relatively limited compared with normalweight concrete (NWC). That is why CEB-FIP in May 2000 published Bulletin 8 about LWAC. The Bulletin gives recommended extensions to CEB-FIB MC 90 and identifies research needs of LWAC. In the following some of the research needs given in CEB-FIB Bulletin 8 is gleaned:

- Adequate description of physical characterisation of aggregates to be able to predict e.g. creep and shrinkage.
- Establishing of reliable methods to determine effective water/binder ratio and specifications for coating of LWA.
- Establishing of reliable procedures and test methods for evaluating compressive strengths and elastic modulus of the aggregates to be applied in e.g. a composite model.
- Establishing of reliable models, as a function of parameters for the aggregates, to describe e.g. short term compressive strength, elastic modulus, creep, redistribution of stresses during creep, ultimate strain and influence of shrinkage.
- Introduction of reduction factors of tensile strength for implications for design.
- Investigation on the softening behaviour and the fracture energy for fracture mechanics.
- Investigation of LWAC under bi-axial compression and tension.
- Investigation of LWAC with respect to shear compression.
- Investigation of cracks on durability.

As far as the author know, only one doctoral study is earlier carried out in Norway concerning masonry. Schjølberg (1987) studied the interaction between brick and mortar in clay-brick masonry. The work has been studied by the author and is unfortunately not found to provide relevant input for the study of material properties of LECA masonry.

The European Prestandard (ENV) for Design of masonry structures (Eurocode 6) was approved by the European Committee for Standardization (CEN) in 1994. Unfortunately, the

pre-standard does not cover LECA masonry in a satisfactory way (Hyrve and Madsø 1996). That may be due to the limited knowledge about the material properties of LECA masonry.

The new Norwegian Technical Regulations, which came into force 1st July 1997, set a high standard for constructions and the products used in construction works. The Technical Regulations call for documented solutions and underline the need for qualified persons carrying out the work. The regulations also emphasise the importance of giving the professional contractors and architects more backing by documentation of the LECA concept. Not only documentation of the masonry unit itself but also of the whole concept with all compounds included is required. Even more important are the detailed descriptions of how to carry out the work. To be able to make sufficient documentation, wide knowledge about the product is required.

Due to the non-linear behaviour of masonry exposed by e.g. creep and shrinkage, possibilities for numerical analysis of masonry have been strongly focused the recent years. Anthoine (1995), Rots (1997), Zijl (2000) and Molnar (2000) are examples of that. DIANA (DIsplacement ANAlyzer) is one example of a general finite element software environment, applicable for structural analysis of masonry. The employment of combined numerical and experimental research tools makes it possible to gain insight into the fundamental behaviour of masonry materials and structures e.g. movement-joint design. However, there is a lack of experimental data on masonry in general from which the material/model parameters can be characterised (Zijl 2000). Such experimental data on LECA masonry is almost completely lacking.

1.2 The aim and the scope of the study

The main objective of this doctoral study is to expand the knowledge about the material properties of masonry made from Light Expanded Clay Aggregate (LECA) concrete blocks. By expanding the knowledge about the material properties of LECA masonry it is assumed that more accurate structural analysis and design of such masonry is made possible. The thesis comprises largely of experimental studies on the material behaviour of LECA masonry. The documentation will hopefully serve as a basis for, and assist further product development of LECA masonry structures.

It is hoped that the work will pave the way for the application of finite element analysis and design of LECA masonry structures through experimental determination of relevant material/model parameters.

Because restrained shrinkage cracking is a major cause of damage to LECA masonry, mapping the behaviour of masonry with obstructed shrinkage is selected as an example. This thesis has performed the experimental analysis of this example. Høiseth at Marintek Department of Structural Engineering will perform the numerical analysis of the same example.

The main emphasis of this thesis has been put on performing laboratory tests in order to determine the deformation process of restrained LECA masonry structures. To be able to determine the deformation process, an identification of material properties of particular interest has been carried out. The identification was based on a restrained shrinkage cracking example. Due to the limited number of experimental data that could be obtained on LECA

masonry, a wide range of material properties has been studied. Only the material properties are covered by this study. But it should be noted that the boundary conditions and geometry of the structure may influence the behaviour of masonry just as much as the material properties.

1.3 Outline

This thesis work deals with material properties for structural analysis and design of LECA masonry. The study does not deal with all conceivable material properties. Chapter 2 identifies areas of particular interest in order to analyse the deformation process of restrained masonry structures. The identification is based on an example of a restrained shrinkage cracking situation. Consequently, the influence of normal compressive loading, shrinkage, creep, temperature and restrained movement on cementitious materials is dealt with separately. The information is gleaned from literature on experimental observation of masonry as well as of concrete. The chapter ends with a brief introduction to modelling strategies for masonry.

Chapter 3 summarises material properties of LECA masonry in particular. While the study does not cover all types of LECA masonry, the chapter starts with a presentation of the investigated qualities. Description of the investigations made are enclosed in the Appendix, see below.

Chapter 4 contains a discussion focusing on relevance and validity of the thesis work. Some aspects concerning the measured material properties and influencing factors are discussed. Finally, some aspects concerning modelling of LECA masonry are discussed.

Chapter 5 presents the main conclusions of the studies. Also recommendations which seems to be appropriate for further development of LECA masonry are presented.

Appendix 1, *A Brief Presentation of Norwegian LECA Masonry*, gives an introduction of the type of masonry focused on in this thesis. Information about the process of manufacturing of LECA blocks as well as typical material properties of the masonry is included. Finally, the appendix tries to identify some of the reasons why LECA masonry has gained such popularity in Norway.

The title of Appendix 2 is *The Influence of Curing Conditions on Shrinkage and Compressive Strength of Masonry Units of LWA Concrete*. In that investigation the effect of different curing regimes on shrinkage and compressive strength of LECA blocks is studied. To reduce the risk of crack development, it is important that the mason uses relatively dry blocks when making the masonry. On the other hand, one can argue that too early drying of the blocks reduces the final strength of the blocks. To study the effects, masonry units from the same production batch were exposed to five different climate conditions during the first month after arriving from the production line.

Appendix 3, *Determination of Creep and Shrinkage in LECA Masonry*, describes an experimental determination of the behaviour of LECA masonry subjected to creep and shrinkage. Knowledge of masonry deformation due to creep and shrinkage is important for the assessment of crack resistance. Lack of such knowledge for LECA masonry was the background for the investigation presented in that report. The main purpose of the

investigation was to establish final creep coefficients and final shrinkage values for LECA masonry. Creep due to both compression and tension load was studied.

The main purpose of the investigation given in Appendix 4, *Tensile Creep Behaviour of LWA Masonry*, was to study the creep behaviour of LECA masonry loaded in tension in the longitudinal direction of the masonry. Normally, such masonry is made without mortar in the perpend joints. When the masonry is exposed to restrained shrinkage, an unclear tensile stress distribution may appear because of the open joints. Instead of using "ordinary" creep tests under compression, the specimens were loaded with constant uni-axial tensile stress in the longitudinal direction of the masonry. The tensile stress distribution close to the open joints was especially focused on.

Appendix 5, *Deformation Controlled Tensile Tests on LECA Masonry*, gives an overview of deformation controlled tensile tests carried out on LECA blocks as well as on small specimens of LECA masonry. The main purpose of the test was to establish the behaviour of LECA masonry in uni-axial tension. The obtained behaviour may be applied for numerical modelling of tensile cracking of LECA masonry.

Appendix 6, *Constitutive Properties of Lightweight Concrete Masonry*, deals with the uni-axial stress-strain relationship of LECA blocks and masonry. The purpose of the study was to demonstrate the capability to reproduce experimental observations by numerical simulations. In the numerical simulations, the mechanical behaviour was represented by a smeared crack model with a non-linear softening diagram.

Appendix 7, *Deformation controlled combined compression and shear tests on LECA masonry*, gives an overview of deformation controlled combined compression and shear tests carried out on LECA masonry. The main purpose of the test was to establish the behaviour of LECA masonry subjected to combined compression and shear actions. The obtained behaviour may be applied for numerical modelling of shear cracking of bed joint in LECA masonry.

The purpose of the investigation given in Appendix 8, *Behaviour of LECA Masonry under Restrained Shrinkage*, was to obtain the shrinkage behaviour of LECA masonry restrained to the bottom by a foundation. This is due to the fact that LECA masonry in most cases are made without a sliding layer between the foundation and the masonry. To control the effect of shrinkage reinforcement, the investigation contains five restrained LECA walls with different amount of reinforcement. In comparison, two walls made on "ideal" sliding layers and three single LECA blocks were tested.

CHAPTER 2

2. THEORETICAL CONTEXT

2.1 Introduction

In order to expand the knowledge about the material properties of LECA masonry, a widest possible range of properties has been studies in this thesis. Because restrained shrinkage cracking is a major cause of damage to LECA masonry, mapping the behaviour of masonry with obstructed shrinkage is selected as an example. In this chapter material properties of particular interest due to a restrained shrinkage cracking example are identified. The different material properties are in the following section dealt with separately. Thesis work concerning the different influences is specified at the end of each section.

The behaviour of cementitious materials when subjected to various influencing factors, is a very complex subject. Even if the material behaviour of concrete has been studied systematically during the 20th century, it is not completely understood yet. Concerning masonry, it may be even more complicated due to the different material properties of masonry units and mortar. Because the LECA masonry contains mortar joints and because the LECA blocks are made with cement binder, it is reasonable to start the study by obtaining more information about the material properties of concrete.

Because of the complexity and the non-linear behaviour of masonry and concrete, the employment of advanced methods such as finite-element analysis is required in order to simulate the deformation behaviour with reasonable accuracy. Consequently, this chapter ends with a brief introduction to non-linear modelling strategies for masonry.

2.2 Behaviour of walls with obstructed shrinkage

As an example, masonry walls are normally somewhat restrained at the foundation. When drying, such walls will shrink and tensile stresses will occur in the walls causing cracks. The example in Figure 2.1 shows a wall restrained at the bottom by a foundation. The dotted lines indicate a likely deformation and crack patterns that may occur in the present case. The presence of an upper floor and/or side piers will introduce restraints from sides and, hence, a different deformation behaviour than indicated may occur. Consequently, the behaviour of such walls depends on quite a number of influencing parameters. The influences may be categorised as boundary conditions, geometry effects and material properties (see Berkers and Rademaker (1992) and Schubert (1988) for more details). However, this thesis is only focusing on those material properties that are influencing the deformations and crack patterns.

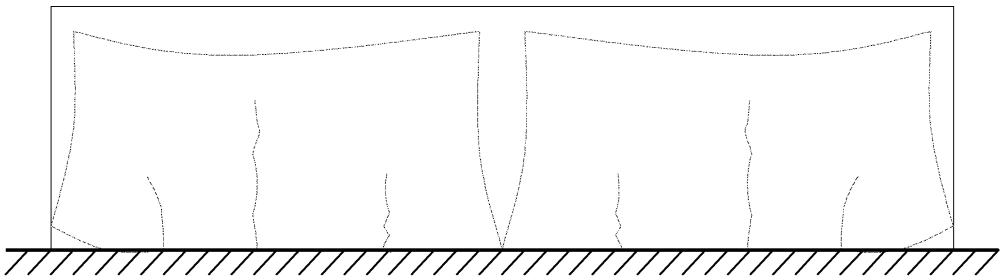

Figure 2.1:
Possible deformation and crack pattern in an unreinforced masonry wall caused by restrained shrinkage at the bottom. The cracks and deformation are strongly magnified to illustrate the effect of the restrained shrinkage.

To summarise, the present restrained shrinkage example may be influenced by:

- normal compressive loading due to erection of an upper floor,
- shrinkage due to loss of water from the masonry,
- creep due to maintenance of the normal compressive loading and to tensile stresses which appear because of the restrained shrinkage,
- change of temperature and
- restrained movement.

Table 2.1 gives an overview over the most important material properties of concrete and LECA masonry with regard to the present restrained shrinkage example. The table also gives some of the variables influencing the material properties as well as examples of references dealing with the influences on concrete and on Norwegian LECA masonry. Due to the limited number of experimental data that could be obtained on LECA masonry, a wide range of material properties has been studied in this thesis work. The investigated properties and investigated relations are given to the right in Table 2.1.

Masonry's response to loads and other actions are dealt with more specifically in Chapter 2.3 and 2.4.

Table 2.1:
Overview of material properties of particular interest for structural analysis of restrained shrinkage of LECA masonry and variables that influence the properties.

Material property	Influencing factor	Examples of references concerning		Studied in this thesis [2]
		concrete	Norwegian LECA masonry [1]	
Compressive stress-strain relationship,	-) *No subdivision*	NS 3473 prEN 1520:1999 Eibl et al. (1995) Neville (1995)	÷	×
	a) Composition of the concrete		÷	
see Chapter 2.3.1 and 3.3	b) Stiffness of the aggregate		÷	
	c) Moisture content		÷	(×)
	d) Age		÷	
	e) Curing conditions		÷	
Poisson's ratio,	-) *No subdivision*	NS 3473 prEN 1520:1999	÷	×
see Chapter 2.3.1 and 3.3	a) Composition of the concrete	Eibl et al. (1995)	÷	
	b) Moisture content		÷	
	c) Age		÷	
	d) Load level		÷	
Final shrinkage value,	-) *No subdivision*	NS 3473 prEN 1520:1999 Eibl et al. (1995) Neville (1995)	Svendsen et al. (1966) Leca 1.000	
see Chapter 2.3.2 and 3.4	a) Ambient humidity		Waldum et al. (1993a) Waldum (1998)	×
	b) Composition of the concrete		÷	
	c) Dimension of the element		÷	×
Creep coefficient,	-) *No subdivision*	NS 3473 prEN 1520:1999 Eibl et al. (1995) Neville (1995)	÷	×
	a) Ambient humidity		÷	
see Chapter 2.3.3 and 3.5	b) Composition of the concrete		÷	
	c) Dimension of the element		÷	
	d) Age at loading		÷	
Coefficient of thermal expansion	-) *No subdivision*	NS 3473 prEN 1520:1999	Svendsen et al. (1966) Leca 1.000	×
	a) Coefficient of the aggregate	Eibl et al. (1995) Neville (1995)	÷	
see Chapter 2.3.4 and 3.6	b) Coefficient of the hydrated cement paste		÷	
	c) Moisture content		÷	×

Table 2.1 (continued):

Material property		Influencing factor	Examples of references concerning		Studied in this thesis [2]
			concrete	Norwegian LECA masonry [1]	
Tensile stress-deformation relationship,	-)	*No subdivision*	Hilleborg et al. (1976)	÷	×
	a)	Composition of the concrete	Eibl et al. (1995)	÷	
see Chapter 2.4.2 and 3.7.4	b)	Stiffness of the aggregate		÷	
	c)	Moisture content		÷	×
	d)	Age		÷	
	e)	Curing conditions		÷	(×)
Shear stress-deformation relationship,	-)	*No subdivision*	Present interest for masonry only, see Pluijm (1999)	÷	×
	a)	Composition of the concrete		÷	
see Chapter 2.4.3 and 3.7.5	b)	Stiffness of the aggregate		÷	
	c)	Moisture content		÷	
	d)	Age		÷	
	e)	Curing conditions		÷	
	f)	Compressive loading		÷	×

[1] ÷ symbolise that no satisfying reference was found.
[2] × symbolise that the actual material property/influencing factor was studied in this thesis work.

2.3 Masonry's response to loads and other actions

2.3.1 Normal compressive loading

Background

During service load conditions, masonry is usually only elastically compressed when a normal compressive loading is applied perpendicular to the bed joint. Simultaneously, a transverse enlarging occurs. In structural design, the stress-strain relationship of the construction material is of great importance. The present section deals with aspects concerning stress-strain relationship of cementitious materials in normal compression.

Instantaneous deformation caused by uni-axial stress is generally characterised by the modulus of elasticity as long as the material behaves linearly. The modulus of elasticity expresses the ability of a material to resist linear elastic deformation. The Poisson's ratio expresses the ratio between the vertical and horizontal deformation.

For many structural applications, the compressive strength of the masonry is the most used mechanical property. The stress-strain relationship is one of the most significant characteristics of a material. In the case of vertically loaded walls (normal compressive loading) the modulus of elasticity only describes the first linear part of the stress-strain diagram, where Hooke's law is valid. Typically, concrete behaves in an approximately linear elastic manner up to about 40 % of the compressive strength (Beeby and Narayanan 1995). Above that, the development of micro-cracks causes a deviation from the linear elastic behaviour. While growth of micro-cracks primarily in the aggregate-cement paste interface is the situation for normalweight concrete, micro-cracks also develop in the aggregate themselves in LWAC (Wischers and Lusche 1972). Consequently, both the strength and the stress-strain relationship of LWAC are more influenced by the properties of the aggregate in LWAC than that of the aggregate in normalweight concrete.

A schematic stress-strain diagram for concrete is given in Figure 2.2. While strain in centric loaded members may not exceed ε_{cl}, the strain of the extreme fibre of members in bending may reach ε_{cu}.

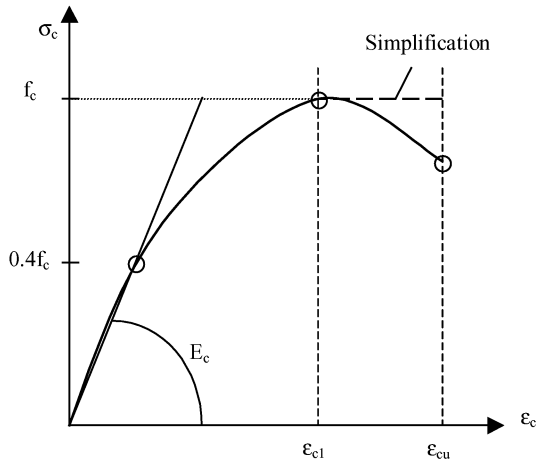

Figure 2.2:
Schematic stress-strain diagram for concrete in compression based on Beeby and Narayanan (1995).

As for most materials the shape and ultimate values of the obtained stress-strain curve is influenced by a number of factors such as:

- the specimen itself,
- the testing equipment and
- the method of testing.

As for cementitious materials, decreasing water/cement-ratio, increasing age and/or increasing stiffness of the aggregate, one may increase the modulus of elasticity as well as the compressive strength. The latter properties may also depend on (Herholdt 1979, Eibl et al. 1995:A6.4.2):

- the volume fraction of the constituents,
- moisture content,
- strength class of the cement,
- additives, type of aggregate and
- curing conditions.

Generally, the modulus of elasticity for concrete may be assumed to be equal for compressive and tensile stresses within the range of service load condition (Mayer 1972, Eibl et al. 1995:A6.4.2).

For concrete, the Poisson's ratio is constant during the linear elastic behaviour of the concrete. The value of Poisson's ratio under tensile load appears to be the same as in compression. Values between 0.15 and 0.25 are very common. LWAC has been reported to have Poisson's ratio at the lower end of the range (Lydon and Balendran 1986). Exceeding 40 % of the compressive strength leads to an increasing of the Poisson's ratio. This is due to the micro-cracking of the concrete. The composition, age and moisture content of the concrete also influence Poisson's ratio (Eibl et al. 1995:A6.4.2).

Thesis work concerning uni-axial compressive loading of LECA masonry

Because the stress-strain relationship of Norwegian LECA masonry has not been very well determined before, some uni-axial compressive tests of such masonry were carried out during this thesis work. Idealised stress-strain relationship as well as design values for modulus of elasticity and Poisson's ratio were established. To be able to establish this, tests were carried out primarily according to prEN 1052-1:1995. However, eccentric loading of specimens as well as testing of smaller specimens had to be performed. The experimentally measured behaviour was then compared with values given by some design standards and with other reported investigations of LECA masonry and LAC, see chapter 3.3.

2.3.2 Shrinkage

Background

Shrinkage is the main time-dependent response to drying effect to be considered in cementitious materials (Beeby and Narayanan 1995). Drying leads to a reduction of size, while moisturising leads to enlarging. The present section deals with aspects concerning shrinkage of cementitious materials.

Shrinkage is defined as stress-free volume reduction of matter due to drying. It should, however, be noted that this definition is theoretical, because drying is never uniform. Consequently, due to non-uniform drying, stresses are introduced in the material. However, the phenomena with introduction of stresses due to non-uniform drying will not be discussed anymore in this thesis.

In concrete, shrinkage is caused by shrinkage of the cement paste since the aggregate used is usually stable. The shrinkage of cement paste may be explained by several shrinkage mechanisms. Wittmann (1982) subdivides the mechanisms into three distinct groups:

- capillary shrinkage,
- chemical shrinkage and
- drying shrinkage.

These mechanisms are discussed in several publications, Bažant and Wittmann (1982), Bažant and Carol (1993) and Sellevold (1993) are examples.

Capillary shrinkage occurs because the water found in capillaries is under a pressure. The capillary pressure results in an attractive force between the walls of the capillary or between two particles separated by a liquid filled capillary. In cement paste the attractive force may lead to reduction of size.

Chemical shrinkage is a term used to cover a number of distinct shrinkage (or swelling) mechanisms caused by chemical reactions. According to Wittmann (1982) the most important mechanisms are:

- hydration shrinkage,
- thermal shrinkage,
- dehydration shrinkage,
- crystallisation swelling,
- carbonation shrinkage and
- conversion shrinkage.

Drying shrinkage of concrete is commonly defined as the time-dependent reduction in volume resulting from loss of water (Basma and Abdel-Jawad 1995).

In general, the shrinkage of concrete is according to Beeby and Narayanan (1995) mainly influenced by the following parameters:

- ambient humidity,
- composition of the concrete and
- dimensions of the element.

Ambient humidity: The most important parameter influencing the magnitude of shrinkage is the water loss after a given duration of drying (Eibl et al. 1995:A6.5.3.2). Experimental results on the effect of the w/c-ratio and ambient humidity on shrinkage are given in Figure 2.3. In concrete, it is normally assumed that 100 % RH is initially present resulting from the fabrication process.

Concerning the *compositions* of LECA blocks, a relatively high w/c-ratio (> 0.7) is typical, see the dotted line in Figure 2.3. Pihlajavaara (1974) points out that the shrinkage increases with increasing w/c-ratio in the high humidity region. The shrinkage of concrete also increases with decreasing modulus of elasticity of the aggregate (Eibl et al. 1995:A6.5.3.2) or decreasing amount of aggregate (Pittman and Ragan 1998, Shimomura and Maekawa 1997). Soft aggregates, such as LWA, restrain shrinkage of the cement paste less effectively than stiff aggregate as found in normalweight concrete. Nevertheless, also an increasing amount of LECA is reported by Bentzon (2000) to reduce the shrinkage of LWAC.

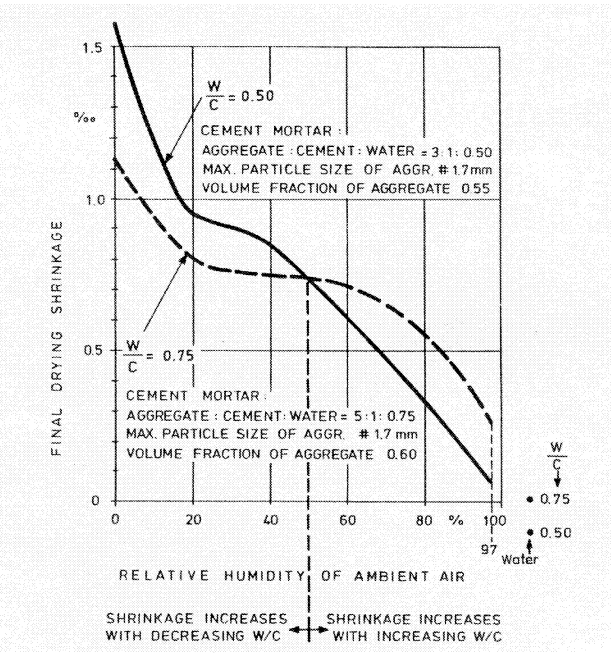

Figure 2.3:
Experimental results of the effect of the water/cement-ratio on shrinkage of cement mortar (Pihlajavaara 1974).

The *dimension of the element*, defined by the notional size (Eurocode 2) or effective thickness (see Equation 2.1), influences the rapidity of the shrinkage. In accordance with test results presented by Schubert (1992) (see Figure 2.4), the shrinkage is delayed with increasing notional size. An increasing notional size indicates a relative reduction of the exposed drying surface.

$$t_{ef} = 2\frac{A_{cs}}{u_{cs}} \qquad \text{Equation 2.1}$$

where t_{ef} is the effective thickness or notional size,
A_{cs} is the component cross-section,
u_{cs} is the perimeter of that area exposed to drying.

According to Beeby and Narayanan (1995) the dimensions of the element also influence the magnitude of the final shrinkage. The size of a concrete member influences shrinkage since small sections lose moisture at a much higher rate than thick sections. Consequently, they shrink much more rapidly. Final shrinkage, however, is according to Hansen and Mattock (1966), independent of the dimension of the member. Since the drying of concrete is usually a rather slow process, the development of shrinkage with time is also slow. Complete drying of thick concrete members may take several decades (Waldum et al. 1993b, Hedenblad 1995, Eibl et al. 1995:A6.5.3.2). That may be why Beeby and Narayanan (1995), among others, report that an increasing notional size gives a decreasing final shrinkage. Influence of size and shape of member on shrinkage is further discussed by Hansen and Mattock (1966) and Nilsson (1979).

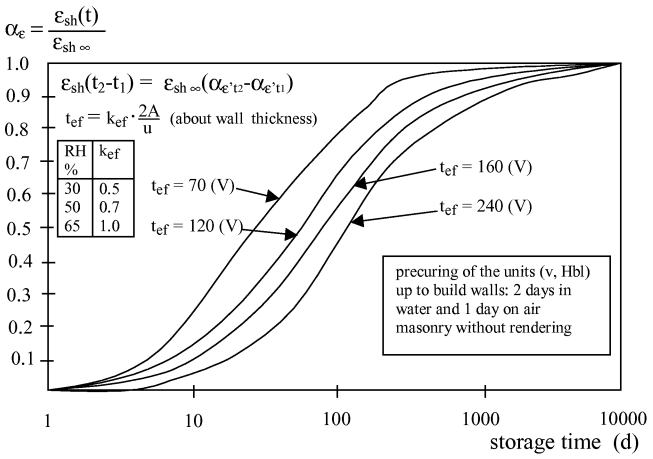

Figure 2.4:
Masonry made from lightweight concrete blocks. Time dependence of shrinkage presented in Schubert (1992). Age at the beginning of shrinkage was 3 to 7 days.

Similarly to notional size, increasing porosity may give faster development of shrinkage. However, no significant effect on the magnitude of final shrinkage was reported when increasing the air content from 2 to 20 volume-% of LWAC (Bentzon 2000).

Subsequent, moisturising of concrete and masonry leads to swelling and, hence further complicates the moisture movement. Figure 2.5 illustrates cyclic drying and re-wetting. The figure indicates that nearly all the irreversible shrinkage appears during the first drying/rewetting cycle. The observation is confirmed by for example Parrot and Young (1982) and Sabri and Illston (1982).

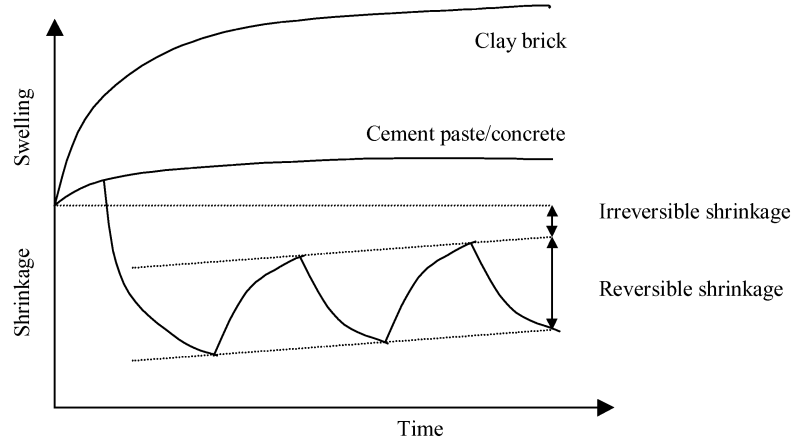

Figure 2.5:
Illustration of typically swelling as well as subsequent shrinkage and moisturing in concrete or masonry constituent materials. Based on L'Hermite et al. (1949), Zijl (2000) and Neville (1995:442).

Thesis work concerning shrinkage of LECA masonry

The shrinkage behaviour of Norwegian LECA masonry has previously not been very well determined. In this thesis work the magnitude of shrinkage and the time-dependent shrinkage behaviour of LECA blocks, small masonry specimens as well as walls were investigated.

The effect of different curing regimes on shrinkage and compressive strength of LECA blocks were studied. The study was carried out in order to see how early after the manufacturing it may be recommended to dry the LECA blocks. Also an investigation of shrinkage behaviour of LECA masonry restrained to the bottom by a foundation were carried out. Concerning the restrained walls, effects of the shrinkage reinforcement amount were studied.

Design values for final shrinkage dependent of ambient humidity may be established by this study. The values are compared with design values given by some design standards. Consideration concerning influences of the dimension of the element have been made. Recommendations for determination of design values as well as for product development are also given. See Chapter 3.4.

2.3.3 Creep

Background

After the initial elastic deformation, a perpetual load leads to a further deformation of the masonry. The deformation ratio reduces gradually and finally it stops after a very long time (Schubert 1992). The present section deals with aspects concerning creep of cementitious materials.

Creep is the increase of deformation caused by long-time loading. Because the creep behaviour of concrete is not completely understood yet, the behaviour may be explained by several real as well as apparent and fictitious creep mechanisms. According to Wittmann (1982) two different real creep mechanisms contribute to the basic creep:

- short-time and
- long-time creep or particle displacement.

Water movement and redistribution of water in the microstructure may explain *short-time creep*, while *long-time creep* is caused by displacement of gel particles.

In addition to basic creep there are several apparent and fictitious creep mechanisms of which drying creep is probably the most important (Wittmann 1982). Drying creep is caused by simultaneous creep and shrinkage and contributes considerably to the total creep. The effect of the drying creep, or Pickett effect (Pickett 1942), is illustrated in Figure 2.6 together with shrinkage and basic creep. Shrinkage is obtained by the drying of an unloaded specimen. Basic creep is obtained from a loaded and sealed specimen, while transient creep is obtained from a loaded specimen free to dry in the same environment as the shrinkage specimen. Drying creep is calculated by subtracting the shrinkage and basic creep from the transient creep.

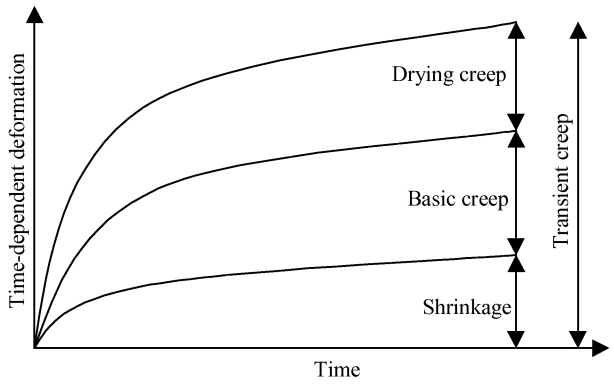

Figure 2.6:
Illustration of the drying creep/Pickett effect. Based on Pickett (1942) and Zijl (2000).

There is still some controversy about the mechanisms that contribute to the drying effect. Bažant (1988) explains that stress-induced shrinkage contributes, while Wittmann (1982) discusses the contribution of crack formation in the shrinkage specimen caused by internal stressing. According to Wittmann (1982), such crack formation is avoided in the creep specimen because of the application of an external compressive load. The compressive load reduces the tensile stresses in the specimen and hence, the risk of cracking. An illustration of the apparent and the fictitious mechanisms' contribution to the drying creep is made by Bažant (1988), see Figure 2.7.

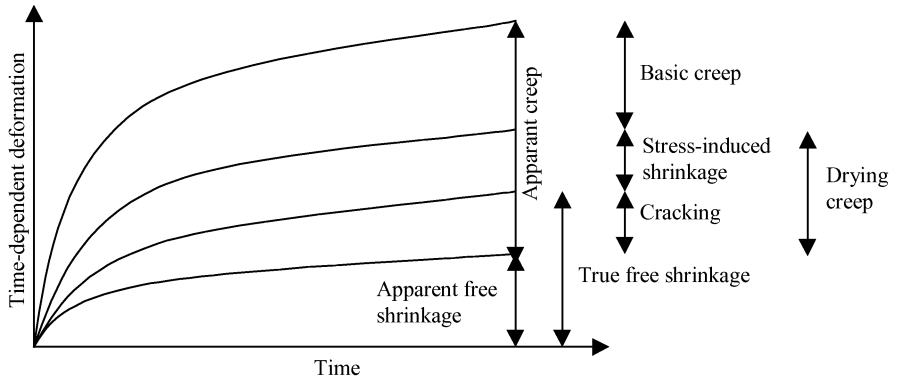

Figure 2.7:
Illustration of the contribution by the cracking and stress-induced shrinkage to the drying creep. Based on Bažant (1988).

The most important real and apparent creep and shrinkage mechanisms are summarised by Wittmann (1982) in Table 2.2. The real and apparent mechanisms can be explained by physical and chemical processes, which can be analysed and simulated numerically. If subdivision in real and apparent mechanisms is not made clearly, fictitious mechanisms have to be introduced. The fictitious mechanisms are, however, not defined mechanisms but based on imaginations.

Table 2.2:
Subdivision of processes involved in creep and shrinkage of concrete in real, apparent and fictitious mechanisms (Wittmann 1982).

	Real mechanisms	Apparent mechanisms	Fictitious mechanisms
Creep (without exchange of moisture)	Short-time creep Particle displacement	Internal stress distribution	
Shrinkage (without external load)	Capillary shrinkage Chemical shrinkage Drying shrinkage	Hygral gradient Crack formation	
Simultaneous creep and shrinkage		Hygral gradient Crack formation	Stress-induced shrinkage Drying creep

The creep is according to Beeby and Narayanan (1995) mainly influenced by:

- ambient humidity,
- composition of the concrete,
- dimensions of the element,
- age at which load is first applied on the concrete and
- duration and magnitude of the loading.

Ambient humidity: The drying creep increases with decreasing relative humidity (Eibl et al. 1995:C5.2.7).

Composition of the concrete: Because the creep of normalweight concrete is almost exclusively due to creep of the hydrated cement paste, the creep is proportional to the volume of cement paste. Like shrinkage, soft aggregates such as LECA restrain creep of the cement paste less effectively than stiff aggregate as in normalweight concrete. Increasing water/cement ratio increases the creep (Bažant 1982).

The *dimensions of the element* do not influence the basic creep. Drying creep, however, increases with decreasing size because the element looses moisture more rapidly (Eibl et al. 1995:C5.2.7).

Decreasing creep appears when the *age at which load is applied* increases (Eibl et al. 1995:C.5.2.7).

Magnitude of load: Creep is approximately proportional to stress up to about 50 % of the strength (Bažant 1982). That is why creep strain is commonly expressed by the creep coefficient, $\phi(t)$, as defined by Equation 2.2:

$$\phi(t) = \frac{\varepsilon_{cr}(t)}{\varepsilon_{el}} \qquad \text{Equation 2.2}$$

where: $\phi(t)$ is the creep coefficient,
$\varepsilon_{cr}(t)$ is the creep strain,
ε_{el} is the elastic strain established immediately after applying the load.

The creep coefficient increases with increasing *duration of the loading*. However, the deformation ratio reduces gradually and finally it stops after a very long time (Schubert 1992). Consequently, a final creep coefficient is given in many design standards e.g. Eurocode 2, Eurocode 6 and NS 3473. Creep in tension and in compression is according to Eibl et al. (1995:A6.5.3.3) equal within the linear elastic part of the stress-strain relationship.

For more information about creep Müller (1993) made a data bank which contains most of the significant results on creep experiments reported in the literature. However, not enough data exists to make design rules for the development of creep of LAC with regard to time (Stemland and Thorenfeldt 1998).

With close relation to creep is relaxation. Relaxation is defined as the stress decrease with time when an imposed strain remains constant. Relaxation depends on the same parameters as the creep. Similar the creep coefficient for the case of constant stress, relaxation may be described by a relaxation coefficient given in Equation 2.3 (Bažant and Asghari 1974, Eibl et al. 1995:A6.5.3.3):

$$\psi_r(t) = \frac{\phi(t)}{[1+\rho_r \cdot \phi(t)]} \qquad \text{Equation 2.3}$$

where $\psi_r(t)$ is the relaxation coefficient,
ρ_r is the ageing coefficient which for long-time loading may be taken as 0.8.

Thesis work concerning creep of LECA masonry

While creep behaviour of Norwegian LECA masonry was not determined earlier, investigations were carried out to obtain the magnitude of creep as well as the time-dependent behaviour.

In this thesis work the total time-dependent deformation due to loading, excluding only the apparent free shrinkage, is attributed to creep.

Caused by restrained shrinkage, tensile stresses and hence tensile creep appears in the longitudinal direction of the wall. Compressive creep normally appears in the vertical direction of a masonry wall caused by vertical compressive loading. That is why creep due to compressive loading normal to the bed joint as well as tensile loading in the longitudinal direction of LECA masonry were studied.

The creep values are compared with design values given by some design standards. Consideration concerning the final creep coefficients and stress distribution around the open perpend joint were also given. See Chapter 3.5.

2.3.4 Temperature

Background

Likewise, change of moisture content and change of temperature lead to deformation of the masonry. An increase in temperature leads to an enlargement of dimensions, while a decrease

in temperature leads to a reduction. The present section deals with some aspects concerning deformation of cementitious materials caused by change of temperature.

The material's ability to change length due to change of temperature is commonly expressed by the coefficient of thermal expansion, see Equation 2.4. The linearity is valid for concrete in the temperature range of about 0 °C to 60 °C.

$$\alpha_T = \frac{\Delta l}{l \cdot \Delta T} \qquad \text{Equation 2.4}$$

where: α_T is the coefficient of thermal expansion,
Δl is the length change,
l is the initial length,
ΔT is the change in temperature.

According to Ziegeldorf et al. (1979) and Eibl et al. (1995:A6.8.4), the coefficient of thermal expansion of concrete depends on the:

- thermal coefficient of the aggregate,
- thermal coefficient of the hydrated cement paste and
- volume fraction of the two constituents.

Consequently, the coefficient of thermal expansion depends to a large extent on the type of aggregate used. Generally, however, the coefficient is somewhat lower for water-saturated aggregates than it is for dry aggregate. The coefficient of thermal expansion of hydrated cement paste decreases slightly with increasing hydration. Nevertheless, the coefficient depends primarily on the moisture content of the paste and is about the same for very dry and for water-saturated paste (about $10 \cdot 10^{-6}$ 1/K). The paste reaches maximum values of about $23 \cdot 10^{-6}$ 1/K at 65-70 % RH (Eibl et al. 1995:A6.8.4).

The temperature may also influence the strength, modulus of elasticity and fracture energy of concrete. CEB-FIB MC 90 indicates decreasing values with increasing temperature. Nevertheless, with temperatures below 80 °C the reduction is in most instances insignificant.

Likewise, creep and shrinkage are influenced by change of temperature. An increasing temperature increases both the magnitude and the rate of the shrinkage, because the increasing temperature accelerates the drying of the concrete and reduces the equilibrium moisture content (Eibl et al. 1995:A6.8.4 and Bažant 1982). Caused by the same reason, drying creep is both accelerated and increased (Wittmann 1982). The basic creep, however, is only accelerated.

Thesis work concerning thermal expansion of LECA masonry

Thermal expansion of LECA blocks with four different moisture contents was measured in order to study the influence of moisture content on the magnitude of thermal expansion. Based on the investigations, a design value of thermal expansion coefficient for LECA masonry was determined, see Chapter 3.6.

2.4 Restrained movement

2.4.1 Actions of restrained movement

Application of load, change of moisture content and change of temperature all lead to deformation of masonry. If the deformations are restrained, stresses appear in the masonry. Figure 2.8 contains an example of masonry prevented from changing dimensions horizontally. Drying shrinkage or reduction of temperature leads to a decreasing length of the masonry. If any obstruction prevents the decreasing from happening, tensile stresses appear in the masonry. If the tensile stresses are higher than the tensile strength, failure of the masonry will occur.

Considering of the relatively low tensile strength perpendicular to the mortar joint, two possible failure cases may occur (Schubert 1992). This may either be because of the limited tensile strength of the masonry unit (see Figure 2.8b) or limited shear strength between the mortar and the unit in the bed joint (Figure 2.8c).

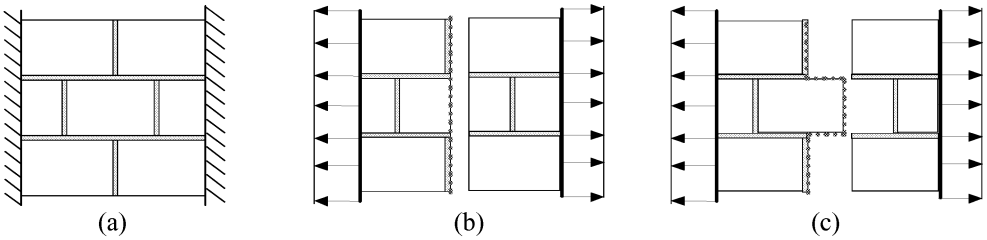

Figure 2.8:
(a) Masonry wall with obstructed shrinkage. (b) Failure du to lack of tensile strength of masonry units and of perpend joints. (c) Failure due to lack of shear strength of bed joint and tensile strength of perpend joints.

2.4.2 Tensile failure

Background

In concrete and masonry, the tensile fracture process may be explained by the idealised stress-displacement relationship presented in Figure 2.9. Materials which may be characterised by such an idealised stress-displacement relationship are known as quasi-brittle materials. The concrete behaves linear elastic up to about 70 % of the tensile strength, when introduction of micro-cracks causes deviation from the linear elastic behaviour (Sturman et al. 1965, Johnston 1970, Eibl et al. 1995:A6.2.2). Further development of strain leads to more micro-cracks and a so-called process zone may start to grow. While the process zone consists of a system of more or less parallel but discontinuous micro-cracks, the stresses decrease with increasing crack opening until a continuous crack has developed (Petersson 1981, Eibl et al. 1995:A6.2.2).

The explanation of the post peak behaviour by the fictitious crack model was original introduced by Hillerborg et al. (1976). While the process zone is located at a very narrow region, the obtained stress-strain diagram depends strongly on the gauge length of the

displacement measurement. Consequently, Hillerborg et al. (1976) and Petersson (1981) illustrates the displacement in a stress-strain diagram for the non-cracked region and a stress-crack opening diagram for the cracked section of the gauge length. The decomposition of the displacement is illustrated in Figure 2.10.

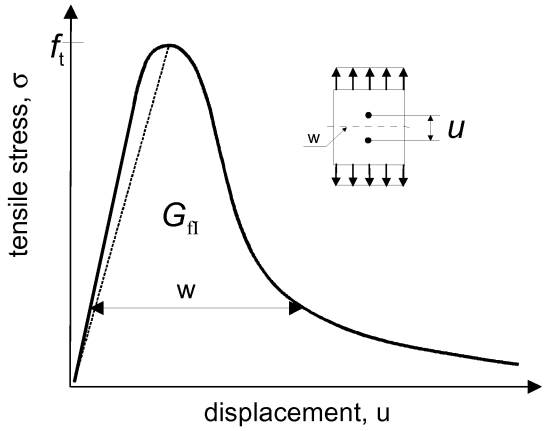

Figure 2.9:
Idealised stress-deformation diagram of a deformation-controlled tensile test.

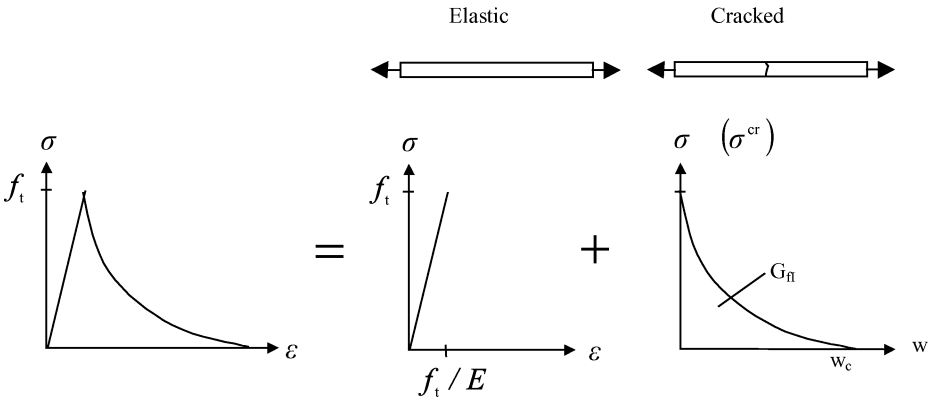

Figure 2.10:
Strain decomposition into an elastic part and another part representing the crack opening. Based on Høiseth (1999).

The stress-crack opening relation is according to Hordijk (1992) undoubtedly the most important input parameter for the non-linear fracture-mechanics calculations of concrete. By defining the mode I fracture energy as the area under the stress/displacement diagram, see Figure 2.9, it is possible to describe the fracture behaviour of concrete subjected to tension by fracture mechanics. The mode I fracture energy is the energy that is needed to create one unit crack surface and may be used to describe the resistance to cracking (Rots 1997). The mode I fracture energy of concrete may in particular depend on the water/cement-ratio, the cement

content, maximum size of the aggregate and age of the concrete (Wittmann et al. 1987, Bažant 1992). Based on the mode I fracture energy, Hordijk and Reinhardt (1990) developed a formula describing the stress-crack opening of concrete subjected to uni-axial tension, see Equation 2.5. Pluijm and Vermeltfoort (1991) proved the validity of the equation for masonry under tension.

$$\frac{\sigma}{f_t} = \left(1 + \left(c_1 \frac{w}{w_c}\right)^3\right) e^{-c_2 \frac{w}{w_c}} - \frac{w}{w_c}\left(1 + c_1^3\right) e^{-c_2} \qquad \text{Equation 2.5}$$

where:

σ is tensile stress,
f_t is tensile (bond) strength,
c_1, c_2 are dimensionless constants, 3.0 and 6.93, respectively.
w is crack width,
w_c is crack width at which no stresses are being transferred any longer :

$$w_c \approx 5{,}14 \frac{G_{fI}}{f_t}$$

G_{fI} is mode I fracture energy, associated with tensile cracking (see Figure 2.9).

Thesis work concerning tensile failure of LECA masonry

Because the behaviour of Norwegian LECA masonry due to uni-axial tensile loading has previously not been determined, the behaviour was studied in this thesis. Both the behaviour of LECA blocks and of mortar joints during tensile failure are studied. The obtained behaviour may be applied for numerical analysis of tensile cracking of LECA masonry, see Chapter 3.7.

2.4.3 Shear failure

Background

Fracture mechanics may also be used to calculate shear failure of masonry. The shear fracture process of bed joint and interface loaded in compression may be presented by the idealised stress-deformation relationship given in Figure 2.11. The shear stress-deformation diagram differs from the tensile stress-deformation diagram mainly because of the descending branch that stabilises at a certain shear stress level, μ. The dry friction of two non-bonded surfaces gives this stress level. The normal-stress level influences the magnitude of the dry friction. The normal-stress also influences the shear strength. In load-bearing masonry, normal-compression stress is a normal situation. An illustration of the influence of normal compression stress on the shear stress-strain relationship is made of Pluijm et al. (2000), see Figure 2.12.

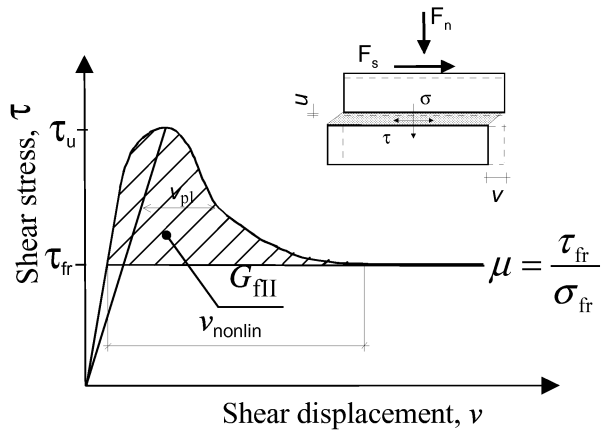

Figure 2.11:
Idealised stress-deformation diagram of a deformation controlled shear test under constant normal compression.

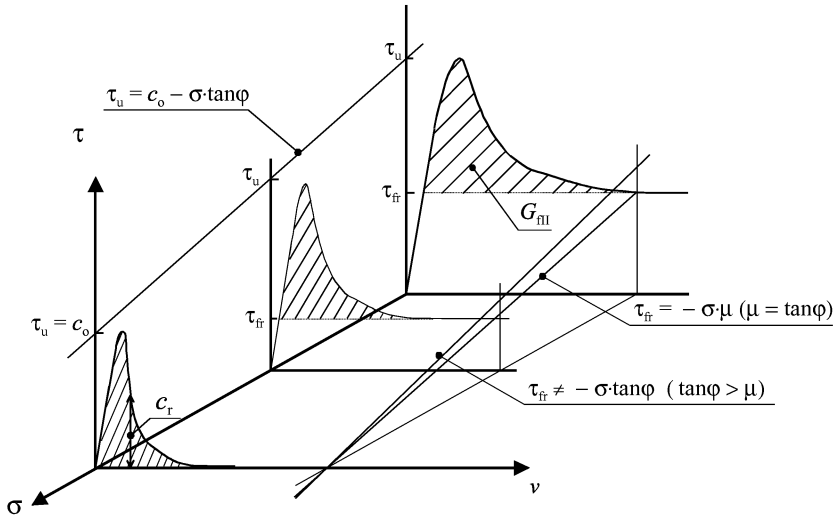

Figure 2.12:
Schematic diagram of deformation controlled shear tests under three different constant normal compression stress levels (Pluijm et al. 2000).

While the descending branch of the tensile stress-displacement relationship is explained by the fictitious crack opening, the corresponding descending branch of the shear stress-displacement relationship may be explained by a softening of the cohesion. The mode II fracture energy corresponds with the area under the cohesion-softening curve, see Figure 2.11, and is defined as the amount of energy that is needed to create one unit area of shear crack (Rots 1997). For non-linear fracture mechanics calculations, the mode II fracture energy and the cohesion-softening relation are necessary input parameters. Lourenço (1996) developed a

formula describing the cohesion softening by including the dependence of mode II fracture energy on the cohesion in the Coulomb's friction failure criterion, see Equation 2.6:

$$\tau_u = c_o \cdot e^{-\frac{c_o}{G_{fII}} \cdot v_{pl}} - \tan\varphi \cdot \sigma \qquad \text{Equation 2.6}$$

where τ_u is the shear bond stress,
c_o is the cohesion or shear bond strength (τ when $\sigma = 0$),
φ is the angle of internal friction,
σ is the normal stress in the bed joint,
G_{fII} is the mode II fracture energy, associated with shear cracking (see Figure 2.11),
v_{pl} is the shear softening distance.

Another description of the cohesion-softening is made by Zijl (1996), by changing the mode I parameters of Equation 2.5 in corresponding mode II parameters, see Equation 2.7:

$$\frac{c_r}{c_o} = \left(1 + \left(c_1 \frac{v_{pl}}{v_{nonlin}}\right)^3\right) e^{-c_2 \frac{v_{pl}}{v_{nonlin}}} - \frac{v_{pl}}{v_{nonlin}}\left(1 + c_1^3\right) e^{-c_2} \qquad \text{Equation 2.7}$$

where: v_{nonlin} is the shear displacement over which the cohesion reduces to zero,
c_1 is dimensionless constant 3.0,
c_2 is dimensionless constant 6.93.

During the shear failure process a displacement perpendicular to the shear deformation also appears. This behaviour of the bed joint during softening is commonly expressed as the dilatancy. When a plastic shear deformation, v_{pl}, of a specimen take place, a plastic transverse deformation, u_{pl}, also appears. The angle between the horizontal and the vertical displacement is of Rots (1997) referred to as the angle of dilatancy, ψ.

In numerical modelling of masonry the dilatancy may be important to simulate the shear failure process. Rots (1997) and Lourenço (1996) both handle dilatancy as a constant during the failure envelope. As a matter of fact this is not the case. Pluijm (1999) describes dilatancy with the following Equation 2.8 as a crude approximation of his experimental results:

$$\Delta\tan\psi = \tan\psi_o \left(2\left(\frac{v_{pl}}{r}\right)^{1,5} - 3\frac{v_{pl}}{r} + 1\right) \qquad : v_{pl} \le r$$

$$\Delta\tan\psi = 0 \qquad : v_{pl} > r \qquad \text{Equation 2.8}$$

where: ψ is the dilatancy angle, where $\tan\psi = \frac{u_{pl}}{v_{pl}}$
$\tan\psi_o$ is the initial (maximum) value of the tangent of the dilatancy angle,
r is a roughness distance depending on the type of masonry over which $\Delta\tan\psi$ reduces to zero,
v_{pl} is the plastic shear displacement,
u_{pl} is the plastic normal displacement.

Thesis work concerning shear failure of bed joint in LECA masonry

Because the behaviour of bed joint in Norwegian LECA masonry due to shear compressive loading has previously not been determined, it was experimentally studied in this study. The obtained behaviour may be applied for numerical analysis of tensile cracking behaviour of LECA masonry, see Chapter 3.7.

2.5 Modelling of masonry

Common approaches

The mechanical behaviour of masonry and of its constituents: units, mortar and the interface between units and mortar show the characteristics of so-called quasi-brittle materials. When subjected to pure compression, tension or shear, as well as combined states of stress, the stress/strain relationship follows the schematised curve in Figure 2.13. When the peak stress has been reached, additional straining leads to increased bridging of micro-cracks which gives a strain softening behaviour of the material. The softening is related to the fracture energy released in connection with crack-formation in the constituents or in the compound masonry. In order to describe the deterioration of masonry due to load induced cracking, the strain softening must be accounted for in a realistic manner.

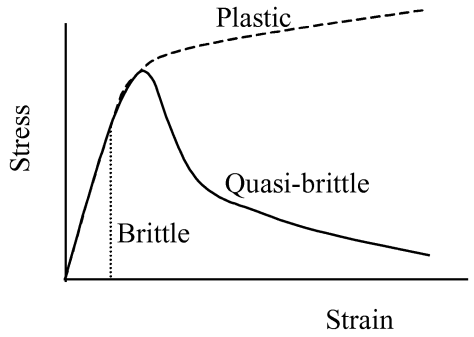

Figure 2.13:
Typical stress/strain relationship for plastic, brittle and quasi-brittle materials (Høiseth and Kvande 1999).

In a Finite Element context, the regular geometric structure of compound masonry suggests that the spacial modelling should follow the constituents, such that units, joints and adhesion zones are treated separately. This way it seems natural to distinguish between continuous areas represented by units and joints (mortar), and regard the adhesion zones as weak planes of discontinuity. Alternatively, the planes of discontinuity may be extended to cover the actions of joints and adhesion zones. Rots (1997) and Lourenço (1996), have termed this micro- and simplified micro-modelling, respectively. Macro-modelling on the other hand, which is more applicable in analysis of real (large) masonry structures, indicates that the masonry is regarded as a continuum, where the material model accounts for the combined actions of the constituents.

The three levels of refinement are illustrated in Figure 2.14, which is taken from Lourenço (1996) and Zijl (2000). The detailed micro-modelling, Figure 2.14b, where the units and joints are represented by continuum elements and the adhesion zone by interface (discontinuum) elements must be considered the most precise description. The continuum element includes stiffness, Poisson's ratio and non-elastic behaviour of the composite it represents, while the interface elements represent a potential crack/slip plane. The simplified micro-modelling is illustrated in Figure 2.14c, where the interface element represents both the joint and the adhesion zone. In this case, the effect of non-elastic behaviour, stiffness and Poisson's ratio of the mortar are neglected. The macro-modelling approach is shown in Figure 2.14d. In ordinary masonry, where especially the stiffness and strength of units are far higher than those of the joints and the adhesion zones, a representative model calls for homogenisation of the joint actions of the constituents. Because macro-modelling is appealing, and, due to efficiency in many practical cases the only suitable approach, much recent research on modelling of masonry focus on homogenisation techniques, see Pande et al. (1998).

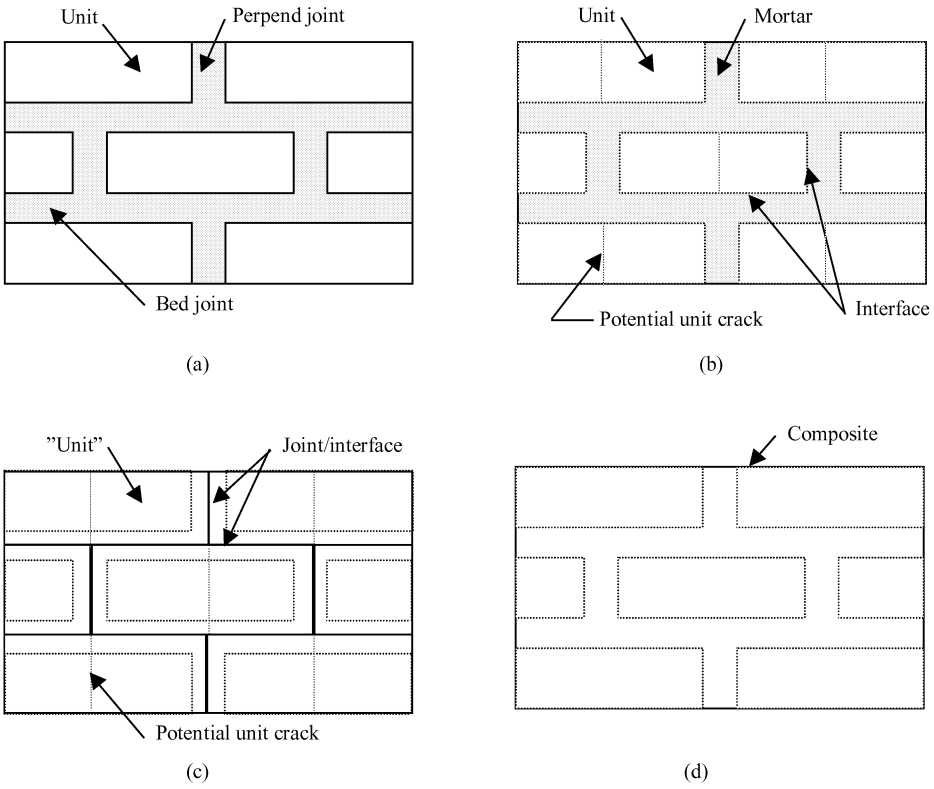

Figure 2.14:
Modelling strategies for masonry structures: (a) Masonry samples, (b) detailed micro-modelling, (c) simplified micro-modelling and (d) macro-modelling (Lourenço 1996, Zijl 2000).

Modelling LECA masonry

The constituent properties of LECA masonry make the mechanical behaviour atypical compared to ordinary masonry. This is illustrated in Figure 2.15, which shows a schematised stress/strain relationship for ordinary clay brick compared to the material behaviour of mortar and LECA blocks. Due to the relatively high stiffness and strength of clay brick, both in tension and compression, compared to the values of mortar, the joints and adhesion zone represent the weak links in ordinary masonry. A realistic description of the constitutive behaviour in these areas is therefore important, while the units in many cases will not be subjected to stress levels exceeding the elastic limit. Concerning LECA masonry, however, the conditions are opposite: the stiffness and strength of mortar are higher than those of the LECA blocks. In structural analysis, this implies that the LECA blocks must also be represented by a material model that takes into account the complete stress/strain relationship, including the softening part.

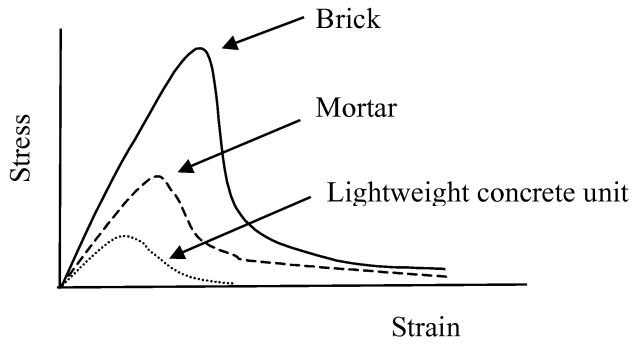

Figure 2.15:
Typical stress/strain relationship for clay brick, mortars and lightweight concrete blocks.

Due to capillar suction from the LECA blocks during curing, the mortar close to the adhesion zone must be expected to be somewhat weaker, both with respect to stiffness and strength than in the middle area of the joint. In spite of this, the rough surface of the LECA blocks and the cementitious character produces a strong mechanical and chemical adhesion between block and joint. The adhesion zone of LECA masonry does therefore not perform as potential planes of discontinuity to the same degree as in ordinary masonry. In essence this justifies that a micro-modelling can be restricted to account for the quasi-brittle material behaviour of the LECA and the average in-situ properties of the applied mortar.

Thesis work concerning modelling of LECA masonry

The experimental results of the present study should provide the necessary constitutive basis for available quasi-brittle material models to allow numerical simulation of LECA masonry by both micro- and macro-modelling.

CHAPTER 3

3. MATERIAL PROPERTIES OF LECA MASONRY

3.1 Introduction

In the previous chapter, some material properties of current importance for structural analysis and design were identified, and main features and mechanisms concerning cementitious materials were introduced. The main goal of the present chapter is to explain the material properties of LECA masonry more specifically. Because of the lack of data, properties of LECA masonry had to be experimentally studied during this thesis work. Material properties measured in this study are given as mean values. The chapter is partly based on the appendixes.

The thesis does not cover all the various qualities of LECA masonry. A selection of investigated qualities has been made based mainly on the Norwegian production volume. The chapter gives first a presentation of the investigated qualities of LECA masonry. A brief presentation of Norwegian LECA masonry in general is enclosed as Appendix 1. The presentation includes the manufacturing process and characteristic material properties for LECA masonry.

3.2 Presentation of investigated LECA masonry

3.2.1 LECA masonry qualities in Norway

Light Expanded Clay Aggregate (LECA) is a type of Lightweight Aggregate (LWA) that is commonly used in Norway. The masonry investigated in this thesis is made from LECA concrete blocks manufactured according to NS 3017. The Norwegian production of LECA masonry units comprises blocks with dry net block density between 600 and 1300 kg/m³ and corresponding compressive strengths as given in Table 3.1.

Table 3.1:
LECA block qualities manufactured in Norway.

Dry net density [kg/m³]	Compressive strength [N/mm²]
600	2
770	2-3
900	4
1 300	8

Block quality “2/600” and “3/770” are by far the most common. Numbers 2 and 3 refer to a gross compressive strength of minimum 2 and 3 N/mm², while number 600 and 770 refer to their average dry net block density of 600 and 770 kg/m³. Normally, block quality “8/1300” is used only where high sound insulation properties are required.

The constituents of the concrete blocks are mainly LECA mixed with small amounts of natural sand, cement, silica fume and water. Normally, LECA grains with diameter 4 – 10 mm represent most of the volume. Blocks with the highest density also contain a significant portion of natural sand. By mainly using aggregate with diameter between 4 and 10 mm, it is possible to obtain the typical porous concrete (LAC) structure of the “2/600” and “3/770” blocks.

LECA blocks are manufactured in a variety of shapes and sizes and with a variety of holes, see examples given in Figure 3.1. Altogether some 30 different types of blocks are produced for the Norwegian market.

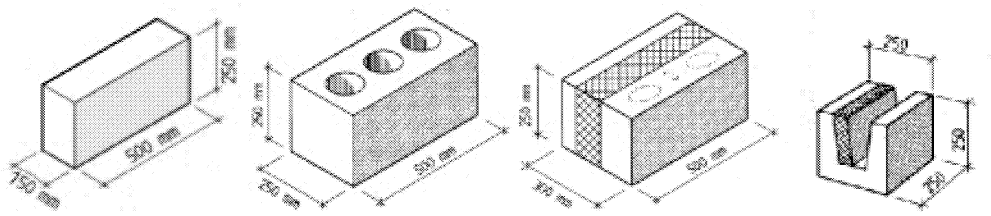

Figure 3.1:
Some typical Norwegian masonry units made of LECA concrete.

In practice, the binder used in the mortar for LECA masonry is usually cement, but a mixture of lime and cement is becoming more and more popular. The cement (CEM) mortar has a mix ration cement:aggregate of about 1:4 by volume, while the lime/cement (L/CEM) mortar has a mix ration lime:cement:aggregate of about 1:1:7 by volume. The 28 days’ flexural and compressive strength for these mortars should be, according to mortar class B of NS 3120, minimum 2.5 N/mm² and 8 N/mm² respectively. (I.e. mortar class M 5 according to prEN 998-2:2000.)

An important distinctive characteristic of Norwegian LECA masonry, which should be noted, is the use of open (free) perpend joints. Normally, Norwegian LECA masonry is made without any mortar in the perpend joints. Masonry is only made with mortar in the perpend joints when a high sound reduction index is recommended or visible perpend joints are requested.

Normally, masonry made of LECA blocks with thickness ≥ 200 mm is made as a shell bedded wall, while masonry of blocks with thickness ≤ 175 mm is made with mortarfilled bed joints. Standardised height of the masonry units is 248 mm, while the most common length of the blocks is 498 mm. (Height and length of the blocks are commonly given as 250 and 500 mm respectively.) Nominal joint thickness is 10-12 mm (Leca teknisk håndbok ’99, Leca 1.000). Consequently, the mortar joints accounts for less than 5 % of the total volume of LECA masonry when made with open perpend joints.

3.2.2 Selection of LECA masonry qualities for sampling

Because of the relatively high number of types of LECA masonry, it was impossible to cover all of them by this study. Based mainly on the Norwegian production volume of LECA blocks, one of the most common qualities were picked out for a throughout investigation. The work of this study is limited dealing with LECA masonry made:

- of blocks of quality "3/770" without holes, see drawing at left hand side of Figure 3.1 (i.e. height 250 mm and length 500 mm), and mixture and characteristics given in Table 3.2,
- of blocks with thickness 150 mm or 100 mm, see list of investigations carried out on the different qualities in Table 3.3,
- of factory made cement mortar or factory made lime/cement mortar, see Table 3.3,
- with open (free) perpend joints,
- with mortarfilled bed joints,
- with bed joint thickness 10-12 mm and
- without rendering.

Consequently, when the subsequent properties of LECA masonry are presented, they will only be applicable to the investigated qualities of LECA masonry.

Selection of the LECA masonry qualities for sampling were based on

- the Norwegian production volume of LECA masonry (block quality "3/770" is among the most common qualities),
- trends in the market (the mortar L/CEM 1:1:7 was assumed to be the most common masonry mortar in the future) and
- a aim of simplify the investigated situation (selection of blocks without holes).

Table 3.2:
Mixture and characteristics for blocks from the three different production runs investigated in this study.

		Production run [1]			Unity
		Kvande (2001-1)	Kvande (2001-3)	Kvande (2001-8)	
Mixture:					
cement		62	78	82	kg/m³ compressed block
silica fume		10	12	13	kg/m³ compressed block
natural sand,	0-1 mm	0.257	0.168	0.156	m³/m³ compressed block
	0.25-4 mm	-	0.116	0.143	m³/m³ compressed block
LECA,	0-4 mm	0.091	-	-	m³/m³ compressed block
	4-10 mm, spheroids	0.769	1.085	0.942	m³/m³ compressed block
	4-10 mm, crushed	0.112		0.142	m³/m³ compressed block
Dry gross density, concrete		800	760	730	kg/m³
Compressive strength, block		3.7	3.0	2.6	N/mm²

[1] Raw material and material properties of the different productions are given in the three references of Kvande (2001-1, 2001-3, 2001-8).

Table 3.3:
Overview of which blocks and mortars that were used for the different type of investigations by Kvande.

	Uni-axial compressive loading	Shrinkage			Creep	Change of temperature	Uni-axial tension	Shear compression
		Blocks	Couplets	Walls				
Production run [1)]	(2001-1)	(2001-3) (2001-8)	(2001-8)	(2001-3)	(2001-8)	(2001-1)	(2001-3)	(2001-3)
Thickness of block	150 mm	150 mm 100 mm	100 mm	150 mm	100 mm	-	-	-
Type of masonry mortar [2)]	CEM 1:4	-	L/CEM 1:1:7	C 1:3 L/CEM 1:1:7	L/CEM 1:1:7	-	L/CEM 1:1:7	L/CEM 1:1:7

1) References to the different production runs of Kvande, see Table 3.2.
2) Volume cement:aggregate or volume lime:cement:aggregate.

LECA blocks for testing were taken from the production line randomly. Table 3.2 shows that the mixture and consequently also the quality of the blocks may vary considerably. The production described of Kvande (2001-8) even showed that some of the blocks did not satisfy the specified strength (f_c = 3 N/mm²). The last production run was carried out especially for this study, and there were no opportunities to make new samples. It should also be noted that the quality of the blocks might vary somewhat depending on the placing in the mould and in the curing chamber during manufacturing. No efforts are made in this thesis to quantify such variations in neither the manufacturing process, nor the influence of the variations on the quality of the LECA blocks. A study of the variations due to manufacturing and deviation from the specified mixtures may, however, be of great importance for optimisation of the manufacturing process. Since the variations in manufacturing are not very well known, the values reported in this thesis work should for the time being be taken as approximate values for the investigated qualities.

Studying only one quality of LECA blocks limit the utilitarian value of the work. No general formulas concerning e.g. the effect of density on the ultimate strain, are possible to develop on the basis of this study. However, due to the limited data on LECA masonry, a relatively thorough study of one particular LECA masonry quality may form an important basis for further studies of other qualities. The last was of importance of this study.

The selected LECA masonry qualities for samplings were made without rendering even though LECA masonry usually are made with. The render may somewhat influence the investigated material properties (i.e. stiffness and strength and ratio of creep and shrinkage). Such influence is, however, neglected in this study.

3.3 Uni-axial compressive loading

3.3.1 Introduction

In Norway, one has argued whether or not the general approaches given in Eurocode 6 for masonry under uni-axial compressive loading normal to the bed joint, is adequate for Norwegian LECA masonry (Hyrve and Madsø 1996). Both the approaches of modulus of elasticity and the value of ultimate compressive strain may not be very adequate for LECA masonry. By this thesis work the stress-strain relationship and modulus of elasticity and Poisson's ratio of LECA masonry are studied, see Section 3.3.3.

In the following, the stress-strain relationship, modulus of elasticity and Poisson's ratio from some design standards are given. The information is given for comparison with the obtained behaviour of LECA masonry. For comparison with other design standards, see CEB-FIP Bulletin 4.

3.3.2 Approaches for structural design given by some design standards

Stress-strain relationship

For construction materials, different idealisations of the stress-strain diagrams are made. According to Eibl et al. (1995:C5.2.5), the two idealised stress-strain diagrams included in the European Pre-standard for design of concrete structures, Eurocode 2, (parabolic-rectangular and bi-linear) are preferred for cross-section design (see Figure 3.2). Similar diagrams are available for masonry according to the European Pre-standard for design of masonry structures, Eurocode 6.

For non-linear or plastic analysis and for the calculation of second order effects, a more detailed stress-strain diagram for short-term loading may according to Eurocode 2 be applied, see Figure 3.3.

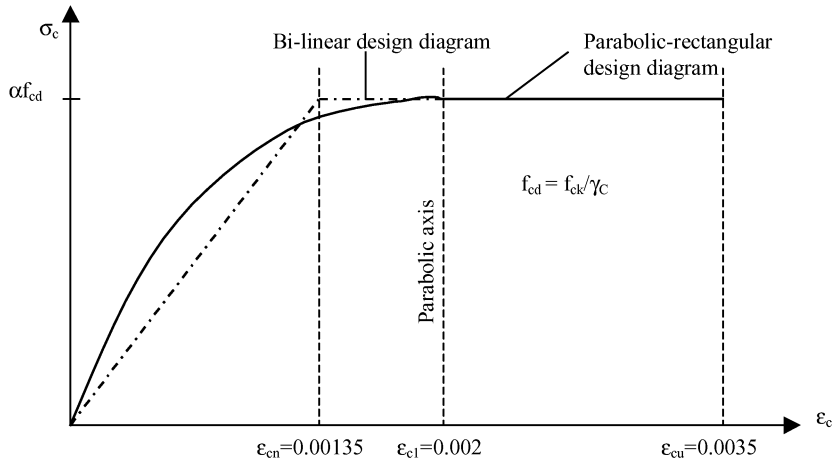

Figure 3.2:
Design stress-strain diagram for concrete in compression. Cross-section design (Eurocode 2, Beeby and Narayanan 1995).

For concrete, the bi-linear stress-strain relationship is defined in Eurocode 2 by the strain values 0.00135 and 0.0035 at design strength and ultimate strain levels respectively. The parabolic stress-strain relationship may be expressed by Equation 3.1 and the ultimate strain 0.0035 (Beeby and Narayanan 1995):

$$\sigma_c = 1000\varepsilon_c(250\varepsilon_c + 1)\alpha f_{cd} \qquad \varepsilon_c \le \varepsilon_{c1} = 0.002 \qquad \text{Equation 3.1}$$

where σ_c is the compressive stress,
f_{cd} is the design value of the compressive strength,
α is a reduction factor, which may generally be assumed to be 0.80 for LAC (prEN 1520:1999).

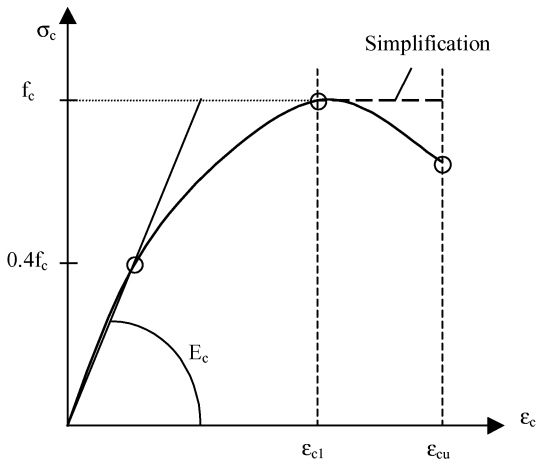

Figure 3.3:
Schematic stress-strain diagram for concrete in compression (Eurocode 2, Beeby and Narayanan 1995).

The schematic stress-strain relationship of Eurocode 2, see Figure 3.3, may be expressed by Equation 3.2 (Beeby and Narayanan 1995):

$$\sigma_c = \frac{f_c(kn - n^2)}{[1 + (k-2)n]} \qquad \text{Equation 3.2}$$

where σ_c is the compressive stress,
f_c is the compressive strength,
n $= \dfrac{\varepsilon_c}{\varepsilon_{c1}}$, both values taken as negative,
ε_{c1} = -0.0022 (strain at peak compressive stress),
k $= 1.1 \cdot E_c \cdot \dfrac{\varepsilon_{c1}}{f_c}$
E_c is the secant modulus of elasticity.

An idealised stress-strain diagram for lightweight aggregate concrete with open structure (LAC) for cross-sectional design is given in the Draft European Standard for prefabricated reinforced components of LAC, prEN 1520:1999, as bi-linear diagram only, see Figure 3.4. The stress-strain relationship is given by the strain 0.002 at design strength level and an estimated ultimate compressive strain. The ultimate compressive strain is calculated from the dry density of the LAC by Equation 3.3:

$$\varepsilon_{cu} = 0.0035 \cdot \eta_1 \qquad \geq 0.002 \qquad \text{Equation 3.3}$$

where ε_{cu} is the ultimate compressive strain, ≤ 0.0035,

η_1 $= 0.40 + 0.60 \cdot \left(\frac{\rho}{2200} \right)$,

ρ is the dry density.

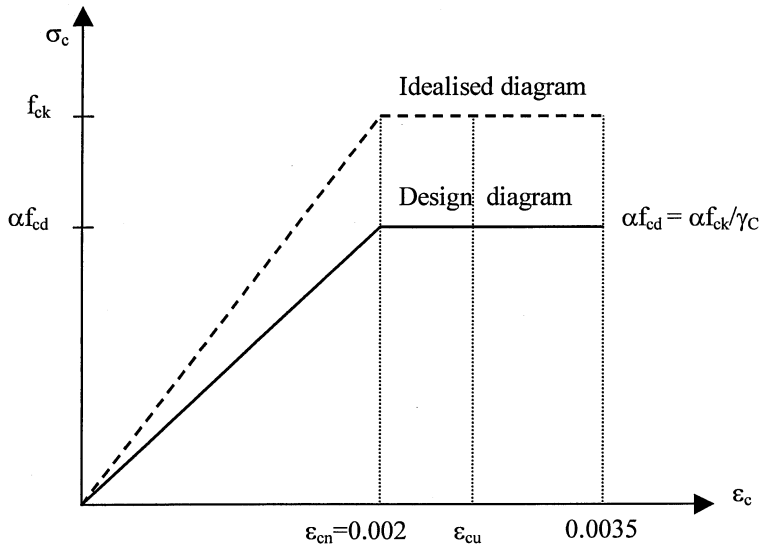

Figure 3.4:
Bi-linear stress-strain diagram for LAC in compression for cross-section design (prEN 1520:1999).

For masonry according to Eurocode 6, the stress-strain relationship may be taken as parabolic-rectangular for the design of masonry in bending and compression. Strain at design strength, ε_{c1}, and ultimate compressive strain, ε_{cu}, is given to 0.002 and 0.0035 respectively. The similarity with Eurocode 2 is obvious. However, no general equation is given for the parabolic-rectangular stress-strain diagram in Eurocode 6. A parabolic-rectangular stress-strain diagram for masonry may be expressed according to the Norwegian Bransjenorm by Equation 3.4:

$$\sigma_c = \frac{\varepsilon_c}{\varepsilon_{c1}}\left[1.1\frac{\varepsilon_{c1}}{\varepsilon_{cn}} - \left(1.1\frac{\varepsilon_{c1}}{\varepsilon_{cn}} - 1\right)\frac{\varepsilon_c}{\varepsilon_{c1}}\right] f_{ck} \qquad \text{Equation 3.4}$$

where σ_c is the compressive stress,
f_{ck} is the characteristic value of the compressive strength,
ε_c is the compressive strain,
ε_{c1} is the strain at the ultimate compressive stress,
ε_{cn} is the ultimate compressive strain.

Finally, it should be noted that no idealised stress-strain relationship at all is given in the Norwegian Standard for design of masonry structures, NS 3475.

Modulus of elasticity

For concrete, the secant modulus of elasticity is commonly determined at 40 % of the compressive strength (Beeby and Narayanan 1995), while the secant modulus for masonry is determined at one third of the maximum load (Eurocode 6). The modulus of elasticity obtained from testing may be stated as mean vales.

Under service conditions, and for use in structural analysis, the secant modulus of elasticity of masonry may accord Eurocode 6 be estimated by Equation 3.5:.

$$E = 1000 \cdot f_k \qquad \text{Equation 3.5}$$

where E is the short term secant modulus of elasticity,
f_k is the characteristic compressive strength of masonry.

Similarly, according to prEN 1520:1999 the modulus of elasticity for LAC can be estimated by Equation 3.6:

$$E_{cm} = 10000 f_{ck}^{1/3} \cdot \eta_2 \qquad \text{Equation 3.6}$$

where E_{cm} is the mean value of the initial modulus of elasticity,
f_{ck} is the characteristic value of the compressive strength,
η_2 $= 0.64 \cdot (\rho/2\,200)$ for $\rho \leq 1\,400$ kg/m³,
ρ is the dry density.

Poisson's ratio

The Poisson's ratio is constant during the linear elastic behaviour of concrete. For concrete design purposes, according to Eurocode 2 and prEN 1520:1999, Poisson's ratio for elastic strain may be taken as 0.2. If cracking is permitted for concrete in tension, the ratio may be taken as 0.

The masonry design standards Eurocode 6 and NS 3475 do not include any value for the Poisson's ratio.

3.3.3 Measured behaviour from compressive tests of LECA masonry

Testing

Determination of the compressive strength of masonry was carried out according to prEN 1052-1:1995 (given by Eurocode 6). According to Crook (1987), tests carried out on small specimens like in prEN 1052-1:1995 provide an accurate reproduction of the behaviour of a real wall.

The specimens were joined together with a cement mortar, C 1:4. Figure 3.5 gives a drawing of the specimen. The 28 days' flexural and compressive strength for the mortar according to prEN 1015-11:1995 were 4.3 N/mm² and 16.8 N/mm² respectively. The specimens were covered by plastic during the first three days after construction, after which they were left uncovered in laboratory environment. The specimens were tested at 28 days.

The test program applied centric loading of the specimen according to prEN 1052-1:1995 as well as eccentric loading over the width (e=t/6) at top and bottom. See right hand side of Figure 3.5 for eccentric loading of specimens. The load was increased steadily so that failure was reached after 15 to 30 minutes from the commencement of loading.

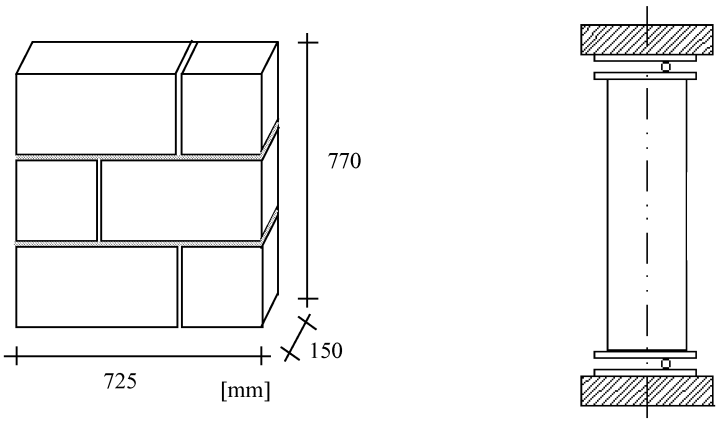

Figure 3.5:
Left: Specimen of LECA masonry for compressive testing. Right: Principle for eccentric application of load.

To obtain the stress-strain relationship, displacement measurements were carried out frequently during the compressive-strength test. By using a special measurement device based on strain gauges, see Figure 3.6, it was possible to measure five parallel displacements spaced approximately 20 mm apart perpendicular to the gauge length. The device contained two rows with equal "claws" located above each other. Consequently, 10 separate displacement measurements were obtained with the same device. Gauge length of each measurement was 135 mm and the resolution of the measurement was 1 μm. (The device is described in detail by Johnsen and Solberg (1991).)

The test program contained displacement measurements taken on the face and on the width of the specimen. By placing the measurement device on the width of the specimens, bending of the specimens was measured during the eccentric loading. Hence, it was possible to obtain an ultimate compressive strain.

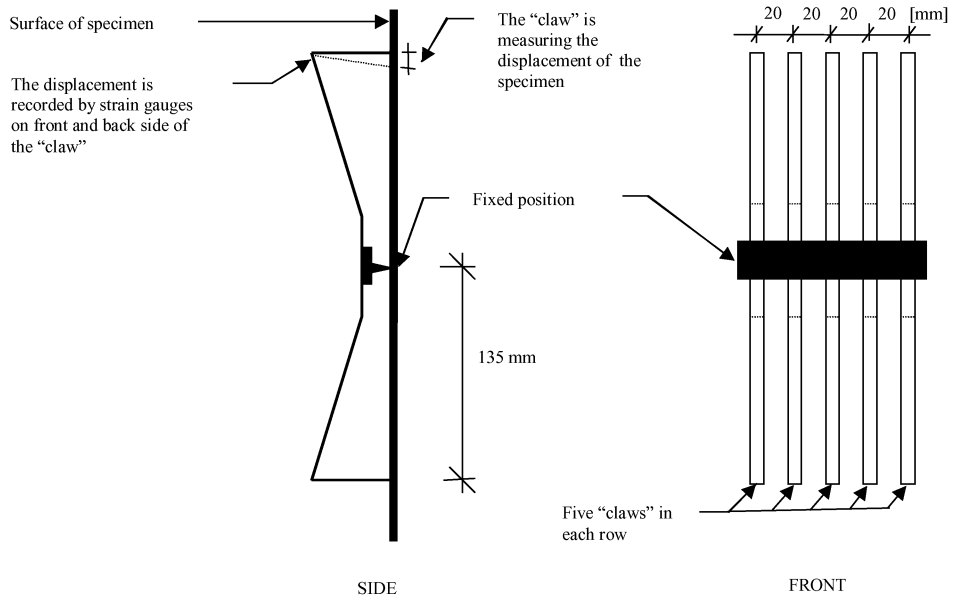

Figure 3.6:
Principal sketch of the device for displacement measurements.

Obtained stress-strain relationship is given in Figure 3.7. Each line represents one test. A summary of mean values is given in Table 3.4. According to prEN 1052-1:1995, the modulus of elasticity is calculated as a secant modulus from the strain and stress equal to one third of the maximum stress achieved. For results in detail, see Olsen (1997).

Table 3.4:
Mean values from uni-axial compressive test of LECA masonry. Coefficient of variation is given parenthetically.

Compressive strength [N/mm²]	Modulus of elasticity [N/mm²]	Compressive strain [mm/m]		
		ε_{cn}	ε_{c1}, e=0	ε_{c1}, e=t/6
2.7 (10 %)	4100 (10 %)	0.66 (10 %)	0.92 (10 %)	1.8 (-)

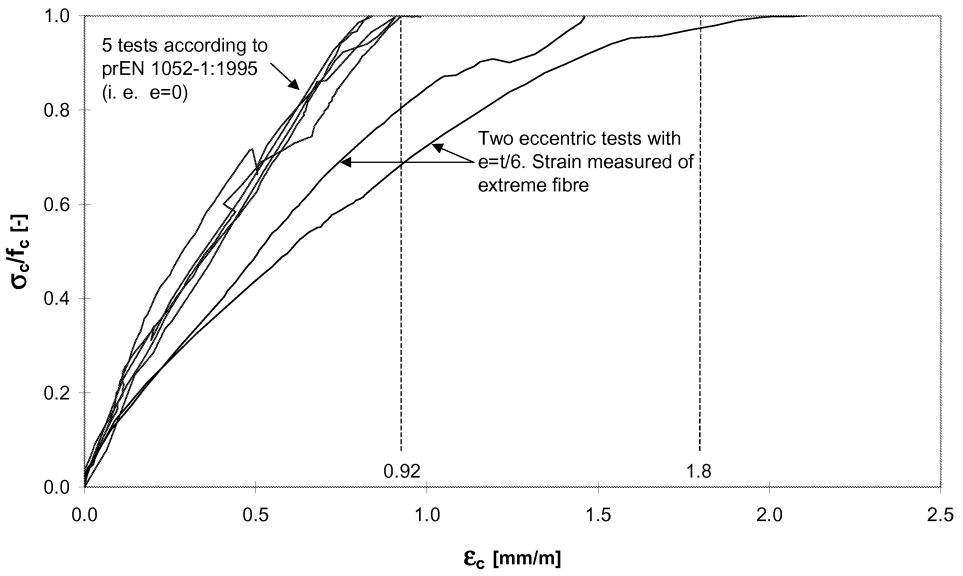

Figure 3.7:
Stress-strain relationship obtained during uni-axial compressive strength test.

Stress-strain relationship

By defining ε_{c1} obtained from the eccentric tests as the ultimate compressive strain, ε_{cu}, it is possible to make an idealised bi-linear diagram for LECA masonry. The idealised bi-linear diagram obtained by testing is compared in Figure 3.8 with the idealised stress-strain diagrams given by Eurocode 2 and prEN 1520:1999. The parabolic-rectangular idealisation of Eurocode 2 is similar the idealisation given by Eurocode 6. None of the diagrams match very well with the obtained results for LECA masonry. ε_{cn}, ε_{c1} and ε_{cu} are given in Eurocode 2 and Eurocode 6 as fixed values independent of type of material. According to Figure 3.8 the strain values seems to be too high for LECA masonry.

Only prEN 1520:1999 takes into account the influence of the concrete density on the ultimate strain.

While this thesis work only contains a limited number of tests, there are some uncertain factors concerning the magnitude of the compressive strains. However, even the obtained compressive strains are less than for normalweight concrete, they are of a magnitude that is reported by Olsen (1998), Stemland and Thorenfeldt (1998) and Johansen (2000). A comparison of the reported results carried out on LECA masonry or LAC made with LECA is enclosed in Table 3.5. It should, however, be noted that the values might not be directly comparable because the values are obtained according to different test methods. E.g. for concrete, the ultimate strain ε_{cu} is normally determined by a four point bending test of beams (or floors) like by Stemland and Thorenfeldt (1998). In this thesis work the ultimate strain is, however, determined by eccentric testing in compression. Due to the tensile reinforcement of the concrete beams, it may be possible to determine higher values of the ultimate compressive strain by testing of such beams. Assuming that the approach of prEN 1520:1999 concerning

ultimate compressive strain (see Equation 3.3) is satisfying also for structural design of LECA masonry, an ultimate strain of 2.1 may be calculated for LECA masonry quality "3/770".

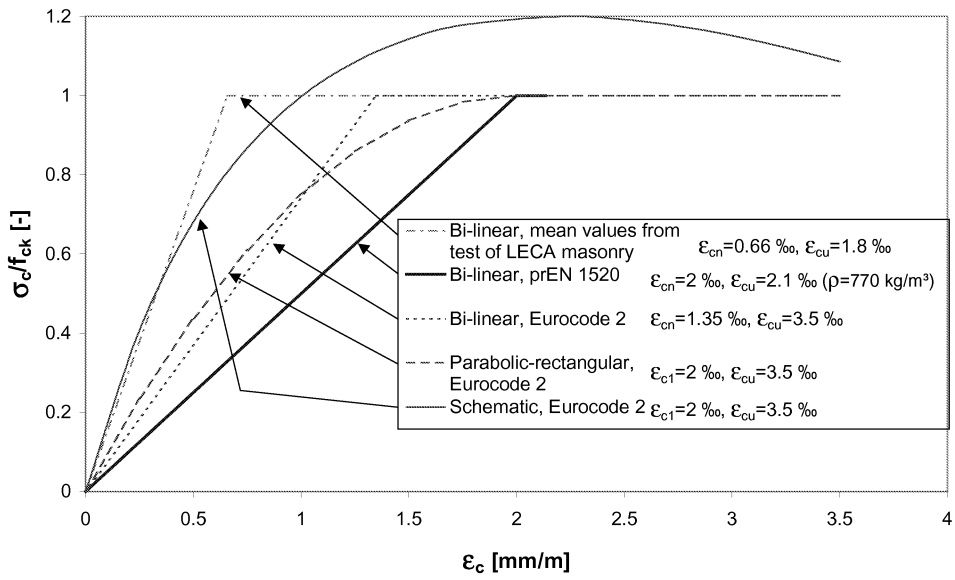

Figure 3.8:
Stress-strain diagrams for design purpose.

Table 3.5:
Comparison of compressive strains obtained on LECA masonry or LAC.

Quality	Reported by	Compressive strain [mm/m]			
		ε_{cn}	ε_{c1}	ε_{cu}	ε_{cu} obtained from
"2/600" LAC	Johansen (2000)	-	0.83	-	
"2/770" masonry	Olsen (1998)	0.66	0.92	1.8	e=t/6
"3/770" masonry	Present thesis work	0.66	0.92	1.8	e=t/6
"3/800" LAC	Stemland and Thorenfeldt (1998)	~1.15	1.25	< 3.5	4 point bending test of floors
"8/1300" masonry	Olsen (1998)	1.00	1.6	3.0	e=t/6

In Figure 3.9, both a bi-linear and a parabolic-rectangular stress-strain diagram for structural design of LECA masonry are introduced. The idealised diagrams may match better for LECA masonry than the approach given in Eurocode 6. The idealisations are based on ε_{cn} and ε_{c1} obtained from the tests, while the ultimate strain, ε_{cu} is calculated from Equation 3.3. The parabolic idealisation is based on Equation 3.4. The diagram matches with the test results that also are enclosed in the diagram.

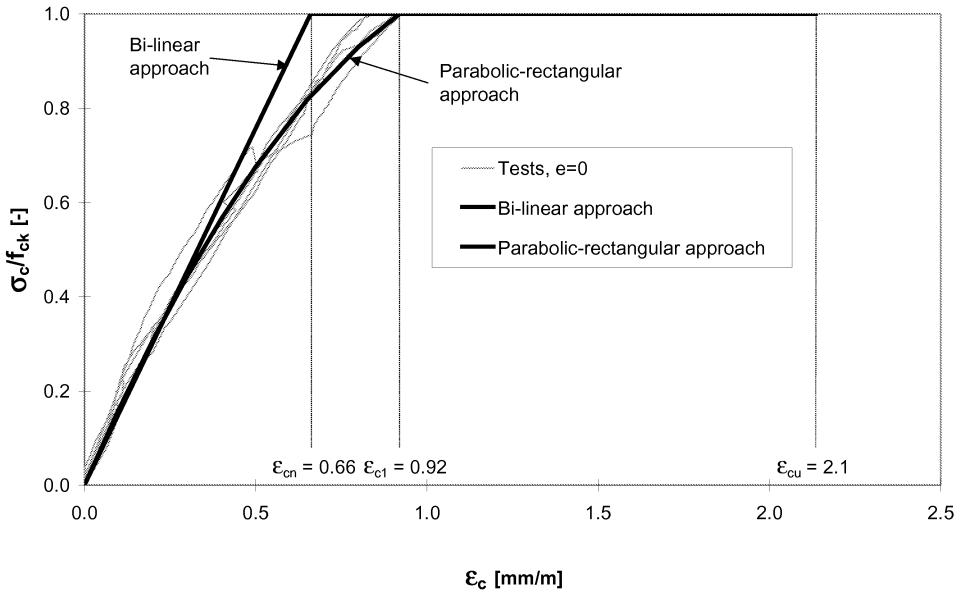

Figure 3.9:
Idealised stress-strain relationship for design of LECA masonry in bending and compression. Test results from Figure 3.7 are included.

Modulus of elasticity

Mean modulus of elasticity determined according to prEN 1052-1:1995 was 4100 N/mm². The value is higher than the short-term secant modulus of elasticity determined according to Equation 3.5 (Eurocode 6). Equation 3.5 is giving a modulus of elasticity of 2300 N/mm², see Table 3.6. The equation is, however, general for masonry and does not cover LECA masonry specifically. While the modulus of LWAC depends on the density of the aggregate (Eibl et al. 1995:A6.4.2), an estimate of the modulus of elasticity of LECA masonry may take the density into account. prEN 1520:1999 does that for LAC, see Equation 3.6. Because the characteristic strength of Equation 3.6 may be derived from the strength of cores with a length equal to the diameter, or cubes, the strength may not be comparable with the strength determined according to prEN 1052-1:1995. Consequently, the present measured strength of LECA masonry might not be used directly within Equation 3.6. While the compressive strength of Equation 3.6 is derived from specimens with a preferred diameter or edge length of 100 mm (NS-EN 1354), converting of the strength determined according to prEN 1052-1:1995 should be carried out. (Determination of strength according to the preferred size of NS-EN 1354 gives the normalised compressive strength.) The present measured strength may be converted to normalised compressive strength by a factor, δ, given in Eurocode 6 Table 3.2. By using the normalised values Equation 3.6 gives a modulus of elasticity of 3200 N/mm² for the present quality of LECA masonry, see Table 3.6. 3200 N/mm² match better with the measured value than the approach of Eurocode 6.

The modulus of elasticity determined according to prEN 1052-1:1995 in this thesis is somewhat higher than the magnitude that is reported by Olsen (1998), Stemland and

Thorenfeldt (1998) and Johansen (2000). A comparison of the reported results carried out on LECA masonry or LAC made with LECA is shown in Table 3.6. It should, however, be noted that the values might not be directly comparable because the values are obtained according to different test methods.

Table 3.6 shows also modulus of elasticity calculated according to Equation 3.5 and 3.6. The calculations are based on the characteristic value of the compressive strength. It should, however, be noted that the reported mean values of the compressive strength are based on different number of specimens. (Range: three to eight specimens.) Consequently, the characteristic strength are influenced by the number of specimens. According to Table 3.6, highest value of modulus of elasticity is calculated by Equation 3.6. The highest value seems to match the measured modulus of elasticity best.

Table 3.6:
Comparison of compressive strength and modulus of elasticity obtained on LECA masonry or LAC.

Quality	Reported by	Compressive strength [N/mm²]		Modulus of elasticity [N/mm²]			
				Measured	Calculated		Calculations based on
		f_c	f_{ck} [1)]		Eq. 3.5	Eq. 3.6	
"2/600" LAC	Johansen (2000)	2.2	1.8	2 700	1 800	2 300	ρ=650 kg/m³, δ=1.00
"2/770" masonry	Olsen (1998)	1.4	1.2	2 100	1 200	1 800	ρ=550 kg/m³, δ=1.15
"3/770" masonry	Present thesis work	2.7	2.3	4 100	2 300	3 200	ρ=800 kg/m³, δ=1.15
"3/770" masonry	- "-	2.3	1.9	2 500	1 900	3 000	ρ=730 kg/m³, δ=1.45
"3/800" LAC	Stemland and Thorenfeldt (1998)	2.9	2.6	3 000 [2)]	2 600	3 500	ρ=800 kg/m³, δ=1.45
"8/1300" masonry	Olsen (1998)	5.9	4.9	6 000	4 900	6 500	ρ=1250 kg/m³, δ=1.15

[1)] Characteristic strength calculated according to prEN 1052-1:1995 (masonry) and prEN 1520:1999 (LAC).
[2)] Determined from four point bending test.

Poisson's ratio

Measurements of vertical as well as horizontal displacements during the compressive testing according to prEN 1052-1:1995 indicate a Poisson's ratio for elastic strain of approximately 0.2. The result matches with the results of Kvande (2001-9), see Appendix 3.

3.3.4 Concluding remarks

Conclusions

The thesis work propose both a bi-linear and a parabolic-rectangular stress-strain diagram which may be better fitted for structural design of LECA masonry than the stress-strain data given in Eurocode 6.

Approach given in prEN 1520:1999, see Equation 3.6, seems to be better fitted for the modulus of elasticity of LECA masonry than the approach given in Eurocode 6, see Equation 3.5. For structural design of LECA masonry the difference between the approaches may not be that important. However, there is a difference between the estimated modulus of elasticity for LECA masonry and the value determined according to prEN 1052-1:1995. The latter should be used in structural analysis.

The ultimate compressive strain given in Eurocode 6 is too high for LECA masonry. The approach given in prEN 1520:1999 seems to be a better match for LECA masonry.

For design purpose Poisson's ratio for elastic strain may be taken as 0.2. If cracking is permitted in tension, the ratio may be taken as zero.

Recommendations for further work

More tests of different types of LECA masonry should be carried out to make a general equation for a better estimate of the ultimate compressive strain (idealised stress-strain relationship) and modulus of elasticity of LECA masonry. A general equation for estimating of ultimate compressive strain should include the density, while an equation concerning the modulus of elasticity should include both compressive strength and density.

3.4 Shrinkage

3.4.1 Introduction

Not much effort has previously been spent on studying the shrinkage behaviour of Norwegian LECA masonry, even though restrained shrinkage cracking of LECA masonry is reported to be a problem (Haugen 2000). In this thesis work, the magnitude of shrinkage as well as the time-dependent behaviour were investigated (Section 3.4.3). The influence of different curing condition on shrinkage and compressive strength of LECA blocks is described in Appendix 2. The shrinkage behaviour of small specimens of LECA masonry is reported in Appendix 3, while Appendix 8 is an investigation of the behaviour of LECA masonry under restrained shrinkage.

In the following, the final shrinkage value from some design standards is given. The information is provided for comparison with the presently measured shrinkage values of LECA masonry. For comparison with other design standards, see CEB-FIP Bulletin 4.

3.4.2 Final shrinkage given by some design standards

Final shrinkage values for structural design are given in different standards for both masonry and concrete. Table 3.7 shows design values provided by some European and Norwegian Standards. Values from European Pre-standard Eurocode 6 and the Norwegian Standard NS 3475 for design of masonry structures, the European Pre-standard Eurocode 2 and the Norwegian Standard NS 3473 for design of concrete structures and the Draft European Standard for prefabricated reinforced components of LAC, prEN 1520:1999 are included. A

more accurate calculation of shrinkage of concrete than included in Table 3.7 is possible in accordance to methods given in Eurocode 2 and NS 3473.

It should be noted that the design values in Table 3.7 are not directly comparable because not all standards cover LAC with density as low as 770 kg/m³. On closer examination of the standards collated in Table 3.7, variations were revealed in the manner of stipulation the final shrinkage. The concrete design standards Eurocode 2, prEN 1520:1999 and NS 3473 distinguish between a dry (inside) and a humid (outside) climate. However, the standards define the humidity of the two typical locations differently. According to Eurocode 2 and prEN 1520:1999, 50 % RH is typical for indoor locations, while 80 % RH is typical for outdoor locations. NS 3473 defines the humidity of these two locations to 40 and 70 % RH, respectively. However, according to Pihlajavaara (1982) the difference between 50 and 40 % RH may not be significant because the equilibrium moisture content of concrete is for practical purposes constant within 10-50 % RH range.

The concrete design standards of Table 3.7 also take both the dimension of the element (notional size, see Equation 2.1) and the composition of the concrete into account. Nevertheless, both masonry design standards, Eurocode 6 and NS 3475, treat masonry equally, irrespective of ambient climate, dimensions of the element and strength class of the LWA blocks. Eurocode 6 and NS 3475 distinguish between type of masonry units.

According to prEN 1520:1999 design values of final shrinkage for LAC are smaller than those of normalweight concrete (NWC).

Table 3.7:
Design values of the final shrinkage according to some selected design standards.

Design Standard		Location	Notional size	Shrinkage	
		[% RH]	[mm]	Design value [mm/m]	Range [mm/m]
Eurocode 6	(LWA masonry)	-	-	-0.4	-1.0 to -0.2
NS 3475	(LWA masonry)	-	-	-	-0.25 to -0.15
Eurocode 2 [1)]	(NWC)	50	≤ 150	-0.60	-
			600	-0.50	-
		80	≤ 150	-0.33	-
			600	-0.28	-
prEN 1520:1999 [2)]	(LAC)	50	≤ 150	-1.20	-
			600	-1.00	-
		80	≤ 150	-0.66	-
			600	-0.56	-
NS 3473 [3)]	(NWC/LWAC)	40	≤ 150	-0.51	-
			150 – 600	-0.42	-
		70	≤ 150	-0.36	-
			150 – 600	-0.30	-

1) Does not cover LAC separately. Values for NWC with slump class S1 and S2 and ambient temperature between –20 °C and 40 °C.
2) Design values from Eurocode 2 adjusted to take into account strength class LAC 2.
3) Does not cover LAC separately. Values for NWC with strength class C35 and initial water content between 155 and 175 l/m³.

3.4.3 Measured shrinkage behaviour of LECA masonry

Test set-up

During this thesis work, several measurements of shrinkage of LECA blocks, small specimens of LECA masonry as well as of walls were carried out, see Conradi (1999), Kvande (2001-5) and Appendix 2, 3 and 8. The different specimens are illustrated in Figure 3.10 to 3.12. Numbering in the illustrations identify gauge locations for measurement of displacement. Shrinkage measurements of blocks were carried out at ambient humidities 30, 50 and 85 % RH, while the small specimens were exposed to 55 % RH. The walls were located indoor, exposed by seasonal variation of the indoor climate.

The measured shrinkage of the LECA blocks and the small specimens will in the following be given as means of three specimens.

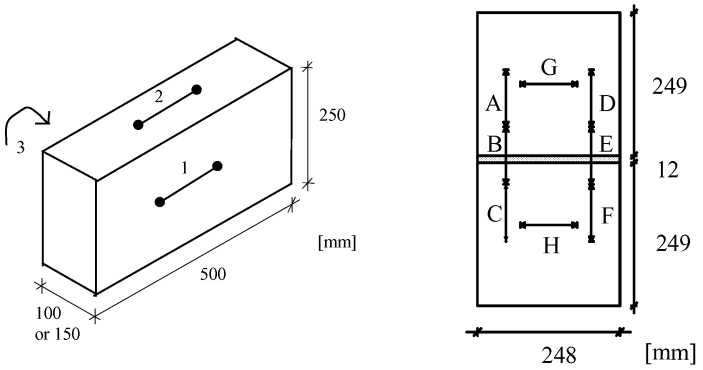

Figure 3.10:
LECA block and small specimen of LECA masonry. The numbering identifies the gauge locations for measurement of displacement.

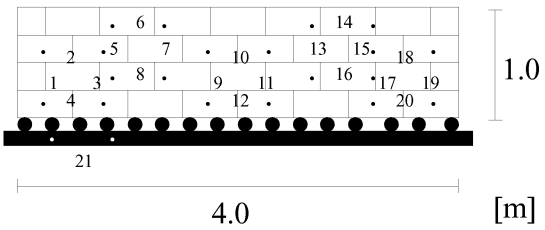

Figure 3.11:
LECA wall built on an "ideal" sliding layer made of steel rollers. The numbers identify the gauge locations.

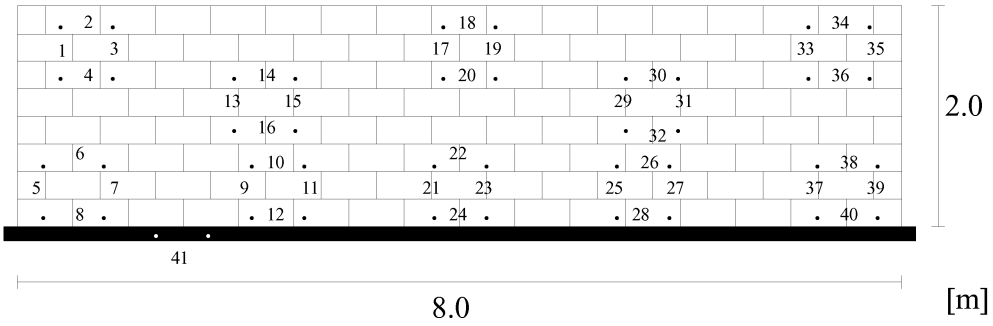

Figure 3.12:
LECA wall restrained to the foundation. The numbers identify the gauge locations.

Shrinkage behaviour of LECA masonry

An initial high moisture content (100 % RH) can be assumed due to the manufacturing process of LECA blocks. One distinctive characteristic of LECA blocks is the rapid loss of moisture when drying out. The rapid loss of weight, compared with normalweight concrete, is caused by the open structure of the concrete. However, the weight stabilises earlier than the shrinkage, see Appendix 2, 3 and 8. This can be explained from the different shrinkage mechanisms explained in Section 2.3.2 (i.e. capillary and chemical shrinkage).

In masonry, both constituents, LECA blocks and mortar, will shrink due to loss of water. The influence of the mortar joint on the shrinkage behaviour of the masonry is illustrated in Figure 3.13. The shrinkage behaviour is studied on specimens illustrated to the right in Figure 3.10. Figure 3.13 shows shrinkage development of block as well as of the mortar joint and masonry calculated from shrinkage measurement on masonry couplets, see Appendix 3. Normal height of a block (248 mm) and normal joint thickness (12 mm) are used in the calculations of shrinkage in masonry. Estimated final shrinkage is summarised in Table 3.8. The table is based on the assumption that 80 % shrinkage is finished after 100 days, see Appendix 3. Calculation of shrinkage of joint reveals a much larger shrinkage than measured on the LECA blocks. The difference can be explained by differences in initial moisture content and hydration of the mortar. However, it is shown in both Figure 3.13 and Table 3.8 that the contribution of the joint is insignificant to the shrinkage of the masonry. This is due to the fact that the mortar joints normally represent less than 5 volume-% of the LECA masonry. The obtained difference between vertical and horizontal shrinkage of blocks may be due to the shape of the specimen affecting the drying rate.

Table 3.8:
Estimated final shrinkage of masonry, block and mortar joint. The estimates are based on assumption that 80 % shrinkage is finished after 100 days. Initial moisture content of the specimens was 6.1 weight-%.

	Final shrinkage [mm/m]
Masonry	-0.52
LECA block, vertical	-0.50
LECA block, horizontal	-0.60
Mortar joint	-1.74

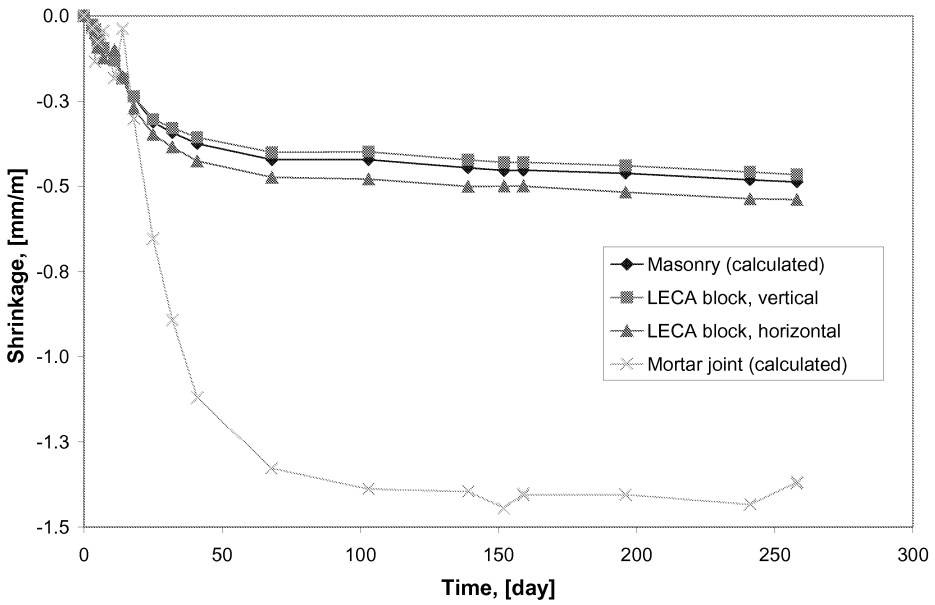

Figure 3.13:
Developments of shrinkage in masonry, block and mortar joint. Ambient climate 20 °C and 55 % RH. Initial moisture content of the specimens was 6.1 weight-%. (Kvande 2001-9)

The dimensions of the specimens were expected to influence the development of shrinkage. In the recommendation reported by Schubert (1994), the side surfaces and the bottom and top surfaces of the specimens were given a water-vapour-proof seal, see Appendix 3. Silicone was used in order to simulate the normal evaporation process for walls as closely as possible. However, shrinkage measurements on blocks without any sealing did not differ significantly from the shrinkage behaviour of the walls reported in Appendix 8. Consequently, sealing according to Schubert (1994) may not be important for the determination of shrinkage of LECA masonry. The insignificant effect of the sealing may mainly be caused by the open structure of the LECA blocks. The open structure may also influence the effect of the thickness of the masonry. Compared with normalweight concrete, the shrinkage behaviour may not be that sensitive to wall thickness. According to Hansen and Mattock (1966), the final shrinkage is independent of the dimension of the element. Consequently, design values for final shrinkage of LECA masonry should be given independently of notional size.

Waldum et al. (1993a), Waldum (1998), Stemland and Thorenfeldt (1998) and Johansen (2000) report shrinkage measurements determined on LECA blocks or LAC made with LECA. Unfortunately, the measurements were carried out with different initial moisture contents. Consequently, it is difficult to compare the magnitude of the shrinkage directly. However, it may be concluded that the final shrinkage is significantly influenced by the ambient humidity even though Eurocode 6 and NS 3475 do not take that into account.

Design values of the final shrinkage of LECA masonry

Moisture content of LECA blocks on leaving the production line is about 10-15 weight-%. Even though the blocks are stored at the factory for about four weeks before transportation to the building site, the moisture content of the LECA blocks is not significantly reduced during

the storage. The insignificant reduction of moisture content is due to a plastic covering during storage and transportation, see Appendix 1 and 2.

According to the experiences of this thesis work, shrinkage of LECA masonry may be derived from tests of single untreated LECA blocks, see Appendix 8. To obtain design values for final shrinkage of LECA masonry, initial moisture content equivalent the moisture content of blocks leaving the production line should be used. Shrinkage measurements similar to Appendix 2 with initial moisture content of 11 weight-% were carried out in order to obtain design values for final shrinkage. The specimens were dried out to ambient humidity levels of 30, 50 or 85 % RH. The shrinkage behaviour is presented in Figure 3.14. The last shrinkage measurements were carried out 450 days after the beginning, while the estimate of final shrinkage are based on the shape of the obtained shrinkage-stress diagram until 450 days and similar diagrams reported for concrete and LWA masonry (Müller and Hilsdorf 1990, Schubert 1992).

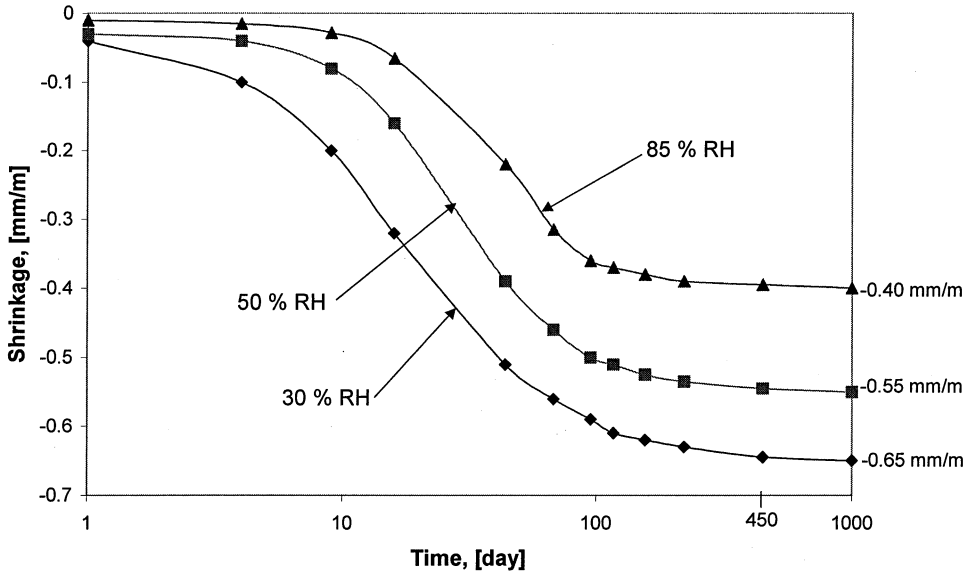

Figure 3.14:
Development of shrinkage and estimated final shrinkage for LECA masonry quality "3/770", block thickness 150 mm and initial moisture content of 11 weight-%. (Last measurements after 450 days.)

According to Figure 3.14, final shrinkage values may be -0.40 mm/m at 85 % RH, -0.55 mm/m at 50 % RH and -0.65 mm/m at 30 % RH. (Moisture contents at equilibrium were 4.4, 1.8 and 0.9 weight-% respectively.) Consequently, the design value of Eurocode 6, see Table 3.7, suit only outdoor conditions in humid climates. The design value is too high. Neither do the design values of prEN 1520:1999 match very well. prEN 1520:1999 gives too low values for both dry and humid climate.

Geving (1998) measured moisture contents of loose LECA (i.e. only the aggregate) during desorption to less than 0.5 weight-% at 94 % RH and less than 0.2 weight-% at 74.5 % RH. Assuming that the aggregate does not behave differently due to the presence of cement paste, the results of Geving (1998) indicate that most of the moisture content in LECA blocks at equilibrium may be absorbed by the cement paste, see Figure 3.14.

It should be noted that the final shrinkage values given in Figure 3.14 may be worst case values. Due to that, the values may be taken as design values for the final shrinkage of LECA masonry. By providing better opportunity for the LECA blocks to dry out before they are applied in the masonry, the final shrinkage of the masonry will be reduced. For example, removing of the plastic covering from the pallets of LECA blocks when they arrive the building site, may contribute to reducing the final shrinkage.

3.4.4 Concluding remarks

Conclusions

Due to the experimental work of this thesis, it is found that determination of shrinkage of LECA masonry may be derived from tests of single untreated LECA blocks.

While the shrinkage behaviour of LECA masonry may not be that sensitive to wall thickness, the design values of the final shrinkage may be given independently of notional size.

The final shrinkage of LECA masonry is significant influenced by the ambient humidity. On the basis of this thesis work, design values for the final shrinkage of LECA masonry may be introduced for three levels of ambient humidity. Design values -0.40, -0.55 and -0.65 mm/m were given for ambient humidity of 85, 50 and 30 % RH respectively. The values are significantly lower than the design value of Eurocode 6.

Recommendations for further work

Only one quality of LECA masonry is studied in this thesis. Final shrinkage values of other qualities may be determined to be able to establish formulas concerning final shrinkage for all types of LECA masonry.

A study identifying different preventive actions to limit the moisture content of LECA blocks before making the masonry should be carried out. Both actions on building site and during manufacturing and storage should be included.

3.5 Creep

3.5.1 Introduction

The creep behaviour of Norwegian LECA masonry has not previously been studied. Traditionally, the creep behaviour of masonry is not taken into account when designing masonry structures in Norway. Caused by compressive loading normal to the bed joint, compressive creep normally appears vertically in a masonry wall. Caused by restrained shrinkage, tensile stress and hence tensile creep may appear in the longitudinal direction of

the wall. Due to the fact that Norwegian LECA masonry is normally made without mortar in the perpend joints, a complicated stress and creep distribution may exists in restrained walls.

In this thesis work, the magnitude of creep and the time-dependent behaviour were investigated, see Section 3.5.3 and Appendix 3 and 4. Creep due to compressive loading normal to the bed joint as well as tensile loading in the longitudinal direction of LECA masonry were studied.

It should be noted that in these tests the total time-dependent deformation due to loading, excluding only the apparent free shrinkage, is assumed attributed to creep (Schubert 1994), see Section 2.3.3.

In the following, the final creep coefficients from some design standards are given. The information is given for comparison with the measured behaviour of LECA masonry. For comparison with other design standards, see CEB-FIP Bulletin 4.

3.5.2 Final creep coefficient given by some design standards

Design values of creep are usually given as final creep coefficients, see Equation 2.2. In Table 3.9 final creep coefficients given by some European and Norwegian Standards are collated. Included in the table are the European Pre-standard Eurocode 6 and the Norwegian Standard NS 3475 for design of masonry structures, the European Pre-standard Eurocode 2 and the Norwegian Standard NS 3473 for design of concrete structures and the Draft European Standard for prefabricated reinforced components of LAC, prEN 1520:1999. A more accurate calculation of final creep coefficient of concrete than shown in Table 3.9 is possible in accordance with methods given in Eurocode 2 and in NS 3473.

It should be noted that the design values in Table 3.9 are not directly comparable because not all standards cover LAC with density as low as 770 kg/m³. On closer examination of the standards referred to in Table 3.9, variations were revealed in the manner of stipulating the final creep coefficient. When estimating the final creep coefficient of concrete Eurocode 2, prEN 1520:1999 and NS 3473 takes into account the:

- location of the construction (dry or humid),
- dimension of the element (notional size, see Equation 2.1 and Section 2.3.3),
- age at loading and
- composition of the concrete.

Eurocode 6 distinguish between type of masonry units, but does not take into account ambient humidity, dimension of the element, age at loading or strength class of the LWA blocks.

It is worth noting that the Norwegian Standard for design of masonry structures, NS 3475, does not cover creep at all.

None of the collated standards of Table 3.9 distinguish between creep in tension and in compression.

According to NS 3473 and prEN 1520:1999, the coefficient of creep of LAC is reduced compared with normalweight concrete (NWC).

Table 3.9:
Design values of the final creep coefficient according to some selected design standards.

Design Standard		Location	Notional size	Creep coefficient [-]				
				Age at loading, [day]				
		[% RH]	[mm]	1	7	28	90	365
Eurocode 6	(LWA masonry)	-	-	← 2.0 → with range 1.0 to 3.0				
NS 3475	(LWA masonry)	-	-	-				
Eurocode 2 [1)]	(NWC)	50	50	5.5	3.9	3.0	2.4	1.8
			150	4.6	3.1	2.5	2.0	1.5
			600	3.7	2.6	2.0	1.6	1.2
		80	50	3.6	2.6	1.9	1.5	1.2
			150	3.2	2.3	1.7	1.4	1.0
			600	2.9	2.0	1.5	1.2	1.0
prEN 1520:1999 [2)]	(LAC)	50	50	2.2	1.6	1.2	1.0	0.7
			150	1.9	1.3	1.0	0.8	0.6
			600	1.5	1.0	0.8	0.6	0.5
		80	50	1.5	1.0	0.8	0.6	0.4
			150	1.3	0.9	0.7	0.6	0.4
			600	1.2	0.8	0.6	0.5	0.4
NS 3473 [3)]	(LWAC)	40	50	1.1	0.8	0.6	0.5	0.4
			150	0.8	0.6	0.5	0.4	0.3
			600	0.7	0.6	0.5	0.4	0.3
		70	50	0.7	0.5	0.4	0.3	0.3
			150	0.6	0.4	0.3	0.3	0.2
			600	0.5	0.4	0.3	0.2	0.2

1) Does not cover LAC separately. Values for NWC with slump class S1 and S2 and ambient temperature between –20 °C and 40 °C.
2) Design values from Eurocode 2 adjusted to density 770 kg/m³ and strength class LAC 2.
3) Design values for NWC with strength class C35 adjusted to density 770 kg/m³. Ambient temperature below 35°C. N.B. the standard does not cover LWAC with strength class <15 N/mm².

3.5.3 Measured creep behaviour of LECA masonry

Test set-up

Specimens for measurement of compressive creep and tensile creep were made according to Figure 3.15. Measurements of displacement were carried out according to the gauge locations illustrated in the figure. To simulate a typical indoor situation, the experiments were carried out in a test chamber equipped with climate control at 20 ±2 °C and 55 ±5 % RH. The creep tests started one week after preparing the specimens, i.e. four weeks after manufacturing of the LECA blocks. The loads were applied in steps up to a compressive level of 1.05 N/mm² and a tensile level of 0.10 N/mm² when dealing with the gross area. In the case of the net area of the tensile specimen, the average stress equalled 0.19 N/mm² in the blocks on both sides of the open joint. The loads represented almost 50 % and 60 % of the compressive and tensile capacity of the specimen respectively. For further explanation of the experimental work in detail, see Appendix 3 and 4.

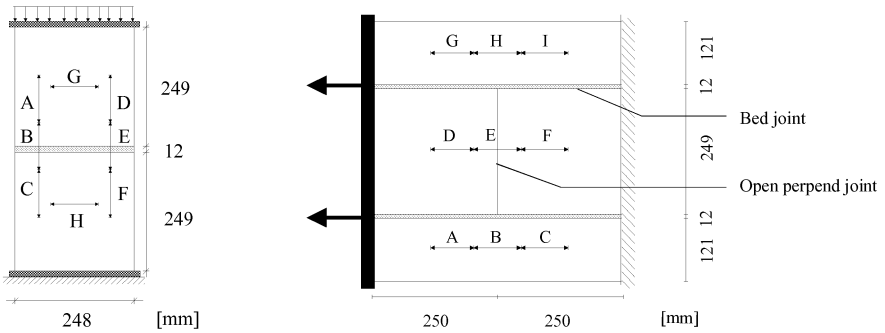

Figure 3.15:
Masonry specimens for measurement of creep due to compressive load and tensile load. Numbering with letters identify the gauge locations.

Compressive creep behaviour of LECA masonry

In a similar manner as for shrinkage, an illustration of the creep contribution made by the mortar and the blocks in the masonry have been obtained, see Figure 3.16 for mean results of three specimens. The figure shows creep coefficient development of joint and block as well as of the masonry. Normal height of a block (248 mm) and normal joint thickness (12 mm) were used in the calculations. As for shrinkage, the creep of the mortar joint is much larger than that of the block. Again the difference can be explained by differences in initial moisture content and hydration of the mortar. However, it is shown in Figure 3.16 that the contribution from the mortar joint is of no significance to the total creep of the masonry. This is due to the fact that the mortar, normally, represents less than 5 volume-% of the masonry.

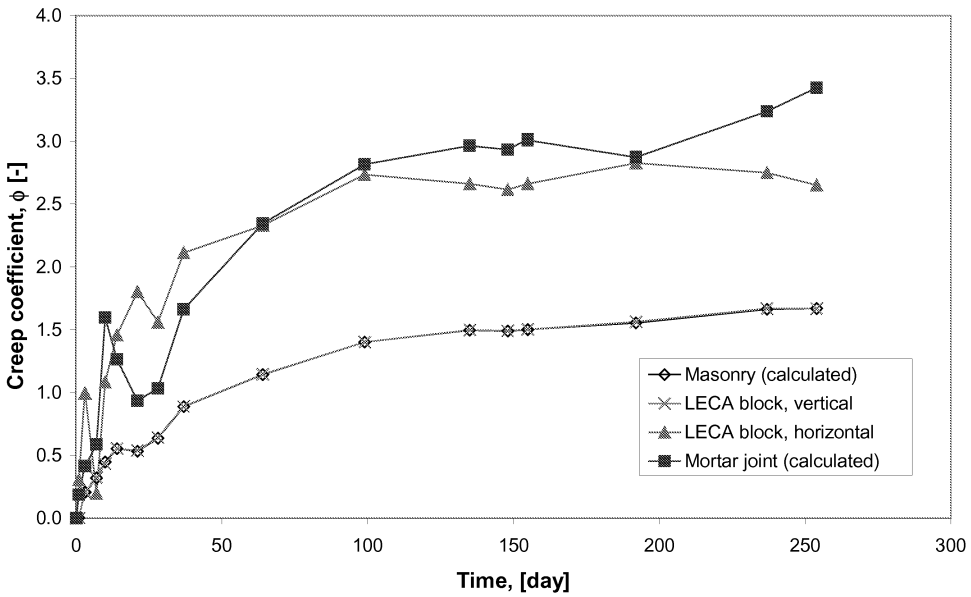

Figure 3.16:
Development of compressive creep coefficients in masonry, block and mortar joint (Kvande 2001-9).

Figure 3.16 indicates that in the tests the creep measurement was stopped a little too early for accurate establishment of the final creep coefficient. To estimate the final creep coefficient, calculations were based on prEN 1520:1999 and on an assumption of 70 % apparent creep after 150 days (Stemland and Thorenfeldt 1998). The estimates and final measurements are compared in Table 3.10. The 70 % assumption of Stemland and Thorenfeldt (1998) was based on small specimens of normal-weight concrete. Nevertheless, the final creep coefficients calculated from that assumption match better with the measurements than the values from prEN 1520:1999. The results show that the creep coefficient in prEN 1520:1999 is too low. Due to the shape of the creep coefficient/time-diagram (Figure 3.16), a creep coefficient for LECA masonry between 1.7 and 1.8 may be expected for the present situation.

Table 3.10:
Creep coefficient after 155 days and at the end of the test (254 days) compared with calculated final creep coefficient.

	Creep coefficient [-]			
	Measurements		Calculated value	
	155 days	254 days	Based on 70 % creep after 150 days	pEN 1520:1999
Masonry (calculated)	1.50	1.67	2.1	1.2
LECA block, vertical	1.50	1.67	2.1	1.2
LECA block, horizontal	2.66	2.65	3.8	1.2
Mortar joint (calculated)	3.01	3.43	4.3	-

Tensile creep behaviour of LECA masonry

Developments of tensile creep coefficients are presented in Figure 3.17. The mean values are obtained from two specimens only. Positions of measurements were grouped as shown in Table 3.11.

Table 3.11:
Elastic strain. Creep strain and creep coefficient at the end of the tensile creep test. Calculated stress based on measured elastic strain and a modulus of elasticity of 2900 N/mm².

Position of measurement [1]	Elastic strain [mm/m]	Creep strain [2] [mm/m]	Creep coefficient [2] [-]	Calculated stress [N/mm²]
D and F	0.01	0.01	0.6	0.03
A, C, G and I	0.05	0.10	2.5	0.15
B and H	0.06	0.23	7.8	0.17
E [3]	*0.18*	*1.26*	*8.0*	-

[1] See Figure 3.15, right.
[2] Mean values based on two specimen only.
[3] Because of the open joint it is incorrect to calculate strain in this area.

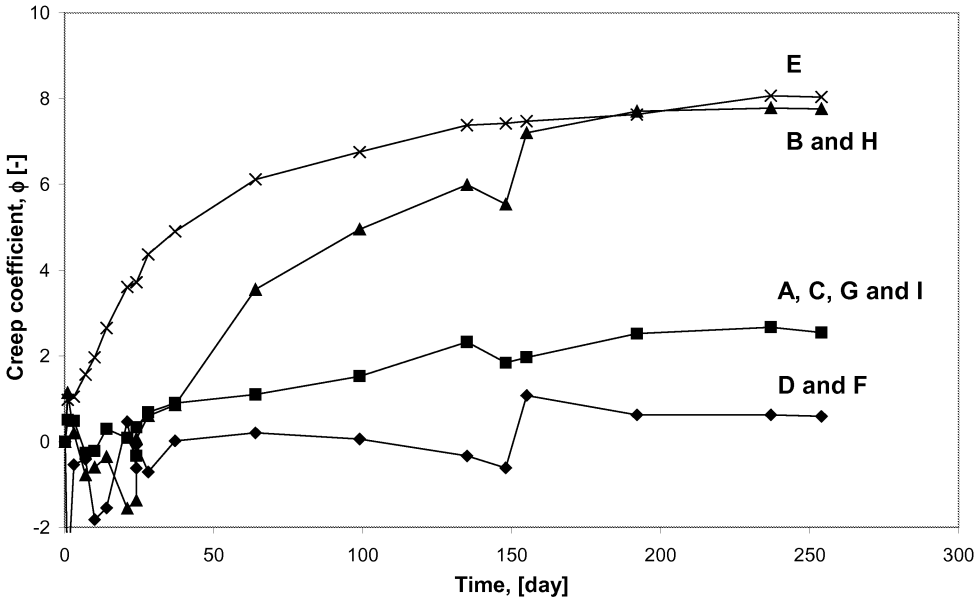

Figure 3.17:
Time-dependent tensile creep coefficients of masonry specimens of LECA concrete 3/770. Displacements are measured in accordance with Figure 3.15. Because of the open joint, it is incorrect to calculate creep coefficient in this area.

Compared to the average deformations of the blocks, a relatively large opening of the open perpend joint was measured. This is in agreement with the results of a linear-elastic analysis, as shown in Figure 3.18. Figure 3.19 illustrates the belonging distribution of the largest principal stress (tension), on both sides of the open perpend joint. The distribution shows that the external tension must be carried by a reverse arch mechanism across the open perpend joint, leaving the areas on both sides free of stress. This implies a stress concentration at both ends of the open perpend joint, which decrease towards a uniform distribution across the adjacent blocks in the extension of the joint. Accounting for creep would hence give a similar shape as in Figure 3.18.

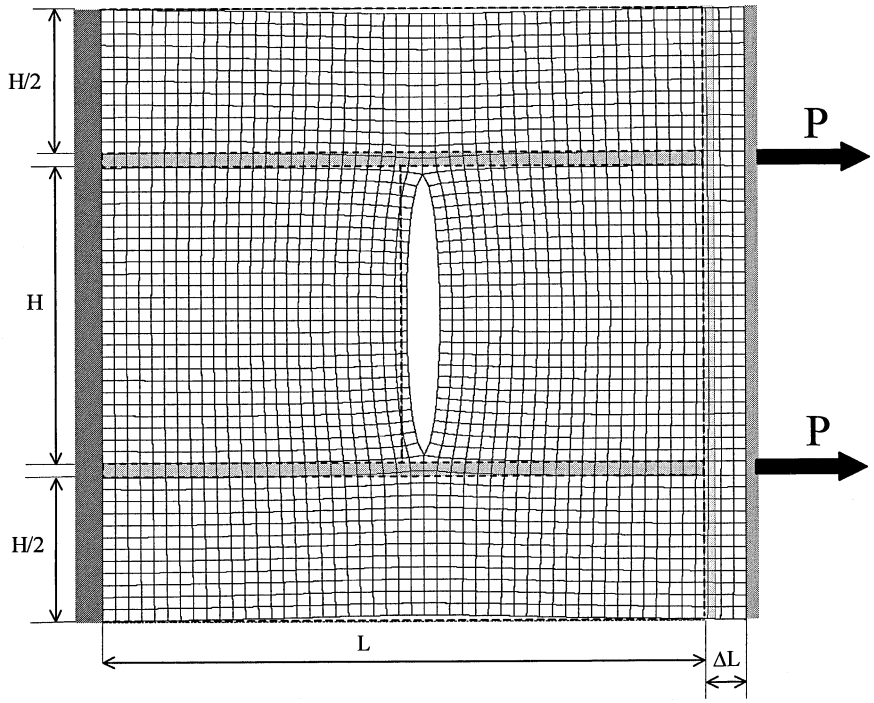

Figure 3.18:
Deformed specimen (Undeformed shape illustrated by dashed lines).

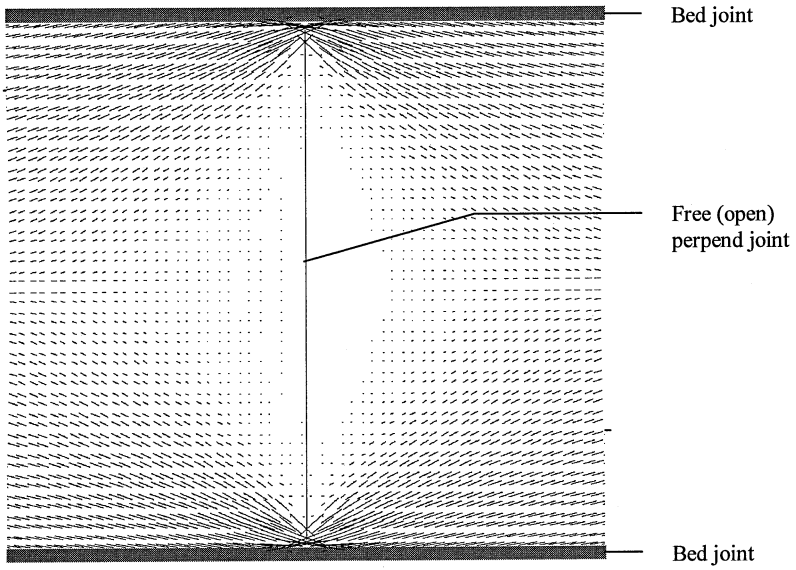

Figure 3.19:
Largest principal stress distribution on both sides of vertical open joint (tension).

Figure 3.17 shows that the test lasted long enough to estimate the final creep coefficient. Hence, the tensile creep coefficients in Table 3.11 can be considered as approximation of final creep coefficients. Experiences from long-time loading of concrete in compression indicate creep coefficients usually between 1.0 and 6.0, with 2.5 as the most typical value (Bažant 1982). The design value of Eurocode 6 is 2.0 with a range from 1.0 to 3.0. Table 3.11 indicates a final creep coefficient of 7.8 in the middle of the continuous blocks (B and H), while coefficients of 2.5 were recorded elsewhere in the continuous blocks (A, C, G and I). The last value match very well with the recommendation in Eurocode 6 and of Bažant (1982). The high creep coefficient at position B and H may be caused by the stress concentration in these parts of the specimen. A tensile load of about 60 % of the tensile strength was maintained during the creep test. Normally, the creep coefficient of concrete is approximately constant up to about 50 % of the compressive strength (Bažant 1982). Due to the equality of the creep coefficient in compression and tension and to the fact that concrete behaves in a linear elastic manner up to about 70 % of the tensile strength (Eibl et al. 1995:A6.2.2&A6.5.3.3), a much lower creep coefficient than 7.8 was expected in the highest stressed area. This is supported by lower creep coefficients obtained by Stemland and Thorenfeldt (1998) during compressive creep tests on low strength LECA concrete. These tests were carried out with stress equal 30, 50 and 70 % of the compressive strength (Stemland and Thorenfeldt 1998), indicating a much smaller creep coefficient than obtained during the investigation of tensile creep in this thesis.

3.5.4 Concluding remarks

Conclusions

In view of the studied creep behaviour of LECA masonry subjected to compression and tension, the creep coefficient design value of Eurocode 6 seems to be reasonable for structural design purposes. However, due to the open perpend joint in LECA masonry, there is a complicated stress distribution in such walls. The stress distribution around the open joint may make the assessment of stress reduction due to creep very complicated.

Recommendations for further work

Only one quality of LECA masonry was studied at one level of ambient humidity in this thesis work. Creep should be determined for other qualities under various levels of ambient humidity, loads and age at loading to establish formulas for the development of creep of LECA masonry.

Further investigations into tensile creep of masonry with open perpend joints should focused on the situation of an entire wall. Both experimental testing and numerical analyses should be applied to yield reliable design methods.

A complementary explanation should also be made for the high creep coefficient in the continuous blocks over and under the open perpend joint. It may be possible that the high measured creep coefficient is explainable by apparent and fictitious mechanisms, such as stress-induced shrinkage and cracking introduced in Section 2.3.3.

3.6 Temperature

3.6.1 Introduction

The coefficient of thermal expansion of concrete depends of the moisture content (Eibl et al. 1995:A6.8.1, Neville 1995:378). Consequently, the experimental determination of the coefficient becomes difficult because of unavoidable moisture movement in the concrete during tests. Internal moisture movement or moisture loss leads to shrinkage. Sealing of specimens and preparing for reduced internal moisture movement have to be carried out before determination of the thermal expansion.

The coefficient of thermal expansion in Leca 1.000 and in Svendsen et al. (1966) are given as $8 \cdot 10^{-6}$/K. However, the origin of this value is not known anymore. During this thesis work, a check of the design value was made. To control the influence of moisture within the material, coefficient of thermal expansion was obtained on LECA blocks with four different moisture contents. The work was first reported by Kvande (1997) and will be reproduced in Section 3.6.3.

In the following, the coefficients of thermal expansion from some design standards are given. The information is given for comparison with the obtained behaviour of LECA masonry. For comparison with other design standards, see CEB-FIP Bulletin 4.

3.6.2 Coefficient of thermal expansion given by some design standards

Coefficients of thermal expansion are given in different design standards for both masonry and concrete. Table 3.12 shows design values from some European and Norwegian Standards. Included in the table are the European Pre-standard Eurocode 6 and the Norwegian Standard NS 3475 for design of masonry structures, the European Pre-standard Eurocode 2 and the Norwegian Standard NS 3473 for design of concrete structures and the Draft European Standard for prefabricated reinforced components of LAC, prEN 1520:1999.

None of the collated design standards take into account different moisture content of the materials.

Table 3.12:
Coefficient of thermal expansion according to some selected standards.

Design Standard		Coefficient of thermal expansion [10^{-6}/K]	
		Design value	Range
Eurocode 6	(LWA masonry)	10	8 to 12
NS 3475	(LWA masonry)	8	-
Eurocode 2 [1)]	(NWC)	10	-
prEN 1520:1999	(LAC)	8	-
NS 3473 [1)]	(NWC/LWAC)	10	-

[1)] Does not cover LAC specifically.

3.6.3 Measured coefficient of thermal expansion for LECA blocks

Testing

Determination of coefficient of thermal expansion was carried out on specimens with dimensions 40 x 40 x 300 mm. The specimens were cut from 6 month old LECA blocks. The sawing was carried out without using water.

Gauge location pads were glued on two sides opposite each other to measure displacements during the test. While the specimens were initially dried to humidity equilibrium of 40 to 50 % RH, water was added to get four different moisture contents.

Totally, three specimens were prepared for each level of moisture content.

After addition of water the specimens were sealed by means of a special aluminium foil covered with polyethylene. Initial weight and length were recorded after the sealing. Recording of length was carried out with a Demec gauge (demountable mechanical gauge) with a gauge length of 250 ±1 mm. The measurements were carried out without breaking the seal. Before starting the test, the specimens were stored at 50 °C to ensure moisture migration. The storage lasted until the length was stabilised.

Determination of coefficient of thermal expansion is based on displacement caused by temperature change from 20 °C to 50 °C and back to 20 °C again. The storage at each temperature lasted until the length was stabilised. Weight of the specimens including the sealing was recorded after determination of the coefficient of thermal expansion. The weighing revealed that no moisture evaporated during the test.

Finally, the sealing was removed and the specimens were dried at 105 °C to find the real moisture content.

Coefficient of thermal expansion

Obtained coefficients of thermal expansion are given in Figure 3.20. The coefficients were calculated according to Equation 2.4. From the figure it is possible to see the effect of moisture content on the coefficient of thermal expansion. Lowest coefficient is recorded on the specimens with the highest and lowest moisture content. LECA blocks with 10.2 weight-% represents 100 % RH, while 1.6 weight-% represents a humidity equilibrium of 40 to 50 % RH. According to Eibl et al. (1995:A6.8.1), the coefficient of thermal expansion of hydrated cement paste depends primarily on the moisture content of the paste, and is about the same for very dry and for water-saturated paste (about $10 \cdot 10^{-6}$ 1/K), see Section 2.3.4. The cement paste reaches maximum values at 65-70 % RH. The high values, recorded on the specimens with the second and third highest moisture content, may be explained by varying moisture content of cement paste. Blocks with 4.8 and 5.6 weight-% represent, however, a moisture content higher than 70 % RH.

The coefficient of thermal expansion of LECA blocks is also influenced by the expansion coefficient of the aggregate. Normally, the thermal coefficient of water-saturated aggregate is lower than for dry aggregate. That level may match with the lowest recorded coefficient of the specimen with the highest moisture content.

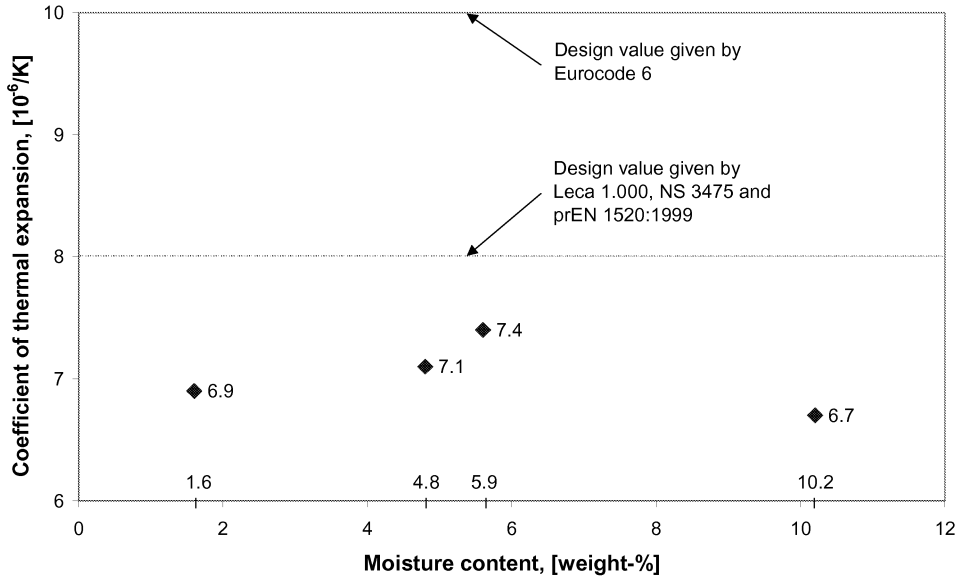

Figure 3.20:
Coefficient of thermal expansion dependent of moisture contents of LECA blocks.

No investigations of the thermal expansion of the mortar were carried out as a part of this thesis work. It is, however, assumed that the thermal expansion of the mortar is of the same magnitude as for concrete. Due to the fact that the mortar normally represents less than 5 volume-% of LECA masonry, the contribution of the mortar joint is insignificant to the thermal expansion of the masonry.

3.6.4 Concluding remarks

Conclusions

During the determination of coefficient of thermal expansion of LECA blocks, values between 6.7 and $7.4 \cdot 10^{-6}$/K depending on moisture content were recorded. Based on the fact that LECA blocks of only four different moisture contents were tested, a design value of $8 \cdot 10^{-6}$/K (Leca 1.000, NS 3475, prEN 1520:1999) seems reasonable for LECA masonry.

Recommendations for further work

It may be possible that the added water of the test (see Section 3.6.3) was not equally distributed in the specimen before starting of the test. This may be corrected by repeating the experimental work.

To get a more complete picture of the influence of moisture content on the coefficient of thermal expansion, an investigation with other moisture contents should be carried out. Such an investigation should comprise of for instance dry and water saturated specimens.

3.7 Behaviour during cracking

3.7.1 Introduction

Today, the availability of employing combined numerical and experimental research tools makes it possible to gain insight into the fundamental behaviour of masonry materials and structures. Establishing of more reliable rules for movement-joint design is one example of results that may be derived from numerical analysis. To be able to analyse e.g. restrained shrinkage cracking, for instance the cracking behaviour of the masonry has to be described. For LECA masonry, however, experimental data did not exist from which material/model parameters for cracking could be determined.

Cracking of masonry due to restrained movement may occur as a result of either tensile or shear failure, see Section 2.4. In this thesis work, the tensile behaviour of LECA blocks and joint, and shear behaviour of bed joints, were studied, see Appendix 5 and 7. The obtained behaviour may be applied for numerical modelling of the cracking behaviour of LECA masonry, see Section 3.7.3 and 3.7.4.

The obtained parameters are adapted to generic material models available in DIANA. The studies of Høiseth (1999, 2000a, 2000b) were carried out to demonstrate the capability of reproducing experimental observations by numerical simulations, see Appendix 6.

3.7.2 Basic theoretical background

Determination of the post-peak behaviour of masonry subjected particularly to tension, but also to shear as well as compression, is very difficult. Reaching the peak stress, the process zone is very unstable and a complete failure can only be avoided by gradually reducing the stress. Consequently, determination of the softening part of the stress-displacement relationship requires a very stiff testing arrangement and a very sensitive control of the test. Regarding the shear behaviour, present of normal stress influence the behaviour significantly. Consequently, sensitive control of the normal stress during the test is also very important to be able to determine reliable data, see Section 2.4.

During the last decade more effort has been made to determine the behaviour of masonry subjected to shear actions as well as tensile actions. A typical main goal has been to establish applicable parameters that are necessary in numerical analysis of failure behaviour. Gottfredsen (1997), Pluijm (1999) and Molnar (2000) are recent examples of works aiming to establish fundamental links between experimental works and numerical analysis. To be able to determine applicable parameters for brick and calcium silicate masonry, Van der Pluijm developed test arrangements for tensile as well as shear testing.

3.7.3 Shear and tensile testing

Deformation controlled uni-axial tensile tests were carried out on specimens made from LECA blocks as well as small masonry specimens including one bed joint. The size and shape of the specimens are illustrated in Figure 3.21.

The tensile test arrangement of Pluijm (1999) was applied for determination of the behaviour of LECA masonry due to uni-axial tension, see Appendix 5. Totally 25 successful tests of the block material and 9 successful tests of masonry specimens were carried out.

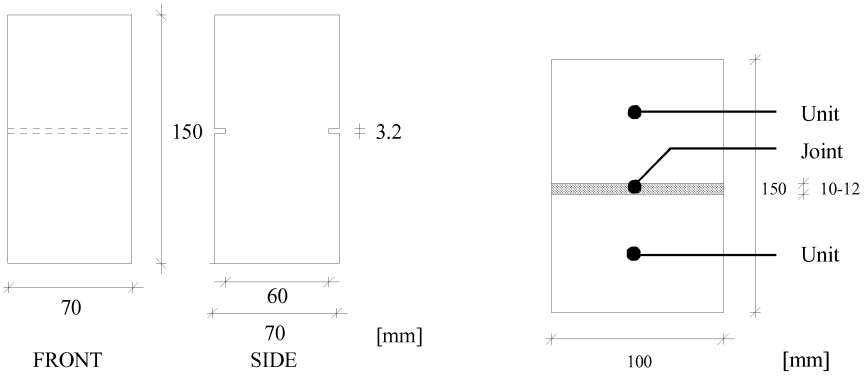

Figure 3.21:
Specimens for tensile test of LECA block material to the left and bed joint in LECA masonry to the right.

Deformation controlled shear compressive tests were carried out on LECA masonry specimens. Size and shape of the specimens are illustrated in Figure 3.22.
The shear test arrangement of Pluijm (1999) was applied for determination of the behaviour of bed joint in LECA masonry due to shear compression, see Appendix 7. In totale 37 specimens were tested.

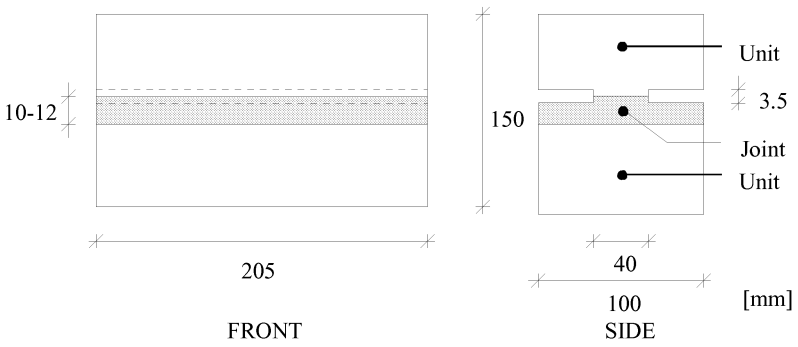

Figure 3.22:
Specimen for shear compressive test of bed joint in LECA masonry

3.7.4 Measured behaviour of tensile failure of LECA masonry

Obtained behaviour of LECA blocks during tensile tests are given in Figure 3.23 and that of joints in Figure 3.24. Both experimental and theoretical curves are included in the figures. The theoretical curve is based on the Hordijk formula given in Equation 2.5 and the obtained mean-values of tensile strength, modulus of elasticity and mode I fracture energy given in Table 3.13.

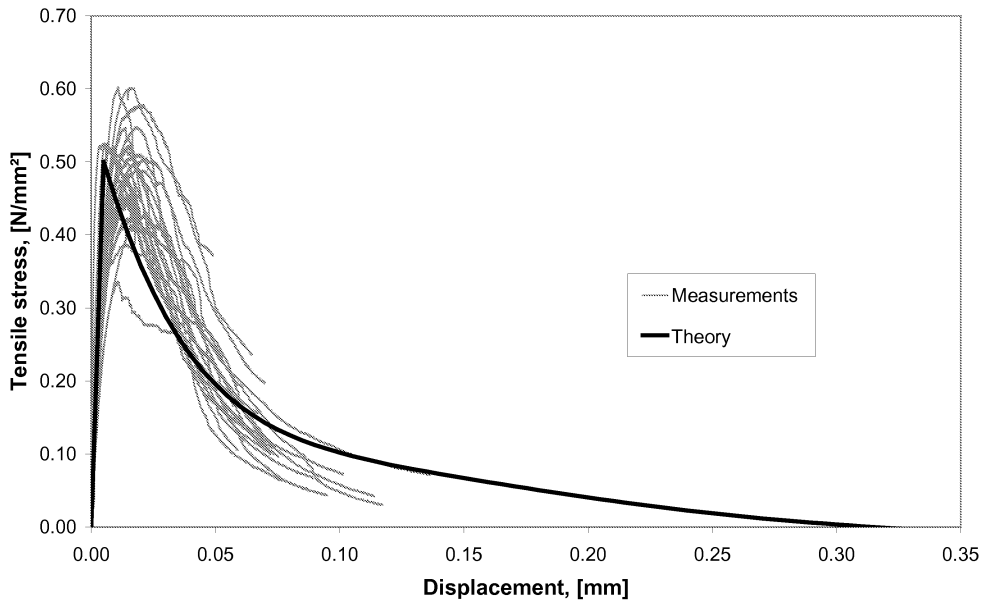

Figure 3.23:
Behaviour of LECA blocks subjected to uni-axial tension compared with a theoretical behaviour based on Hordijk softening (Equation 2.5).

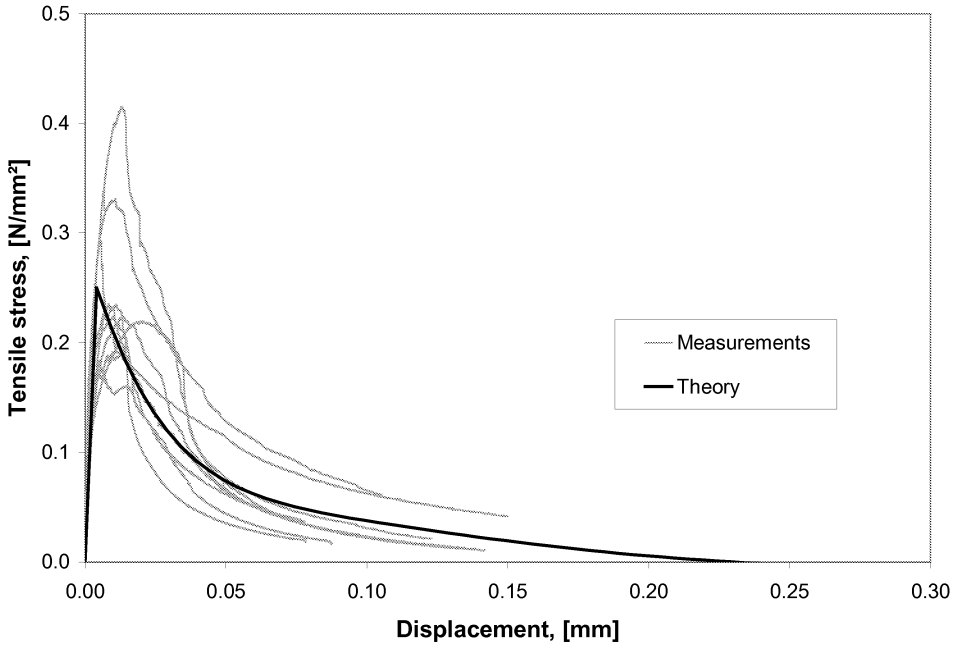

Figure 3.24:
Behaviour of mortar joints subjected to uni-axial tension compared with a theoretical behaviour based on Hordijk softening (Equation 2.5).

Table 3.13:
Obtained mean values of material properties.

	Tensile strength [N/mm²]	Modulus of elasticity [N/mm²]	Mode I fracture energy [N/mm]
Block	0.5	3000	0.030
Joint [1)]	0.25	1300	0.011

[1)] Mortar joint including the interface between mortar and block.

Regarding the presented data for mortar joints, it should be noted that the mortar itself is expected to be stiffer and stronger than the block. However, that is not the situation for the presented data. The properties of mortar joints may vary considerably, especially over the thickness, because of variations in hardening conditions. Capillary suction from the blocks dries out the interfaces, while a more optimal hardening condition is maintained in the middle of the joint. Seep introduces an additional reduction of the interface strength by leaving a small area without contact between block and joint along the circumference of the upper interface, see Figure 3.25. However, due to practical reasons and due to lack of possibilities to make a distinction, the determined behaviour of the mortar joint is considered the mean behaviour of the mortar joint itself and the interface. The effect of the weaker interface is observed during testing, but is not "included" in the presented data.

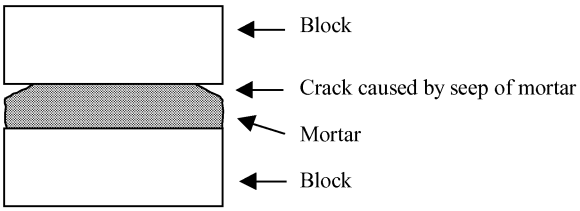

Figure 3.25:
Reduced contact between the upper block and the mortar joint due to seep of the mortar.

In the numerical simulations of Høiseth (1999), the mechanical behaviour of LECA blocks was represented by a smeared crack model with a linear softening diagram and a softening diagram proposed by Hordijk (Equation 2.5). The obtained crack-pattern and crack-propagation was in good agreement with the experiments, almost independent of the applied softening diagrams.

Regarding the stress-deformation relationship, the study of Høiseth (1999) demonstrates the dependency of the crackband-width on the smeared crack model. Agreement with the experimentally measured fracture energy assumes the use of a realistic crackband-width in the simulations. The closest relationship with the experimental softening was obtained with Hordijk softening, confirming the results of Kvande (2001-6) and Pluijm (1999) for other types of masonry.

Numerical simulations of the mechanical behaviour of LECA couplets made with one mortar joint was carried out by Høiseth (2000a). Again, a smeared crack model with a softening diagram proposed by Hordijk (Equation 2.5) represented the specimen. The obtained crack-

pattern and crack-propagation, however, did not harmonise perfectly with the experimental observations. The non-linear analysis showed a fracture in the middle of the joint, while the experimental results showed that a complete fracture occurred in the interface between block and joint. This is due to the determination of experimental data representing an average behaviour of the mortar and the interface.

3.7.5 Measured behaviour of shear failure of bed joint in LECA masonry

Obtained behaviour of bed joint in LECA masonry during combined compression and shear tests are given in Figure 3.26. Both experimental and theoretical curves are included in the figure. The theoretical curve is based on exponential cohesion softening of Equation 2.6 with obtained mean values of shear strength, shear modulus and mode II fracture energy given in Table 3.14.

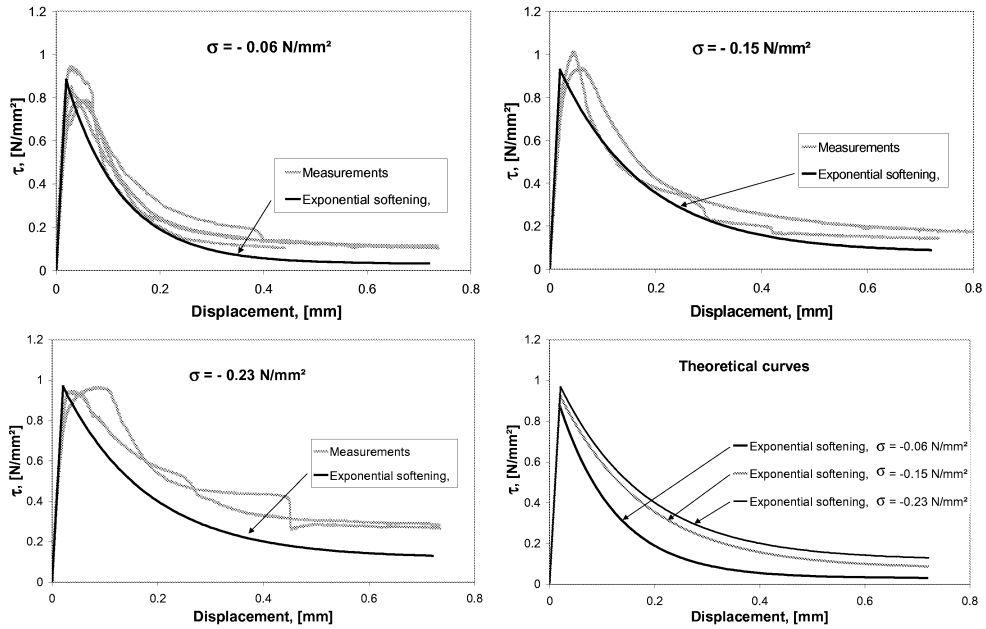

Figure 3.26:
Behaviour of bed joints in LECA masonry subjected to shear compression compared with theoretical behaviour based on exponential cohesion softening (Equation 2.6).

Table 3.14:
Obtained mean values of material properties of mortar joint including the mortar/block interface.

		Compression level during shear testing [N/mm²]		
		0.06	0.15	0.23
Shear bond strength	[N/mm²]	0.88	0.93	0.97
Shear modulus	[N/mm²]	1500	1500	1500
Mode II fracture energy	[N/mm]	0.092	0.137	0.138

In Section 2.4.3 cohesion softening is expressed in two different ways, see Equation 2.6 and 2.7. The exponential formula of Equation 2.6 gives the best agreement with the experimentally obtained behaviour. The formula matches best in the beginning of the descending branch. At the end of the descending branch the theoretical curves drops too much. This is due to the increase of τ_{fr} when normal stress-increase is different from the increase of τ_u ($\Delta\tau_u = \tan\varphi \cdot \sigma$), see Figure 2.12.

The experimental results demonstrate that the dilatancy is not constant during the failure envelope. Expression by the formula of Pluijm (1999), Equation 2.8, seems to match reasonably well when 1,0 mm is chosen for r and $\tan\psi_o$ are 0.82, 0.75 and 0.59 for precompression 0.06, 0.15 and 0.23 N/mm² respectively, see Appendix 7.

In the numerical simulations of Høiseth (2000b), a coarse 3-dimensional element mesh was used to study the mechanical behaviour of the Fixed Smeared Crack model, in combination with various shear retention descriptions, and the Rotating Smeared Crack model. With the Rotating Smeared Crack model, a limit load and subsequent global softening was obtained. In the first instance, this was due to rotation of the crack directions, such that increasing shear stress produced crack-planes in the joint element which approached the horizontal orientation, i.e. parallel to the interface between units and joint. Subsequently, the softening behaviour was obtained by a realistic description for compressive states of stress.

It should be noted that there are some arguing whether shear failure of masonry should be considered as mode I or mode II fracturing. In the concrete community it has over the years become accepted that failure of plain concrete (quasi-brittle materials) is a Mode I phenomenon, regardless of the state of stress. The present study of Høiseth (2000b) show that Mode I fracturing is a plausible criterion also for initiation of the failure mechanism in the joints of LECA masonry subjected to shear. A complete simulation of the failure process requires however that the remaining capacity in compression is treated properly.

The constitutive properties of LECA block and mortar, especially in the interface, are quite similar or at least comparable. Therefore, in all the analyses of Høiseth (2000b), cracks developed also in the upper and lower units. This suggests that structural analysis of LECA masonry may be performed by macro-modelling, with sufficiently accurate results.

3.7.6 Concluding remarks

Conclusions

The behaviour of LECA masonry due to tensile as well as shear compression failure is studied in this thesis work. A close relationship with the experimental softening due to tension was obtained with Hordijk-softening (Equation 2.5) for both LECA block and mortar joint. The cohesion softening due to shear may be described by exponential cohesion softening according to Equation 2.6. Similarly, the development of dilatancy may be described by the formula of Pluijm (1999) (Equation 2.8), when 1,0 mm is chosen for r and $\tan\psi_o$ are 0.82, 0.75 and 0.59 for precompression 0.06, 0.15 and 0.23 N/mm² respectively.

Restrained shrinkage cracking will normally appear as tensile failure. This is due to a higher shear capacity of the bed joint than the tensile capacity of the LECA blocks and that the masonry is made without mortar in the perpend joints.

Recommendations for further work

Test of other LECA qualities may be carried out to establish formula giving the fracture energy depending on compressive strength and maximum aggregate size. Such a formula is available for normalweight concrete in CEB-FIP MC 90.

CHAPTER 4

4. RELEVANCE AND VALIDITY OF THE THESIS WORK

4.1 Investigated material properties of LECA masonry

Introduction

The main objective of this study is to expand the knowledge about the material properties of LECA masonry to enable more accurate structural analysis and design of such masonry. In order to limit the number of investigated material properties, properties of particular interest were identified, see Table 4.1. Because restrained shrinkage cracking is a major cause of damage to LECA masonry, the identification of material properties was based on a restrained shrinkage cracking example. Table 1 also gives some of the variables influencing the material properties. Some aspects concerning the material properties and the influencing factors given in Table 4.1 are discussed in the following.

Investigated material properties and combination effects

In order to do accurate analysis of the deformation process of LECA masonry due to restrained shrinkage, all the significant material properties for the task have to be known, see Table 4.1. Essential material properties may be missing in the table. It should, however, be noted that e.g. the compressive stress-strain relationship covers compressive strength, modulus of elasticity as well as ultimate compressive strain. Taking such relations in account the material properties of Table 4.1 should be rather complete, see Chapter 3.

While the material properties are studied under specific conditions, combination effects may, however, be omitted. For instance, the compressive strength is reduced if there is tension normal to the compression direction. The validity of the existing strength reduction formula of CEB-FIP MC 90 due to LWAC and LECA masonry, should be checked. The formula is originally established for NWC.

Other combination effects of simultaneous creep and shrinkage, and of temperature on strength, modulus of elasticity, fracture energy, creep and shrinkage are dealt with in Chapter 2.

Table 4.1:
Overview of material properties of particular interest for structural analysis of restrained shrinkage of LECA masonry and variables that influence the properties.

Material property	Influencing factor	Examples of references concerning: concrete	Examples of references concerning: Norwegian LECA masonry [1]	Studied in this thesis [2]
Compressive stress-strain relationship, *see Chapter 2.3.1 and 3.3*	-) *No subdivision*	NS 3473 prEN 1520:1999 Eibl et al. (1995) Neville (1995)	÷	×
	a) Composition of the concrete		÷	
	b) Stiffness of the aggregate		÷	
	c) Moisture content		÷	(×)
	d) Age		÷	
	e) Curing conditions		÷	
Poisson's ratio, *see Chapter 2.3.1 and 3.3*	-) *No subdivision*	NS 3473 prEN 1520:1999	÷	×
	a) Composition of the concrete	Eibl et al. (1995)	÷	
	b) Moisture content		÷	
	c) Age		÷	
	d) Load level		÷	
Final shrinkage value, *see Chapter 2.3.2 and 3.4*	-) *No subdivision*		Svendsen et al. (1966) Leca 1.000	
	a) Ambient humidity	NS 3473 prEN 1520:1999 Eibl et al. (1995) Neville (1995)	Waldum et al. (1993a) Waldum (1998)	×
	b) Composition of the concrete		÷	
	c) Dimension of the element		÷	×
Creep coefficient, *see Chapter 2.3.3 and 3.5*	-) *No subdivision*	NS 3473 prEN 1520:1999 Eibl et al. (1995) Neville (1995)	÷	×
	a) Ambient humidity		÷	
	b) Composition of the concrete		÷	
	c) Dimension of the element		÷	
	d) Age at loading		÷	
Coefficient of thermal expansion *see Chapter 2.3.4 and 3.6*	-) *No subdivision*	NS 3473 prEN 1520:1999	Svendsen et al. (1966) Leca 1.000	×
	a) Coefficient of the aggregate	Eibl et al. (1995) Neville (1995)	÷	
	b) Coefficient of the hydrated cement paste		÷	
	c) Moisture content		÷	×

Table 4.1 (continued):

Material property		Influencing factor	Examples of references concerning		Studied in this thesis [2]
			concrete	Norwegian LECA masonry [1]	
Tensile stress-deformation relationship,	-)	*No subdivision*	Hilleborg et al. (1976)	÷	×
	a)	Composition of the concrete	Eibl et al. (1995)	÷	
see Chapter 2.4.2 and 3.7.4	b)	Stiffness of the aggregate		÷	
	c)	Moisture content		÷	×
	d)	Age		÷	
	e)	Curing conditions		÷	(×)
Shear stress-deformation relationship,	-)	*No subdivision*	Present interest for masonry only, see Pluijm (1999)	÷	×
	a)	Composition of the concrete		÷	
see Chapter 2.4.3 and 3.7.5	b)	Stiffness of the aggregate		÷	
	c)	Moisture content		÷	
	d)	Age		÷	
	e)	Curing conditions		÷	
	f)	Compressive loading		÷	×

[1] ÷ symbolise that no satisfying reference was found.

[2] × symbolise that the actual material property/influencing factor was studied in this thesis work.

Influencing factors

Table 4.1 shows some influencing factors on the different material properties.

The composition of the LECA blocks/masonry obviously has an influence on all the investigated material properties. Effects of variations in composition were, however, not a important task of this thesis. Due to the limited data on LECA masonry, a relatively thorough study of one particular LECA masonry quality was carried out in order to form a basis for further studies of other qualities. It may be argued that studying only one quality of LECA blocks limits the utilitarian value of the work since no general formulas concerning e.g. the effect of density on the ultimate strain are possible to develop on the basis of this study. Most of the "voids" in the right column of Table 4.1 are explainable by the limited number of qualities of LECA masonry investigated.

It should also be noted that the quality of the LECA blocks might vary somewhat depending on the placing in the mould and in the curing chamber during manufacturing. No efforts are made in this thesis to quantify such variations in neither the manufacturing process, nor the influences of the variations on the quality of the LECA blocks. A study of the variation due to manufacturing and deviation from the specified mixtures may, however, be of great

importance for optimisation of the manufacturing process. Since the variations in manufacturing are not very well known, values reported in this thesis work should for the time being be taken as approximate values for the investigated qualities. For design purpose, however, the LECA block quality "3/770" may be sufficiently covered by this study.

The moisture content and the ambient humidity of the masonry may also influence all the investigated material properties. However, their effects on stress-deformation relationship may not be significant for design purposes within the normal service conditions bracket. A control of the influence of moisture content was carried out during determination of tensile stress-deformation relationship of LECA blocks, see Appendix 5. Tests were carried out on both specimens conditioned at 20 °C and 60 % RH and specimens dried at 105 °C. No significant difference in the measured values were found.

Concerning the value of creep, shrinkage and thermal expansion, the influence of moisture content and the ambient humidity of the masonry is significant. That is why establishing of final shrinkage values at different ambient humidities were focused on in this study. According to NS 3473 and prEN 1520:1999, establishing of design values for shrinkage at 30, 50 and 85 % RH may be sufficient for design purposes.

Also, the influence of moisture content of LECA blocks on the coefficient of thermal expansion was controlled in this study. For design purposes, the effect on thermal expansion under normal structural conditions, may be neglected.

Concerning creep, a drier environment leads to an increase of the drying creep. Due to limited time, establishment of creep coefficients at different ambient humidities was not carried out in this thesis study. In order to determine a typical value of the creep coefficient, creep tests were carried out in a normal indoor situation (20 ±2 °C and 55 ±5 % RH) four weeks after manufacturing of the LECA blocks and one week after preparing the specimens, see Appendix 3 and 4. However, creep should also be determined for other conditions in order to establish design values that can be used for other situations.

Due to plastic covering over the LECA blocks during storage, the moisture content of the blocks is maintained approximately at the same level as leaving the curing chamber. Creep and shrinkage were measured in this study from blocks with this moisture content.

The effect of *age and curing conditions* on the investigated qualities are not dealt with in detail in this thesis work. Because the LECA blocks usually arrive at the building site more than four weeks after manufacturing, it is assumed that the development of block strength is finalised. Consequently, it was an ultimate scope of this work to study material properties of well-cured blocks. Due to the use of plastic covering over the pallets, a high humidity level during curing is maintained. However, due to an outdoor storage, the temperature under the plastic covering varies considerable. However, all LECA blocks investigated by this thesis work got at least four week of hydration covered by plastic at > 15 °C. According to CEB-FIP MC 90, 28 day of curing at 15 °C reduces the temperature adjusted concrete age to 22 compared with curing at 20 °C.

The average storage temperature in January at the factory location Lillestrøm (reference year) is about –9 ° C (Geving and Torgersen 1997). 28 days of curing at –9 °C represent, according

to CEB-FIP MC 90, 6 day of curing at 20 °C. The lower curing temperature is by the producers compensated by extending the storage of the LECA blocks during winter time.

A study of the effect of different curing regimes on shrinkage and compressive strength of LECA blocks is enclosed in Appendix 2. According to that investigation, most of the block strength is built up during the manufacturing process. (Storage at 50 °C for two days represents 7 days of curing at 20 °C.)

Due to the curing time and the manufacturing process, it is assumed that the curing process of all blocks arriving at the building site is finalised. Consequently, it is assumed that with regard to curing, the measured material properties match the properties of typical LECA blocks arriving at the building site.

The load level influences the obtained Poisson's ratio and creep coefficient. However, the properties are approximately constant within service load conditions (Eibl et al. 1995:A6.4.2, Bažant 1982). In the present restrained shrinkage example, only the situation within service load condition is of particular interest for this study.

Regarding the shear stress-deformation relationship, the influence of compressive loading is significant. Consequently, the behaviour during shear compression is of interest in this thesis work.

4.2 Structural analysis of LECA masonry

Introduction

To pave the way for non-linear Finite Element analysis and design of LECA masonry structures, experimental determination of relevant material/model parameters is required. Although the theoretical basis for current mechanical material models is in general universal, without restrictions to state of stress or stress path, the governing material parameters can usually be obtained experimentally under well-defined uni-axial or two-dimensional loading conditions. Consequently, this thesis study has focused on uni-axial tensile failure and shear failure under bi-axial shear compression through experimental observations, see Appendix 5 and 7.

The experiments have been simulated numerically by Høiseth, see (1999, 2000a, 2000b), where appropriate models have been outlined, and their capabilities to reproduce the experimental results have been demonstrated. The high Finite Element mesh resolution which was used in these analyses is however inappropriate for practical purposes. Even with modern computers, modelling an entire masonry structure in the same manner would be too time-consuming. A macro-modelling approach, for instance by homogenisation of the masonry constituents, seems necessary. In the following section some aspects concerning modelling of LECA masonry are discussed.

Modelling LECA masonry

Because micro-modelling of masonry tends to be less efficient for practical purposes, much effort has recently been made in the development of homogenisation techniques. Different homogenisation techniques have been proposed by Gottfredsen (1997) and Molnar (2000). Because the constituents of masonry are arranged in a highly periodic way, it is possible to predict the global behaviour of masonry by the introduction of so-called basic cells. A basic cell is a small domain that represents a given volume of the masonry, i.e. including masonry unit and mortar. By homogenisation, a constitutive relation between the volume average of stress and strain can be established.

To which extent the basic cell is consistent with the volume it represents, depends on the in homogeneity of the masonry. The more inhomogeneous the masonry structure is, the smaller the basic cell should be (Gottfredsen 1997). According to Lourenço (1996) homogenisation leads to unreliable results if the stiffness difference between mortar and masonry units exceeds a value of about 10. This is due to an increasing non-uniform stress field caused by this difference within the volume represented by the basic cell.

Even though homogenisation has been used successfully to approximate the mechanical behaviour of masonry, it can for the time being only be regarded as a research tool (Lourenço 1996, Gottfredsen 1997). This is due to the fact that complex homogenisation techniques require powerful calculation facilities. Neither are current techniques capable of accounting for the non-linear behaviour during cracking in an adequate manner (Molnar 2000).

As pointed out in Section 2.5, however, the joints and units in LECA masonry are more consistent than in ordinary masonry. For practical design or reassessment purposes, treating the combined actions of units and mortar as an isotropic material with the non-linear properties of LECA blocks may therefore give sufficiently accurate results, with respect to both global deformations and cracking as well as load-carrying capacity. Such an approach would allow a reduced mesh-resolution, and hence increase the efficiency with respect to computer-time.

The idea is appealing also because:

- The mechanical properties of mortar and LECA blocks are compatible quantities. The compressive strength of mortar is three to four times higher than for LECA blocks. At present, development works are being carried out in Norway, aiming at production of mortars which matches the stiffness of LECA blocks better than today.

- The experienced difficulties in obtaining shear failure in the interface mortar/block during the bi-axial shear compression tests, demonstrates the small difference between the mechanical properties of the mortar and those of the LECA blocks, see Appendix 7. Preparation of deep notches in the interface was necessary to study the shear behaviour of the bed joint.

- The tensile strength of the LECA masonry specimen was about 50 % of the strength of the blocks. Due to scale effects of the tested specimens, the strength differences for the constituents of a wall are expected to be even less. Similar tests of Pluijm (1999) on dry brick masonry showed that the tensile strength of the bricks was more than four times stronger than the masonry. It should also be noted that the tests of LECA masonry were carried out on similar shaped specimens as Pluijm (1999). However, the

larger dimension of the LECA blocks compared to those of the bricks is not taken into account in the test program. Consequently, the obtained tensile strength of the masonry tested may be smaller than if whole blocks were used. This is due to that seep and drying shrinkage along the surface of the joints may influence the tensile strength of small specimens more significantly than for larger specimens.

The validity of modelling LECA blocks and mortar as a joint isotropic material with the properties of LECA blocks remains however to be verified. The results from the full-scale tests (e.g. Appendix 8) of restrained shrinkage should in this connection be used as reference for numerical simulations. It must yet be emphasised that the open perpend joint of LECA masonry makes the compound behaviour highly anisotropic. This anomaly represents discontinuity planes, which may be accounted for by interface elements representing predefined discrete cracks.

Application of the experimental results to structural analysis

The material properties of LECA blocks and LECA masonry, which have been found during the present study, constitute the necessary basis for numerical modelling. In this connection, also the measured relationship between loading and deformation under various conditions apply as reference for numerical formulations. By adopting the experimental results in generic material models available in general FEM-packages like DIANA, the models should generally permit analysis of structures with random geometry, boundary conditions and loading. Such analyses will cover the complete deformation process, from elastic behaviour via cracking to global failure.

As pointed out, restrained shrinkage in LECA walls is a matter of current interest. The full-scale testing of restrained shrinkage should therefore serve as suitable verification case for global analysis.

Having established appropriate numerical formulations, the following issues are important with respect to LECA masonry, and should be subjected to numerical investigations:

- out-of-plane bending due to wind load,
- out-of plane bending of basement walls due to ground pressure,
- expansion due to temperature gradients and
- settlements.

LECA masonry is usually strengthened by reinforcement elements to provide the necessary tensile strength under given conditions. Although appropriate models for the mechanical behaviour of embedded reinforcement in concrete are available, experimental evidence is necessary to apply these formulations in connection with masonry joints.

CHAPTER 5

5. CONCLUDING REMARKS

5.1 Conclusions

General

In order to expand the knowledge about the material properties for structural analysis and design of LECA masonry, a relatively wide range of material properties has been investigated in this study. In order to limit the number of investigated material properties, properties of particular interest were identified. Because restrained shrinkage cracking is a major cause of damage to LECA masonry, the identification of material properties was based on a restrained shrinkage cracking example. To be able to determine the deformation process of restrained LECA masonry structures, the following material properties were investigated in this thesis study:

- compressive stress-strain relationship,
- Poisson's ratio,
- final shrinkage value,
- creep coefficient,
- coefficient of thermal expansion,
- tensile stress-deformation relationship and
- shear stress-deformation relationship.

The study was limited to the LECA block quality "3/770" only. Consequently, no relationships including the influence of different qualities and compositions of LECA blocks/masonry on the properties were established.

By determining a relatively wide range of important material properties, this thesis study has been largely instrumental in expanding the knowledge about the material behaviour of LECA masonry. Studied material properties are given in Table 5.1. For comparison, design values of Eurocode 6 are also included in Table 5.1. While also the composition and the properties of the raw materials of the LECA blocks are documented in this study, the study may form an important basis for more accurate analysis of structural performance as well as further product development of such masonry.

Table 5.1:
Summary of material properties obtained in this thesis work

Material property	Symbol [1]	Obtained value of LECA masonry in this thesis work	Design value of Eurocode 6 [2]	Unit
Compressive stress-strain relationship	f_c	2.7	-	N/mm²
	E_c	4 100	2 300	N/mm²
	ε_{cn}	0.66	-	mm/m
	ε_{c1}	0.92	2	mm/m
	ε_{cu}	1.8	3.5	mm/m
Poisson's ratio	ν	0.2	-	-
Final shrinkage value	ε_{sh}	30 % RH: -0.65 50 % RH: -0.55 85 % RH: -0.40	-0.4	mm/m
Creep coefficient	ϕ_∞	1.7 – 8.0	2.0	-
Coefficient of thermal expansion	α_T	$6.7 – 7.4 \cdot 10^{-6}$ dependent of moisture content	$10 \cdot 10^{-6}$	1/K
Tensile stress-deformation relationship	f_t^u	0.5	-	N/mm²
	f_t^j	0.25	-	N/mm²
	E_o^u	3 000	-	N/mm²
	E_o^j	1 300	-	N/mm²
	G_{fI}^u	0.030	-	N/mm
	G_{fI}^j	0.011	-	N/mm
		Support Hordijk-softening		
Shear stress-deformation relationship	τ_u	σ_c = 0.06 N/mm²: 0.88	-	N/mm²
		σ_c = 0.15 N/mm²: 0.93	-	N/mm²
		σ_c = 0.23 N/mm²: 0.97	-	N/mm²
	G_o	σ_c = 0.06 N/mm²: 1 500	-	N/mm²
		σ_c = 0.15 N/mm²: 1 500	-	N/mm²
		σ_c = 0.23 N/mm²: 1 500	-	N/mm²
	G_{fII}	σ_c = 0.06 N/mm²: 0.0.92	-	N/mm
		σ_c = 0.15 N/mm²: 0.137	-	N/mm
		σ_c = 0.23 N/mm²: 0.138	-	N/mm
	μ	0.88	-	-
		Support partly exponential cohesion-softening and dilatancy softening		

[1] See list of symbols for explanations.
[2] Due to general application only design values from the European Prestandard for design of masonry structures is included in the Table.

Compressive stress-strain relationship

The thesis work proposes both a bi-linear and a parabolic-rectangular stress-strain diagram which may be better fitted for structural design of LECA masonry than the stress-strain data given in Eurocode 6.

Approach given in prEN 1520:1999, see Equation 3.6, seems to be better fitted for the modulus of elasticity of LECA masonry than the approach given in Eurocode 6, see Equation 3.5. For structural design of LECA masonry the difference between the approaches

may not be that important. However, there is a difference between the estimated modulus of elasticity for LECA masonry and the value determined according to prEN 1052-1:1995. The latter should be used in structural analysis.

The ultimate compressive strain given in Eurocode 6 (3.5 ‰) is too high for LECA masonry. The approach given in prEN 1520:1999 (2.1 ‰) seems to be a better match for LECA masonry.

Poisson's ratio

For design purposes, Poisson's ratio for elastic strain may be taken as 0.2. If cracking is permitted in tension, the ratio may be taken as zero.

Shrinkage

Due to the experimental work described in this thesis, it is found that determination of shrinkage of LECA masonry may be derived from tests on single untreated LECA blocks.

Since the shrinkage behaviour of LECA masonry may not be that sensitive to wall thickness, the design values of the final shrinkage may be given independently of notional size (see Equation 2.1).

The final shrinkage of LECA masonry is significantly influenced by the ambient humidity. On the basis of this thesis work, design values for the final shrinkage of LECA masonry may be introduced for three levels of ambient humidity. Design values -0.40, -0.55 and -0.65 mm/m were given for ambient humidity of 85, 50 and 30 % RH respectively. The values are significantly lower than the design value of Eurocode 6.

In order to study the effect of different curing conditions on shrinkage and compressive strength of LECA blocks, masonry units from the same production batch were exposed to five different climate conditions during the first month after arriving from the production line. The results seems to indicate that an early drying of LECA blocks does not significantly influence the compressive strength of the blocks. Since the use of relatively dry blocks when making masonry will reduce the risk of cracking, it may be recommended to dry the LECA blocks as early as possible after they have left the production line.

The behaviour of restrained shrinkage LECA walls was experimentally studied in this thesis study. In order to control the effect of shrinkage reinforcement, five LECA walls restrained to the foundation were studied. The walls contained different amounts of shrinkage reinforcement. Even though no cracking of LECA blocks were observed during the test period of 1½ year, the test results indicate that the amount and placement of the shrinkage reinforcement influence the magnitude of the horizontal shrinkage. Smallest horizontal shrinkage was obtained on the wall with most reinforcement ($A_s/A_M \approx 0.67$ ‰). The effect of the reinforcement, however, seems to be limited. Consequently, the amount of shrinkage reinforcement required today (Bransjenorm, Leca 1.000) may be of limited significance for prevention of restrained shrinkage cracking of LECA masonry.

Creep coefficient

In view of the investigated creep behaviour of LECA masonry subjected to compression and tension, the creep coefficient design value of Eurocode 6, given as 2.0, seems to be reasonable for structural design purposes. However, due to the open perpend joint in LECA masonry, there is a complicated stress distribution in such walls. The stress distribution around the open joint may make the assessment of stress reduction due to creep very complicated.

Coefficient of thermal expansion

During the determination of coefficient of thermal expansion of LECA blocks, values between 6.7 and $7.4 \cdot 10^{-6}$/K depending on moisture content were recorded. Based on the fact that LECA blocks of only four different moisture contents were tested, a design value of $8 \cdot 10^{-6}$/K (Leca 1.000, NS 3475, prEN 1520:1999) seems reasonably accurate for LECA masonry.

Tensile stress-deformation relationship

Values for tensile strength, modulus of elasticity and mode I fracture energy for LECA blocks and bond has been established in this thesis work. These parameters are necessary input when applying in finite-element method programs to describe the behaviour of tensile failure of masonry. A close relationship with the experimental softening due to tension, i.e. the post peak behaviour, was obtained with Hordijk-softening (Equation 2.5) for both LECA block and mortar joint.

Shear stress-deformation relationship

Parameters necessary as input in the finite-element method programs to describe the behaviour of bed joints in LECA masonry subjected to combined compression and shear action, have been established in this thesis work. The results include mean values for shear strength, shear stiffness, mode II fracture energy and dry friction coefficient. The results support partly the validity of exponential cohesion-softening (Equation 2.6) and dilatancy softening (Equation 2.8) of the bond interface to describe the post peak behaviour.

Restrained shrinkage cracking of LECA masonry will normally appear as tensile failure. This is due to a higher shear capacity of the bed joint than the tensile capacity of the LECA blocks.

Modelling LECA masonry

In order to pave the way for finite element analysis and design of LECA masonry structures, experimental determination of relevant material/model parameters were carried out in this thesis study. A micro-modelling can be restricted to account for the quasi-brittle material behaviour of the LECA blocks and the average in-situ properties of the applied mortar. By application generic material models in DIANA, the current tests of LECA masonry subjected to uni-axial tension and compression/shear, this approach gave satisfactory results, see Høiseth and Kvande (2000) and Høiseth (2000b).

Although the average stiffness and strength of mortar is usually somewhat higher than for the LECA units, a macro-modelling based on the LECA block properties should in general give

sufficiently accurate results in global analysis of real structures. It must however be emphasised that the open perpend joint of LECA masonry makes the compound behaviour highly anisotropic. This anomaly represents discontinuity planes, which may be accounted for by interface elements representing predefined discrete cracks.

By adopting the experimental results of this study in generic material models available in general FEM-packages like DIANA, the models should generally permit analysis of structures with random geometry, boundary conditions and loading. Such analyses will cover the complete deformation process, from elastic behaviour via cracking to global failure. The full-scale testing of restrained shrinkage carried out in this study, should serve as suitable verification case for global analysis of LECA masonry.

5.2 Recommendations

For further development of LECA masonry, the following recommendations seem to be appropriate:

- Due to the amount of restrained shrinkage cracking, more effort should be made to ensure that the LECA blocks adequately dry before making the masonry. Appropriate actions on building site, in manufacturing, and during storage, should be developed. The opportunities for development of practical and economical arrangements to expose the masonry units to early drying seem very favourable. Presently, no specific requirement to moisture content is suggested in this study because more tests should be carried out to identify appropriate levels of moisture content.

- Only one quality of LECA masonry is studied in this thesis work. Other LECA masonry qualities should be subjected to similar tests. By testing a wider range of qualities, it may be possible to establish general formulas that may be used for estimation of different material properties depending on mix ratios and other production variables.

- Further investigations of restrained shrinkage of LECA masonry of various types should be performed. Both experimental testing and numerical analysis should be applied to give reliable guidelines for the amount and position of shrinkage reinforcement as well as the design of movement joints. The work may be based on the material/model parameters obtained during this study.

- The adapted material models in DIANA are certainly applicable for other structural situations than restrained shrinkage. In order to evaluate the applicability, comparing experimental observations of an out-of-plane bending situation of LECA masonry and numerical simulations should be carried out.

- LECA masonry is usually strengthened by reinforcement elements to provide the necessary tensile strength under given conditions. Although appropriate models for the mechanical behaviour of embedded reinforcement in concrete are available, experimental evidence is necessary to apply these formulations in connection with masonry joints.

- This thesis work has studied material properties of LECA masonry. An aim of further research should lead to the development of advanced software programs for design of LECA masonry. Based on tools for numerical analysis and existing design standards, such software programs may be possible to develop. The programs should be designed especially for structural engineers and architects in order to secure improved design of LECA masonry. Design of movement-joints and guidelines for reinforcement should be important constituents of such a program.

REFERENCES

Anthoine (1995) — Anthoine, A. – Derivation of the in-plane elastic characteristics of masonry through homogenization theory. *International Journal of Solids and Structures*, Vol. 32, No. 2. pp. 137-163, 1995.

Basma and Abdel-Jawad (1995) — Basma, A.A. and Abdel-Jawad, Y. – Probability Model for the Drying Shrinkage of Concrete, *ACI Materials Journal*, Vol. 92, No. 3, 1995.

Bažant (1982) — Bažant, Z.P. – Chapter 7: Mathematical Models for Creep and Shrinkage of Concrete, *Creep and Shrinkage in Concrete Structures*, (Editors Bažant, Z.P. and Wittmann, F.H.) Wiley & Sohns, ISBN 0-471-10409-4, New York 1982.

Bažant (1988) — Bažant, Z.P – Chapter 2: Material models for structural creep analysis, *Mathematical modeling of creep and shrinkage of concrete*, (Editor: Bažant, Z.P.) Wiley & Sohns, ISBN 0-471-92057-6, Chichester 1988.

Bažant (1992) — Bažant, Z.P (Editor) – *Fracture Mechanics of Concrete Structures*, Part I, Elsevier, ISBN 1-85166-869-1, London 1992.

Bažant and Asghari (1974) — Bažant, Z.P. and Asghari, A. – Computation of Age-Dependent Relaxation Spectra. *Cement and Concrete Research*, Vol 4, pp. 567-579, 1974.

Bažant and Carol (1993) — Bažant, Z.P. and Carol, I. (Editors) – *Creep and Shrinkage of Concrete. 5th International RILEM Symposium*, Barcelona, Spon, ISBN 0-419-18630-1, London 1993.

Bažant and Wittmann (1982) — Bažant, Z.P. and Wittmann, F.H. – *Creep and Shrinkage in Concrete Structures*, Wiley & Sohns, ISBN 0-471-10409-4, New York 1982.

Beeby and Narayanan (1995) — Beeby, A.W. and Narayanan, R.S. – *Designers' handbook to Eurocode 2 Part 1.1: Design of concrete structures*. Telford, ISBN 0-7277-1668-9, London 1995.

Bentzon (2000) — Bentzon, L.C. – *Reduktion af svind i letklinkerbeton* (Reduction of shrinkage in lightweight aggregate concrete), SBI report 327, Danish Building Research Institute, ISBN 87-563-1060-9, Hørsholm 2000 (in Danish).

Berkers and Rademaker (1992) — Berkers, W.G.J. and Rademaker, P.D. – *Cracking in long walls – Final report*, RCK report no. CK015.1, Research Centre Calcium Silicate Industry, Barneveld 1992.

Bransjenorm — *Bransjenorm, Veiledning til ENV 1996-1-1:1995, Prosjektering av murverk. Beregning og dimensjonering* (Draft National Application Document for ENV 1996-1-1:1995) Arbeidsdokument pr. 2000.01.19, Utarbeidet av Mur-Sentret, Oslo 2000 (in Norwegian).

CEB-FIP Bulletin 4 — *Lightweight Aggregate Concrete. Codes and standards. State-of-art report.* Bulletin No. 4, CEB-FIP fédération internationale du beton, Sprint-Druck Stuttgart, ISBN 2-88394-044-4, Lausanne 1999.

CEB-FIP Bulletin 8 — *Lightweight Aggregate Concrete. Recommended extensions to Model Code 90. Identifications of research needs. Case studies.* Bulletin No. 8, CEB-FIP fédération internationale du beton, Sprint-Druck Stuttgart, ISBN 2-88394-048-7, Lausanne 2000.

CEB-FIP MC 90 — CEB-FIP Model code 1990, Bulletins d'Information No. 213-214, Comité Euro-International du Béton, Thomas Telford, ISBN 0-7277-1696-4, Lausanne 1993.

Conradi (1999) — Conradi, T. – *Måling av herde- og tørkesvinn i lettklinkerbetongblokker* (Measurement of shrinkage in LECA units), Project work, Department of Building and Construction Engineering – NTNU, Trondheim 1999 (in Norwegian).

Crook (1987) — Crook, R.N. – *An investigation into the performance of concrete block masonry using couplets subjected to axial and eccentric loading*, Technical Report 567, Cement and Concrete Association, ISBN 0-7210-1357-0, Wexham Springs 1987.

DIANA — *DIANA, User's Manual release 7 – Nonlinear Analysis*, TNO Building and Construction Research, Delft 1998.

Eibl et al. (1995) — Eibl, J. et al. – *Concrete Structures. Euro-Design Handbook*. Ernst & Sohn, Berlin 1995.

Eibl et al. (1995:A6.2.2) — Ibidem, Chapter A6.2.2.

Eibl et al. (1995: A6.2.2&A6.5.3.3) — Ibidem, Chapter A6.2.2 and A6.5.3.3 (the first of them).

Eibl et al. (1995:A6.4.2) — Ibidem, Chapter A6.4.2.

Eibl et al. (1995:A6.5.3.2) — Ibidem, Chapter A6.5.3.2.

Eibl et al. (1995:A6.5.3.3) — Ibidem, Chapter A6.5.3.3 (the first of them).

Eibl et al. (1995:A6.8.1)	Ibidem, Chapter A6.8.1.
Eibl et al. (1995:A6.8.4)	Ibidem, Chapter A6.8.4.
Eibl et al. (1995:C5.2.5)	Ibidem, Chapter C5.2.5.
Eibl et al. (1995:C5.2.7)	Ibidem, Chapter C5.2.7.
Eurocode 2	European Prestandard ENV 1992-1-1:1991. Eurocode 2: *Design of Concrete Structures. Part 1-1: General rules and rules for buildings*, European Committee for Standardization CEN, Brussels 1993.
Eurocode 6	European Prestandard ENV 1996-1-1:1995. Eurocode 6: *Design of masonry structures. Part 1-1: General rules for buildings – Rules for reinforced and unreinforced masonry*, European Committee for Standardization CEN, Brussels 1995.
Geving (1998)	Geving, S. – *Måling av fukt og varmetekniske materialegenskaper til løs lettklinker* (Measurements of hygrothermal material properties for LECA loose fill materials), Report N 8267, Norwegian Building Research Institute, Trondheim, 1998 (in Norwegian).
Geving and Torgersen (1997)	Geving, S. and Torgersen, S.E. – *Klimadata for fuktberegninger. Referanseår for 12 steder i Norge og klimadata for konstruksjoner mot grunnen* (Climatic data for moisture calculations. Reference years for 12 locations in Norway and climatic data for structures on the ground), Project report 227, Norwegian Building Research Institute, Oslo 1997 (in Norwegian).
Gottfredsen (1997)	Gottfredsen, F.G. – *Laterally Loaded Masonry. Properties and Behaviour*. Dissertation. SBI report 289, Danish Building Research Institute, ISBN 87-563-0976-7, Hørsholm 1997.
Hansen and Mattock (1966)	Hansen, T.C. and Mattock, A.H. – Influence of Size ad Shape of Member on the Shrinkage and Creep of Concrete, *Journal of the American Concrete Institute,* Vol. 63, No. 2, pp. 267-289, 1966.
Haugen (2000)	Haugen, O.P. (Editor) – *Masonry and rendering mortar for LWA masonry. Phase 1: State of the art - LWA masonry*. Exclay project 19.2, as Norsk Leca, Oslo 2000 (restricted).
Hedenblad (1995)	Hedenblad, G. – *Uttorking av byggfukt i betong: torktider och fuktmätning* (Drying of construction water in concrete: drying times and moisture measurement), Byggforskningsrådet 12:1995, Stockholm 1995 (in Swedish).

Herholdt (1979) Herholdt, A. D. (Editor) – *Beton-bogen* (Concrete), Chapter 3, Aalborg Portland, ISBN 87-980816-0-8, Aalborg 1979 (in Danish).

Hillerborg et al. (1976) Hillerborg, A., Modéer, M. and Petersson, P.E. – Analysis of crack formation and crack growth in concrete by means of fracture mechanics and finite elements, *Cement and Concrete Research*, Vol. 6, No. 6, pp. 773-781, 1976.

Hordijk (1992) Hordijk, D.A - Tensile and tensile fatigue behaviour of concrete; experiments, modelling and analyses, *Heron* Vol. 37 No. 1, pp. 1-79 1992.

Hordijk and Reinhardt (1990) Hordijk, D.A. and Reinhardt, H.W. – *Testing and modelling of plain concrete under mode I loading*, Micro Mechanics of failure of quasi brittle materials, Elsevier Applied Science, pp. 559-568, ISBN 1-85166-511-0, 1990.

Hyrve and Madsø (1996) Hyrve, O. and Madsø, F.M. – Materialegenskaper knyttet til konstruktiv bruk av lettklinkerbetongmurverk (Material properties for masonry of lightweight aggregate concrete as a constructive material). *Mur*, No. 4, pp. 13-15, 1996 (in Norwegian).

Høiseth (1999) Høiseth, K.V. – *Uniaxial Tension*, Report no. R-15-99, Department of Structural Engineering – NTNU, Trondheim 1999.

Høiseth (2000a) Høiseth, K.V. – *Uniaxial Tension of Masonry*, Report no. R-3-00, Department of Structural Engineering – NTNU, Trondheim 2000.

Høiseth (2000b) Høiseth, K.V. – *Combined Compression and Shear in Masonry*, Report no. R-11-00, Department of Structural Engineering – NTNU, Trondheim 2000.

Høiseth and Kvande (1999) Høiseth, K.V. and Kvande, T. – Material Modelling of Lightweight Concrete Masonry, *17th Symposium on Nordic Concrete Research*, Icelandic Concrete Association, Reykjavik 1999.

Høiseth and Kvande (2000) Høiseth, K.V. and Kvande, T. – Constitutive properties of Lightweight Aggregate Concrete Masonry, *12th International Brick and Block Masonry Conference*, pp. 1025-1037, Madrid 2000 (see Appendix 6).

Johansen (2000) Johansen, K. – *Testing of cementitious blocks with LECA/Poraver aggregate*. Report no. 32977/1, SINTEF, Trondheim 2000 (restricted).

Johnsen and Solberg (1991) Johnsen, T. and Solberg, B. – Utbygging av beregningsgrunnlaget for murverk. Korte og slanke søyler utsatt for kombinerte lasttilfeller (M-N), (Development of design rules for structural masonry. Columns). Master thesis, Institutt for husbyggingsteknikk – NTH, Trondheim 1991 (in Norwegian).

Johnston (1970) Johnston, C.D. – Strength and deformation of concrete in uniaxial tension and compression, *Magazine of Concrete research*, Vol. 22, No. 70, 1970.

Jong (1992) Jong, P. de – Bouwschade ter lering (I) (Lessons from damage in building industry (I)), *Cement*, No. 2, pp. 26-28, 1992 (in Dutch).

Kvande (1997) Kvande, T. – *Lettklinkerbetongblokker. Måling av porefordeling og termisk dilatasjon* (LECA units. Determination of pore-structure and coefficient of thermal expansion), Project work, Fag 37986 Betongstruktur, Norwegian University of Science and Technology, Trondheim 1997 (in Norwegian).

Kvande (1998) Kvande, T. – *Eksamensarbeid i Informasjonssøking* (Examination paper in Information retrieval). Department of Building and Construction Engineering – NTNU, Trondheim 1998 (in Norwegian).

Kvande (2001-1) Kvande, T. – *Råstoff og materialeigenskapar for tre ulike lettklinkerbetongblokk-kvalitetar. Prøveuttak frå a.s Norsk Leca sitt fabrikkanlegg på Lillestrøm.* (Three different qualities of Light Expanded Clay Aggregate (LECA) Concrete Units: Raw material and material properties). Report N 8330-1, Norwegian Building Research Institute, Trondheim, 2001 (in Norwegian).

Kvande (2001-3) Kvande, T. – *Råstoff og materialeigenskapar for lettklinkerbetongblokk kvalitet 3/770 150x250x500 mm. Prøveuttak frå a.s Norsk Leca sitt fabrikkanlegg på Lillestrøm 17.08.98.* (Light Expanded Clay Aggregate (LECA) Concrete Units, Quality 3/770 150 x 250 x 500: Raw material and material properties). Report N 8330-3, Norwegian Building Research Institute, Trondheim, 2001 (in Norwegian).

Kvande (2001-5) Kvande, T. – *Lengdeendring av lettklinkerbetongblokker på grunn av fukt. Samling av måleresultat frå ulike målingar av svinn og fuktbevegelser på tre ulike blokk-kvalitetar.* (Determination of displacement subjected to change of moisture-content in masonry of LECA. Collection of measurements), Report N 8330-5, Norwegian Building Research Institute, Trondheim, 2001 (in Norwegian).

Kvande (2001-6) Kvande, T. – *Deformation controlled tensile tests on LECA masonry*, Report N 8330-6, Norwegian Building Research Institute, Trondheim, 2001 (see Appendix 5).

Kvande (2001-7) Kvande, T. – *Deformation controlled combined compression and shear tests on LECA masonry*, Report N 8330-7, Norwegian Building Research Institute, Trondheim, 2001 (see Appendix 7).

Kvande (2001-8) Kvande, T. – *Råstoff og materialeigenskapar for lettklinkerbetong-blokk-kvalitet 3/770 100x250x500 mm. Prøveuttak frå a.s Norsk Leca sitt fabrikkanlegg på Lillestrøm 19.01.99.* (Light Expanded Clay Aggregate (LECA) Concrete Units, Quality 3/770 100 x 250 x 500: Raw material and material properties). Report N 8330-8, Norwegian Building Research Institute, Trondheim, 2001 (in Norwegian).

Kvande (2001-9) Kvande, T. – *Determination of creep and shrinkage in LECA masonry.* Report N 8330-9, Norwegian Building Research Institute, Trondheim, 2001 (see Appendix 3).

Leca 1.000 *Leca murverk prosjektering* (Design of LECA masonry), anvisning 1.000, as Norsk Leca, Oslo 1995 (in Norwegian).

Leca teknisk håndbok '99 *Leca teknisk håndbok '99* (LECA technical handbook '99), as Norsk Leca, Oslo 1999 (in Norwegian).

L'Hermite et al. (1949) L'Hermite, R., Chefdeville, J. and Grieu, J.J. – Nouvelle contribution à l'étude du retrait des ciments, *Annales de l'Institut Technique du Bâtiment et de Travaux Publics No. 106, Liants Hydrauliques No. 5*, 1949 (in French).

Lourenço (1996) Lourenço, P. B. – *Computational Strategies for Masonry Structures*. Dissertation, Delft University of Technology, ISBN 90-407-1221-2, Delft 1996.

Lydon and Balendran (1986) Lydon, F.D. and Balendran, R.V. – Some observations on elastic properties of plain concrete, *Cement and Concrete Research*, Vol. 16, pp. 314-324, 1986.

Madsø (1997) Madsø, F.E. – Bevegelser og bevegelsesfuger i murverk. Del 1 (Movement and Movement Joints in Masonry. Part 1), *Mur*, No. 2, pp. 27-30, 1997 (in Norwegian).

Mayer (1972) Mayer, F. – Einfluβ unterschiedlicher Zuschläge auf die Druckfestigkeit und den E-modul von Normalbeton, *Beton*, Vol. 22, No. 2, pp. 61-62, 1972 (in German).

Molnar (2000) Molnar, M. – *In-Plane Tension Behaviour of Horizontally Loaded Masonry. Experimental and Numerical Study*. Licentiate Thesis, Lund University, Lund 2000.

Müller (1993) Müller, H.S. – Considerations on the development of a data base on creep and shrinkage tests, *Creep and Shrinkage of Concrete. 5th International RILEM Symposium*, (Editors: Bažant, Z.P. and Carol, I.) pp. 859-872, Spon, ISBN 0-419-18630-1, London 1993.

Müller and Hilsdorf (1990) Müller, H.S. and Hilsdorf, H.K. – *Evaluation of the time dependent behaviour of concrete; summary report on the work of General Task Group 9*. CEB bulletin d'information No. 199, ISBN 2-88394-005-3, Lausanne 1990.

Neville (1995) Neville, A.M. – *Properties of concrete*, Longman, ISBN 0-582-23070-5, Harlow 1995.

Neville (1995:378) Ibidem, pp. 378-385.

Neville (1995:442) Ibidem, pp. 442-443.

Nilsson (1979) Nilsson, L.O. – *Byggfukt i betongplatta på mark. Torknings- och mätmetoder*. (Drying of concrete floors) Del 1, 2, 3. Tekniska Högskolan i Lund, Lund 1979 (in Swedish).

Norwegian Technical Regulations *Tekniske forskrifter til plan og bygningsloven 1997* (Technical Regulations under the Planning and Building Act 1997) Established by the Ministry of Local Government and Labour. Norsk Byggtjenestes Forlag, ISBN 82-7258-245-7, Oslo 1997 (in Norwegian).

NS 3017 Norwegian Standard NS 3017 – *Lettklinkerbetong. Blokk for muring.* (Lightweight aggregate concrete building blocks), The Norwegian Standards Association, 1. utg. 1970 (in Norwegian).

NS 3120 Norwegian Standard NS 3120 – *Murmørtler. Egenskaper og klassifisering* (Mortars. Properties and Classification), The Norwegian Standards Association, 1. utg. 1998 (in Norwegian).

NS 3473 Norwegian Standard NS 3473: *Prosjektering av betongkonstruksjoner. beregnings- og konstruksjonsregler (innbefattet rettelsesblad AC:1999).* (Concrete structures. Design rules (Corrigendum AC:1999 incorporated)) The Norwegian Standards Association, 5. utg., Oslo 1998 (in Norwegian).

NS 3475 Norwegian Standard NS 3475: *Prosjektering av murverk. Beregning og dimensjonering.* (Masonry structures. Design rules) The Norwegian Standards Association, 1. utg., Oslo 1981 (in Norwegian).

NS-EN 1354 Norwegian Standard NS-EN 1354: *Bestemmelse av trykkfasthet for lettklinkerbetong med åpen struktur* (Determination of compressive strength of lightweight aggregate concrete with open structure), The Norwegian Standards Association, 1. utg., Oslo 1997.

Olsen (1997) Olsen, G.O, - *Trykkprøving av korte lettklinkersøyler. Arbeidsdiagram og trykkfasthet*, (Determination of compressive strength and stress-strain relationship of LECA masonry), Project work, Department of Buildings and Energy, Technical University of Denmark, Lyngby 1997 (in Norwegian).

Olsen (1998) Olsen, G.O, – *Materialegenskaper knyttet til konstruktiv bruk av lettklinkerbetongmurverk.* (LECA masonry in load-bearing constructions), Master thesis, Department of Buildings and Energy, Technical University of Denmark, Lyngby 1998 (in Norwegian).

Pande et al. (1998) Pande, G.N., Middleton, J. and Kralj, B. – *Computer Methods in Structural Masonry – 4*, *Proceedings of the Fourth International Symposium on Computer Methods in Structural Masonry*, Florence, Spon, ISBN 0-419-23540-X, London 1998.

Petersson (1981) Petersson, P.E. – Crack growth and development of fracture zones in plain concrete and similar materials, Dissertation, Report TVBM-1006, Lund Institute of Technology, Lund 1981.

Parrot and Young (1982) Parrot, I.J. and Young, J.F. – Shrinkage and swelling of two hydrated alite pastes, *Fundamental Research on Creep and Shrinkage of Concrete*, (Editor: Wittmann, F.H.), pp. 35-48, Marthinus Nijhoff, ISBN 90-247-2549-6, The Hague 1982.

Pickett (1942) Pickett, G. – The effect of change in moisture content on the creep of concrete under a sustained load, *Journal of the American Concrete Institute* Vol. 38 pp. 333-355, 1942.

Pihlajavaara (1974) Pihlajavaara, S.E. – A review of some of the main results of a research on the ageing phenomena of concrete: effect of moisture conditions on strength, shrinkage and creep of mature concrete, *Cement and Concrete Ressearch*, No. 4, pp. 761-771, 1974.

Pihlajavaara (1982) Pihlajavaara, S.E. – Chapter 4: Estimation of Drying of Concrete at Different Relative Humidities and Temperatures of Ambient Air with Special Discussion about Fundamental Features of Drying and Shrinkage, *Creep and Shrinkage in Concrete Structures*, (Editors: Bažant, Z.P. and Wittmann, F.H.) Wiley & Sons, ISBN 0 471 10409 4, New York 1982.

Pittmann and Ragan (1998) Pittmann, D.W. and Ragan, S.A. – Drying Shrinkage of Roller-Compacted Concrete for Pavement Applications, *ACI Materials Journal*, Vol. 95, No. 1, 1998.

Pluijm (1999) Pluijm, R. van der – *Out-of-Plane Bending of Masonry. Behaviour and Strength*, Dissertation, Technische Universiteit Eindhoven, ISBN 90-6814-099-X, Eindhoven 1999.

Pluijm et al. (2000) Pluijm, R. van der, Rutten, R., Ceelen, M. – Shear behaviour of bed joints, *12th International Brick and Block Masonry Conference*, pp. 1849-1862, Madrid 2000.

Pluijm and Vermeltfoort (1991) Pluijm, R. van der, Vermeltfoort, A.Th. - *Deformation Controlled Tensile and Compression Tests on Units, Mortar and Masonry*, TNO-report B-91-0561, 1991 (in Dutch).

prEN 998-2:2000 Draft European Standard prEN 998-2: *Specification for mortar for masonry. Part 2: Masonry mortar*, European Committee for Standardization CEN, Brussels 2000.

prEN 1015-11:1995 Draft European Standard prEN 1015-11: *Method of test for mortar for masonry - Part 11: Determination of flexural and compressive strength of hardened mortar*, European Committee for Standardization CEN, Brussels 1995.

prEN 1052-1:1995 Draft European Standard prEN 1052-1: *Method of test for masonry - Part 1: Determination of compressive strength*, European Committee for Standardization CEN, Brussels 1995.

prEN 1520:1999 Draft European Standard prEN 1520: *Prefabricated reinforced components of lightweight aggregate concrete with open structure,* Final draft, European Committee for Standardization CEN, Brussels 1999.

Rots (1997) Rots, J.G (Editor) – *Structural Masonry. An Experimental/Numerical Basis for Practical Design Rules*. CUR, Balkema, ISBN 90 54-10-680-8, Rotterdam 1997.

Sabri and Illston (1982) Sabri, S. and Illston, J.M. – Isothermal drying shrinkage and wetting swelling of hardened cement paste, *Fundamental Research on Creep and Shrinkage of Concrete*, (Editor: Wittemann, F.H.), pp. 63-72, Marthinus Nijhoff, ISBN 90-247-2549-6, The Hague 1982.

Sellevold (1993) Sellevold, E.J. – Svind/svellning. Fysiske mekanismer. (Shrinkage/ swelling. Physical processes), UM 8 Fag 37986 Betongstruktur, Norwegian University of Science and Technology, Trondheim 1993 (in Danish).

Schjølberg (1987) Schjølberg, K.E. – Samvirket mellom stein og mørtel i teglmurverk. (Interaction between brick and mortar in clay-brick masonry), Dissertation, The Norwegian Institute of Technology, Trondheim 1987 (in Norwegian).

Schubert (1988) Schubert, P. – Zur rissfreien Läge von nichttragenden mauerwerks-wänden. *Mauerwerk-kalender 1988*, pp. 473-488, Ernst & Sohn, Berlin 1988 (in German).

Schubert (1992) Schubert, P. – Strength and deformation properties of masonry made from lightweight concrete units, *6th Canadian Masonry Symposium,* University of Saskatchewan, pp. 489-498, Saskatoon 1992.

Schubert (1994) Schubert, P – Test methods for the determination of creep and shrinkage in masonry, *10th International Brick and Block Masonry Conference*, Masonry Council of Canada, The University of Calgary, Calgary, pp. 777-786, 1994.

Shimomura and Maekawa (1997) — Shimomura, T. and Maekawa, K. – Analysis of the drying shrinkage behaviour of concrete using a micromechanical model based on the micropore structure of concrete, *Magazine of Concrete Research*, Vol. 49, No. 181, 1997.

Stemland and Thorenfeldt (1998) — Stemland, H. and Thorenfeldt, E. – *Lett konstruksjonsbetong* (Lightweight concrete), Delprosjekt 2: Konstruktive aspekter, Delrapport 2.1: Superlette betongkvaliteter, Report STF22 A98742, SINTEF, Trondheim 1998 (in Norwegian).

Sturman et al. (1965) — Sturman, G.M., Shah, S.P. and Winter, G. – Microcracking and inelastic behaviour of concrete, *Proceedings of the International Symposium on Flexural Mechanics of Reinforced Concrete*, ASCE-1965-50 and American Concrete Institute ACI SP-12, pp. 473-499, Detroit 1965.

Svendsen et al. (1966) — Svendsen, S. et al – (*Mørtel - Mur - Puss)* (Mortar - Masonry - Rendering), Handbook 20, Norwegian Building Research Institute, Oslo 1966 (in Norwegian).

Waldum et al. (1993a) — Waldum, A.M. et al – *Prosjektet "sprekkfri utførelse av Leca Isoblokkvegg"* (Masonry of LECA sandwich units. Making crack-free façades), Report O 3583, Norwegian Building Research Institute, Trondheim 1993 (in Norwegian, restricted).

Waldum et al. (1993b) — Waldum, A.M., Askeland, A. and Vesterlid, A. – *Keramiske fliser på betongunderlag* (Tile glued to concrete flooring), Project report 139, Norwegian Building Research Institute, Oslo 1993 (in Norwegian).

Waldum (1998) — Waldum, A.M. – *Sprekkfrie fasader med Leca Isoblokk. Krav til mur- og pussmørtel* (Masonry of LECA sandwich units. Rendering mortars for crack-free façades), Report O 8227, Norwegian Building Research Institute, Trondheim, 1998 (in Norwegian, restricted).

Wischers and Lusche (1972) — Wischers, G. and Lusche, M. – Einfluβ der inneren Spannungs-verteilung auf das Tragverhalten von druckbeanspruchtem Normal- und Leichtbeton, *Beton*, Vol. 22, No. 8 pp. 343-347 and No. 9, pp. 397-403, 1972 (in German).

Wittmann (1982) — Wittmann, F.H. – Chapter 7: Creep and Shrinkage Mechanisms. *Creep and Shrinkage in Concrete Structures*, (Editors: Bažant, Z.P. and Wittmann, F.H.) Wiley & Sohns, ISBN 0-471-10409-4, New York 1982.

Wittmann et al. (1987) — Wittmann, F.H. et al. – Influence of age at loading, water/cement ratio and rate of loading on fracture energy of concrete, *Materials and structures*, Vol. 20, pp. 103-110, 1987.

Ziegeldorf et al. (1979) — Ziegeldorf, S., Kleiser, K. and Hilsdorf, H.K. – Vorherbestimmung und Kontrolle des thermischen Ausdehnungskoeffizienten von Beton. *Schriftenreihe des Deutschen Ausschuβ für Stahleton*, No. 305, pp. 1-35, 1979 (in German).

Zijl (1996) — Zijl, van G.P.A.G – *Shear transfer across bed joints in masonry: A numerical study*, Technical report 03.21.0.22.28, Delft University of Technology, Delft 1996.

Zijl (2000) — Zijl, van G.P.A.G – *Computational Modelling of Masonry Creep and Shrinkage*. Dissertation, Delft University of Technology, ISBN 90-9013475-1, Delft 2000.

APPENDIXES

Reading guide for appendixes

Appendix 1

Kvande, T.
A Brief Presentation of Norwegian LECA Masonry.
Unpublished.

Appendix 2

Kvande, T. and Conradi, T.
The Influence of Curing Conditions on Shrinkage and Compressive Strength of Masonry Units of LWA Concrete.
Submitted for publication in Masonry International, November 2000.

Appendix 3

Kvande, T.
Determination of Creep and Shrinkage in LECA Masonry.
Report N 8330-9, Norwegian Building Research Institute, Trondheim 2001.

Appendix 4

Kvande, T., Vermeltfoort, A.T., Pluijm, R. van der and Høiseth, K.V.
Tensile Creep Behaviour of LWA Masonry.
Submitted for publication in Masonry International, November 2000.

Appendix 5

Kvande, T.
Deformation Controlled Tensile Tests on LECA Masonry,
Report N 8330-6, Norwegian Building Research Institute, Trondheim 2001.

Appendix 6

Høiseth, K.V. and Kvande, T.
Constitutive Properties of Lightweight Concrete Masonry,
12th International Brick and Block Masonry Conference, Madrid 2000.

Appendix 7

Kvande, T.
Deformation Controlled Combined Compression and Shear Tests on LECA Masonry,
Report N 8330-7, Norwegian Building Research Institute, Trondheim 2001.

Appendix 8

Kvande, T. and Høiseth, K.V.
Behaviour of LECA Masonry under Restrained Shrinkage.
Submitted for publication in Masonry International, January 2001.

READING GUIDE FOR APPENDIXES

Appendix 1

The appendix gives general information about LECA masonry. The author is Tore Kvande.

Appendix 2

The enclosed investigation of curing conditions influence on shrinkage and compressive strength of LECA blocks is based on a limited number of specimens and on only one quality of LECA blocks. That should be noted reading the conclusions. The results is given as mean values. Three blocks were exposed to each climate condition. Totally the mean values were based on nine shrinkage measurements. The coefficient of variations of shrinkage of the different test series were less than 20 %, see Table 1. Due to the equality of the measurement no advanced statistics analysis were carried out. The results seems to indicate that an early drying of LECA masonry blocks does not significantly influences the compressive strength of the blocks.

Table 1
Determined coefficient of variation from the test.

Series number	Drying shrinkage [1]			Moisture expansion [1]	Moisture content [2]	Dry density [2]	Compressive strength [2]
	after 28 days	at 33°C and 25 % RH	at 80°C				
	[%]	[%]	[%]	[%]	[%]	[%]	[%]
A, unit 2,4 & 6	11	-	-	5	3	5	21
A, unit 1,3 & 5	18	5	5	-	3	3	9
B	11	10	10	5	1	1	10
C	20	9	11	7	9	7	21
D	6	6	7	8	7	2	5
E	13	6	6	4	8	1	9
F	-		8 - 10 [3]	4 - 7 [3]	10	3	-

[1] Based on nine measurements.
[2] Based on three measurements.
[3] Dependent of cycle.

The work was partly carried out as a student project by *Thorbjørn Conradi*. *Tore Kvande* took the initiative to the student project by describing the problem and he has also been the teaching supervisor. Some additional shrinkage measurement including the irreversible shrinkage measurement and the determination of compressive strength are carried out afterwards the student project. The article is written by Tore Kvande. All tables and figures are made by Tore Kvande.

Concerning reference 9:

See Neville, A.M. – *Properties of concrete*, pp. 442, Longman, Harlow 1995.

Concerning reference 10:

See Kvande, T. – *Jamførande prøving av trykkfasthet. Prøving utført ved a.s Norsk Leca Lillestrøm og Institutt for bygg- og anleggsteknikk, NTNU* (Comparative test of compressive strength), Report N 8330-9, Norwegian Building Research Institute, Trondheim 2001 (in Norwegian).

Concerning reference 11:

Technical documentation of the cement used in LECA blocks is for the time being (01.02.2001) found at http://www.norcem.no/kunde/fa.pdf.

Appendix 3

The appendix describes an experimental determination of the behaviour of LECA masonry subjected to creep and shrinkage. The author is Tore Kvande.

Appendix 4

The work gives a study of the creep behaviour of LECA masonry loaded in tension in the longitudinal direction of the masonry. The submitted article is based on the work presented in Kvande (2001-9), see Appendix 3. That is why there are a lot of overlap concerning the tensile creep in Kvande (2001-9). In addition to Kvande (2001-9) results from ESPI measurements and a linear-elastic analysis are incorporated in the article.

Ad Th. Vermeltfoort has taken care of the ESPI measurement by writing i.a. Chapter 3.3, third section of Chapter 3.4 and fourth section of Chapter 4. He is also responsible for Figure 3 and 6.

Rob van der Pluijm has contributed in the planning of the research.

Karl Vincent Høiseth has made Figure 7 and 8.

Tore Kvande have been responsible for this part of the project. He took the initiative, planned and co-ordinated the work and he has been the main writer of the article.

All the authors have contributed by improving the outlines made of Tore Kvande.

Concerning reference 12:

See Eibl et al. – *Concrete Structures. Euro-Design Handbook*, Chapter A6.2.2 and A6.5.3.3 (the first one), Ernst & Sohn, Berlin 1995.

Appendix 5

The appendix gives an overview of deformation controlled tensile tests carried out on LECA blocks as well as on small specimens of LECA masonry. The author is Tore Kvande.

Appendix 6

The paper deals with the uni-axial stress-strain relationship of LECA blocks and masonry. The purpose of the study was to demonstrate the capability to reproduce experimental observations by numerical simulations.

Karl Vincent Høiseth has carried out the numerical simulations with DIANA and been the main writer of the paper.

Tore Kvande took the initiative to the work and contributed in the accomplishment of the work by frequent discussions. All experimental data is delivered by Tore Kvande.

Concerning reference 4:

> See Kvande, T. – *Deformation controlled tensile tests on LECA masonry,* Report N 8330-6, Norwegian Building Research Institute, Trondheim 2001.

Appendix 7

The appendix gives an overview of deformation-controlled combined compression and shear tests carried out on LECA masonry. The author is Tore Kvande.

Appendix 8

The submitted article deals with an investigation of the shrinkage behaviour of LECA masonry restrained to the bottom by a foundation.

Tore Kvande is the main author of the submitted article. He took the initiative to this work and has been responsible for the planning and accomplishment of the research.

Karl Vincent Høiseth has contributed in the planning of the research.

APPENDIX 1

Kvande. T.
A Brief Presentation of Norwegian LECA Masonry.
Unpublished.

A Brief Presentation of Norwegian LECA Masonry

by

TORE KVANDE
Department of Building and Construction Engineering, Norwegian University of Science and Technology

Introduction

Masonry made from Light Expanded Clay Aggregate (LECA) concrete blocks is by far the most commonly made masonry in Norway today. LECA is a type of lightweight aggregate (LWA). This paper gives a brief presentation of the manufacture of LECA blocks and typical material properties of the masonry. Finally, the paper tries to identify some of the reasons why this type of masonry has gained such popularity in Norway.

Background

In Norway production of LECA masonry started in the early 1930s. In those days with most of the aggregate and also some of the blocks were imported. Since 1954 both aggregate and blocks have mainly been produced in Norway. Today the company Norsk Leca is the only producer of both aggregate and blocks in Norway. About 15 % of the Norwegian LECA masonry market is today covered by imported LECA blocks by BMC.

Traditionally, masonry made from LECA blocks are used as basement walls in private dwellings (Figure 1a), outer walls above the ground (Figure 1b), fire-resistant walls, sound-insulated walls, etc.

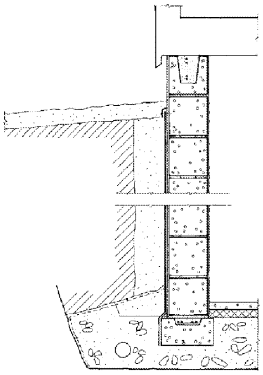

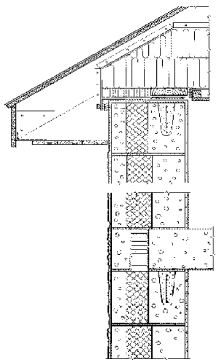

Figure 1
a) Typical Norwegian basement wall.
b) Outer wall with connections between flooring and roof.

Stovepipes and floor elements are other prefabricated products in the Norwegian market made of LECA concrete. In addition loose LECA pellets are used for thermal insulation of floors and roofs, lightweight railway- and roadbed fillings and as a cleansing agent for water.

Today, 1.0 – 2.0 million m² LECA masonry is produced annually. The amount is calculated from the production volume divided by an average wall thickness of 220 mm. 1.0 – 2.0 million m² represent almost 80 % of the total annual masonry market in Norway. According to the production volume, as much as 80 million m² wall may be built of LECA masonry in Norway since 1954.

Production of LECA blocks

Today, light expanded clay aggregate is produced in Norway at two locations. LECA blocks are manufactured at six locations. The production consists of blocks with dry net density between 600 and 1300 kg/m³ and corresponding compressive strength of block between 2 and 8 N/mm². The density depends on product and area of application. Block qualities "2/600" and "3/770" are by far most common. Number 2 and 3 indicate a gross compressive strength of the blocks of approximately 2 and 3 N/mm², while 600 and 770 indicate a dry net block density of about 600 and 770 kg/m³.

The aggregate is made from clay in a rotary kiln. Suitable clay for production of aggregate is fine-grained with minimum 35 % of the grains smaller than 2 μm and no large grains. The clay should be of great plasticity and contain a minimum of calcium. Typical contents is 55 – 78 % SiO_2, 12 – 25 % Al_2O_3 and minimum 6 % Fe_2O_3.

Prior to being fed into the rotary kiln, the clay is thoroughly kneaded together with petroleum and some additives. The rotary kiln is divided into a drying zone, a burning zone and a cooling zone. In the drying part rotation and cutting devices divide the clay into small pellets. The pellets expand like popcorn at about 1100 – 1200 °C making aggregate containing 70 – 75 volume-% air pores with a ceramic shell. At 1100 – 1200 °C the clay almost reaches its melting point. Expansion of the clay pellets is caused by release of gas when transformation of the clay mineral occurs and lack of oxygen in the burning zone. By controlling the process of expansion, LECA with a specified dry loose bulk density between 200-900 kg/m³ may be produced.

The masonry concrete units are mainly made of LECA together with small amounts of natural sand, cement, silica fume and water. Normally, LECA with diameter 4 – 10 mm and dry loose bulk density of 250-350 kg/m³ represents most of the volume. Blocks with the highest density also contain an important part of natural sand. By mainly using aggregate with diameter between 4 and 10 mm it is possible to obtain the typical porous concrete structure of the Norwegian LECA blocks. Typically for LECA concrete with density 600-900 kg/m³, cement paste and silica gel represent about 8 % of the total volume of the LECA concrete, while LECA represents about 55 – 60 % and sand about 10 – 15 %. The rest of the volume is formed by voids.

The LECA blocks are produced in fully automated and computerised plants. A principal sketch of a typical production line is shown in Figure 2. From the silos correct dosage of the constituents are transported to the mixer. The fresh LECA concrete is moulded with great accuracy and the units are directly transported to the curing chamber after being released from the mould. Addition of steam makes an initial climate in the chamber of approximately 50 °C and 100 % RH. The temperature is gradually reduced during the time inside the chamber.

After 1-2 days in the curing chamber the LECA blocks are loaded onto pallets and wrapped with plastic foil, see Figure 2. The blocks are relatively humid when they arrive from the

curing chamber. The wrapping ensures favourable moisture content for hydration of the blocks. The plastic wrapping also protects the blocks against rain and snow, as well as holding them together during transportation. Normally, the pallets are stored outdoors for at least four weeks before transportation to the building site.

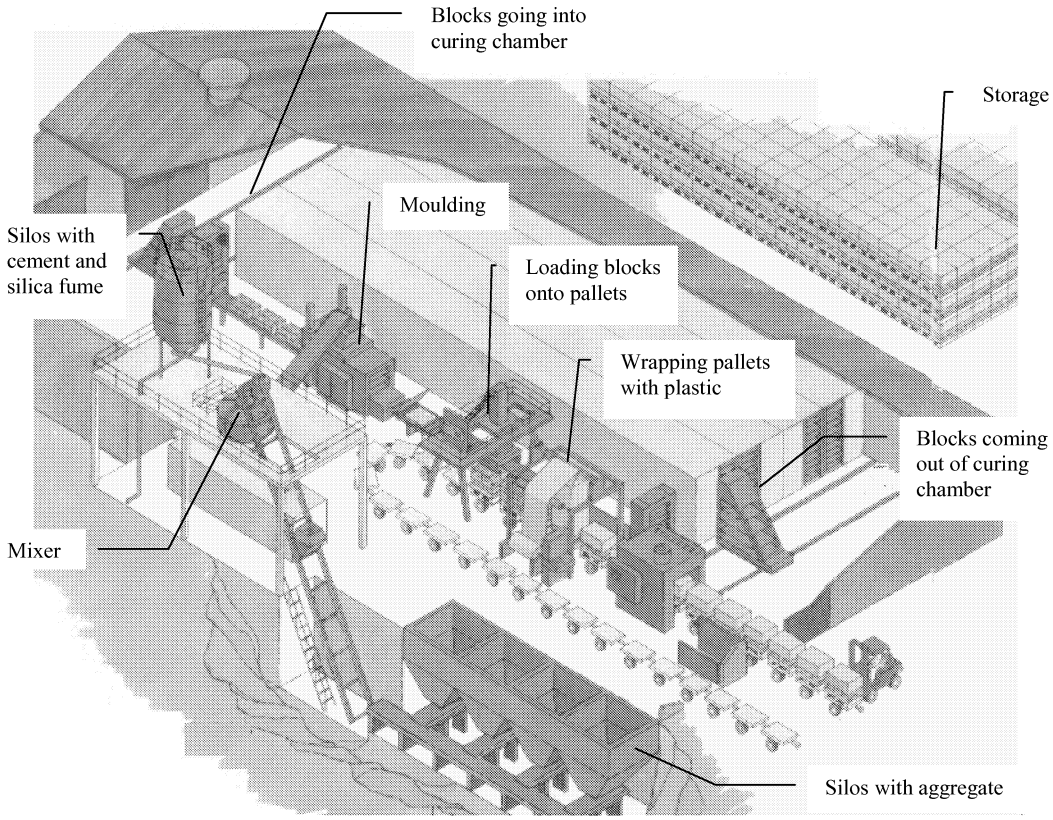

Figure 2
Example of factory making LECA blocks.

Altogether some 30 different types of LECA blocks are produced for the Norwegian market. Some typical blocks can be viewed in Figure 3. Blocks number three and four from the left in the figure (*Sandwich-blocks*) are probably the most special. The blocks contain thermal insulation between two thin blocks made of LECA concrete. By filling the three last blocks with reinforcement and concrete block 5 and 6 from the left are used as lintels and rims, while the last one is used for footing.

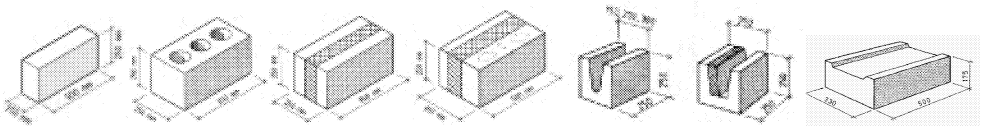

Figure 3
Some typical Norwegian LECA blocks.

The thermal-insulation-blocks are produced in special production plants. The thin LECA parts are taken directly from the curing chamber and automatically placed in pairs on a conveyor belt. On the conveyor belt the pairs of blocks are foam-bonded together with polyurethane. The polyurethane is suitably cured during the time it takes to pass the conveyor.

Material properties

Typical for LECA masonry is the combination of [1]:

- low density,
- adequate load-bearing capacity,
- low water absorption,
- high frost resistance,
- favourable base for rendering and plastering,
- thermal insulation,
- high fire resistance,
- advantageous sound insulation and
- resistance to chemicals.

Some quality specifications are listed in Tables 1 and 2. The tables are based on [2,3,4,5,6,7].

Table 1
Typical material properties of LECA masonry [2, 3, 4, 5, 6].

Material property	Value	
Coefficient of thermal expansion	0.008	mm/(m°C)
Moisture expansion or shrinkage	0.15 – 0.40	mm/m
Vapour permeability	30 – 60	10^{-12} kg/(msPa)
Water absorption	12 – 20	volume-%
Thermal conductivity (density 600-900 kg/m³)	0.20 – 0.27	W/(mK)

Table 2
Typical material properties for masonry made from LECA concrete blocks [2, 3, 7].

Density, net [kg/m³]	Compressive strength [N/mm²]	Thickness of wall [mm]	Thermal resistance [m²K/W]	Side of the wall with rendering/ plastering [-]	Sound reduction index [dB]	Classification of fire resistance [-]
600	2	300	1.65	2	abt. 53	REI-M 240
770	2-3	150	0.66	2	abt. 45	REI-M 240
		250	1.11	2	abt. 52	REI-M 240
900 [1)]	4	-	-	-	-	-
1 300	8	175	0.32	2	abt. 52	REI-M 240
		250	0.46	2	abt. 55	REI-M 240

[1)] Produced specially as leafs for thermal insulated blocks.

The special thermal-insulated blocks are produced with thicknesses of 250 and 300 mm. By making masonry of such blocks it is possible to achieve thermal transmittance of 0.26 and 0.22 W/(m²K) respectively. Using ordinary blocks with density 770 kg/m³ and thickness 250 mm it is possible to achieve thermal transmittance of 0.80 W/(m²K).

Closing remarks

In the last few decades, LECA masonry has totally dominated the market for basement walls. The success was mainly based on the "do it yourself"/private market. By making a product concept including literally everything you needed to facilitate making your own basement wall, the system was quite unique in Norway. Today, the concept covers "all types" of masonry units including special blocks for footings, lintels, rims, corners and thermal-insulation blocks. It also includes all kinds of mortar and supplements, for example, reinforcement and equipment to cut blocks and to distribute mortar in the bed face. Thanks to the product concept, building LECA masonry is quick and simple. The size of the blocks, and the fact that such masonry is usually made without mortar in the perpend joints, makes it possible to build much faster than for example brickwork.

However, the success is not only based on the LECA masonry itself. Teaching people how to make the masonry is another essential factor. By holding brief practical lessons and making illustrative brochures, many people have been persuaded to make their own house, garage or basement wall using LECA blocks.

The leading producer in Norway has made LECA masonry easy to build and economically competitive. Together with favourable material properties, individual attention to customers and skilled marketing, the result is a masonry concept with a good reputation in Norway today.

Acknowledgements

The financial support of The Research Council of Norway and Norsk Leca is gratefully acknowledged. Thanks are also due to Arne Monsen and Ole Petter Haugen for their important contribution of information.

References

[1] Haavaldsen, T. et al. – *Dimensjonering av murkonstruksjoner etter NS 3475* (Design of masonry structures), Institutt for husbyggingsteknikk-NTH, Trondheim 1991 (in Norwegian).

[2] *Murkatalogen* (Masonry catalogue), Mur-Sentret, Oslo (in Norwegian).

[3] *Byggforskserien* (Building Research Design Sheets), Norwegian Building Research Institute, Oslo (in Norwegian).

[4] European Prestandard ENV 1996-1-1 Eurocode 6: *Design of masonry structures – Part 1-1: General rules for buildings – Rules for reinforced and unreinforced masonry*, European Committee for Standardization, Brussels 1995.

[5] Norwegian Standard NS 3031: *Varmeisolering. Beregning av bygningers energi- og effektbehov til oppvarming og ventilasjon* (Thermal insulation. Calculation of the energy and power demand for heating and ventilation in buildings), The Norwegian Standards Association, 4. utg. Oslo 1987 (in Norwegian).

[6] Svendsen, S. et al. – *Mørtel - Mur - Puss* (Mortar - Masonry - Rendering), Håndbok 20, Norwegian Building Research Institute, Oslo 1966 (in Norwegian).

[7] *Leca teknisk håndbok ’99* (LECA technical handbook ’99), as Norsk Leca, Oslo 1999 (in Norwegian).

APPENDIX 2

Kvande. T. and Conradi, T.
The Influence of Curing Conditions on Shrinkage and Compressive Strength of Masonry Units of LWA Concrete.
Submitted for publication in Masonry International in November 2000.

The Influence of Curing Conditions on Shrinkage and Compressive Strength of Masonry Units of LWA Concrete

by

T. KVANDE and T. CONRADI
Department of Building and Construction Engineering, Norwegian University of Science and Technology

ABSTRACT

To reduce the risk of cracking of masonry it is important to use relatively dry units when making the masonry. But, too early drying of concrete may reduce the final strength by influencing the curing conditions. The main purpose of the presented investigation in this paper was to study the effect of different curing conditions on shrinkage and compressive strength of masonry units of lightweight aggregate (LWA) concrete. Masonry units from the same production batch were exposed to five different climate conditions during the first month after arriving from the production line. The different curing conditions did not significantly influence the total drying shrinkage or the compressive strength. To reduce the risk of cracking of masonry made of LWA concrete blocks, it is recommended to dry the blocks as early as possible after they have left the curing chamber.

1. INTRODUCTION

In Norway, Light Expanded Clay Aggregate (LECA) concrete blocks are by fare the most popular units for masonry. LECA is a type of lightweight aggregate (LWA). The blocks are produced by fully automated and computerised plant, where fresh blocks spend 1 to 2 days in a curing chamber (50°C, 100 % RH) before they are loaded onto pallets and wrapped with plastic. The LECA blocks are relatively humid when they arrive from the curing chamber. The wrapping ensures favourable moisture content for hydration of the blocks. The plastic wrapping also protects the blocks against rain and snow, as well as holding them together during transportation.

Before transportation to the building site, the pallets are stored outdoor at the factory, normally for about four weeks. For economic reasons, the producer does not want to store the blocks longer. The outdoor storage influences the curing conditions. The temperature varies over the season, while the moisture content is more stable because of the plastic wrapping.

The risk of cracks in masonry walls normally increases with increased moisture content of the masonry units. This is due to the fact that changes in climate conditions influences the strain within the masonry [1]. The ambient humidity of concrete influences both the development rate and the ultimate value of "delayed strain" [2]. To reduce the ultimate value of shrinkage strain in concrete block masonry, it is required to reduce the moisture content of the blocks before making the wall. Unfortunately, an early reduction of the moisture content of the concrete blocks may negatively influence the hydration conditions. Hence, an apparent conflict appears between reducing shrinkage and maintaining strength.

In this paper, shrinkage will be used to denote changes in length or strain due to loss of moisture from masonry unit.

2. OBJECTIVE

The purpose of this investigation was to quantify the effect of an early drying of concrete blocks on compressive strength and shrinkage of the LECA blocks. Therefore, LECA blocks were stored under five different curing climates. Deformation of the blocks was measured frequently during the whole test. Afterwards, the blocks were dried and the compressive strength was measured.

3. TEST PROCEDURE

Norsk Leca produced the LECA blocks tested in this investigation. These blocks are mainly made of LECA, sand, cement, silica and water. By mainly using LECA with diameter between 4 and 10 mm it is possible to obtain the typical porous concrete structure of the Norwegian LECA blocks. After moulding, the blocks are transported directly to the curing chamber. Addition of steam makes an initial climate in the chamber of approximately 50°C and 100 % RH. The temperature is gradually reduced in the chamber. Usually the blocks are kept inside the curing chamber for 1-2 days. Typical material properties of the tested blocks are shown in Table 1.

Immediately after the LECA blocks arrived from the curing chamber, the specimens were picked out from the production line and gauge location pads were glued on them. Measurements of deformation were carried out on each face of the unit and on the bed face turned up during the production (see Figure 1). After gluing of gauge location pads, initial weight and length were recorded and the specimens were transported closed covered with plastic to the lab at Norwegian University of Science and Technology (NTNU). Shrinkage was measured with a Demec gauge (demountable mechanical gauge) with a gauge length of 250 ±1 mm. The specimens were stabilised at 20°C before the first measurement.

During the first 28 days after the production, series of specimens were exposed to five different climate conditions. Test Series A was tested according to prEN 772-14 [4] (two weeks in airtight bags and then two weeks in air at $\geq$ 15 °C and $\leq$ 65 % RH). Series B was exposed to an early drying. Series C was stored at an "ideal" curing climate (wrapped with plastic at 20°C), while Series D (25°C and 50 % RH) and Series E (3°C and 85 % RH) were exposed to climate conditions between Series B and C. Three specimens were prepared for each series. The complete environmental history of each test series is given in Table 2.

After the initial four weeks of curing, all specimens were dried at 33°C and 25 % RH to stabilise the weight. Deformation and weight were measured frequently. When the weight was stabilised, moisture expansion was measured after having stored the blocks in water. Thereafter, the blocks were dried at 80°C. The length of the dry specimens was measured after the specimens had been cooled down to 20°C. These measurements were carried out approximately 6 hours after the specimens had left the heater.

The last series (F), was cyclicly soaked in water and dried to determine reversible moisture movement (five cycles). This part of the test program was carried out with four months old specimens. The blocks were close covered with plastic at 20°C during the four months storage. The length of the dry specimens was measured after the specimens had been cooled down to 20°C.

Finally, compressive strength of the LECA blocks was measured according to prEN 772-1 [5].

4. RESULTS

In the following, a negative elongation expresses a decreasing length (shrinkage) and a positive elongation an increasing length (moisture expansion). The moisture movement and weight change of the specimens developed differently for the six series during the first four week in individual climate and during the following drying period at 33°C and 25 % RH (Figure 2 and 3). At the end of the test program, the total shrinkage of all series stabilised at about the same level. The two figures also show that the weight of the specimens was stabilised earlier than the length.

During the first 28 days, the different series lost different amount of weight (Figure 3). Compared with the change of weight (Figure 3), a larger difference of displacement was expected during the same period. The results seem a bit confusing because the length was measured in the current environment of the different series. Consequently, the results are influenced by the thermal expansion of the concrete. The drying shrinkage of Table 3 is adjusted for deviation in temperature from 20°C by using a coefficient of thermal expansion of 0.008 mm/(m°C) [6]. It can be seen that different climate conditions during the first 28 days after production cause a great variation of moisture movement between the series. However, no significant difference of the final drying shrinkage was recorded after the drying at 33°C and 25 % RH. A drying shrinkage of approximately –0.45 mm/m was obtained for all test series. It should be noted that the tests probably were stopped too early to reach the finale value of shrinkage.

Table 3 also includes the moisture expansion, the moisture content at the beginning of the test, the dry density and the compressive strength of each series after the various stage of the test program. Also results from Series F, exposed to cyclic soaking in water and drying at 80°C, are shown in the table. The coefficient of variation of the elongation of series F was less than 10 %. The coefficients of variations for the rest of the measurement were less than 20 %.

Series number A was tested according to prEN 772-14 [4]. A moisture expansion coefficient of 0.26 mm/m (after 96 hours) and a drying shrinkage coefficient of 0.20 mm/m (after 21 days) were recorded. Hence, the total movement coefficient was found to be 0.46 mm/m.

A detailed overview of the moisture movements is given in [7].

5. DISCUSSION

After arriving from the production line, blocks were exposed to one extreme moisture conditions, the 25 % RH (Series B). Covering in plastic (Series C) should represent an "ideal" curing condition similar to the intended situation today, while the environment with 50 % RH (Series D) and 85 % RH (Series E) are between the extreme and the ideal curing climate. Further drying of the specimen from 25 % RH at 80°C did not increase the drying shrinkage significantly. Only an additional shrinkage of 0.05 mm/m was recorded. The low additional displacement may be influenced by a high water/cement-ratio (w/c-ratio > 0.7) of the concrete and the size of the pores in the aggregate [8].

About the same drying shrinkage was recorded for Series B and D after 28 days. This is due to the fact that equilibrium moisture content of concrete is for practical purpose constant within 10-50 % RH [8].

Cyclic soaking of the specimens in water followed by drying at 80°C revealed that the moisture expansion was approximately the same for each cycle. During the first cycle, an additional drying shrinkage of 0.10 mm/m was recorded. No significant difference between the next four cycles was recorded. Hence, a reversible shrinkage of about 0.45 mm/m was recorded. The obtained reversible shrinkage fit very well with the moisture movement recorded according to prEN 772-14 [4]. The large initial irreversible shrinkage is probably caused by the formation of new links in the cement gel when the particles are in closer contact upon shrinkage [9].

An early drying worsens the curing condition for the concrete blocks. Different climate conditions during the first 28 days after production was therefore expected to influence the strength of the blocks. However, the compressive strength of the different series listed in Table 3 gives no definite answer about the effect of different curing conditions. A more clarified picture appears when the measured compressive strength is presented as a function of the density of the blocks. Figure 4 shows the correlation between compressive strength and density based on the results from this test program and results from another test program [10]. Compressive strength from [10] are measured in accordance with prEN 772-1 [5] on blocks from a similar production batch as used in this program. The figure shows that the compressive strength is strongly influenced by the density of the blocks. Linear trends are calculated assuming a linear relation between density and compressive strength within the limited dispersion of density. A gradient of $9.4 \cdot 10^{-3}$ is calculated for the results from all blocks of this test program (A-E). In comparison, a gradient of $9.6 \cdot 10^{-3}$ is calculated for the results from [10]. The fact that the two gradients are practically identical indicates that the climate conditions during the first 28 days after the production has insignificant effect on the compressive strength of the LECA blocks.

The results from this test program show that the compressive strength of the blocks is mainly build up during the time inside the curing chamber. According to the technical documentation [11] of the cement used in LECA blocks, 43 % of the total 28 days compressive strength has been established after one day only. The similar shares for two and seven days storage is 57 % and 76 %, respectively. The results reported in [11] are determined on mortar specimens in accordance with [12]. When no significant difference in compressive strength was recorded during the present investigation, it may be explained from the compound of the blocks. Cement paste and silica gel represent about 8 % of the total volume in the masonry units, while LECA represents about 55 – 60 % and sand about

10 – 15 %. The rest of the volume is air pores. The compressive strength of the blocks mainly depends on the LECA (density, shape and strength of the aggregate grain and particle size distribution). The aggregate with the greatest diameter make a load-bearing skeleton glued together by the cement paste and the silica gel. The fine grained aggregate make it possible for the fresh concrete to retain its shape from the moulding, but may not contribute very much to the finale compressive strength of the unit. The effect of the gluing built up during the time inside the curing chamber is strong enough to keep the skeleton together. Further hydration may not contribute very much to the compressive strength because the weakest parts are already the large grain aggregates and the structure of the load-bearing skeleton itself. This theory is supported by observation during the test of compressive strength of the blocks. Testing of compressive strength revealed that the failure appears largely through the aggregate. Measurements of compressive strength carried out 7 and 28 days after the production do not show a significant increasing of compressive strength.

The investigation that is reported in this paper, concerns only one quality of LECA concrete. Future research should also include other qualities of LECA blocks. Furthermore, a practically and economically arrangement to expose the LECA blocks to an early drying may be developed.

6. CONCLUSIONS

The results from this test program shows that the climate conditions where the LECA blocks were exposed to during the first month after arriving from the curing chamber, did not significantly influence the final drying shrinkage of the blocks. Neither did the climate conditions significantly influence the compressive strength of the concrete blocks. Variation of compressive strength recorded during this test program was explainable by the variation of density of the blocks.

The results have shown that an early drying of LECA concrete blocks does not significantly influences the compressive strength of the blocks. Since the use of relatively dry blocks when making masonry will reduce the risk of cracking, it is recommended to dry the LECA blocks as early as possible after they have left the production line.

ACKNOWLEDGEMENTS

The Research Council of Norway and Norsk Leca has financially supported this study. The authors gratefully acknowledge this support. Thanks also due to Noralf Bakken for his help in carrying out the experimental work and Lars Myhre and Rob van der Pluijm for their many important corrections.

REFERENCES

1. HUGHES, T.G. AND HARVEY, R.J. – Environmental influences on the shrinkage of concrete block masonry, *Materials and Structures*, Vol. 30, pp. 225-232, 1997.

2. MENZES, N.C. AND TRINH, J.K. – Influence of water content on the time-dependent properties of concrete, *Creep and shrinkage of concrete. Fifth International RILEM Symposium*, Editor Bažant, Z. and Carol, I. Spon, ISBN 0-419-18630-1, pp. 277-282, London 1993.

3. EUROPEAN COMMITTEE FOR STANDARDIZATION CEN – prEN 771-3: Specification for masonry units – Part 3: Aggregate concrete masonry units (Dense and lightweight aggregates), Brussels 1996.

4. EUROPEAN COMMITTEE FOR STANDARDIZATION CEN – prEN 772-14: 1996, Methods of test for masonry units: Determination of moisture movement of aggregate concrete masonry units, Brussels 1996.

5. EUROPEAN COMMITTEE FOR STANDARDIZATION CEN – prEN 772-1: 1996, Methods of test for masonry units: Determination of compressive strength (draft), Brussels, January 1996.

6. as NORSK LECA – *Leca murverk prosjektering*, (Design of LECA masonry) Anvisning 1.000, Oslo 1995 (in Norwegian).

7. CONRADI, T. – *Måling av herde- og tørkesvinn i lettklinkerbetongblokker* (Measurement of shrinkage in LECA masonry), Student project, Department of Building and Construction Engineering – NTNU, Trondheim 1999 (in Norwegian).

8. PIHLAJAVAARA, S.E. – Chapter 4: Estimation of Drying of Concrete at Different Relative Humidities and Temperatures of Ambient Air with Special Discussion about Fundamental Features of Drying and Shrinkage, *Creep and Shrinkage in Concrete Structures*, (Editor Bažant, Z.P. and Wittmann, F.H.) Wiley & Sons, ISBN 0 471 10409 4, New York 1982.

9. NEVILLE, A.M. – *Properties of concrete*, Longman, Harlow 1995.

10. KVANDE, T. – *Jamførande prøving av trykkfasthet. Prøving utført ved a.s Norsk Leca Lillestrøm og Institutt for bygg- og anleggsteknikk, NTNU* (Comparative test of compressive strength), Working report 4. Department of Building and Construction Engineering – NTNU, Trondheim 1998 (in Norwegian).

11. http://www.norcem.no (January 2000)

12. THE NORWEGIAN STANDARDS ASSOCIATION – NS 3086: Portlandsementer. Krav til sammensetning og egenskaper (Portland cements. Specifications of composition and properties), 1.utgave, Oslo 1995 (in Norwegian).

Table 1
Material properties of LECA blocks of quality "3/770" in accordance with prEN 771-3 [3].

Dimension	99 x 249 x 500 mm
Dry density	730 kg/m³
Compressive strength	2.6 N/mm²
Modulus of elasticity	2900 N/mm²
Poisson's ratio	0.2

Table 2
Climate history for the seven test series.

Series number	Climate and duration in each climate				
	Day 1 to 14	Day 15 to 28	To stabilise weight	To stabilise weight	To stabilise weight
A, unit 2,4 & 6	Wrapped with plastic at 20°C	In air at 20°C and 50 % RH	In water	In air at 80°C	-
A, unit 1,3 & 5	Wrapped with plastic at 20°C	In air at 20°C and 50 % RH	In air at 33°C and 25 % RH	In water	In air at 80°C
B	In air at 33°C and 25 % RH		In air at 33°C and 25 % RH	In water	In air at 80°C
C	Wrapped with plastic at 20°C		In air at 33°C and 25 % RH	In water	In air at 80°C
D	In air at 23°C and 50 % RH		In air at 33°C and 25 % RH	In water	In air at 80°C
E	In air at 3°C and 85 % RH		In air at 33°C and 25 % RH	In water	In air at 80°C
F [1)]	Wrapped with plastic at 20°C				In water / 80°C

1) Five times cyclic wetted and dried.

Table 3
Determined mean values from the test.

Series number	Drying shrinkage			Moisture expansion [2)]	Moisture content [3)]	Dry density [4)]	Compressive strength [5)]
	after 28 days [1)]	at 33°C and 25 % RH [1)]	at 80°C				
	[mm/m]	[mm/m]	[mm/m]	[mm/m]	[volume-%]	[kg/m³]	[N/mm²]
A, unit 2,4 & 6	-0.24	-	-	0.27	5.55	725	2.4
A, unit 1,3 & 5	-0.24	-0.48	-0.53	-	6.08	730	2.3
B	-0.39	-0.43	-0.48	0.19	6.10	715	2.3
C	+0.07	-0.44	-0.48	0.20	6.00	720	2.5
D	-0.39	-0.47	-0.52	0.18	6.11	745	2.8
E	-0.12	-0.45	-0.50	0.19	5.75	745	2.7
F [6)]	-		-0.55 /- 0.45 [7)]	0.52 / 0.43 [8)]	5.58	740	-

1) The values of drying shrinkage after 28 days and at 33°C are adjusted for deviation from 20°C by using a coefficient of thermal expansion of 0.008 mm/(m°C).

2) Moisture expansion when storage in water specimens first dried at 33°C and 25% RH.

3) Moisture content at the beginning of the test calculated from drying at 80°C.
4) Dried at 80°C.
5) Measured in accordance with prEN 772-1.
6) Specimens cyclic wetted and dried five times.
7) Drying shrinkage from saturated blocks. Value from first and last cycle.
8) Moisture expansion from drying at 80°C. Value from second and last cycle.

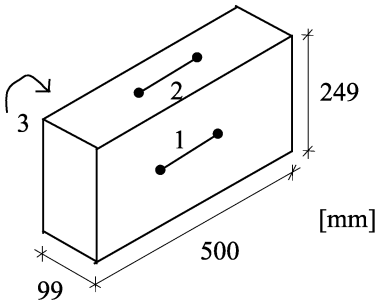

Figure 1 – Positioning of gauge location pads on the LECA block.

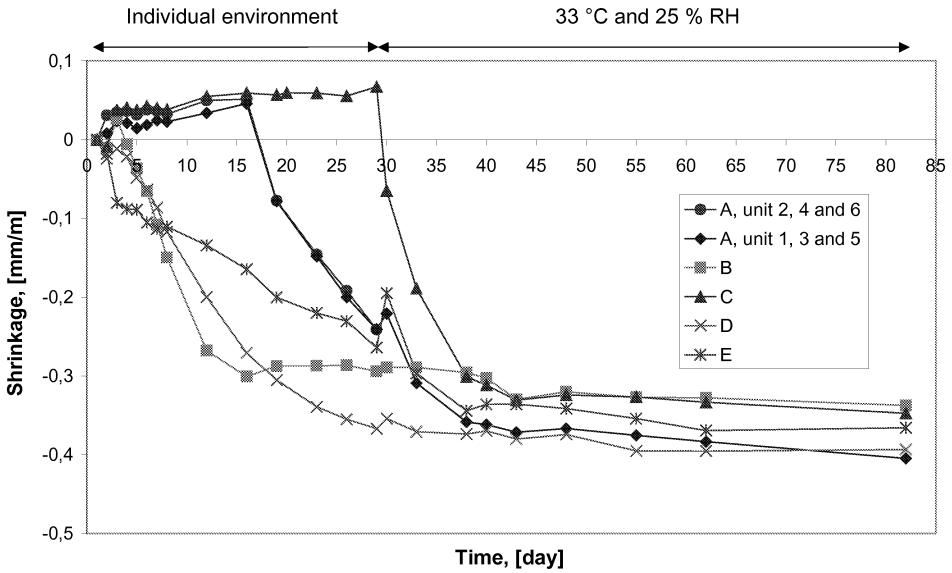

Figure 2 – Mean moisture movement of LECA blocks exposed to different climate conditions. It should be noted that Series A, unit 2, 4 and 6 were not exposed to 33°C and 25 % RH,

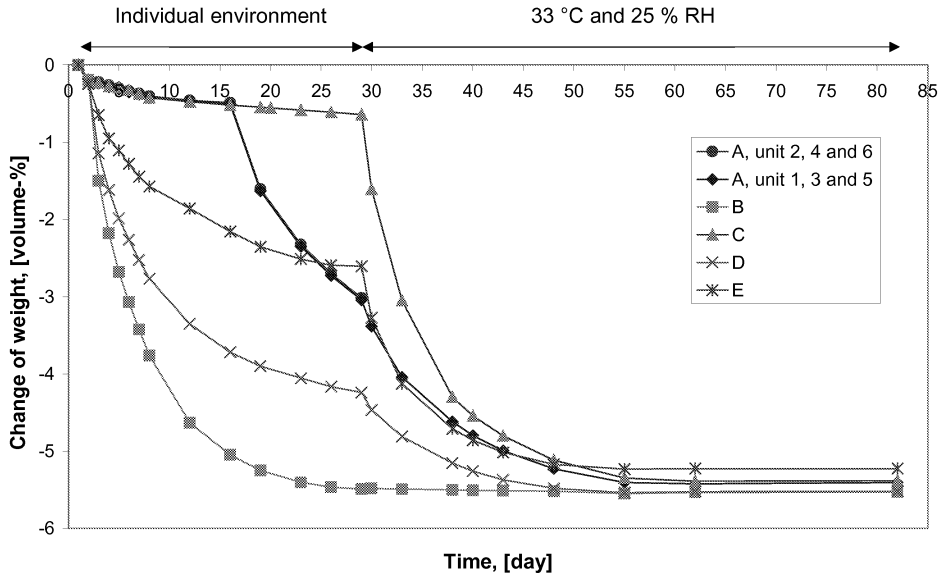

Figure 3 – Mean change of weight of LECA blocks exposed to different climate conditions. It should be noted that Series A, unit 2, 4 and 6 were not exposed to 33°C and 25 % RH,

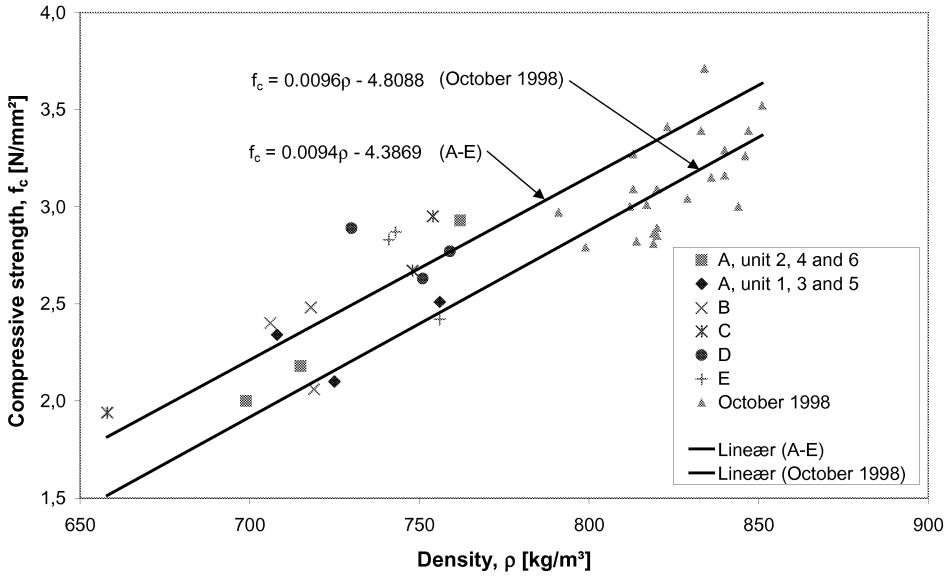

Figure 4 – Compressive strength as a function of the density of the LECA blocks measured in accordance with [3]. Results from this test program (A-E) and results from a similar test program in October 1998 [10]. Linear trends of series A-E together and of [10] are enclosed in the diagram.

APPENDIX 3

Kvande. T.
Determination of Creep and Shrinkage in LECA Masonry.
Report N 8330-9, Norwegian Building Research Institute, Trondheim 2001.

BYGGFORSK
Norwegian Building Research Institute

Head Office
Forskningsveien 3b
P.O.Box 123 Blindern
N-0314 OSLO
Tel. +47 22 96 55 55
Fax +47 22 69 94 38

Local Department
Høgskoleringen 7
N-7491 TRONDHEIM
Tel. +47 73 59 33 90
Fax +47 73 59 33 80

E-mail firmapost@byggforsk.no
Internet www.byggforsk.no
Registration No. NO 943 813 361 VAT

Clients
Mur-Sentret and
Department of Building and
Construction Engineering - NTNU

Client's addresses
Pb. 53 Blindern, 0313 Oslo
and
7491 Trondheim

Client's contact-persons
Geir Wold-Hansen og
Jan Vincent Thue

Project/archive no.	Date	Rev. date	No. of pages	Appendixes	Classification	Author(s)
N 8330-9	31.01.2001		22		Unrestricted	Tore Kvande

Project leader	Sign.	Responsible manager	Sign.	Quality assurance	Sign.
Tore Kvande		Terje Jacobsen		Tore Haavaldsen	

Assignment Report

Deformation of creep and shrinkage in LECA Masonry

Summary

This report gives an overview of the behaviour of LECA masonry subjected to shrinkage, compressive creep and tensile creep. The behaviour is obtained during tests carried out at Pieter van Musschenbroek Laboratory at Technische Universiteit Eindhoven.

Creep and shrinkage deformations were found to be larger than the elastic ones. Hence, it emphasises the importance of taking creep and shrinkage into account in the design of masonry structures.

The determined final compression creep coefficient is found to be a little lower than the design value of Eurocode 6 for LWA masonry. A lower design value of final shrinkage than that given in Eurocede 6 should be used according to the established final shrinkage in this test program. Obtained tensile creep coefficients in the highest stressed area was larger than expected from information retrieval. A relatively large widening of the open perpend joint is also recorded.

This work has been a part of the dr.ing-project "Material Properties for Masonry of Light Expanded Clay Aggregate Concrete as a Constructive Material". The doctoral study has been funded by The Research Council of Norway and Norsk Leca (presently Optiroc). The study has been a part of the research program "Loadbearing Masonry 1997-2000" co-ordinated by Mur-Sentret. The current report is based on Working Report 9 of 31. December 1999.

Address of the building	Built (year)

Activity code	Keywords	Filename
3.4	Lettbetong, Styrke, Stivhet, Mørtel, Formstabilitet	N8330-9.doc

Contents

1. Introduction

Knowledge of masonry deformation due to creep and shrinkage is important for the assessment of crack resistance and for design. Lack of such knowledge for masonry of Light Expanded Clay Aggregate (LECA) concrete blocks was the background for the investigation presented in this report. The report represents an experimental research for determining the behaviour of LECA masonry subjected to creep and shrinkage. The main purpose of the investigation was to establish final creep coefficients and final shrinkage values for LECA masonry. Creep due to both compression and tension loads were studied.

Compressive creep normally appears in the vertical direction of a masonry wall caused by vertical compressive loading. Caused by restrained shrinkage, tensile stresses and hence tensile creep appears in the longitudinal direction of the wall. Due to this fact it was "necessary" to measure compressive creep in the vertical direction of the masonry and tensile creep in the longitude direction. It was desirable that the long-term stresses were within the range of service load conditions.

In this report "shrinkage" will be used to denote changes in volume or length or strains due to loss of moisture from masonry in the hardened state or after a certain initial hardening. The deformation caused by long-term loading is referred to as "creep." The definitions are in accordance with Schubert (1994). To obtain creep, one must consider two identical specimens subjected to exactly the same environmental history. One specimen must be loaded and the companion specimen must be load-free. The creep plus instantaneous deformation are obtained from the difference of the deformation of these two specimens (Bažant 1982).

The tests were carried out in the Pieter van Musschenbroek Laboratory at Technische Universiteit Eindhoven, TUE, during the period from February to November 1999. Cor Naninck, TUE, and Tore Kvande, Norwegian University of Science and Technology (NTNU) have been responsible for the practical work carrying out the experiments valuable supported by Sip Overdijk, TUE.

A detailed overview of the results is given in Kvande (2001-12).

2. Materials and specimens

The LECA blocks used in these tests were produced by Norsk Leca's factory at Lillestrøm, Norway. Identification of the blocks is *Leca kompaktblokk 10 cm 3/770*. "3/770" indicates the quality, telling about a gross compressive strength of the blocks of approximately 3 N/mm² and a net block density of approximately 770 kg/m³. Kvande (2001-8) describes material properties and material composition. The size of the blocks were approximately 96 x 249 x 500 mm (width x height x length).

The dimensions of the specimen were chosen in accordance with guidelines given by Schubert (1994) and Van der Pluijm and Vermeltfoort (1998). Similar specimens for the measurement of shrinkage and compressive creep were made as shown in Figure 1. Such specimens were made by LECA blocks divided in two horizontally (half the length of a block), representing the illustrated location in a wall in Figure 2.

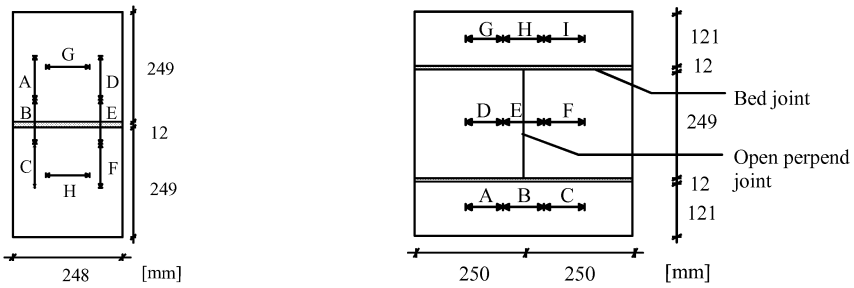

Figure 1:
Left: Masonry specimen for measurement of shrinkage and for measurements of creep due to compressive load. Right: Specimen for measurement of creep due to tensile load. Numbering with letters identify the gauge locations.

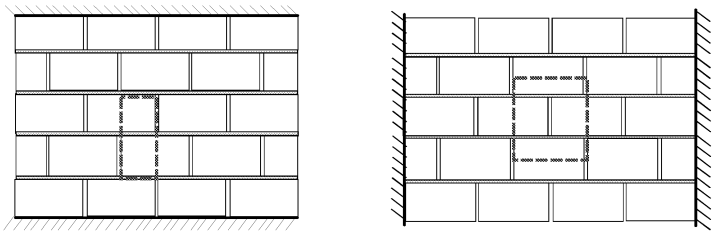

Figure 2:
Specimens for measurement of compressive and tensile creep being member for a masonry walls.

Figure 1 also shows the specimens used for measurement of tensile creep. The specimens comprise one LECA block divided in two horizontally (half the height of the block) and one block divided in two vertically (half the length of the block). Normally, Norwegian LECA masonry is made without mortar in the perpend joint. Hence, the specimens contained two bed joints with mortar and one open (free) perpend joint. The thickness of all specimens corresponded with the width of the blocks (96 mm). The LECA blocks were cut without the addition of water one day after production of the blocks.

The specimens were made 21 days after production of the blocks, mortared together with a factory made mortar 1:1:7 (volume lime:cement:aggregate). Three specimens were made for each type of testing. The 28-day's flexural and compressive strength for the mortar was in accordance with prEN 1015-11 3.3 N/mm² and 11.2 N/mm² respectively.

After manufacturing, the specimens were enclosed in plastic until, one week later, the measurements were started. The two small side surfaces and the bottom and top surfaces of the specimens were given a watervapour-proof seal. (The side surfaces of the tensile creep specimen, that were glued later, were not sealed.) The sealing was used to simulate as closely as possible the normal evaporation process for walls. Gauge location pads were glued on each face of the specimens in order to measure displacements during the test (see Figure 1).

3. Test arrangement

3.1 Experimental procedure

To simulate a typical indoor situation, the experiments were carried out in an environmental test chamber at 20 ±2 °C and 55 ±5 % RH. Measurement of shrinkage started three days after making the specimens. Both changes of length and weight were recorded.

The creep tests started one week after making the specimens. Fibreboard was placed between the specimens and the steel plates at the top and bottom of the compressive creep specimens in the test rig. The fibreboard layers were intended to distribute the load equally on the bed surfaces. The load was applied in steps up to a level of 1.05 N/mm², which should represent almost half of the compressive capacity of the specimen. The compression creep arrangement is shown in Figure 3.

The tensile creep specimens were turned 90° and glued in the test rig as shown in Figure 4 and 5. Tensile stresses were obtained by using a lever. The load was applied in successive steps up to a level of 0.10 N/mm² when dealing with the gross area. In the case of the net area, the averages stress equalled 0.19 N/mm² in the blocks on both sides of the open joint.

Creep and shrinkage were measured with a Demec gauge (demountable mechanical gauge) with a gauge length of 100 ±1 mm. Measuring positions are shown in Figure 1. The displacement of the creep specimens was measured regularly during the test program. Changes in length and weight of the shrinkage specimens were recorded at the same time. Measurements made just before applying the load were taken as zero-values for the calculation of the total strain in the creep specimens. The zero-values for time-dependent behaviour were measured one hour after applying the load.

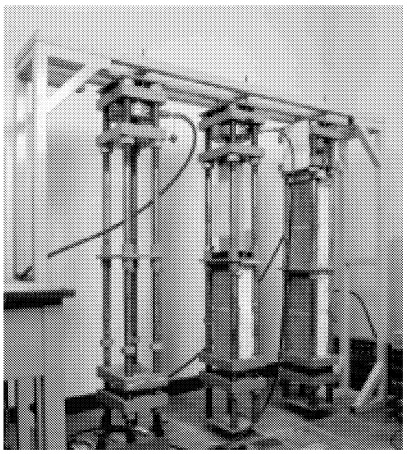

Figure 3:
Compressive creep test set-up. (Photo: Ben Elfrink, TUE)

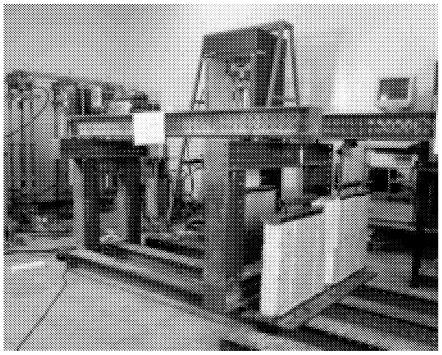

Figure 4:
Tensile creep test set-up. (Photo: Ben Elfrink, TUE)

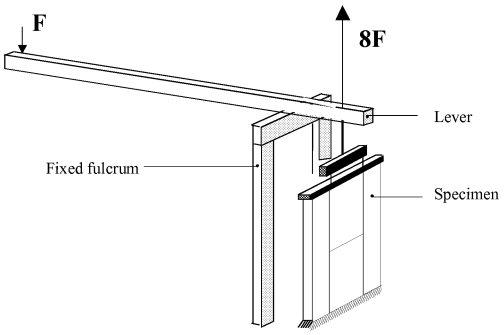

Figure 5:
Principal sketch of the tensile creep test rig. It should be noted that the specimen were turned 90° before gluing in the test rig.

Compressive strength of the compression creep specimens was determined at the end of the test program. During the compressive strength testing, displacement measurements were carried out on the specimens by using LVDTs glued to the specimens as shown in Figure 6. Their gauge length was 65 mm.

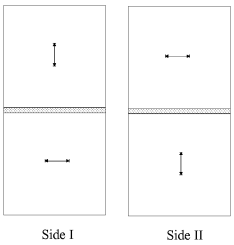

Figure 6:
Placing of LVDTs during measuring of compressive strength.

Tensile strengths of the tensile creep specimens were tested at the end of the test program by loading the lever in the test arrangement in small steps until failure occurred. Before testing the specimens were unloaded.

Finally the shrinkage specimens were dried at 80 °C to a constant mass to be able to establish the moisture content during the test.

3.2 Calculations

Total strain of the creep specimen consists of the following three components as:

$$\varepsilon_{total}(t) = \varepsilon_{el} + \varepsilon_{sh}(t) + \varepsilon_{cr}(t) \qquad \text{Equation 1}$$

where: $\varepsilon_{total}(t)$ is the measured total strain in the creep specimens,
$\varepsilon_{cr}(t)$ is the creep strain,
ε_{el} is the elastic strain established immediately after applying the load,
$\varepsilon_{sh}(t)$ is the shrinkage strain.

The coefficient of creep, $\phi(t)$, can be calculated in accordance with Eurocode 6 as follows:

$$\phi(t) = \frac{\varepsilon_{cr}(t)}{\varepsilon_{el}} \qquad \text{Equation 2}$$

4. Results

4.1 Shrinkage

In Figure 7 the shrinkage (strain) and change of weight during are presented during the test period. A negative strain reveals shortening. Only mean results are presented. Figure 7 shows that the weight of the specimens stabilised after about 100 days. The reduction was approximately 4.5 weight-% with respect to the dry mass. Deformations stabilised much later. At the end of the test, the shrinkage strains were -0.47 mm/m vertically (average A, C, D and F), -0.54 mm/m horizontally (average G and H) and -0.57 mm/m vertically including the bed joint (average B and E). The last point on each curve was the result of measurements after drying to a constant mass at 80 °C.

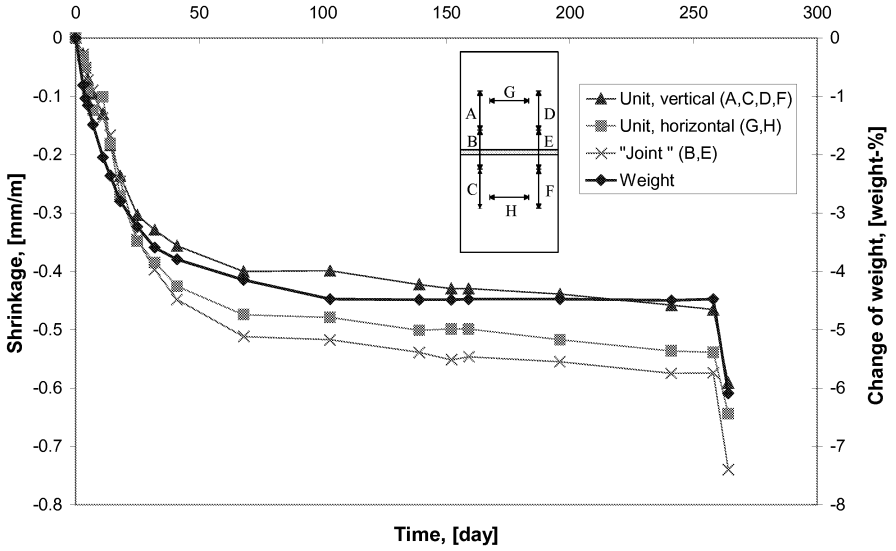

Figure 7:
Shrinkage of specimens. Displacements are measured in accordance with the figure enclosed in the diagram.

4.2 Compressive creep

The development of strain during the compressive creep tests is presented in Figure 8. A negative strain reveals shortening, while positive strain expresses elongation. The figure includes horizontal and vertical creep of the LECA blocks as well as vertical creep measured over the bed joint. The last two points on each curve were the results of measurements after un-loading. The development of creep coefficients, $\phi(t)$, calculated in accordance with Equation 2 is presented in Figure 9. Only mean values are presented.

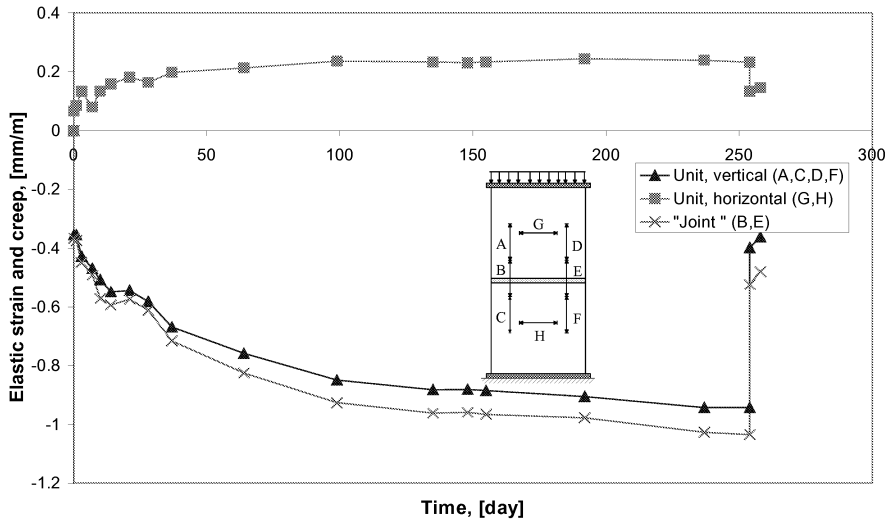

Figure 8:
Elastic strain plus compressive creep of specimens. Displacements are recorded in accordance with the figure enclosed in the diagram.

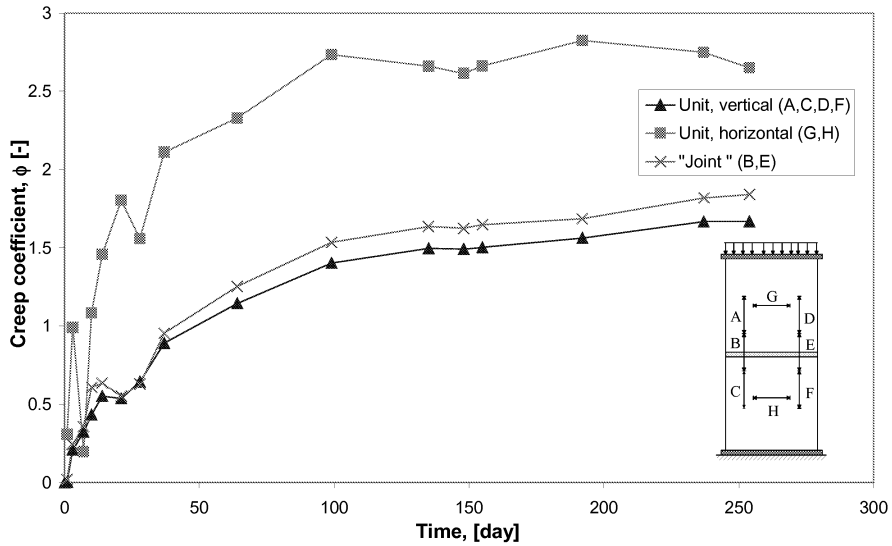

Figure 9:
Time-dependent compressive creep coefficients of specimens. Displacements are measured in accordance with the figure enclosed in the diagram.

At the end of the creep test, total creep (ε_{total} - ε_{el}) strains were 0.17 mm/m for the block horizontally (average G and H), -0.57 mm/m for the block vertically (average A, C, D and F) and -0.67 mm/m for the specimen vertically including the bed joint (average B and H). Correspondingly, creep coefficients at the end of the test were calculated approximately 2.65, 1.67 and 1.84 respectively (Figure 9).

Measurements of length were carried out just before, and after, load application. Calculation of modulus of elasticity and Poisson's ratio in Table 1 was based on those measurements. Modulus of elasticity and Poisson's ratio were also calculated from the measurements carried out during the test of compressive strength. The results can be seen in Table 2. Modulus of elasticity and Poisson's ratio are calculated from the situation at 33 % and 50 % of the compressive strength. The difference between the situation at 33 % and 50 % of the strength was insignificant. Compressive strength of each specimen is included in Table 2.

Table 1:
Modulus of elasticity and Poisson's ratio calculated from the instantaneous deformation caused by load application of the creep specimens.

Specimen	Modulus of elasticity [N/mm²]		Poisson's ratio [-]
	Mean measurement on blocks (A, C, D, F)	Mean of all measurements (A, B, C, D, E, F)	
C1	3182	3000	0.22
C2	2917	2838	0.19
C3	2917	2917	0.16
Mean (CV)	3000 (5 %)	2900 (4 %)	0.2 (16 %)

Table 2:
Compressive strength, modulus of elasticity and Poisson's ratio calculated from the measurements during determination of compressive strength of the specimens. Modulus of elasticity and Poisson's ratio are calculated from the situation at 50 % of the compressive strength.

Specimen	Compressive strength [N/mm²]	Modulus of elasticity [N/mm²]	Poisson's ratio [-]
C1	2.41	3213	0.22
C2	2.39	1916	0.12
C3	2.09	2323	0.14
Mean (CV)	2.3 (8)	2500 (27)	0.2 (31)

4.3 Tensile creep

138 days after applying the load, specimen T1 failed. In Figure 10 the development of strain ($\varepsilon_{el} + \varepsilon_{cr}$) during the tensile creep testing is presented. Positive values express a elongation. Because of the failure of specimen T1 the creep behaviour of T1 is presented with separate curves in the figure. The behaviour of specimens T2 and T3 are presented as mean values. The diagram is made for a comparison between the deformation of the failed specimen and the two remaining specimens. The diagram shows a very good conformity between the results of specimen T1 until failure and the mean of T2 and T3. In the following, tensile creep is given as mean creep of specimen T2 and T3 (Figure 11). The last two points on each curve were the results of measurements after un-loading. The

The elastic strain and the tensile creep in the specimen at the end of the creep tests are given in Table 3. Table 3 contains mean values of measurements at similar positions. D and F (block above and under the open joint in the test arrangement), A, C, G and I (block above and under the highest stressed area) and B and H (block at the highest stressed area beside the open joint) were similarly positioned. The result of measurement E (over the open perpend joint) is presented separately. The developments of creep coefficients are presented in Figure 12. Positions of measurements were grouped as in Table 3.

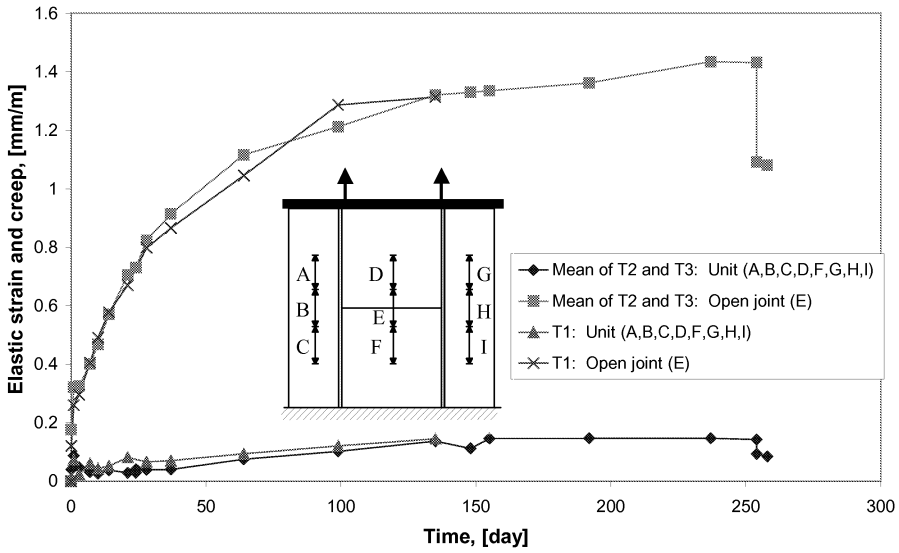

Figure 10:
Elastic strain plus tensile creep of specimens. Displacements are measured in accordance with the figure enclosed in the diagram. Because of the open joint it is not correct to calculate strain in this area.

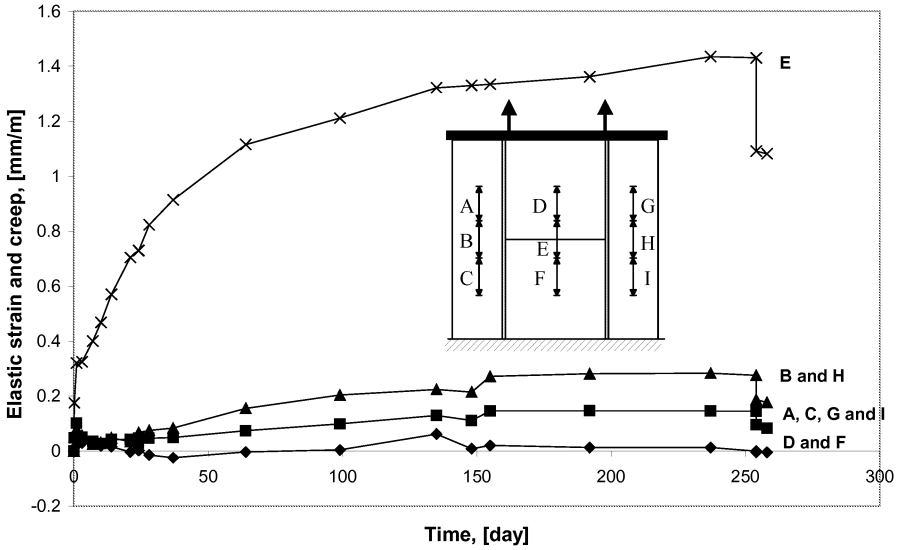

Figure 11:
Elastic strain and tensile creep of specimens. Displacements are measured in accordance with the figure enclosed in the diagram. Because of the open joint it is not correct to calculate strain in this area.

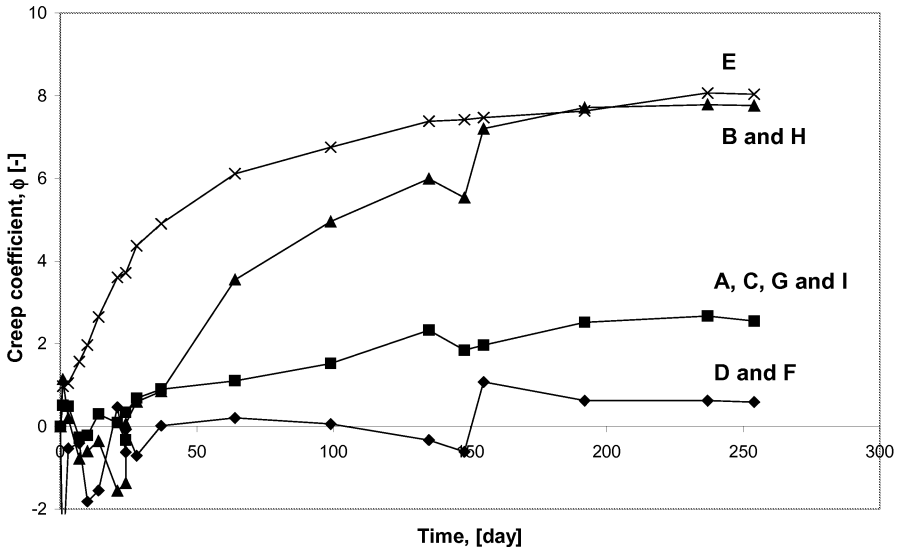

Figure 12:
Time-dependent tensile creep coefficients of masonry specimens of LECA concrete 3/770. Displacements are measured in accordance with Figure 1. Because of the open joint it is not correct to calculate creep coefficient in this area.

Table 3:
Elastic strain. Creep strain and creep coefficient after 254 days at the end of the tensile creep test. Calculated stresses are based on measured elastic strain and a modulus of elasticity of 2900 N/mm².

Position of measurement	Elastic strain [mm/m]	Creep strain [1] [mm/m]	Creep coefficient [1] [-]	Calculated stress [1] [N/mm²]
D and F	0.01	0.01	0.6	0.03
A, C, G and I	0.05	0.10	2.5	0.15
B and H	0.06	0.23	7.8	0.17
E [2]	*0.18*	*1.26*	*8.0*	*0.52*

[1] Mean values based on specimen T2 and T3 only.
[2] Because of the open joint it is not correct to calculate strain and stress in this area.

The tensile strength (gross area) of specimen T2 and T3 was 0.16 N/mm². Both specimens failed within the highest stressed area via the open joint. Using the net area by subtracting the open joint almost doubles the average strength of the highly stressed area to 0.32 N/mm².

4.4 Compressive and flexural strength of mortar

Flexural strength and compressive strength of the mortar were measured in accordance with prEN 1015-11. Mean values and development of the strengths are given in Table 4.

Table 4:
Development of flexural and compressive strength. Strengths measured in accordance with prEN 1015-11.

Age when testing	Flexural strength		Compressive strength	
		Change		Change
[day]	[N/mm²]	[%]	[N/mm²]	[%]
8	1.6	-	6.1	-
28	3.3	106	11.2	84
267	3.3	106	11.9	95

5. Discussion

5.1 Comments on the test program

In agreement with the recommendation of Schubert (1994) and Van der Pluijm and Vermeltfoort (1998) it could be concluded that the small specimens chosen for this test program are representative for the behaviour of masonry. The test is carried out in a climate chamber at 20 ±2 °C and 55 ±5 % RH. The environment represents a normal indoor climate. In this experimental program the shrinkage tests were carried out together with the creep tests to obtain the creep part of the total measured strain on the creep tests. For shrinkage tests in general, however, a very low relative humidity should be selected in order to allow for extreme cases.

Normally, masonry LECA blocks are wrapped in plastic and stored for about four weeks before transportation to the building site. In this study, the blocks were wrapped in plastic for three weeks before the specimens were prepared. The moisture content of the specimens at the start of testing was assumed to correspond with the normal situation at the building site (about 10 weight-%). However, due to the manufacturing of the specimens, some drying out occurred and about 6 weight-% moisture remained. Consequently, the determined shrinkage and drying creep may be too high (N.B. negative values) compared to starting the measurement with a moisture content of 10 weight-%.

It should be noted that small stepwise changes of displacement were measured during the test program. Applying the tensile load caused, for example, a measured elastic deformation on parts of the specimens of less than 1 µm. The uncertainty of the Demec gauge was given as ±1 µm. Repeated measurements of the same position in succession, however, indicated an uncertainty of ±2 µm (k=2) rather than ± 1 µm. An uncertainty of ±2 µm would influence the measurements considerably, since for instance the elastic deformation caused by the tensile load was less than 1 µm for parts of the specimen. Consequently, some of the variation seen in the time dependence of, for example, tensile creep coefficients could account for the uncertainty of the measurements. In spite of the uncertainty of the Demec gauge, the coefficients of variation of the strains were less than 10 % (with exception of «horizontal creep», see section 5.3).

5.2 Shrinkage behaviour

Development of shrinkage was given in Figure 7. At the end of the shrinkage tests, the greatest strain was obtained in connection to the bed joint (-0.57 mm/m). This was expected because of higher initial moisture content in the mortar compared with the blocks. The initial moisture content of the mortar was 17 weight-% when making the mortar, while the LECA blocks contained about 6 weight -%. The situation is also influenced by a lack of hydration of the mortar compared with the three weeks older LECA block.

A slight difference between displacement recorded on LECA block parallel and perpendicular to the bed joint can be observed in Figure 7 (-0.54 and –0.47 mm/m). The trend was recorded in all three specimens and may be due to geometrical reasons.

The shrinkage test was stopped too early to obtain the final shrinkage. According to experimental results presented by Schubert (1992) (see Figure 13), 45 – 80 % of the shrinkage in lightweight masonry appears after 100 days. The specimen of Schubert were tested under

roughly constant conditions and the shrinkage was largely completed after three to five years. The rapidity of the shrinkage depends on effective thickness, see Equation 3:

$$t_{ef} = 2\frac{A_{cs}}{u_{cs}} \qquad \text{Equation 3}$$

where t_{ef} is the effective thickness,
A_{cs} is the component cross-section,
u_{cs} is the circumference of the component cross-section exposed to drying.

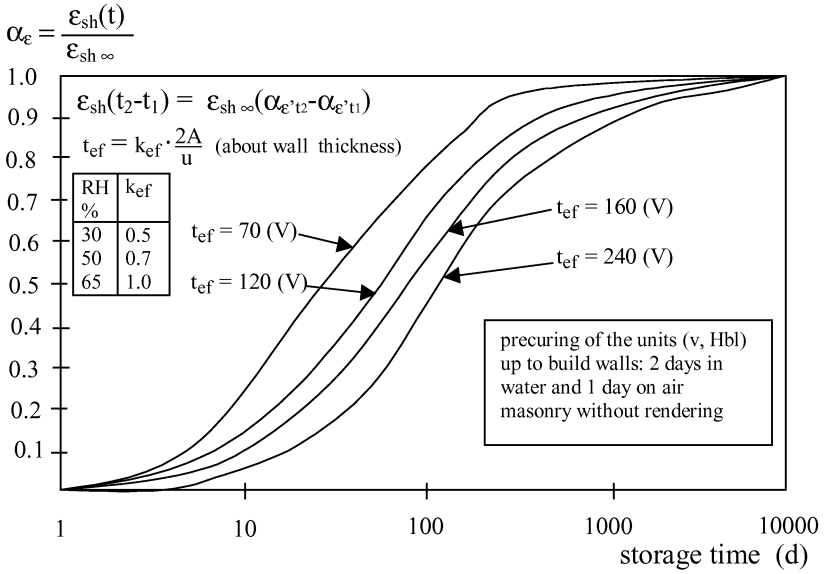

Figure 13:
Shrinkage of masonry made from lightweight concrete blocks. Age at the beginning of shrinkage was 3 to 7 days. (Schubert 1992)

Regarding the specimens tested in this report, Equation 3 gives an effective thickness of 96 mm. According to Schubert (1992), about 70 % of the final shrinkage should appear within 100 days for that effective thickness. To compare the results with (Schubert 1992) a presentation of the shrinkage with time on a logarithmic scale is made in Figure 14. The figure is made assuming 70 % of the shrinkage appears after 100 days. Completion of shrinkage is supposed to be three years.

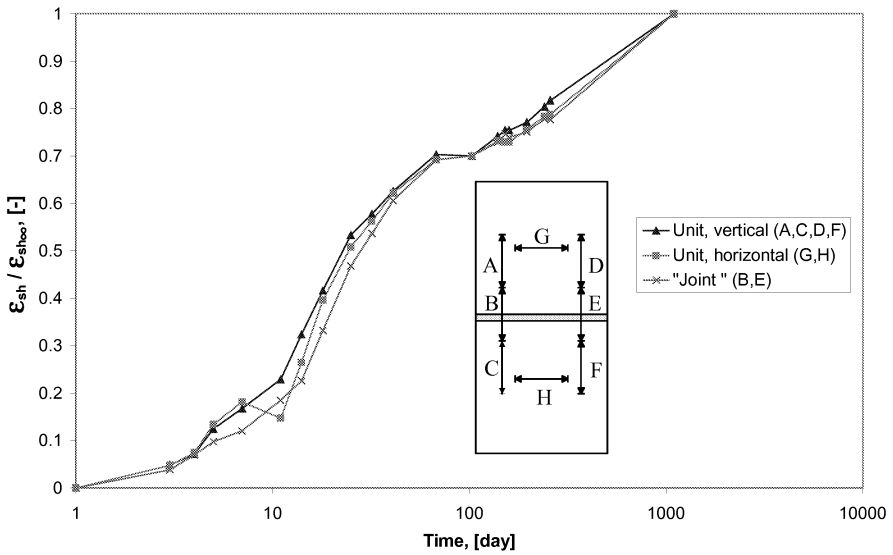

Figure 14:
Time-dependent shrinkage presented with assumption of 70 % of the shrinkage appearing after 100 days and with completion of shrinkage within three year.

Comparison between the shape of the curves in Figure 13 and 14 indicates that more than 70 % of the shrinkage appeared within 100 days. A more correct estimate of the final shrinkage seems to be the appearance of at least 80 % shrinkage after 100 days as illustrated in Figure 15. The estimate is based on the development of time- dependent shrinkage presented of Müller and Hilsdorf (1990) and Schubert (1992).

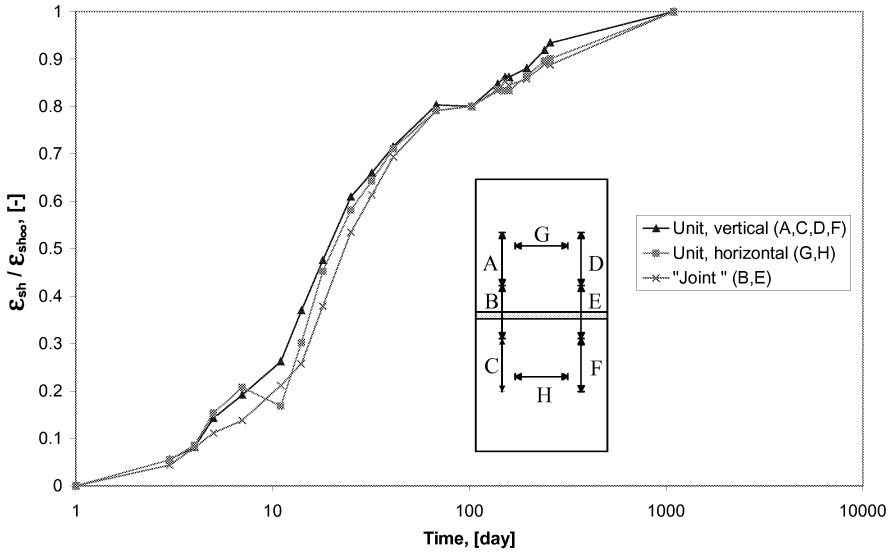

Figure 15:
Time-dependent shrinkage presented with an assumption of 80 % of the shrinkage appearing after 100 days and with completion of shrinkage within three years.

The shrinkage is measured with a gauge length of 100 mm. Shrinkage of the joint alone can be calculated as follows:

$$\varepsilon_{sh}^{j}(t) = \frac{\left[\varepsilon_{sh}^{j+u}(t) \cdot \left(t^{j} + t^{u}\right) - \varepsilon_{sh}^{u}(t) \cdot t^{u}\right]}{t^{j}} \qquad \text{Equation 5}$$

where: $\varepsilon_{sh}^{j}(t)$ is the shrinkage of joint,
$\varepsilon_{sh}^{j+u}(t)$ is the shrinkage of the specimen within the gauge length (follows directly from measurements)
$\varepsilon_{sh}^{u}(t)$ is the shrinkage of the block,
t^{j} is the thickness of the mortar joint,
t^{u} is the sum of the length of the concrete block parts within the measurement length,

Shrinkage of an element representing the masonry can be calculated according to Equation 6. The element contains one block and half of a joint.

$$\varepsilon_{sh}^{M}(t) = \frac{\left[\varepsilon_{sh}^{u}(t) \cdot t^{u} + \varepsilon_{sh}^{j}(t) \cdot ½t^{j}\right]}{h^{M}} \qquad \text{Equation 6}$$

where: $\varepsilon_{sh}^{M}(t)$ is the shrinkage of the masonry element,
h^{M} is the height of the masonry element.

Development of shrinkage of joint (Equation 5) and block (measurement) as well as of the masonry (Equation 6) is given in Figure 16. Normal height of a block (248 mm) and normal joint thickness (12 mm) are used for the calculations of shrinkage of masonry. Estimated final shrinkage is summarised in Table 5. The estimate is made on the assumption of 80 % shrinkage after 100 days. The shrinkage of joints is much larger than shrinkage of the block. The difference can be explained by differences in initial moisture content and age. However, the contribution from the joint is insignificant on the shrinkage of the masonry, see Figure 16 and Table 5. This is due to the joint representing less than 5 volume-% of the masonry.

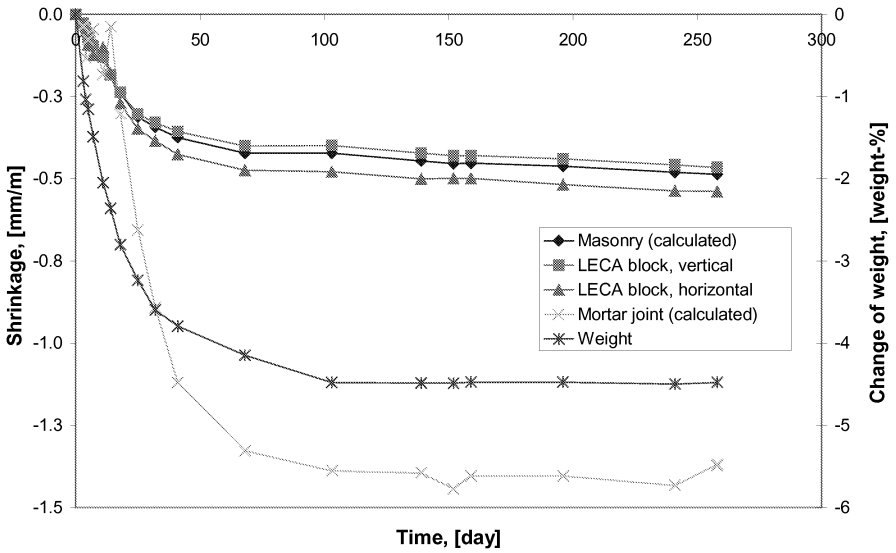

Figure 16:
Developments of shrinkage in masonry, LECA block and mortar joint.

Table 5:
Estimated final shrinkage of masonry, LECA block and mortar joint. Estimate based on assumption of 80 % shrinkage after 100 days.

Component	Final shrinkage [mm/m]
Masonry	-0.52
LECA block, vertical	-0.50
LECA block, horizontal	-0.60
Mortar joint	-1.74

Design value for final shrinkage or moisture expansion given in Eurocode 6 for LWA masonry is –0.4 mm/m with a range of –1.0 to –0.2 mm/m. In concrete, shrinkage typically attains values from –0.2 to –0.8 mm/m (Bažant 1982). Initial moisture content and shrinkage climate mainly influence the final value. Shrinkage obtained during this test program should represent a normal indoor situation for LECA masonry regarding initial moisture content as well as environmental climate.

5.3 Compressive creep behaviour

Development of compressive creep is presented in Figure 8. The creep deformation is larger than the elastic deformation. Largest creep was recorded over the bed joint. Experience from Hughes and Harvey (1997) explains the great variation between displacement of the LECA block and the mortar by differences in initial moisture content.

Based on a modification of Equation 5 and 6 (change ε_{sh} with ε_{cr}) it is possible to present development of compressive creep coefficient of joint and block as well as of the masonry

(Figure 17). The figure shows that the contribution from the joint on the creep of the masonry is insignificant (creep of masonry ≈ creep of masonry unit).

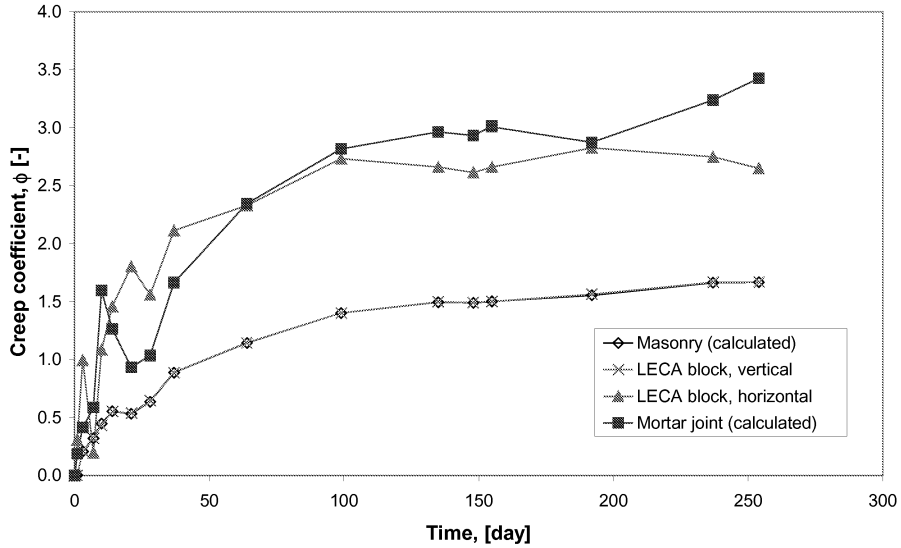

Figure 17:
Developments of compressive creep in masonry, LECA block and mortar joint.

Figures 8 and 17 indicate that the test was stopped somewhat too early to measure the final creep. To be able to estimate a final creep coefficient experiences from Stemland and Thorenfeldt (1998) and prEN 1520 could be used. Stemland and Thorenfeldt (1998) refer to experiences with creep of small specimens of normalweight concrete. On cylindrical specimen with a diameter of 103 mm, about 70 % of the creep normally appear after 150 days. It is also possible to establish creep coefficients in accordance with prEN 1520 (Equation 7). prEN 1520 covers prefabricated reinforced components of lightweight aggregate concrete with open structure intended to be used in building constructions.

$$\varphi(\infty,t_o) = \varphi_o(\infty,t_o)\cdot\eta_2\eta_4 \qquad \text{Equation 7}$$

where $\varphi(\infty,t_o)$ is the design value of the creep coefficient,
t_o is the age at loading, in this case 28 days for the masonry units,
$\varphi_0(\infty,t_o)$ is the creep coefficient of normal weight concrete, in this case 2.84,
η_2 is a coefficient adjusting for modulus of elasticity, in this case 0.23,
η_4 is a coefficient compensating for strength of the concrete, in this case 1.8.

Estimated final creep coefficients are given in Table 6. Estimations based on the 70 % experience as well as on prEN 1520 are included in the table. The table indicates best agreement between experimentally obtained creep coefficients and the 70 % assumption. Values given by prEN 1520 are too low. However, it should be noted that the calculation in accordance with prEN 1520 is based on the age of the LECA block at loading and not on the age of the masonry itself. This decision is due to the insignificant contribution from the joint on the creep of the masonry (Figure 17).

Table 6:
Creep coefficient at 155 days and at the end of the test (254 days) compared with calculated final creep coefficient.

	Creep coefficient [-]			
	Measurements		Calculated value	
	155 days	254 days	Based on 70% creep after 150 days	pEN 1520
Masonry	1.50	1.67	2.1	1.2
LECA block, vertical	1.50	1.67	2.1	1.2
LECA block, horizontal	2.66	2.65	3.8	1.2
Mortar joint	3.01	3.43	4.3	-

Obtained «horizontal creep» coefficient of LECA block may be too high compared with the vertically obtained coefficient. Measured changes of horizontal displacement are very small. Uncertainty in the measurement of length and too low resolution influences the measurements quite considerably. From (Kvande 1999-12) it is clear that the variation of the «horizontal creep» coefficient is very high (CV > 50 %) compared with the vertical ones (CV ≤ 10 %). According to that the measurements should be stated as unreliable.

Experiences from long-term loading of concrete referred by Bažant (1982) states that the creep coefficients usually are between 1.0 and 6.0, with 2.5 as the most typical value. Eurocode 6 gives a design value of 2.0 with range 1.0 to 3.0. Due to the shape of the creep coefficient/time-diagram (Figure 3.17), a creep coefficient for LECA masonry between 1.7 and 1.8 may be expected for the present situation. This is a little lower than the final creep coefficient estimated by the 70 % assumption and the design value of Eurocode 6. However, for structural design purpose the design value of Eurocode 6 seams reasonable.

5.4 Tensile creep behaviour

Figure 12 indicates that the test lasted almost long enough to measure the final creep. Hence, the tensile creep coefficients in Table 3 can be considered as final creep coefficients. Table 3 indicates a final creep coefficient of about 8 for in the middle of the continuous blocks (B and H), while coefficients of 2.5 were recorded elsewhere in the continuous blocks (A, C, G and I). The last value fits very well with the recommendation in Eurocode 6 and Bažant (1982). The high creep coefficient at position B and H may be caused by stress concentration in this part of the specimen. A tensile load of about 60 % of the tensile strength was maintained during the creep test. Normally, the creep coefficient of concrete is approximately constant up to about 50 % of the compressive strength Bažant (1982). Due to the equality of the creep coefficient in compression and tension and the fact that concrete behaves in a linear elastic manner up to about 70 % of the tensile strength, a much lower creep coefficient than 8 was expected in the highest stressed area (Eibl et al. 1995). This is supported by lower creep coefficients obtained by Stemland and Thorenfeldt (1998) during compressive creep tests on low strength LECA concrete. These tests were carried out with stresses equal 30 %, 50 % and 70 % of the compressive strength, indicating a much smaller creep coefficient than obtained during this investigation of tensile creep.

6. Conclusions

The behaviour of LECA masonry when subjected to shrinkage, compressive and tensile creep were determined during this test program. Creep and shrinkage deformations were found to be larger than the elastic ones. Hence, it emphasises the importance of taking creep and shrinkage into account in the design of masonry structures.

The determined final compression creep coefficient is found to be a little lower than the design values of 2.0 of Eurocode 6 for LWA masonry. However, for structural design purpose the design value of Eurocode 6 seams reasonable.

A lower design value of final shrinkage than that given in Eurocede 6 should be used according to the established final shrinkage in this test program.

Obtained tensile creep coefficients in the highest stressed area was larger than expected from information retrieval. A relatively large widening of the open (free) perpend joint is also recorded.

Creep and shrinkage of the mortar joint are far larger than in the blocks. However, the contribution from the joints to the creep and shrinkage of the masonry is insignificant. This is due to the fact that the joint represents less than 5 volume- % of masonry.

7. References

Bažant (1982)
Bažant, Z.P. – Chapter 7: Mathematical Models for Creep and Shrinkage of Concrete, *Creep and Shrinkage in Concrete Structures*, (Editors: Bažant, Z.P. and Wittmann, F.H.) Wiley, ISBN 0-471-10409-4, New York 1982.

Eibl et al. (1995)
Eibl, J. et al. – *Concrete structures. Euro-Design Handbook*, Chapter A6.2.2 and A6.5.3.3 (the first one) Ernst & Sohn, Berlin 1995.

Draft European Standard prEN 1015-11*: Method of test for mortar for masonry – Part 11: Determination of flexural and compressive strength of hardened mortar,* European Committee for Standardization CEN, Brussels 1995.

European Prestandard ENV 1996-1-1 Eurocode 6: *Design of masonry structures – Part 1-1: General rules for buildings – Rules for reinforced and unreinforced masonry*, European Committee for Standardization CEN, Brussels 1995.

Draft European Standard prEN 1520*: Prefabricated reinforced components of lightweight aggregate concrete with open structure*, Final draft, European Committee for Standardization CEN, Brussels 1999.

Hughes and Harvey (1997)
Hughes, T.G. and Harvey, R.J. – Environmental influences on the shrinkage of concrete block masonry, *Materials and Structures*, Vol. 30, pp. 225-232, 1997.

Kvande (2001-8)
Kvande, T. – *Råstoff og materialeigenskapar for lettklinkerbetongblokk-kvalitet 3/770 100x250x500 mm. Prøveuttak frå a.s Norsk Leca sitt fabrikkanlegg på Lillestrøm 19.01.99.* (Light Expanded Clay Aggregate (LECA) Concrete Blocks, Quality 3/770 100 x 250 x 500: Raw material and material properties). Report N 8330-8, Norwegian Building Research Institute, Trondheim 2001 (in Norwegian).

Kvande (2001-12)
Kvande, T – *Determination of creep and shrinkage in LECA masonry. Collection of results,* Report N 8330-12, Norwegian Building Research Institute, Trondheim 2001.

Müller and Hilsdorf (1990)
Müller, H.S. and Hilsdorf, H.K. – *Evaluation of the time dependent behaviour of concrete; summary report on the work of General Task Group 9*. CEB bulletin d'information No. 199, ISBN 2-88394-005-3, Lausanne 1990.

Van der Pluijm and Vermeltfoort (1998)
Pluijm, R. van der and Vermeltfoort, A.Th. – Influence of the type of mortar joint on the time dependent behaviour of masonry, *8th Canadian Masonry Symposium.* Alberta, Canada 1998.

Schubert (1992)
Schubert, P. – Strength and deformation properties of masonry made from lightweight concrete units, *6th Canadian Masonry Symposium,* University of Saskatchewan, Saskatoon, Canada 1992.

Schubert (1994)
Schubert, P. – Test methods for the determination of creep and shrinkage in masonry, *10th International Brick and Block Masonry Conference*, Masonry Council of Canada, The University of Calgary, pp. 777-786, Calgary 1994.

Stemland and Thorenfeldt (1998)
Stemland, H. and Thorenfeldt, E. – *Lett konstruksjonsbetong* (Lightweight concrete*)*, Delprosjekt 2: Konstruktive aspekter, Delrapport 2.1: Superlette betongkvaliteter, STF22 A98742, SINTEF, Trondheim 1998 (in Norwegian).

Symbols

A_{cs}	component cross-section	[mm²]
CV	coefficient of variation	[%]
E	modulus of elasticity	[N/mm²]
h	height	[mm]
t	thickness	[mm]
t_0	age at loading	[day]
t_{ef}	effective thickness	[mm]
u_{cs}	circumference of the component cross-section exposed to drying	[mm]
ε_{cr}	creep strain	[-]
ε_{el}	elastic strain	[-]
ε_{total}	total strain in specimen	[-]
ε_{sh}	shrinkage strain	[-]
ϕ	creep coefficient	[-]
ϕ_∞	final creep coefficient	[-]
σ	normal stress	[N/mm²]
ν	Poisson's ratio	[-]

Superscripts

u	of masonry unit
M	of masonry
j	of (mortar)joint
j+u	of joint + masonry unit within measuring length

APPENDIX 4

Kvande. T., Vermeltfoort, A.T., Pluijm, R. van der and Høiseth, K.V.
Tensile Creep Behaviour of LWA Masonry.
Submitted for publication in Masonry International in November 2000.

Tensile Creep Behaviour of LWA Masonry

by

T. KVANDE[1], A.T. VERMELTFOORT[2], R. VAN DER PLUIJM[3] and K.V. HØISETH[4]

ABSTRACT

Knowledge of masonry deformation caused by creep and shrinkage is important when designing for crack resistance. The main purpose of the presented investigation was to study the creep behaviour of typical Norwegian masonry made of Light Expanded Clay Aggregate (LECA) concrete blocks. Normally such masonry is made without mortar in the perpend joint. When the masonry is exposed to restrained shrinkage, an unclear tensile stress distribution may appear because of the free (open) joint. Instead of using "ordinary" creep tests under compression, specimens were loaded with constant uni-axial tensile stress in the longitudinal direction of the masonry. The ESPI measurements showed a relatively large opening of the free perpend joint, which was due to the stress distribution in the specimen. The obtained creep coefficient was especially large for the highest stress levels.

1. INTRODUCTION

Restrained shrinkage cracking of masonry walls is a major cause for damage of buildings [1, 2]. Cracking occurs because the masonry has limited tensile strength. Knowledge of masonry deformation caused by creep and shrinkage is important when designing for crack resistance [3]. Due to restrained shrinkage, tensile stresses and hence tensile creep appears in the longitudinal direction of the wall.

In Norway, Light Expanded Clay Aggregate (LECA) concrete blocks are the most commonly used blocks for masonry. LECA is a type of lightweight aggregate (LWA). Normally, Norwegian LECA masonry is made without mortar in the perpend joints. Because of the free (open) perpend joints, a complicated stress distribution exists in restrained walls, making the assessment of stress reduction due to creep difficult. As far as the authors know, no earlier studies on tensile creep of masonry with free perpend joints have been reported.

In this paper, shrinkage will be used to denote changes in length due to loss of moisture from masonry unit and mortar in the hardened state or after a certain initial hardening. The deformation caused by long-term loading is referred to as creep. The definitions are in accordance with [4]. To obtain creep one must consider two identical specimens subjected to exactly the same environmental history. One specimen must be loaded and the companion specimen must be load-free. The creep plus instantaneous deformation are obtained from the difference of the deformation of these two specimens [5].

[1] Norwegian University of Science and Technology, Norway
[2] Technische Universiteit Eindhoven, The Netherlands
[3] TNO Building and Construction Research, The Netherlands
[4] MARINTEK Department of Structural Engineering, Norway

2. OBJECTIVE

The purpose of the present work has been to study the creep behaviour of typical Norwegian LECA masonry exposed to uni-axial tensile loading. Determination of a creep coefficient is of particular interest. The creep tests were carried out by applying a constant tensile load in the longitudinal direction of the masonry. By using an optical measurement technique the strain distribution around the open joint was established.

3. TEST PROCEDURE

3.1 Materials and specimens

Norsk Leca produced the LECA blocks used in the tests. Typical material properties of the blocks used are given in Table 1.
The dimensions of the specimens were chosen in accordance with the guidance given in [4, 7]. For the shrinkage measurements, specimens were made of two half masonry blocks as shown in Figure 1, left. For the tensile creep measurements, the specimens were made of horizontally cut LECA blocks (half the height of ordinary block) and vertically cut blocks (half the length of ordinary block), Figure 1, right. The latter specimen contained two bed joints with mortar and one free perpend joint. The thickness of all specimens corresponded with the width of ordinary blocks. The LECA blocks were cut one day after production of the blocks. The sawing was carried out under dry conditions to avoid addition of water.
Three specimens were made for each type of testing, noted T1, T2 and T3. The specimens were made 21 days after the blocks were produced with a factory made 1:1:7 (lime:cement:aggregate-ratio by volume) mortar. The 28 days' flexural and compressive strength for this mortar according to prEN 1015-11 [8] were 3.3 N/mm² and 11.2 N/mm², respectively.

After production, the specimens were covered with tight plastic for one week until the measurements started. The two small side surfaces and the bottom and top surface of the specimens were provided with a water vapour proof seal of silicone. (The later glued side-surfaces of the tensile creep specimens were not sealed.) Sealing was recommended to simulate the normal evaporation process for walls as close as possible [4]. Gauge location pads were glued on each face of the specimens in order to measure displacements during testing (see Figure 1).

3.2 Test arrangement

The creep tests were carried out in the longitudinal direction of the masonry in order to gather data in the direction in which walls are normally restrained. To obtain creep coefficients, two sets of specimens were exposed to exactly the same environmental history. One set was unloaded and subjected to unrestrained shrinkage. The other set was loaded. The creep, in addition to the instantaneous deformations was obtained from the difference in deformations between the two sets.

To simulate a typical indoor situation, the experiments were carried out in an environmental test chamber at 20 ±2 °C and 55 ±5 % RH. The tensile creep specimens were turned 90° and glued in the test arrangement as shown in Figure 2. The principal of a lever obtained tensile stresses. Load was applied in successive steps up to a level of

0.10 N/mm² when referred to the gross area. Referred to the net area, the average stress in the blocks on both sides of the open joint was 0.19 N/mm².

3.3 ESPI

In order to obtain information about strain distributions around the free perpend joint, deformation measurements were carried out using Electronic Speckle Pattern Interferometry, ESPI [9]. The functioning of the system is as follows: The ESPI instrument illuminates the surface on a specimen from two positions with a laser beam via a splitter over mirrors in various phases of testing. The reflected light is captured and analysed by a computer with a monitor. At first speckle patterns are found, and by subtracting speckle patterns from various phases of testing, interference fringes are formed [10, 11]. The number of fringes and their widths are measures of displacements in the illuminated area. The technique is similar to the Moire'method but the accuracy can be much higher dependency of the size of the illuminated area.

The ESPI system consists of the ESPI head with CCD camera lens and laser mirrors, a control unit, and a computer with monitor and optionally a printer and a video recorder. Automatic evaluation of the measurement by real-time subtraction and phase-shifting algorithms is possible. Displacements in X, Y and Z direction can be obtained, using mirrors. From a fringe pattern of 572 by 768 pixels the displacements can be determined. The steps in the applied measuring process includes:

- Generation of a speckle pattern for two different loads,
- Generation of fringe patterns by subtraction of the two speckle patterns,
- calculation the vertical and horizontal displacements in a number of points,
- storage of the X and Y value and the displacement in X and Y direction of one of every ten pixels in an ASCI file for further analysis.

3.4 Measurements

Creep and shrinkage were measured with a Demec gauge (demountable mechanical gauge) with a gauge length of 100 ±1 mm. The measuring positions are shown in Figure 1. The displacements of the creep specimens were measured regularly during the test program. Changes in length and weight of the shrinkage specimens were recorded at the same time. Measurements made just before applying the load were taken as zero-values for the calculation of the total strain in the creep specimens. The zero-values for time dependent behaviour were measured after applying the load.

The tensile strength of the creep specimen was determined at the end of the test program. This was done by increasing the lever load in small steps until failure occurred.

The ESPI measurements were carried out during the tensile strength test of one of the creep specimen (T1). An area near the free perpend joint was observed by using ESPI, see in Figure 3. The observed area covered about 220x150 mm². The free perpend joint is visible to the left. The ESPI tensile test was carried out in a separate rig in which the specimen and the ESPI equipment were mounted at the same solid steel base, to avoid disturbance of the ESPI measurements due to movements of the test arrangement itself.

At the end of the test period the shrinkage specimens were dried to a constant mass at 80 °C in order to assess the moisture content during testing.

3.5 Calculations

The total strain of creep specimens consists of the following three components:

$$\varepsilon_{total}(t) = \varepsilon_{el} + \varepsilon_{sh}(t) + \varepsilon_{cr}(t) \quad (1)$$

where: $\varepsilon_{total}(t)$ is the measured strain in the creep specimens,
$\varepsilon_{cr}(t)$ is the creep strain,
ε_{el} is the elastic strain immediately after applying the load,
$\varepsilon_{sh}(t)$ is the shrinkage strain.

The creep coefficient, $\phi(t)$, can be calculated in accordance with [3] according to:

$$\phi(t) = \frac{\varepsilon_{cr}(t)}{\varepsilon_{el}} \quad (2)$$

4. RESULTS

In the following, a negative strain expresses a shortening (shrinkage), while a positive strain expresses an increasing length (tensile creep). In Figure 4 the change of weight and shrinkage are presented as a function of time. The figure shows that the weight of the specimens stabilised after about 100 days. The reduction was approximately 4.5 weight-% with respect to the dry mass. Deformations stabilised much later. At the end of the test, the shrinkage strains were -0.47 mm/m vertically (average A, D, C and F), -0.54 mm/m horizontally (average G and H) and -0.57 mm/m vertically including the bed joint (average B and E). The last point on each curve was the result of measurements after drying to a constant mass at 80 °C.

Specimen T1 failed 138 days after applying the load. It was not clear whether the specimen broke because of the applied creep load or because of any external influences. Specimen T1 was glued to be used for the ESPI measurement. Because of the failure of specimen T1, only tensile creep results of T2 and T3 are given. However, the measurements of T1 until 135 days indicated that it behaved similar to T2 and T3.

The elastic strain and the tensile creep in the specimen at the end of the creep tests are given in Table 2. Table 2 contains mean values of measurements at similar positions. Similar were the positions D and F (block above and under the open joint in the test arrangement), A, C, G and I (block above and under the highest stressed area) and B and H (block at the highest stressed area beside the open joint). The result of measurement E (over the free perpend joint) is presented separately. The developments of creep coefficients are presented in Figure 5. Position of measurements was grouped like in Table 2.

Deformations were also derived from the ESPI measurements. In Figure 6, the displacements at several heights relatively to the bottom of the monitored area (see Figure 3) are plotted versus their horizontal position. Displacements near the bottom of the observed surface are quite small on the left hand side under the open joint. At 143 mm from the bottom of the observed area the displacements were largest at the left hand side (0.012 mm). The effect of the open joint is clear. Points at 73 mm hardly moved, while points at 79 mm had a displacement of almost 0.0012 mm. At the right hand side, the displacements were proportional to the distance from the bottom, indicating uniform stress distribution.

The tensile strength (gross area) of specimen T2 and T3 was 0.16 N/mm². Both specimens failed within the highest stressed area via the open joint. Using the net area as basis, the average strength of the most stressed area was 0.32 N/mm².

5. DISCUSSION

Under production, masonry LECA blocks are wrapped in plastic and stored for about four weeks before transportation to the building site. In this study, the blocks were wrapped in plastic for three weeks before the specimens were prepared. The moisture content of the specimens at the start of testing was assumed to be in correspondence with the normal situation at the building site (about 10 weight-%). However, due to the manufacturing of the specimens drying appeared and about 6 weight-% moisture remained. Consequently, some of the drying creep may be lost compared with expected “worst case”.

Compared to the average deformations of the blocks, a relatively large opening of the free perpend joint was measured. This is in agreement with the results of a linear-elastic analysis, as shown in Figure 7. Figure 8 illustrates the belonging distribution of the largest principal stress (tension), on both sides of the free perpend joint. The distribution shows that the external tension must be carried by a reverse arch mechanism across the free perpend joint, leaving the areas on both sides free of stress. This implies a stress concentration at both ends of the free perpend joint, which decrease towards a uniform distribution across the adjacent blocks in the extension of the joint. Accounting for creep would hence give a similar shape as in Figure 7, which is also indicated by the ESPI results in Figure 6.

Figure 5 indicates that the test lasted almost long enough to measure the final creep. Hence, the tensile creep coefficients in Table 2 can be considered as final creep coefficients. Experiences from long-time loading of concrete in compression indicate creep coefficients usually between 1.0 and 6.0, with 2.5 as the most typical value [5]. The design value of Eurocode 6 [3] is 2.0 with a range from 1.0 to 3.0. Table 2 indicates a final creep coefficient of 7.8 in the middle of the continuous blocks (B and H), while coefficients of 2.5 were recorded elsewhere in the continuous blocks (A, C, G and I). The last value fits very well with the recommendation in [3, 5]. The high creep coefficient at position B and H may be caused by the stress concentration in this part of the specimen. A tensile load of about 60 % of the tensile strength was maintained during the creep test. Normally, the creep coefficient of concrete is approximately constant up to about 50 % of the compressive strength [5]. Due to the equality of the creep coefficient in compression and tension and the fact that concrete behaves in a linear elastic manner up to about 70 % of the tensile strength [12], a much lower creep coefficient than 7.8 was expected in the highest stressed area. This is supported by lower creep coefficients obtained by [13] during compressive creep tests on low strength LECA concrete. These tests were carried out with stresses equal 30 %, 50 % and 70 % of the compressive strength [13], indicating a much smaller creep coefficient than obtained during this investigation of tensile creep.

Further investigations into tensile creep of masonry with free perpend joints should be focused on the situation in a whole wall. Both experimental testing and numerical analyses should be involved to give reliable design methods. A complementary explanation should also be made for the high creep coefficient in the continuous blocks besides the open joint.

6. CONCLUSIONS

The behaviour of LECA masonry exposed to tensile creep has been analysed during this test program. A relatively large opening of the free perpend joint is explained by the stress distribution in the specimens. Obtained creep coefficient in the highest stressed area was larger than expected from information retrieval.

ACKNOWLEDGEMENTS

The experiments were carried out at the Pieter van Musschenbroek Laboratory at Technische Universiteit Eindhoven. The authors gratefully acknowledge the financially support from The Research Council of Norway and Norsk Leca. Thanks are also due to Cor Naninck, Sip Overdijk and Erik Wijen for their support in carrying out the experiments.

REFERENCES

1. JONG, P. DE – Bouwschade ter lering (I) (Lessons from damage in building industry (I)), *Cement*, (2) pp. 26-28, 1992 (in Dutch).

2. MADSØ, F. E. – Bevegelser og bevegelsesfuger i murverk. Del 1 (Movement and Movement Joints in Masonry. Part 1), *Mur*, (2) pp. 27-30, 1997 (in Norwegian).

3. EUROPEAN PRESTANDARD: ENV 1996-1-1 Eurocode 6: Design of masonry structures – Part 1-1: General rules for buildings – Rules for reinforced and unreinforced masonry, CEN, Brussels 1995.

4. SCHUBERT, P. – Test methods for the determination of creep and shrinkage in masonry, *Proc. of 10th Int. Brick and Block Masonry Conf.* Masonry Council of Canada, The University of Calgary, Calgary, pp. 777-786, 1994.

5. BAŽANT, Z.P. – Chapter 7: Mathematical Models for Creep and Shrinkage of Concrete, *Creep and Shrinkage in Concrete Structures*, (Editor Bažant, Z.P. and Wittmann, F.H.) Wiley, ISBN 0-471-10409-4, New York 1982.

6. DRAFT EUROPEAN STANDARD: prEN 771-3: Specification for masonry units – Part 3: Aggregate concrete masonry units (Dense and lightweight aggregates), CEN, Brussels 1996.

7. PLUIJM, R. VAN DER and VERMELTFOORT, A.T. – Influence of the type of mortar joint on the time dependent behaviour of masonry, *Proc. of 8th Canadian Masonry Symposium*, Alberta, Canada 1998.

8. DRAFT EUROPEAN STANDARD: prEN 1015-11: Method of test for mortar for masonry – Part 11: Determination of flexural and compressive strength of hardened mortar, CEN, Brussels 1995.

9. VERMELTFOORT, A.T. – ESPI for research into mechanical compressive behaviour of masonry, *Proc. of 11th International Brick/Masonry Conf.* Shanghai, pp. 385-394, 1997.

10. VERMELTFOORT, A.T. – The application of Electronic Speckle Pattern Interferometry for measurements of Masonry/mortar stiffness, *Proc. 5th Int. Mas. Conf.* London, pp. 77-84, 1998.

11. JONES, R. and WYKES, C. – *Holographic and speckle interferometry*. Cambridge university press, Cambridge 1983.

12. EIBL, J. et al. – *Concrete Structures. Euro-Design Hanbook*, Ernst & Sohn, Berlin 1995.

13. STEMLAND, H. and THORENFELDT, E. – *Lett konstruksjonsbetong* (Lightweight concrete), Delprosjekt 2: Konstruktive aspekter, Delrapport 2.1: Superlette betongkvaliteter, STF22 A98742, SINTEF, Trondheim 1998 (in Norwegian).

Table 1
Material properties of LECA blocks according to prEN 771-3 [6].

Dimension	96 x 249 x 500 mm
Dry density	730 kg/m³
Compressive strength	2.6 N/mm²
Modulus of elasticity	2900 N/mm²
Poisson's ratio	0.2

Table 2
Elastic strain. Creep strain and creep coefficient at the end of the tensile creep test. Calculated stresses based on measured elastic strain and a modulus of elasticity of 2900 N/mm².

Position of measurement [1]	Elastic strain [mm/m]	Creep strain [2] [mm/m]	Creep coefficient [2] [-]	Calculated stress [N/mm²]
D and F	0.01	0.01	0.6	0.03
A, C, G and I	0.05	0.10	2.5	0.15
B and H	0.06	0.23	7.8	0.17
E [3]	*0.18*	*1.26*	*8.0*	-

[1] See Figure 1, right.
[2] Mean values based on specimen T2 and T3 only.
[3] Because of the open joint, it is not correct to calculate strain in this area.

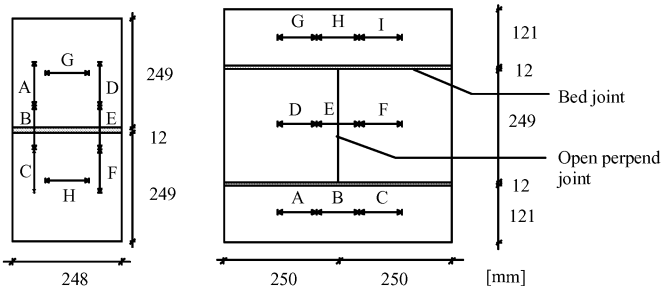

Figure 1 – Left: masonry specimens for measurement of shrinkage. Right: masonry specimens for measurements of creep caused by tensile load. The letters identifies the gauge locations.

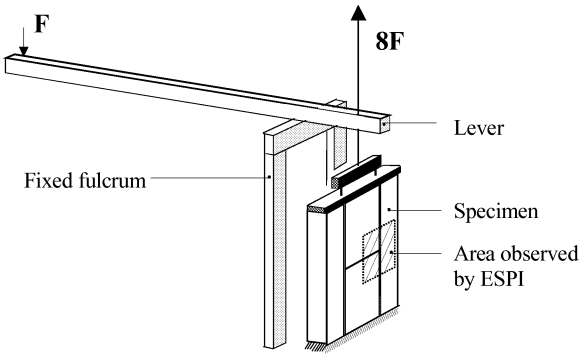

Figure 2 – Principal sketch of the tensile creep test arrangement. It should be noted that the specimen is turned 90° before gluing in the test arrangement.

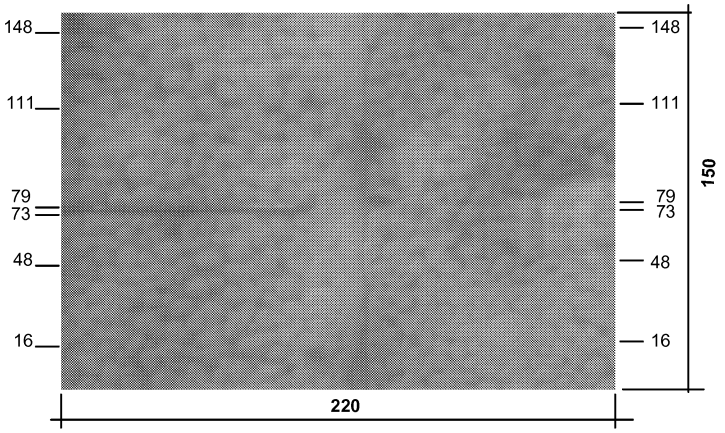

Figure 3 – Photo of the surface area that was observed by ESPI. Free perpend joint at half the height at the left hand side.

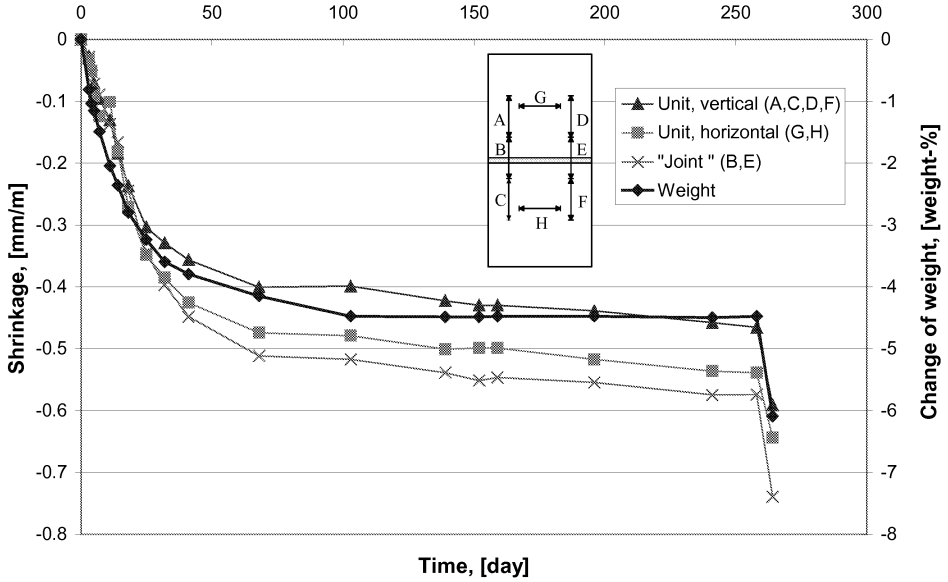

Figure 4 – Mean development of shrinkage. Displacements are measured in accordance with the figure enclosed in the diagram.

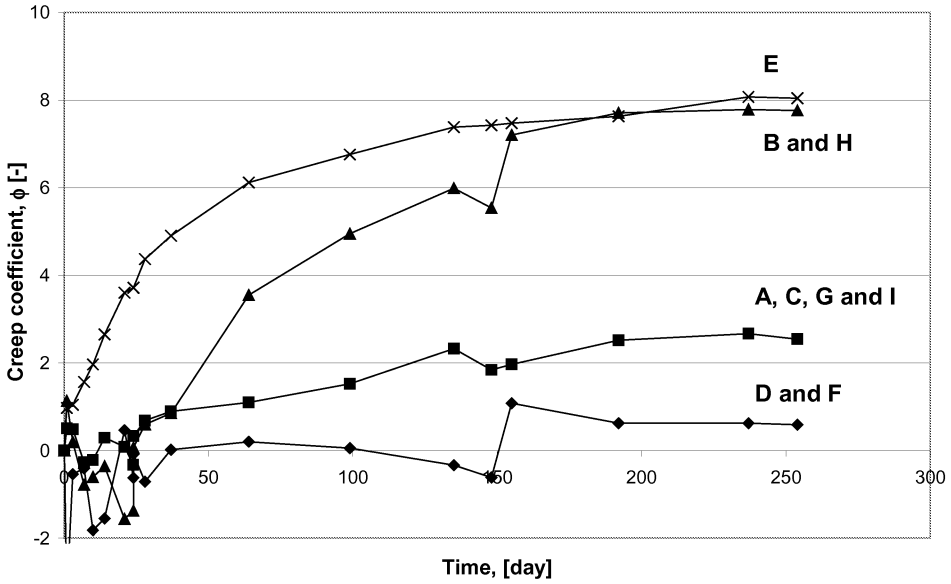

Figure 5 – Mean development of tensile creep coefficients obtained from specimen T2 and T3. Strains are measured in accordance with Figure 1. Because of the open joint, it is not correct to calculate creep coefficient in this area, see curve E.

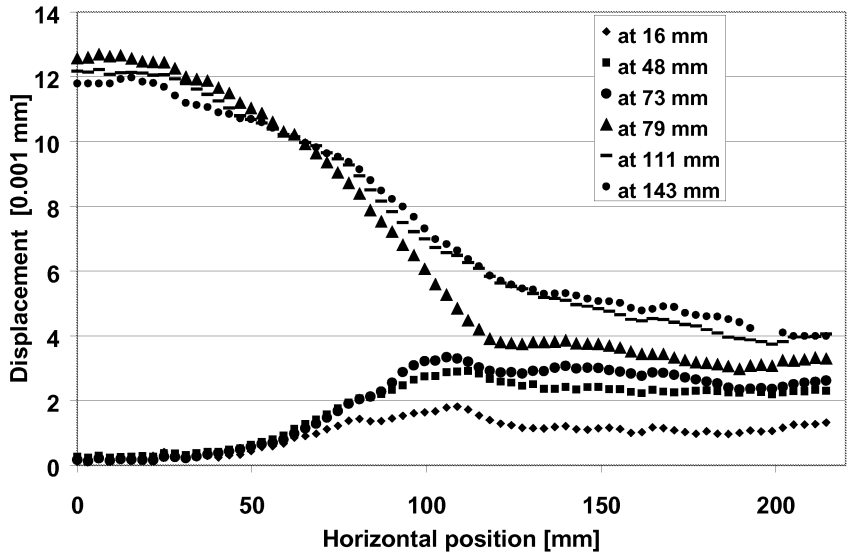

Figure 6 – Displacements in vertical direction with respect to the specimen in the test arrangement. Postion of measurement according to legend are indicated in Figure 3.

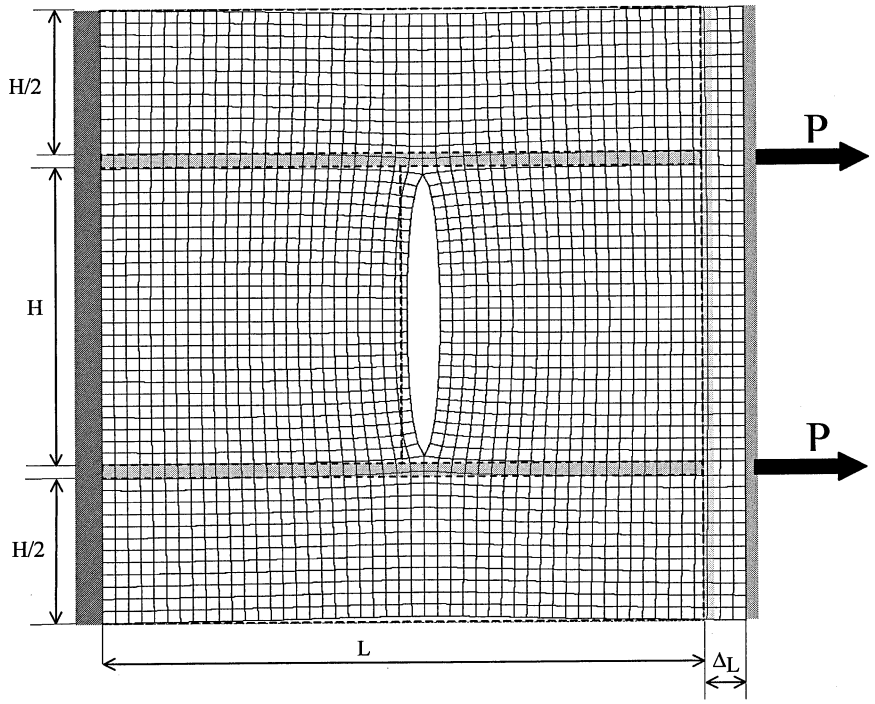

Figure 7 – Deformed specimen (Undeformed shape illustrated by dashed lines).

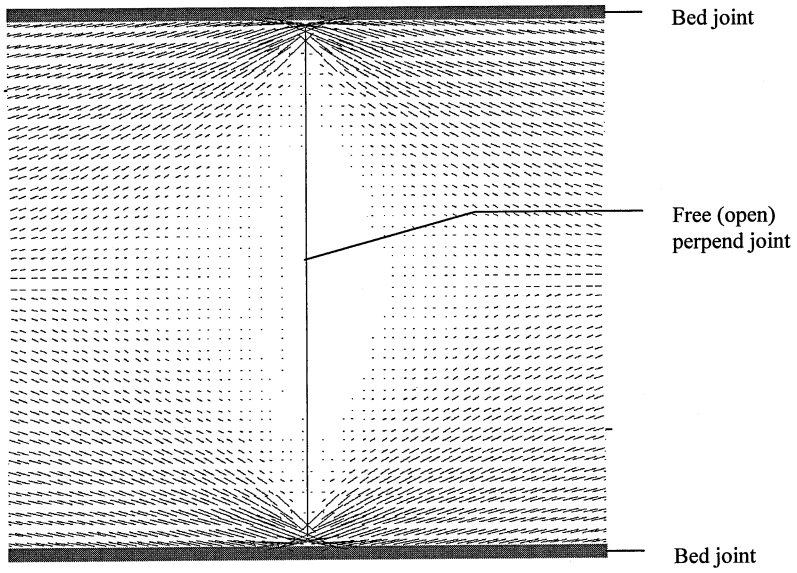

Figure 8 – Largest principal stress distribution on both sides of vertical open joint (tension).

APPENDIX 5

Kvande. T.
Deformation Controlled Tensile Tests on LECA Masonry.
Report N 8330-6, Norwegian Building Research Institute, Trondheim 2001.

BYGGFORSK
Norwegian Building Research Institute

Head Office
Forskningsveien 3b
P.O.Box 123 Blindern
N-0314 OSLO
Tel. +47 22 96 55 55
Fax +47 22 69 94 38

Local Department
Høgskoleringen 7
N-7491 TRONDHEIM
Tel. +47 73 59 33 90
Fax +47 73 59 33 80

E-mail firmapost@byggforsk.no
Internet www.byggforsk.no
Registration No. NO 943 813 361 VAT

Clients
Mur-Sentret and
Department of Building and
Construction Engineering - NTNU

Client's addresses
Pb. 53 Blindern, 0313 Oslo
and
7491 Trondheim

Client's contact-persons
Geir Wold-Hansen og
Jan Vincent Thue

Project/archive no.	Date	Rev. date	No. of pages	Appendixes	Classification	Author(s)
N 8330-6	31.01.2001		21	3	Unrestricted	Tore Kvande

Project leader	Sign.	Responsible manager	Sign.	Quality assurance	Sign.
Tore Kvande		Terje Jacobsen		Karl Vincent Høiseth	

Assignment Report

Deformation controlled tensile tests on LECA Masonry

Summary

This report gives an overview of deformation-controlled tensile tests on masonry of Light Expanded Clay Aggregate (LECA) concrete blocks. The main purpose of the test was to establish the behaviour of LECA masonry in uni-axial tension. The determined behaviour may be applied for numerical modelling of tensile cracking of LECA masonry.

The tests are carried out in a tensile testing arrangement developed at the Pieter van Musschenbroek Laboratory at Technische Universiteit Eindhoven, the Netherlands.

Values for tensile strength, modulus of elasticity and fracture energy for LECA blocks and bond has been established during the test program. The results from the test program support the validity of Hordijk softening (Equation 2) for blocks and bond interface to describe the post peak behaviour on the basis of non-linear fracture mechanics.

This work has been a part of the dr.ing-project "Material Properties for Masonry of Light Expanded Clay Aggregate Concrete as a Constructive Material". The doctoral study has been funded by The Research Council of Norway and Norsk Leca (presently Optiroc). The study has been a part of the research program "Loadbearing Masonry 1997-2000" co-ordinated by Mur-Sentret. The current report is based on Working Report 6 of 20. October 1999.

Address of the building	Built (year)

Activity code	Keywords	Filename
3.4	Lettbetong, Styrke, Stivhet, Mørtel	N8330-6.doc

Contents

1. Introduction

This report gives an overview of deformation controlled tensile tests on masonry of Light Expanded Clay Aggregate (LECA) concrete blocks. The main purpose of the test was to establish the behaviour of LECA masonry in uni-axial tension. The behaviour should be expressed applicable for numerical modelling of tensile cracking of LECA masonry.

During his Ph.D-study, Van der Pluijm (1999) developed the test set-up used for the testing. The tests were carried out in the Pieter van Musschenbroek Laboratory at Technische Universiteit Eindhoven, TUE, during the period from January to March 1999. Martien Ceelen, TUE, and Tore Kvande, Norwegian University of Science and Technology - NTNU, have been responsible for the performance of the testing.

A detailed overview of the test results is given in Kvande (2001-10).

2. Materials and specimens

The LECA blocks used as test specimens were produced 17.08.98 by Norsk Leca's factory at Lillestrøm, Norway. The blocks are known as *Leca kompaktblokk 15 cm 3/770*. "3/770" indicates the quality of the concrete, namely a compressive strength of 3 N/mm² and a density equal to 770 kg/m³. Material properties and material composition of these blocks are described in Kvande (2001-3).

Deformation controlled tensile tests were carried out on blocks and on masonry couplets containing one mortar joint.

The block specimens, with dimensions 150x70x70 mm, were sawn out of LECA blocks. A 5 mm deep notch on two opposite sides made the fracture area 60x70 mm as shown in Figure 1. After cutting, the specimens were acclimatised by 20 °C and 60 % RH before testing. Specimens were made for testing in the three orthogonal directions of the LECA block, see Figure 2: Vertically direction of the blocks (set I), in the width of the blocks (horizontally, set IV) and in the length of the blocks (horizontally, set V). Set V were tested both acclimatised by 20 °C and 60 % RH and dried by 105 °C (set V-D). Specimens with letter V-D were tested within a few hours after they were removed from the heater.
In total 60 specimens were made.

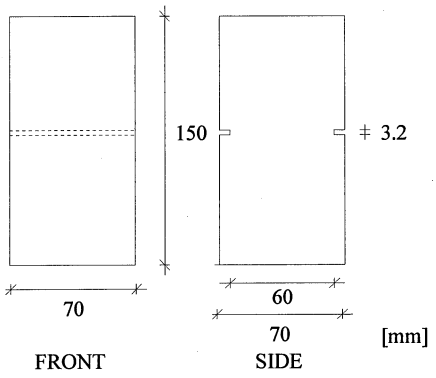

Figure 1:
Specimen for tensile test of block.

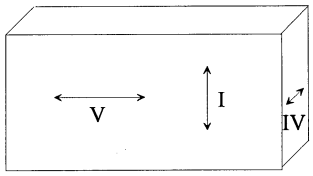

Figure 2:
Test directions of block.

For tensile testing of the masonry, pieces of 69x100x100 mm were sawn from the LECA blocks. In order to achieve representative joints, mortar was applied on original bonding surfaces. Before making the specimens, the sawn pieces were acclimatised by 20 °C and 60 % RH.

A factory made mortar *Leca fasadepuss* (LC 35/65/520) was used as joint material in the specimens. When mixing the mortar in the laboratory, 2.5 l water was added to 15 kg dry mortar.

After the specimens were made, they were enclosed in plastic for four days and afterwards stored for at least 24 days by 20 °C and 60 % RH. In total 20 masonry specimens were made for deformation-controlled tensile test, see Figure 3.

A preliminary test of tensile strength was carried out on 12 specimens by force control. The tests were carried out to estimate the effect of two different curing regimes. Half of the specimens were stored as mentioned, the remainders were enclosed in plastic until testing 29 days after manufacturing.

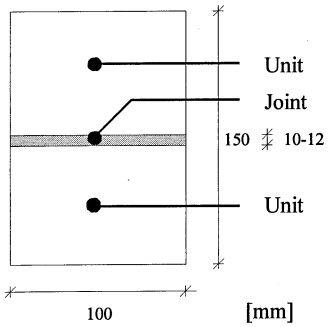

Figure 3:
Specimen for tensile test of masonry.

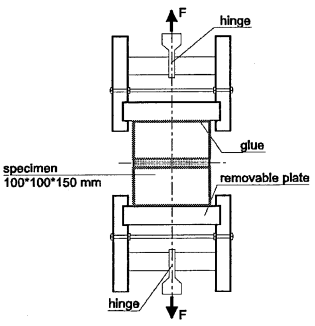

Figure 4:
Tensile test set-up for preliminary test (Van der Pluijm 1995).

3. Testing arrangement

3.1 Preliminary test of tensile strength of masonry

Preliminary tests of tensile strength of masonry with one mortar joint were carried out as shown in Figure 4. The tests were carried out by force control.

3.2 Deformation controlled tensile tests

In Figure 5 to 7 the tensile testing arrangement of the Pieter van Musschenbrock Laboratory is illustrated. The test set-up is designed to avoid rotation of the plates between which the specimens are glued. It consists of two horizontal steel arms and a rectangular hollow section making a parallelogram together with the HE300B frame. The parallelogram allows the hollow section to move straight up or down without any rotation. The hollow section is denoted “red box” in Figure 5. Figure 7, shows a cross section of the red box and its contents. The dead weight of the hollow section and the spring-force of the steel arms must be subtracted from the measured load.

The Linear Variable Differential Transducers, LVDTs, is controlling the increase of deformation over a crack that develops during testing. The LVDTs are glued to the specimen as shown in Figure 6, with measuring length 30 mm.

A detailed description of the test set-up is given in Van der Pluijm (1997).

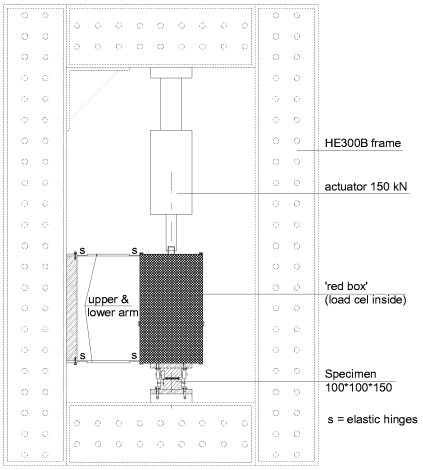

Figure 5:
Deformation controlled tensile test arrangement (Van der Pluijm 1995).

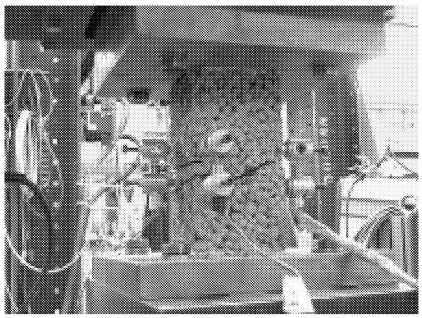

Figure 6:
A specimen mounted in the test rig. The results from this specimen are rejected because the failure appeared outside one of the LVDTs.

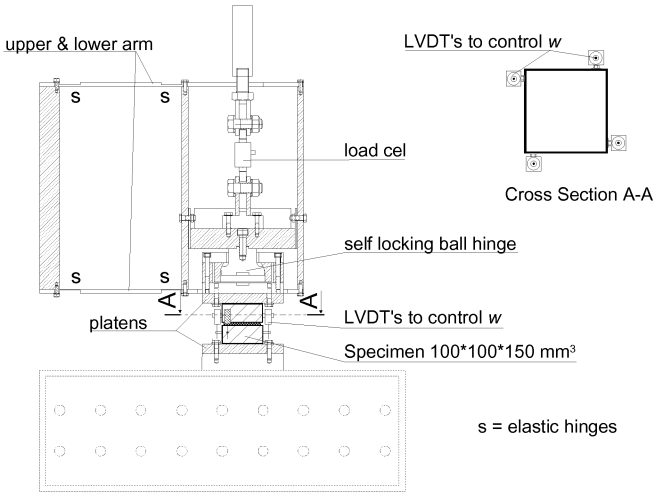

Figure 7:
Deformation controlled tensile testing arrangement in detail. The figure was made at the Pieter van Musschenbrock Laboratory.

The test arrangement contains of a self locking ball lump that allows for non parallel specimens that are glued between steel plates outside the arrangement. Because it was suspected that the ball lump did not loch correctly anymore, the rig was modified by a plate of aluminium. The aluminium plate was fixed to the bottom of the hollow section as seen in Figure 8. Rotation of the parallelogram and the upper steel plate, which the specimens were glued to, was measured during testing before and after modification. The effect of the modification will be discussed in chapter 5.

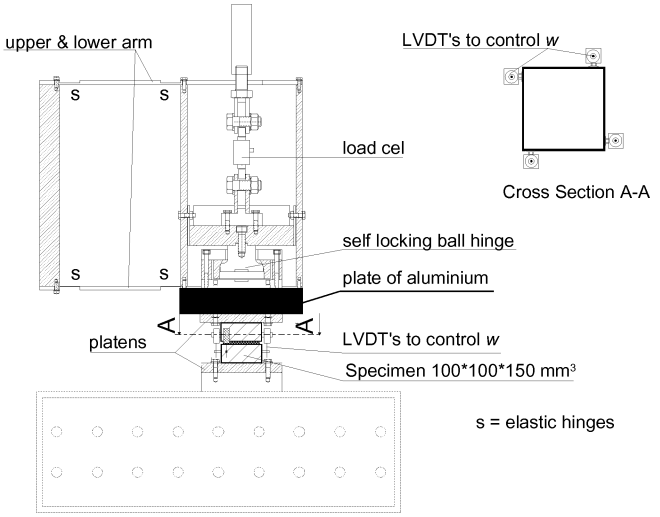

Figure 8:
Deformation controlled tensile testing arrangement after modification.

3.3 Calculation of f_t, E and G_{fl}

The main purpose of the tensile testing was to determine the behaviour of LECA masonry in uni-axial tension. An idealised stress-deformation relationship is presented in Figure 9. To do non-linear analysis of tensile cracking of LECA masonry the complete stress-displacement relationship has to be known. The stiffness, strength and stress-crack width relation may accord to Rots (1997), express the relationship.

The tensile strength, f_t, is calculated by:

$$f_t = \frac{F_u}{A} \qquad \text{Equation 1}$$

where: F_u is the maximum load,
A is cross sectional area of the specimen.

Before the onset of cracking, the specimen behaves almost linear, with a modulus of elasticity denoted as E_o. In numerical modelling, the mechanical behaviour is frequently considered linear until the tensile strength has been reached. In the present work, a secant modulus at the strength, E_u, are also calculated, see Figure 9.

Regarding the block specimens, tensile values were determined on specimens with notches. As the specimens had a notch in the area where the measurements were taken, no representative stiffness values could be obtained. In accordance with (Van der Pluijm 1999) too low values may have been obtained. Because of the notches themselves and the changes of the cross sectional area within the load direction, a non-uniform stress distribution occurs in the specimens. The non-uniform stress distribution leads to lower stiffness values than expected.

The area under the stress-deformation is defined as the mode I fracture energy, G_{fI}. The fracture energy is the energy that is needed to create one unit crack surface (Rots 1997).

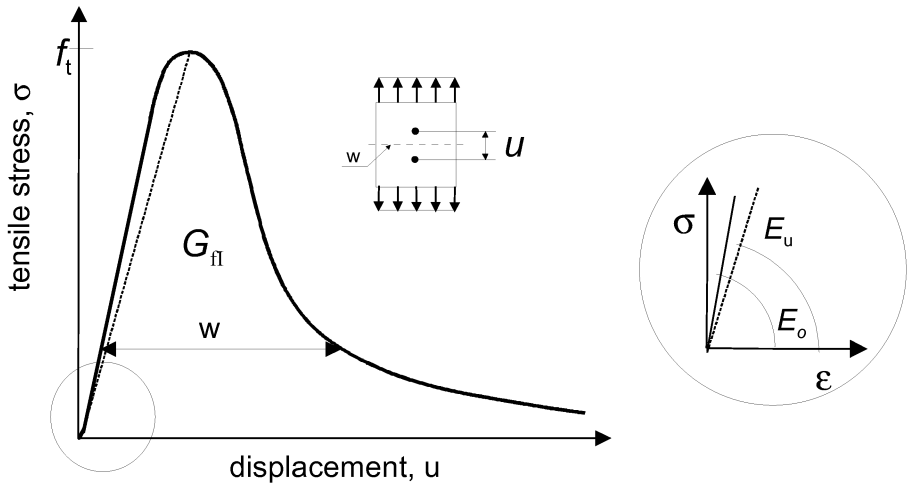

Figure 9:
Schematic diagram of a deformation controlled tensile test. The figure contains analysed quantities.

After the tensile strength has been reached, the mechanical behaviour of the specimen is difficult to control. Instant global failure occurred in some of the specimens because of the sensibility of the test. In these cases, the complete descending branch was not traced, and the contribution to G_{fI} of the post peak stress/deformation curve was lost.

In Hordijk (1992) a formula describing the descending branch for concrete is presented (Equation 2). Van der Pluijm and Vermeltfoort (1991) prove the validity of the equation for masonry under tension.

$$\frac{\sigma}{f_t} = \left(1 + \left(c_1 \frac{w}{w_c}\right)^3\right) e^{-c_2 \frac{w}{w_c}} - \frac{w}{w_c}\left(1 + c_1^3\right) e^{-c_2} \qquad \text{Equation 2}$$

where: σ is tensile stress,
f_t is tensile (bond)strength,
c_1, c_2 is dimensionless constants, respectively 3.0 and 6.93,
w is crack width,
w_c is crack width at which no stresses are being transferred any more:

$$w_c = 5{,}14 \frac{G_{fI}}{f_t}$$

G_{fI} is mode I fracture energy.

By using Equation 2 it is possible to calculate a theoretical value of G_{fI} if the tail is incomplete. The difference between G_{fI} and $G_{fI:theory}$ are illustrated in Figure 10.

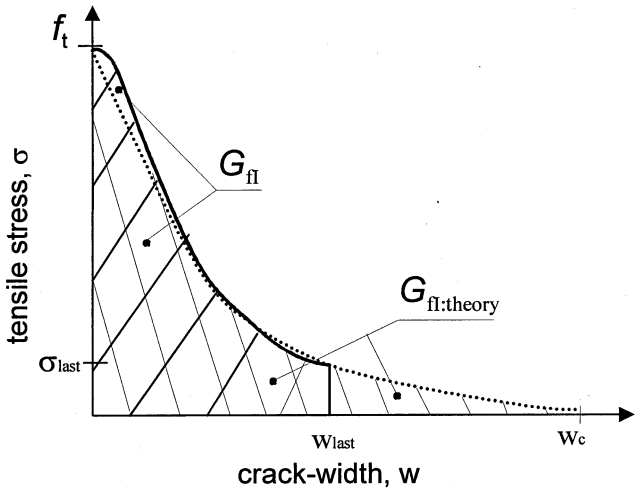

Figure 10
Schematic diagram of the difference between G_{fI}, calculated from the measurement up to w_{last} and $G_{fI:theory}$, calculated from the theoretical line up to w_c.

The calculation of the modulus of elasticity of the mortar joint is based on Equation 3. The equation is based on the assumption that Poisson's ratios are equal for block and mortar. It should be noted that, according to Equation 3, the effect of the interface is included in the calculated modulus of elasticity of the joint.

$$E^j = \frac{t^j \cdot E^{j+u} \cdot E^u}{E^u\left(t^u + t^j\right) - E^{j+u} \cdot t^u} \qquad \text{Equation 3}$$

where: E^j is the modulus of elasticity of the joint,
E^u is the modulus of elasticity of the masonry unit,
E^{j+u} is the modulus of elasticity of the specimen within the gauge length, follows directly from the measurements,
t^j is the thickness of the mortar joint,
t^u is the sum of the thickness of the concrete block parts within the gauge length.

4. Results

4.1 Preliminary test of tensile strength of masonry

The results from the preliminary test of tensile strength of masonry specimens with one joint are presented in Table 4.a. Specimens 1-6 were enclosed in plastic for 4 days and afterwards stored in 20 °C and 60 % RH for 23 days. Specimens 7-12 were stored under plastic cover for 29 days.

Table 4.a:
Mean values of tensile strength, f_t, of LECA masonry. CV is coefficient of variation.

Specimen	Tensile strength		Failure
1-6	*Mean* *CV*	0.26 N/mm² 28 %	Interface
7-12	Mean CV	0.29 N/mm² 24 %	Interface / (LECA)
All	***Mean*** ***CV***	***0.28 N/mm²*** ***25 %***	**-**

The flexural- and compressive strength of plain mortar was measured to 2.9 N/mm² and 9.7 N/mm² respectively. The measurements were carried out in accordance with prEN 1015-11.

4.2 Deformation controlled tensile test of LECA blocks

In total 32 specimens were tested. In 25 specimens, the ultimate crack was initiated inside the notch, and propagated through the cross section within the measuring length of the LVDTs. For the remaining tests, the ultimate crack was either initiated outside, or propagated outside the LVDTs, which made it impossible to control the deformation. The results are given in Table 4.b. Figure 11 and Appendix 1 concerns merely the tests where the failure appeared within the LVDT. For some of the tests, failure appeared at a too high stress level to give a representative value of G_{fl}. Table 4.b and Appendix 2 contains only the values of G_{fl} and last displacement and stress reading for those specimens were it was possible to calculate representative values of G_{fl}.

The picture in Figure 12 illustrates a typical crack surface after failure. Figure 13 shows a sketch of the characteristic irregular crack propagation through the cross-section of the specimens. Close to the notches, two cracks were frequently observed, which bridged into a main crack in some small distance from the notch surface. This is due to stress-concentrations in each corner of the notches (Van Mier et al. 1994).

Table 4.b:

Mean values from tensile test of LECA block. The numbers in parenthesis are coefficient of variation, CV, in %.

Type of specimen	Tensile strength f_t [N/mm²]	Mode I fracture energy G_{fI} [N/mm]	Last displacement w_{last} [mm]	Last stress $_{last}$ [N/mm²]	Mode I fracture energy, theory $G_{fI;theory}$ [N/mm]
I	0.48 (21)	0.019 (15)	0.08 (24)	0.11 (62)	0.028 (37)
IV	0.50 (12)	0.020 (13)	0.08 (19)	0.09 (45)	0.026 (31)
V	0.50 (14)	0.022 (12)	0.08 (34)	0.10 (60)	0.030 (20)
V-D	0.49 (8)	0.022 (21)	0.07 (41)	0.14 (37)	0.037 (24)
Mean all	***0.49 (13)***	***0.021 (16)***	***0.08 (29)***	***0.11 (49)***	***0.030 (29)***

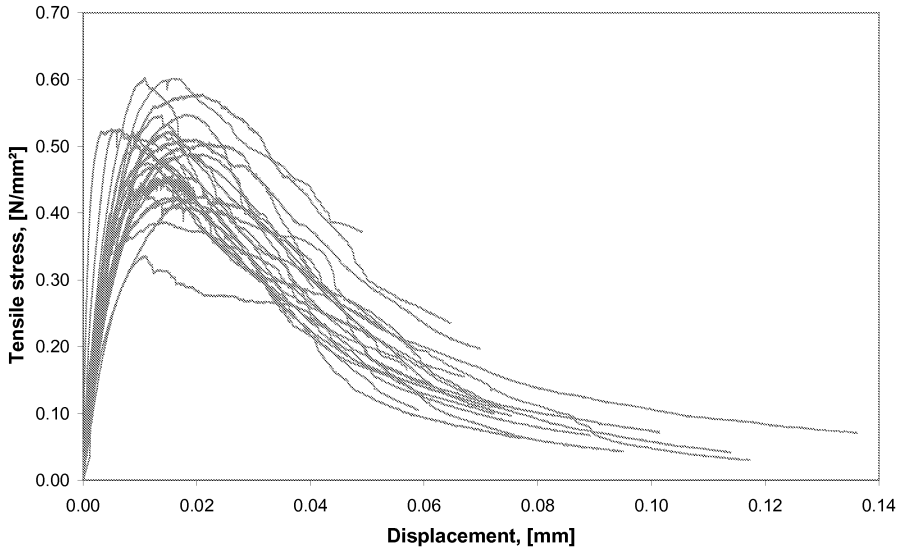

Figure 11:

Summary of all tensile tests of LECA block.

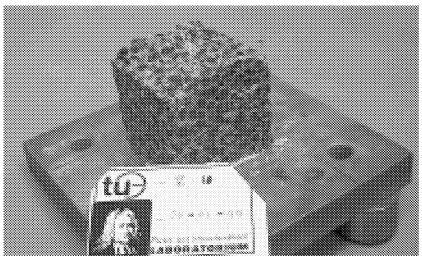

Figure 12:
Crack surface after failure of specimen V-11.

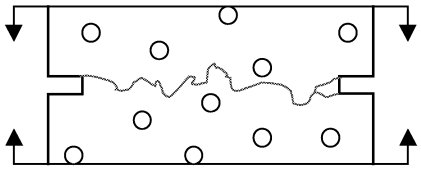

Figure 13:
Principal sketch of a typical failure of specimens of block.

4.3 Deformation controlled tensile test of masonry specimens

In total 11 tensile tests of small masonry specimens were carried out. In two cases, however, the specimens were subjected to eccentric loading because of incomplete gluing between test specimens and steel plates, see Figure 6. The results of these tests have been neglected. The test results are given in Appendix 3 and Figure 14. The summary in Table 4.c contains the mean values from testing. The table also contain theoretical fracture energy, $G_{fl;theory}$, calculated from last measured displacement and stress according to Equation 2. Calculation of the modulus of elasticity of joint is based on E_o^u= 3000 N/mm², see section 5.2.

It should be noted that the presented data for mortar joint is the mean behaviour of the mortar joint itself and the interface.

Table 4.c:
Mean values from tensile test of LECA masonry. CV is coefficient of variation.

Material property		Mean	CV, [%]
Tensile strength	f_t	0.25 N/mm²	29
Modulus of elasticity	E_o^{j+u}	2100 N/mm²	36
	E_o^j	1800 N/mm²	44
	E_u^{j+u}	800 N/mm²	42
	E_u^j	300 N/mm²	51
Mode I fracture energy	G_{fl}	0.011 N/mm	35
	$G_{fl;theory}$	0.011 N/mm	32
Last displacement	σ_{last}	0.11 mm	26
Last stress	w_{last}	0.03 N/mm²	62

The flexural- and compressive strength of the mortar was measured to 3.0 N/mm² and 9.9 N/mm² respectively. The strengths were measured in accordance with prEN 1015-11.

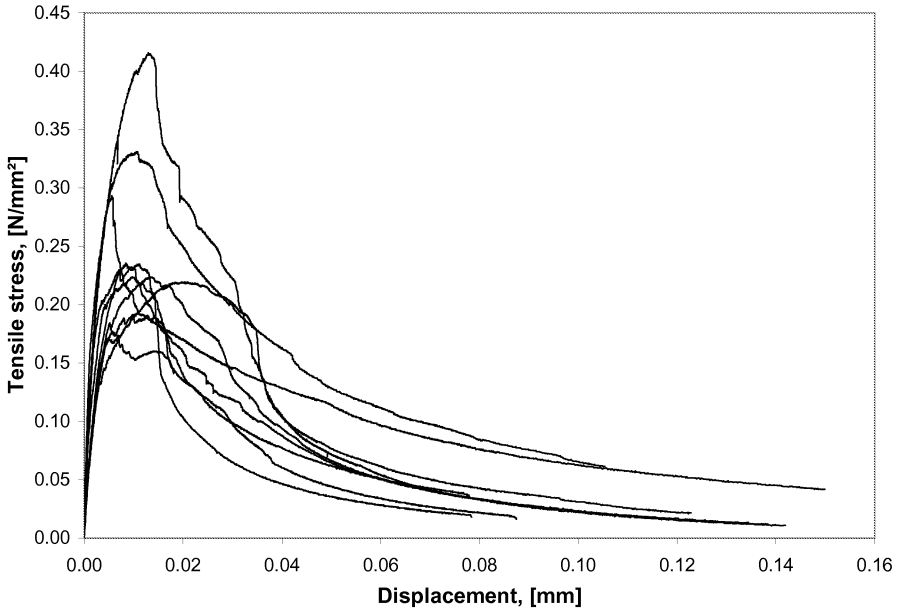

Figure 14:
Summary of all tensile tests of LECA masonry.

A typical example of failure is shown in Figure 15. Apart from cracking through a few aggregates, the failure appeared in the interface between mortar and block.

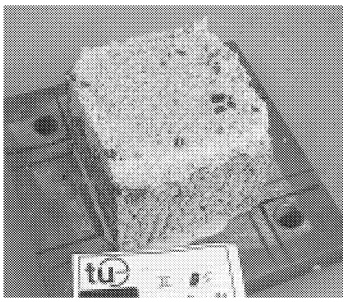

Figure 15:
Crack surface after failure of specimen II-5.

5. Discussion

5.1 Control of the test arrangement

The main goal with the tensile test program was to determine the stress-crack width diagram and the corresponding fracture energy. To get representative data, it is important that the test specimens are subjected to pure uni-axial conditions. Normally, the greatest challenge making a tensile test set-up is to get a sufficient stiff arrangement and a sensitive enough controlling of the test (Eibl et al. 1995). A sufficient stiffness is achieved by the parallelogram arrangement in the rig at Pieter van Musschenbroek Laboratory, see chapter 3.2. The arrangement allows the hollow section (the load head) to move in a vertical direction, accompanied by a negligible horizontal displacement, see Figure 16. The vertical displacement during the tensile testing was less than 0.5 mm, which involved a horizontal displacement less than 0.4 μm. In Van Mier et al. (1994) the influence of the boundary conditions of the testing arrangement on the fracture energy is discussed in detail.

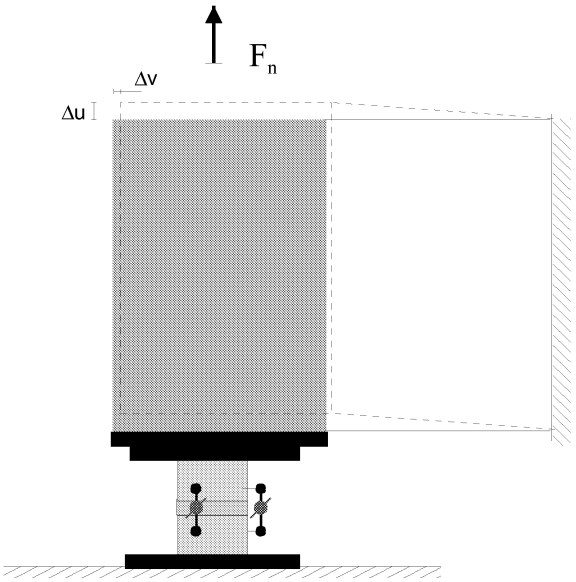

Figure 16
"Unintended" horizontal displacement, Δv, because of vertical movement, Δu of the parallelogram.

As a control of the test rig during testing measurement of rotation were made, see Kvande (2001-10). Before starting the tensile test of the masonry, the test set-up was modified by avoiding the movable hinge inside the hollow section. A plate of aluminium was fixed to the bottom of the hollow section (see Figure 8). By avoiding the rotation, a better controlling of the opening of the crack was intended. The test results indicate success with the test design modification. Now displacement of 0.10 mm with a corresponding tensile stress level of 12 % of the maximum (mean values) was recorded. For the test of the LECA block, 0.07 mm and 33 % (mean values) was recorded respectively. After the design modification the difference between G_{fI} and $G_{fI;theory}$ was strongly reduced (see Table 4.b and 4.c). This supports the validity of Equation 2 (Hordijk 1992) also for masonry of LECA.

Another proves of the success with the test design modification, were the measurements of the rotation during the test of specimens II-6 to II-9, see Kvande (2001-10). The rotation of the upper steel plate during the elastic part of the test is reduced. A rotation of the upper plate of less than 0.0015° was recorded. The rotation introduces a difference in deformation over the specimen of less than 2.5 μm.

The notches made in the specimens of LECA blocks intended to ensure failure within the LVDTs. Due to the shape of the notch stress-concentration appears in the corners of the notches during testing. Making notches without sharp corners are usually recommended to avoid such stress-concentration. However, making of notches with another shape will introduce micro-cracking in the LECA blocks as well. Consequently, stress-concentrations might appear no matter of shape of the notches.

5.2 Idealised tensile behaviour for numerical modelling

When the uncontrolled failure appear too early in the descending branch, the calculated mode I fracture energy is too small. Based on Equation 2 and the last measurement it is possible to calculate a theoretically mode I fracture energy. Consequently, also the validity of the $G_{fI;theory}$ depends on the length of the measured descending branch. This is why the presentation of mean values of G_{fI} an $G_{fI;theory}$ in Table 4.b and 4.c is not based on all the individual values. Tests where the final failure appeared higher than approximately 40 % of the maximum stress level are not counted in these tables. The decision is based on Van der Pluijm (1998).

Because the Hordijk softening (Equation 2) gives a nice correlation with the experimental diagrams, the theoretical fracture energy of Table 4.b may be used in numerical analysis. $G_{fI;theory}$ take in account the complete theoretical descending branch.

Figure 17 describes the idealised behaviour of LECA block. The elastic part of the diagram is expressed by E_o^u = 3000 N/mm² and a tensile strength of 0.5 N/mm². The descending branch in the diagram is calculated from Hordijk (1992) with fracture energy of 0.03 N/mm.

As the specimens had a notch in the area where the measurements were taken, no stiffness values may be obtained. E_o^u is taken from “Bransjenorm” obtained from compressive tests. According to Eibl et al. (1995) the modulus of elasticity may be assumed to be the same for compressive and tensile stresses within the range of working stresses.

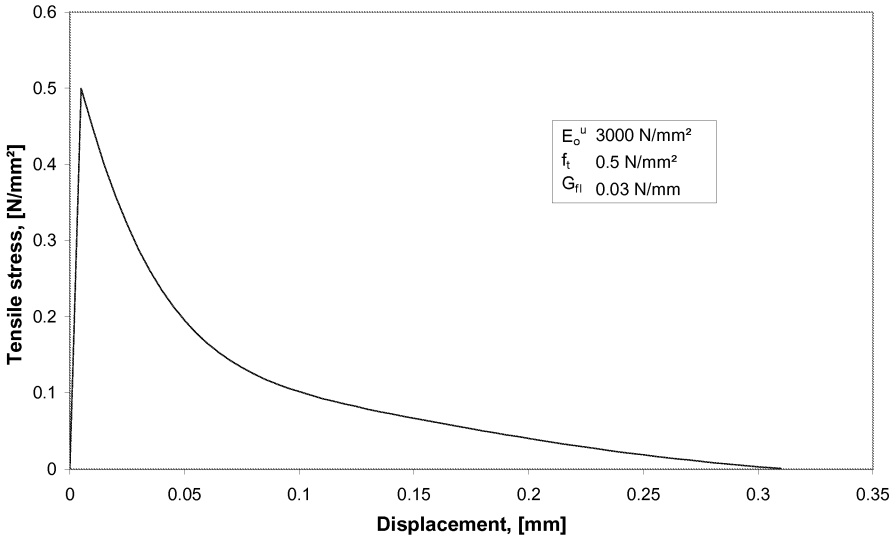

Figure 17:
Idealised behaviour of LECA block during deformation controlled tensile test.

The idealised behaviour of bed joint in LECA masonry is described in Figure 18. The diagram is based on f_t and G_{fI} ($G_{fI} = G_{fI;theory}$) from Table 4.c and Hordijk softening. It should be noted that calculation of E^j according to Equation 3 gives 1300 N/mm² (mortar joint thickness 10 mm). The value differ from the mean value given in Table 4.c because of variation of the mortar joint thickness. In numerical control of the experimental, the calculated E^j may be used as seen in Figure 18.

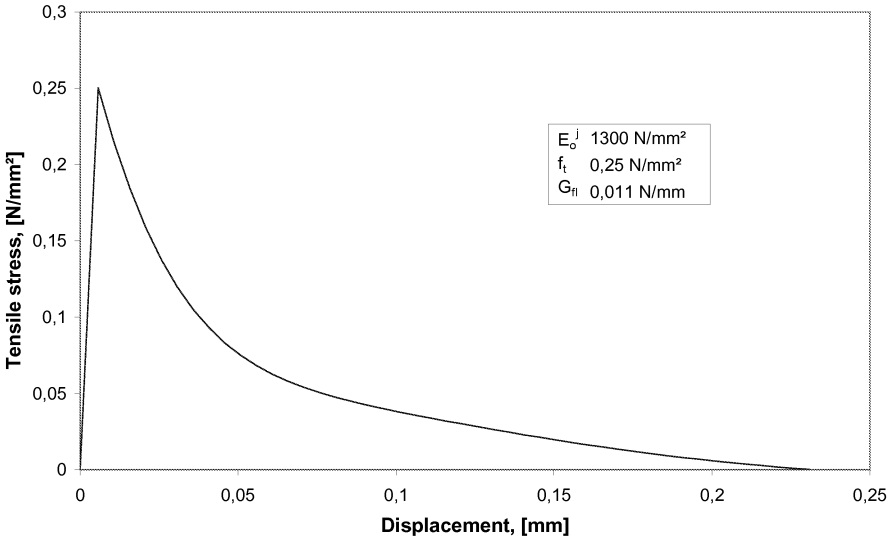

Figure 18:
Idealised behaviour of joint in LECA masonry during deformation controlled tensile test.

5.3 Homogeneity of the LECA block and influences of the humidity

To study the homogeneity of the LECA block, the specimens were tested in the three orthogonal directions, see Figure 2. No significant differences in the measured values were found.

The tested specimens were conditioned at 20 °C and 60 % RH. To check the effect of the humidity level, specimens of LECA block dried at 105 °C were also tested. No significant differences in the measured values were found.

6. Conclusions

Values for tensile strength, modulus of elasticity and mode I fracture energy for LECA blocks and bond has been established during the test program. The results from the test program support the validity of Hordijk softening (Equation 2) for blocks and the bond interface to describe the post peak behaviour on the basis of non-linear fracture mechanics.

No significant differences in the measured values were found in the three orthogonal directions of the block.

No significant differences in the measured values were found in specimens of masonry conditioned at two humidity levels.

7. References

Bransjenorm
Bransjenorm, Veiledning til ENV 1996-1-1:1995, Prosjektering av murverk. Beregning og dimensjonering (Draft National Application Document for ENV 1996-1-1:1995) Arbeidsdokument pr. 2000.01.19, Utarbeidet av Mur-Sentret, Oslo 2000.

Eibl et al. (1995)
Eibl, J. et al. – *Concrete Structures. Euro-Design Handbook*. Chapter A6.4.4, Ernst, Berlin 1995.

Hordijk (1992)
Hordijk, D.A - Tensile and tensile fatigue behaviour of concrete; experiments, modelling and analyses, *Heron* Vol. 37 No. 1, pp. 1-79.

Kvande (2001-3)
Kvande, T. – *Råstoff og materialeigenskapar for lettklinkerbetongblokk-kvalitet 3/770 150x250x500 mm. Prøveuttak frå a.s Norsk Leca sitt fabrikkanlegg på Lillestrøm 17.08.98.* (Light Expanded Clay Aggregate (LECA) Concrete Blocks, Quality 3/770 150 x 250 x 500: Raw material and material properties). Report N 8330-3, Norwegian Building Research Institute, Trondheim 2001 (in Norwegian).

Kvande (2001-10)
Kvande, T – *Deformation controlled tensile tests on LECA masonry. Collection of results,* Report N 8330-10, Norwegian Building Research Institute, Trondheim 2001.

prEN 1015-11
Draft European Standard prEN 1015-11:1995: *Method of test for mortar for masonry – Part 11: Determination of flexural and compressive strength of hardened mortar*, European Committee for Standardization CEN, Brussels 1995.

Rots (1997)
Rots, J.G (Editor) – *Structural Masonry. An Experimental/Numerical Basis for Practical Design Rules*. CUR, Balkema, ISBN 90 54-10-680-8, Rotterdam 1997.

Van Mier et al. (1994)
Mier, J.G.M. van, Vervuurt, A and Schlangen, E – Boundary and Size Effects in Uniaxial Tensile Tests: A Numerical and Experimental Study, *Fracture and Damage in Quasibrittle Structures*, Editor Bažant, Z.P., pp. 289-302, Spon, ISBN 0-419-19280-8, London 1994.

Van der Pluijm and Vermeltfoort (1991)
Pluijm, R. van der, Vermeltfoort, A.Th - *Deformation Controlled Tensile and Compression Tests on Units, Mortar and Masonry*, TNO-report B-91-0561, 1991 (in Dutch).

Van der Pluijm (1995)
Pluijm, R. van der. – Measuring of Bond. A Comparative Experimental Research, *The 7th North American Masonry Conference,* University of Notre Dame, School of Architecture, Notre Dame, Indiana, USA, pp. 267-281.

Van der Pluijm (1997)
Pluijm, R. van der. - Non-linear Behaviour of Masonry under Tension. *Heron* Vol. 42 No. 1, pp. 25-54.

Van der Pluijm (1998)
Pluijm, R. van der. – *Overview of deformation controlled tensile tests carried out during the period 1996-1998*. TUE/BCO/98.19, Faculty of Architecture, Building and Planning, Eindhoven University of Technology, Eindhoven 1998.

Van der Pluijm (1999)
Pluijm, R. van der. – *Out-of-Plane Bending of Masonry. Behaviour and strength.* Dissertation, Technische Universiteit Eindhoven, ISBN 90-6814-099-X, Eindhoven 1999.

Symbols

CV	coefficient of variation	[%]
E	modulus of elasticity E_o is calculated from best-fit true linear part from origin E_u is calculated from secant at ultimate load	[N/mm²]
G_{fI}	mode I fracture energy	[N/mm]
$G_{fI;theory}$	mode I fracture energy calculated after Hordijk (1992)	[N/mm]
f_t	tensile strength	[N/mm²]
u	normal displacement of specimen	[mm]
w	crack width	[mm]
w_c	crack width at which no stresses are transferred any more	[mm]
w_{last}	last measured crack width	[mm]
ε	strain	[-]
σ_{last}	last measured stress in descending branch	[N/mm²]

Superscripts

u	of masonry unit
m	of mortar
j	of (mortar)joint
j+u	of joint + masonry unit within measuring length

Appendix 1

TEST RESULTS FROM TENSILE TEST OF UNIT

Test period: 05.01.99 - 20.01.99

Specimen	f_t [N/mm²]	E_o *) [N/mm²]	E_u *) [N/mm²]	G_{fl} [N/mm]	w_{last} [mm]	σ_{last} [N/mm²]	$G_{fl;theory}$ [N/mm]
I-1	0,51	3245	1676	0,0185	0,08	0,06	0,0185
I-2	0,34	1618	925	0,0156	0,07	0,10	0,0283
I-3	0,42	2430	799	0,0227	0,10	0,07	0,0227
I-4	0,6	2156	1133	0,0228	0,05	0,37	0,0775
I-5	0,52	1970	1108	0,0196	0,06	0,21	0,0424
Mean	*0,48*	*2284*	*1128*	*0,0198*	*0,07*	*0,16*	*0,0379*
St.dev.	*0,10*	*613*	*335*	*0,0030*	*0,02*	*0,13*	*0,0239*
CV, [%]	*21*	*27*	*30*	*15*	*29*	*80*	*63*
IV-1	0,53	14897	3113	0,0217	0,07	0,15	0,039
IV-2	0,42	2728	772	0,0163	0,06	0,11	0,0277
IV-3	0,47	2748	1156	0,0199	0,09	0,07	0,0199
IV-4	0,43	1969	616	0,0199	0,10	0,04	0,0199
IV-7	0,55	2319	924	0,017	0,04	0,29	0,0462
IV-8	0,51	2505	881	0,0233	0,08	0,10	0,0233
IV-9	0,58	3045	824	0,0267	0,06	0,24	0,0578
Mean	*0,50*	*4316*	*1184*	*0,0207*	*0,07*	*0,14*	*0,0334*
St.dev.	*0,06*	*4678*	*866*	*0,0036*	*0,02*	*0,09*	*0,0147*
CV, [%]	*12*	*108*	*73*	*17*	*26*	*64*	*44*
V-1	0,48	1889	932	0,0184	0,07	0,13	0,0317
V-2	0,46	2042	860	0,0227	0,11	0,04	0,0227
V-3	0,39	2355	837	0,0128	0,04	0,27	0,054
V-6	0,55	2564	1190	0,0225	0,07	0,12	0,037
V-7	0,53	5768	2408	0,0142	0,04	0,24	0,0331
V-8	0,49	1885	814	0,0253	0,12	0,03	0,0253
V-11	0,6	3253	1662	0,02	0,06	0,17	0,0352
Mean	*0,50*	*2822*	*1243*	*0,0194*	*0,07*	*0,14*	*0,0341*
St.dev.	*0,07*	*1385*	*596*	*0,0046*	*0,03*	*0,09*	*0,0102*
CV, [%]	*14*	*49*	*48*	*24*	*46*	*63*	*30*
V-D-1	0,51	1811	684	0,0247	0,07	0,20	0,0516
V-D-2	0,52	1877	1074	0,0205	0,06	0,14	0,0359
V-D-3	0,46	2278	957	0,0073	0,02	0,43	0,1785
V-D-5	0,43	3294	1210	0,029	0,14	0,07	0,029
V-D-6	0,48	3042	1264	0,0172	0,06	0,18	0,0357
V-D-7	0,52	2954	1632	0,0196	0,07	0,11	0,0315
Mean all	*0,49*	*2543*	*1137*	*0,0197*	*0,07*	*0,19*	*0,0604*
St.dev. All	*0,04*	*637*	*319*	*0,0074*	*0,04*	*0,13*	*0,0584*
CV all, [%]	*8*	*25*	*28*	*37*	*55*	*67*	*97*
Mean	***0,49***	***3066***	***1178***	***0,0199***	***0,07***	***0,16***	***0,0410***
St.dev.	***0,06***	***2601***	***564***	***0,0047***	***0,03***	***0,10***	***0,0318***
CV, [%]	***13***	***85***	***48***	***23***	***38***	***66***	***78***

*) The stiffness may not be representative because the values were obtained from specimens with notches.

Appendix 2

TEST RESULTS FROM TENSILE TEST OF UNIT

Test period: 05.01.99 - 20.01.99

Specimen	f_t [N/mm²]	E_o *) [N/mm²]	E_u *) [N/mm²]	G_{fl} [N/mm]	w_{last} [mm]	σ_{last} [N/mm²]	$G_{fl;theory}$ [N/mm]	
I-1	0,51	3245	1676	0,0185	0,08	0,06	0,0185	
I-2	0,34	1618	925	0,0156	0,07	0,10	0,0283	
I-3	0,42	2430	799	0,0227	0,10	0,07	0,0227	
I-4	0,6	2156	1133					**)
I-5	0,52	1970	1108	0,0196	0,06	0,21	0,0424	
Mean	*0,48*	*2284*	*1128*	*0,0191*	*0,08*	*0,11*	*0,0280*	
St.dev.	*0,10*	*613*	*335*	*0,0029*	*0,02*	*0,07*	*0,0104*	
CV, [%]	*21*	*27*	*30*	*15*	*24*	*62*	*37*	
IV-1	0,53	14897	3113	0,0217	0,07	0,15	0,039	
IV-2	0,42	2728	772	0,0163	0,06	0,11	0,0277	
IV-3	0,47	2748	1156	0,0199	0,09	0,07	0,0199	
IV-4	0,43	1969	616	0,0199	0,10	0,04	0,0199	
IV-7	0,55	2319	924					**)
IV-8	0,51	2505	881	0,0233	0,08	0,10	0,0233	
IV-9	0,58	3045	824					**)
Mean	*0,50*	*4316*	*1184*	*0,0202*	*0,08*	*0,09*	*0,0260*	
St.dev.	*0,06*	*4678*	*866*	*0,0026*	*0,01*	*0,04*	*0,0080*	
CV, [%]	*12*	*108*	*73*	*13*	*19*	*45*	*31*	
V-1	0,48	1889	932	0,0184	0,07	0,13	0,0317	
V-2	0,46	2042	860	0,0227	0,11	0,04	0,0227	
V-3	0,39	2355	837					**)
V-6	0,55	2564	1190	0,0225	0,07	0,12	0,037	
V-7	0,53	5768	2408					**)
V-8	0,49	1885	814	0,0253	0,12	0,03	0,0253	
V-11	0,6	3253	1662	0,02	0,06	0,17	0,0352	
Mean	*0,50*	*2822*	*1243*	*0,0218*	*0,08*	*0,10*	*0,0304*	
St.dev.	*0,07*	*1385*	*596*	*0,0027*	*0,03*	*0,06*	*0,0062*	
CV, [%]	*14*	*49*	*48*	*12*	*34*	*60*	*20*	
V-D-1	0,51	1811	684	0,0247	0,07	0,20	0,0516	
V-D-2	0,52	1877	1074	0,0205	0,06	0,14	0,0359	
V-D-3	0,46	2278	957					**)
V-D-5	0,43	3294	1210	0,029	0,14	0,07	0,029	
V-D-6	0,48	3042	1264	0,0172	0,06	0,18	0,0357	
V-D-7	0,52	2954	1632	0,0196	0,07	0,11	0,0315	
Mean all	*0,49*	*2543*	*1137*	*0,0222*	*0,08*	*0,14*	*0,0367*	
St.dev. All	*0,04*	*637*	*319*	*0,0047*	*0,03*	*0,05*	*0,0088*	
CV all, [%]	*8*	*25*	*28*	*21*	*41*	*37*	*24*	
Mean	***0,49***	***3066***	***1178***	***0,0209***	***0,08***	***0,11***	***0,0304***	
St.dev.	***0,06***	***2601***	***564***	***0,0033***	***0,02***	***0,05***	***0,0087***	
CV, [%]	***13***	***85***	***48***	***16***	***29***	***49***	***29***	

*) The stiffness may not be representative because the values were obtained from specimens with notches.
**) Failure to early in the descending branch.

Appendix 3

TEST RESULTS FROM TENSILE TEST OF MASONRY

Test period: 01.03.99 - 09.03.99

E_o^u = 3000 N/mm²

All specimens

Spesimen	f_t [N/mm²]	E_o^{j+u} [N/mm²]	E_o^j [N/mm²]	E_u^{j+u} [N/mm²]	E_u^j [N/mm²]	G_{fl} [N/mm]	w_{last} [mm]	σ_{last} [N/mm²]	$G_{fl;theory}$ [N/mm]
II-1	0,23	1691	903	723	287	0,0059	0,08	0,02	0,0059
II-2	0,22	2464	1815	702	277	0,0072	0,09	0,02	0,0072
II-3	0,22	1408	683	333	120	0,0111	0,12	0,02	0,0111
II-4	0,42	2185	1520	960	458	0,014	0,14	0,01	0,014
II-5	0,17	1630	852	761	305	0,007	0,08	0,04	0,0111
II-6	0,19	1279	642	585	245	0,009	0,14	0,01	0,0084
II-7	0,24	2872	2661	841	360	0,0036	0,02	0,14	0,0115
II-8	0,29	2273	1493	1566	771	0,0148	0,15	0,04	0,0148
II-9	0,33	3713	7077	937	394	0,016	0,11	0,06	0,016
II-11	0,22	1610	836	510	236	0,0091	0,09	0,03	0,0091
Mean	***0,25***	***2113***	***1848***	***792***	***345***	***0,0098***	***0,10***	***0,04***	***0,0109***
St.dev.	***0,07***	***756***	***1942***	***333***	***176***	***0,0041***	***0,04***	***0,04***	***0,0033***
CV, [%]	***29***	***36***	***105***	***42***	***51***	***42***	***39***	***102***	***30***

Without the last 4 columns for specimen II-7

Spesimen	f_t [N/mm²]	E_o^{j+u} [N/mm²]	E_o^j [N/mm²]	E_u^{j+u} [N/mm²]	E_u^j [N/mm²]	G_{fl} [N/mm]	w_{last} [mm]	σ_{last} [N/mm²]	$G_{fl;theory}$ [N/mm]
II-1	0,23	1691	903	723	287	0,0059	0,08	0,02	0,0059
II-2	0,22	2464	1815	702	277	0,0072	0,09	0,02	0,0072
II-3	0,22	1408	683	333	120	0,0111	0,12	0,02	0,0111
II-4	0,42	2185	1520	960	458	0,014	0,14	0,01	0,014
II-5	0,17	1630	852	761	305	0,007	0,08	0,04	0,0111
II-6	0,19	1279	642	585	245	0,009	0,14	0,01	0,0084
II-7 *)	0,24	2872	2661	841	360				
II-8	0,29	2273	1493	1566	771	0,0148	0,15	0,04	0,0148
II-9	0,33	3713	7077	937	394	0,016	0,11	0,06	0,016
II-11	0,22	1610	836	510	236	0,0091	0,09	0,03	0,0091
Mean	***0,25***	***2113***	***1848***	***792***	***345***	***0,0105***	***0,11***	***0,03***	***0,0108***
St.dev.	***0,07***	***756***	***1942***	***333***	***176***	***0,0037***	***0,03***	***0,02***	***0,0035***
CV, [%]	***29***	***36***	***105***	***42***	***51***	***35***	***26***	***62***	***32***

*) II-7 failed to early in the descending branch

APPENDIX 6

Høiseth, K.V. and Kvande. T.
Constitutive Properties of Lightweight Concrete Masonry,
12th International Brick and Block Masonry Conference, Madrid 2000.

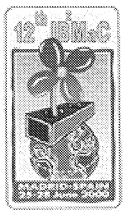

Constitutive Properties of Lightweight Concrete Masonry

K. V. Høiseth, T. Kvande

ABSTRACT
The present paper deals with the uniaxial stress-strain relationship of lightweight concrete units and masonry. The purpose of the study was to demonstrate the capability to reproduce experimental observations by numerical simulations. In the numerical simulations, the mechanical behaviour was represented by a smeared crack model with a nonlinear softening diagram. The obtained relationship between load and deformation, as well as the crack-pattern and crack-propagation was in good agreement with the experiments. Concerning the stress/deformation relationship, the smeared crack models dependency of the crackband-width has been demonstrated. The study has shown the significance of shear retention in crack-planes even under uniaxial conditions

KEY WORDS
Lightweight Concrete Masonry, Experimental Testing, Material Modelling, Uniaxial Tension

INTRODUCTION
A proceeding doctoral study at NTNU, Faculty of Civil and Environmental Engineering, “Material properties for masonry of lightweight concrete as a constructive material” aims at providing documentation of structural properties and options as basis for product development and improvements in structural utilisation.

In this connection, experimental testing is being performed in order to investigate the mechanical properties of lightweight aggregate concrete units of the LECA[1] type, the properties of the joints between units and the properties of the combined action of units and joints in masonry. The material testing, which concerns stress/strain relationship under various loading conditions, strength parameters, creep and shrinkage, as well as fracture energy, is carried out at TU-Eindhoven

An important part of the study is to adapt the results of the testing to generic material models available in DIANA[2], which are applicable for structural analysis of masonry. The adapted models will allow analysis of structures with random geometry, -boundary conditions and loadings, with respect to the complete deformation process, from elastic behaviour via cracking to global failure. The models are also necessary for reassessment purposes, or in order to simulate the structural behaviour after the appearance of a local failure, and hence estimate the redundant loadcarrying capacity under service life conditions. In the current project, specifically, the quality of the models will be evaluated by comparing numerical results and experimental observations.

---

[1] LECA® Light Expanded Clay Aggregate
[2] DIANA (Displacement ANAlyzer) is a general finite element software environment

The current paper deals with masonry and units subjected to uniaxial tension. The purpose of the study was to demonstrate the capability of numerical simulations to reproduce the experimental observations [4].

CHARACTERISTIC PROPERTIES

The mechanical behaviour of masonry and of its constituents: units, mortar and the interface between units and mortar shows the characteristics of so-called quasi-brittle materials. When subjected to pure compression, tension or shear, as well as combined states of stress, the stress/strain relationship follows the schematised curve in Figure 1a. When the peak stress has been reached, additional straining leads to increased bridging of microcracks and hence a softening of the material.

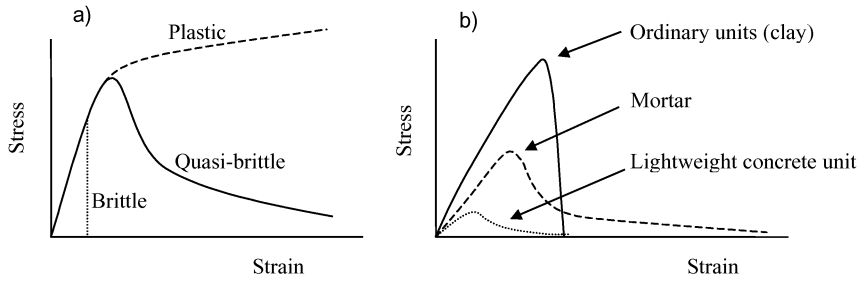

Figure 1. *a) Stress/strain relationship for plastic, brittle and quasi-brittle materials.*
b) Relationship for ordinary units, mortars and lightweight concrete units.

Figure 1b shows a schematised stress/strain relationship for ordinary units compared to the constitutive behaviour of mortar and lightweight concrete units. Due to the relatively high stiffness and strength of ordinary units, both in tension and compression, compared to the values of mortar, the joints and adhesion zone represents the weak links in ordinary masonry. A realistic description of the constitutive behaviour in these areas are therefore important, while the units in most cases will not be subjected to stress levels exceeding the elastic limit.

Concerning lightweight concrete masonry, however, the conditions are opposite, compared to the stiffness and strength of units, the values for mortar is higher. In structural analysis, this implies that also the units must be represented by a material model which accounts for the complete stress/strain relationship, including the softening part.

MATERIAL MODELLING

The smeared crack model

Analyses of the tension tests have been performed with a smeared crack model representing the LECA as well as the joint. The smeared crack approach is based on the assumption that the discrete properties of cracks can be distributed over a so-called equivalent length of a continuum. Instead of treating crack widths and sliding between crack planes as displacements, they are included in the strain tensor. In a Finite Element context, this implies that the constitutive behaviour of cracking is being accounted for in the integration points of the elements.

In the current model, this is done by decomposing the strain in an elastic strain component, and a crack strain component. As long as the material is subjected to stresses less than the tensile strength, the mechanical behaviour is linear elastic, according to Hooke's law. A smeared crack is initialised when the maximum principal stress exceeds the tensile strength of the material (mode-1 fracture criteria). If the deformation is increased, the capacity of the crack to transfer tension diminish.

A schematised stress/strain relationship of such an event is shown in Figure 2, which illustrates a bar subjected to uniaxial tension (mode-I fracture). At the onset of tension, the bar behaves linearly elastic.

When the tensile strength is reached, a crack is initiated in the bar. The elastic strain component is at its maximum, f_t/E, while the crack strain is still zero. From this point on, further stretching leads to a stress reduction as the crack strain increases and the elastic strain decreases. Eventually, the crack will be fully opened without any resistance to transfer tensile stress, the crack strain has reached ε^{cr}_{ult} and the elastic strain component is back to zero.

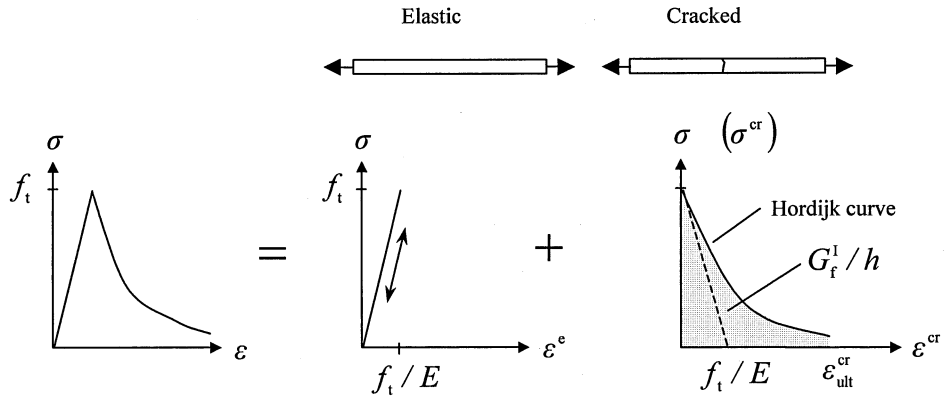

Figure 2. Strain decomposition illustrated by uniaxial tension (Mode-I fracture)

The relationship between the tensile stress and the crack strain is usually referred to as the softening diagram. In the present study, a nonlinear formulation proposed by Hordijk [5] was used. The shape of the softening diagram, which is illustrated in Figure 2, reads:

$$\frac{\sigma}{f_t} = \left(1 + \left(c_1 \frac{\varepsilon^{cr}}{\varepsilon^{cr}_{ult}}\right)^3\right) e^{-c_2 \frac{\varepsilon^{cr}}{\varepsilon^{cr}_{ult}}} - \frac{\varepsilon^{cr}}{\varepsilon^{cr}_{ult}}\left(1 + c_1^3\right) e^{-c_2} \qquad (1)$$

$$\varepsilon^{cr}_{ult} \approx 5.14 \frac{G_f^I}{f_t}$$

C_1 and C_2 are dimensionless constants, taken as: C_1=3,C_2=6.93

It should be noticed that the area under the σ-ε^{cr}_{ult} curve is equal to the fracture energy related to mode-I fracture, G_f^I, divided by the so-called equivalent length *h*. The fracture energy is a material parameter which represents the amount of potential energy required to create one unit of fractured area. Also the equivalent length may be considered a material parameter. In this physical case, the equivalent length represents the thickness of the fracture zone. Fracture in quasi-brittle materials like concrete (LECA) is namely not a completely discrete phenomenon, the fracture zone is an area where microscale cracking take place before an ultimate crack develops. The thickness of this area in front of-, and around the ultimate crack- tip, is approximately 3 times the maximum aggregate size [2].

In smeared crack models, the equivalent length is also known as the crackband-width, and often considered to be an element-related property. Equation (2) shows the relation between the fracture energy and the crackband-width.

$$G_f^I = h \int_{\varepsilon^{cr}=0}^{\varepsilon^{cr}=\infty} \sigma^{cr} \varepsilon^{cr} d\varepsilon^{cr} \qquad (2)$$

where $h\varepsilon^{cr} = w$ (Crack width)

*Figure 3*a shows a simple test modelled by a single membrane element with 2x2 Gauss integration points. The crackband-width *h* is taken as the height of the element. The global P/δ curve, and thus

also the energy content, is equal to that in *Figure 3*c. The same result is achieved if the specimen is modelled by two elements, as shown in *Figure 3*b. This is however only true if the crackband-width *h* is kept equal in both cases. If the crackband-width is taken equal to the element-height, the energy content in the latter case, *Figure 3*b, would be twice as large as that of *Figure 3*a.

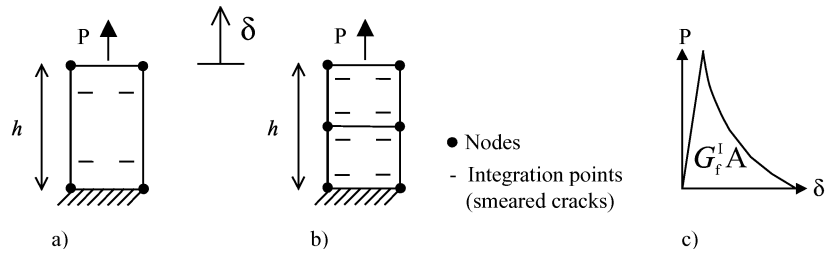

Figure 3. Mesh-objectivity with respect to crackband-width, h.

The example illustrates a deficiency of the smeared crack approach, namely that the solutions need not be objective with respect to the element mesh resolution. The choice of *h* must therefore be adapted to the crackband-width, which is obtained by numerical analysis and which can be judged as representing discrete cracks.

Under general and unproportional loading conditions, the directions of the principal stresses change. When cracking has been initiated, this implies that a shear deformation will appear parallel to the crack plane. The shear resistance on a crack plane will of course be less than in the uncracked state. In the present study, a linear relation between shear stress and – strain is maintained also after cracking, however the shear-modulus on the crack-plane is reduced by a constant shear retention factor β.

The smeared crack model allows multiple cracks to develop in each integration point. After the first crack has been initiated, subsequent cracks in an integration point are formed when the following criteria are satisfied simultaneously:

- The principal tensile stress is larger than the tensile strength.
- The angle between existing cracks and the direction of the principal tensile stress exceeds the value of a given threshold value.

A detailed description of this multidirectional smeared crack model as well as the implementation of the model in a Finite Element context is given in [1] and [3].

Material properties

The material properties were taken from the experiments [4], and it was the mean values which were used, see Table 1. Young's modulus refers to the initial tangent modulus.

Table 1. Material properties unit testing [4]

	Young's modulus E (Mpa)	Poisson's ratio ν	Tensile strength f_t (Mpa)	Shear retention β	Fracture Energy G_f^I (Nm/m^2)	Crackband width h (m)
LECA	3000	0.2	0.5	0.03	30	0.0015

Table 2. Material properties masonry testing [4]

	Young's modulus E (Mpa)	Poisson's ratio ν	Tensile strength f_t (Mpa)	Shear retention β	Fracture Energy G_f^I (Nm/m^2)	Crackband width h (m)
LECA	3000	0.2	0.5	0.03	30	0.0015
Joint	1313	0.2	0.25	1.0 (0.03)	11	0.0015

NONLINEAR ANALYSIS OF UNIT

Geometric model, boundary conditions and loading

The test specimen was modelled under the assumption of two-dimensional plane stress conditions. Due to symmetry about the vertical centre-line, merely half the test specimen was represented, see Figure 4. The model was assembled by eight-node quadrilateral isoparametric membrane elements (CQ16M), with a 2x2 Gauss integration scheme.

In the experimental testing, the top and bottom face of the specimens were glued to stiff steel platens. The nodes at the top and bottom of the model were therefore fixed in the horizontal direction. Symmetric conditions were achieved by fixing the nodes along the line of symmetry in the horizontal direction. In line with the experiments, the nodes in the bottom of the model were fixed also in the vertical direction.

The length between the points P and S corresponds with the measuring length of the LVDT's which were used in the experiments.

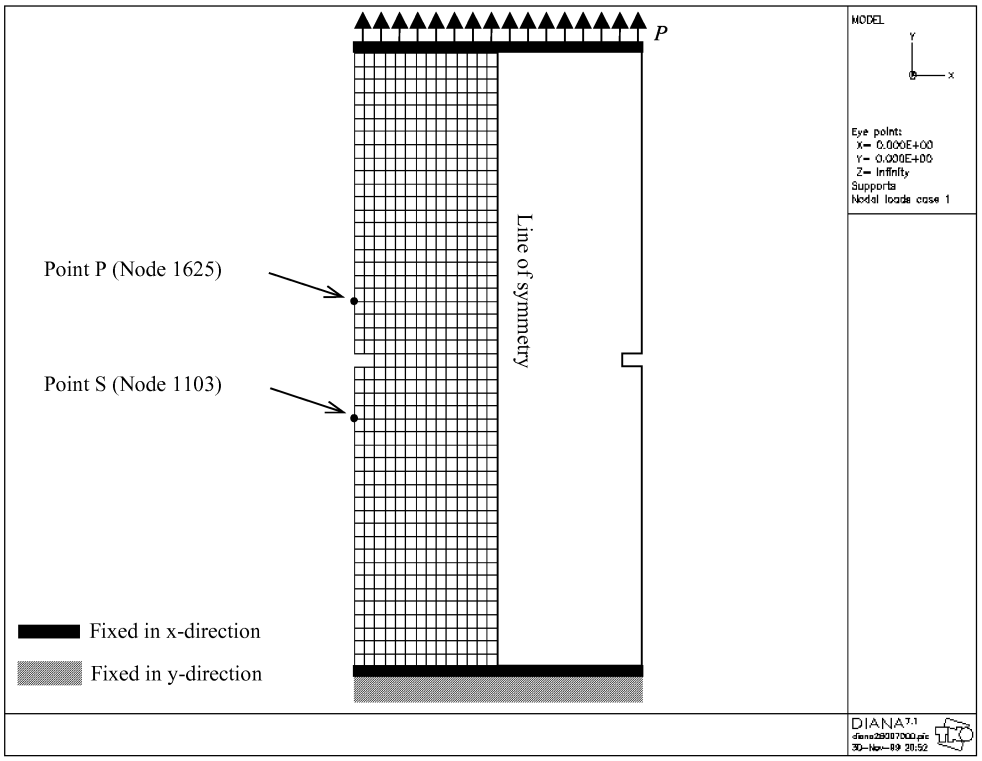

Figure 4. FE-model of tension tests

Results

Initial analysis had indicated that a global, fully opened crack would develop through a horizontal row of integration points. With the applied 2x2 integration rule, the crackband-width was therefore taken equal to half the element height.

Figure 5 shows the relationship between the load and the extension of the distance between the points P and S. The curve obtained in the analysis is compared to a curve representing an average of the

experimental results, fitted to the softening diagram of Hordijk, see [4]. It should be noticed that the fracture energy, both in the smeared crack model as well as in the empirical expression, was entered with the same value. Hence, one should expect the area under the curves to be fairly equal. The tensile stress in the diagram represents the externally applied load divided by the cross-sectional area through the notches of the specimen.

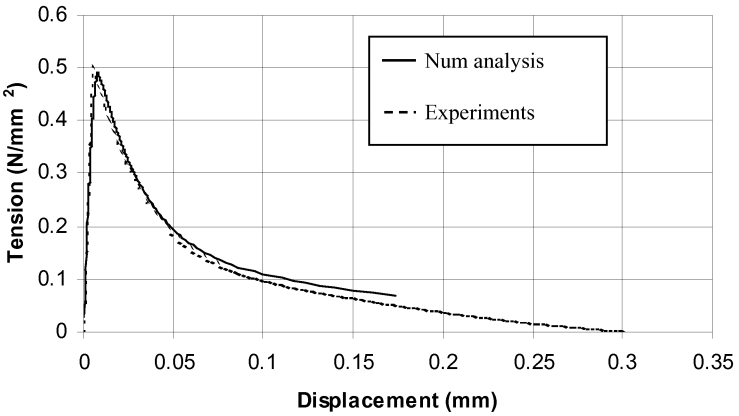

Figure 5. Relationship between load and displacement (P-S extension, see Figure 4)

The fully developed crack pattern is illustrated in
Figure 6, which also shows a close view of the crack-propagation in relation to the stress level. Due to stress concentration, cracking is initiated in the integration points nearest to the notch, with a crack plane normal to the direction of the principal stress. Because of the notch, the direction of the principal stress is not vertical. A closed-form solution under linear elastic conditions would have given an infinite principal stress in the corners of the notch. This is not achieved by the discretization inherent in the Finite Element method, however also in the numerical results the stress concentration in the corners of the notch was significant. The direction of the initial crack planes was in agreement with observations made during testing.

Figure 6 shows that, as the cracking propagates towards the interior, the angle of the crack-planes become horizontal, and the direction of the principal stresses increasingly vertical. This explains the crack-branching above and under the main horizontal crack, in the area close to centre of the specimen. After the crack-pattern was established, these branches closed, and a global crack developed trough the cross section along the lower line of integration points in the elements extending horizontally from the notch. It should be emphasised that the analysis was unstable at the point of maximum load, when the crack pattern was about to be fully developed, ie run through the entire cross-section. At this stage, the analysis was performed with arc-length control, with very small load-steps. That the main crack opened merely along the lower row of integration points and not the upper, or both, must therefore be regarded as a numerical coincidence.

An additional analysis was performed, where the nonlinear formulation of Hordijk was replaced by a linear softening diagram. This produced a similar crack-pattern, with the same fracture energy, however the final deformation after unloading was obviously less.

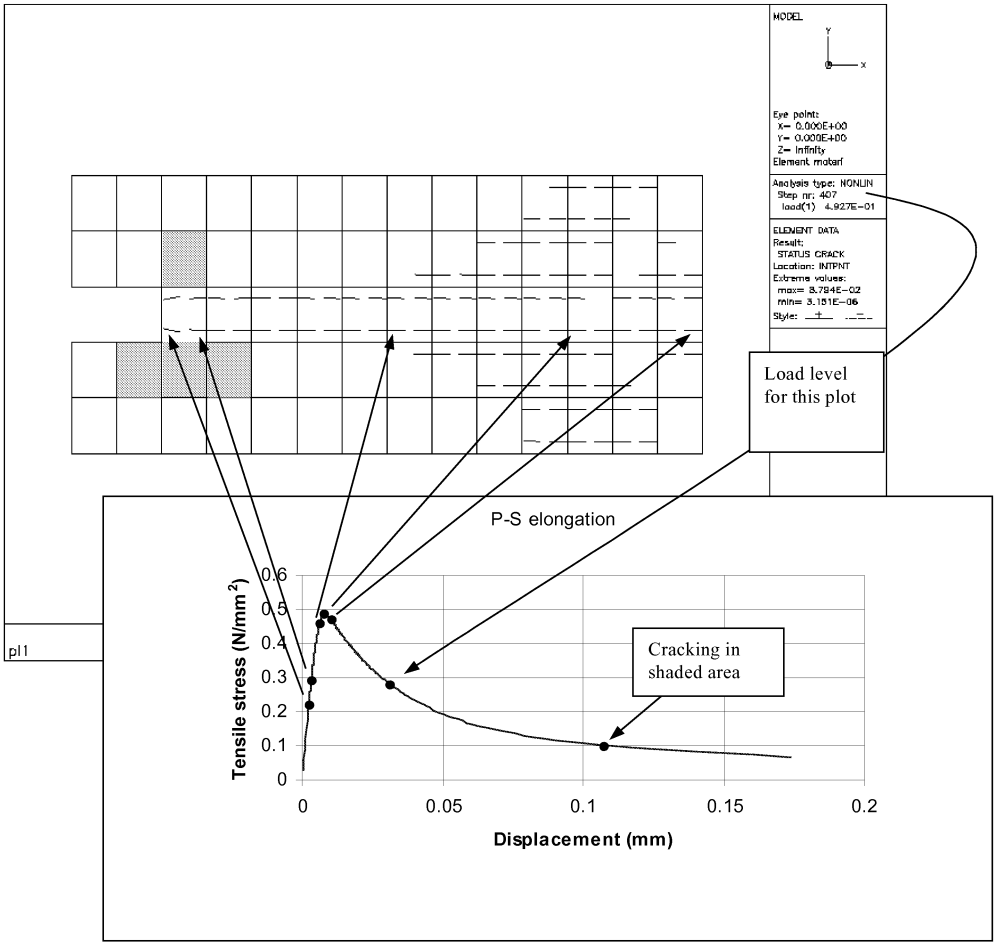

Figure 6. Crack propagation

NONLINEAR ANALYSIS OF MASONRY

Geometric model, boundary conditions and loading

The test specimen was modelled under the assumption of two-dimensional plane stress conditions. Due to symmetry about the vertical centre-line, merely half the test specimen was represented, see *Figure 7*. The model was assembled by eight-node quadrilateral isoparametric membrane elements (CQ16M), with a 2x2 Gauss integration scheme.

In the experimental testing, the top and bottom face of the specimens were glued to stiff steel platens. The nodes at the top and bottom of the model were therefore fixed in the horizontal direction. Symmetric conditions were achieved by fixing the nodes along the line of symmetry in the horizontal direction. In line with the experiments, the nodes in the bottom of the model were fixed also in the vertical direction.

The top-row of elements were subjected to consistent edge loading with a constant distribution.

The length between the points P and S corresponds with the measuring length of the LVDT's, which were used in the experiments.

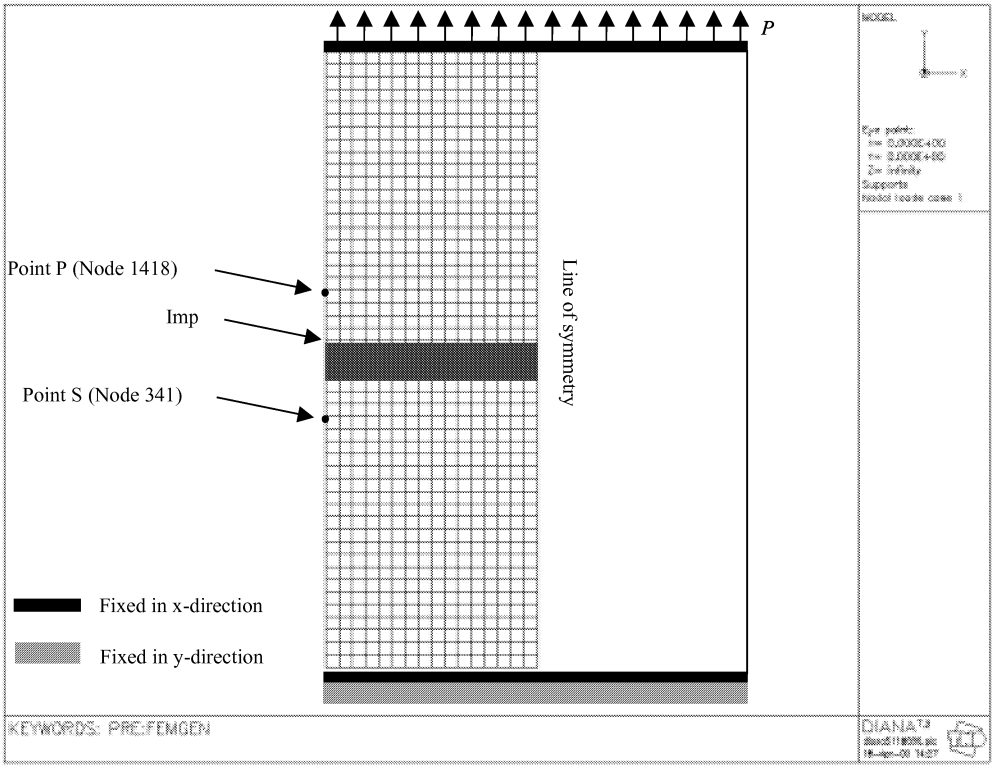

Figure 7. FE-model of masonry test

Results

The extension between the points P and S in relation to the loading, is given by the curve denoted ”Num analysis” in Figure 8. The curve ”Experiments” belongs to an average of the experimental results, inserted in Equation (1).

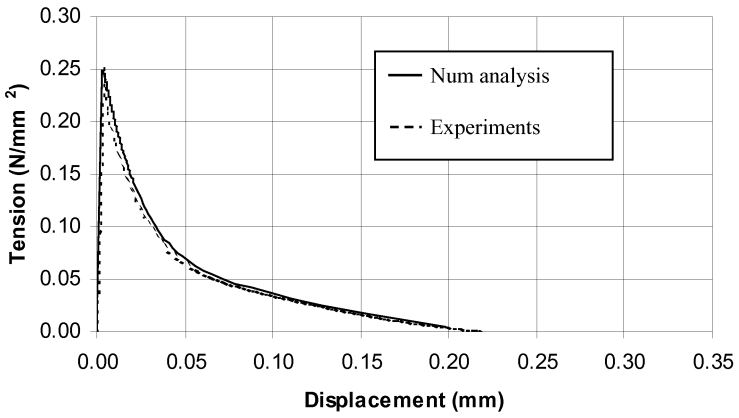

Figure 8. Relationship between load and displacement (P-S extension)

The crack pattern at the end of the analysis is given in *Figure 9*. Cracking is initiated in centre of the joint, and in the middle of the specimen. This is due to the different material properties of LECA and joint, which implies that the principal stress in the middle of the specimen becomes slightly higher than at the surface. From this area, the cracking propagates horizontally towards the surface. At the end of loading, a global and fully opened crack run through a horizontal row of integration points, while in the adjacent elements, crack-closure have taken place.

The localisation of the crack-band in combination with the anticipated crack-band width, which was taken equal to the influence length of one integration point (Table 1), explains the close agreement between the deformation curves in Figure 8.

As a first approach, the analysis was performed with a low shear retention factor, β=0.03. This produced a horizontal, but wave-like global crack, which gave unrealistic large shear deformations in the joint during unloading.

During casting and curing of the specimens, it was observed that due to seep and drying creep of mortar, contact was lost between joint and unit along the circumference of the joint. The result was a small notch, which may act as a crack initiator. In order to demonstrate this effect, numerical analyses were performed on a model with a small imperfection, by means of removing the contact between the outermost two nodes at the surface of the specimen between the upper unit and the joint, see the area denoted Imp in Figure 7. Due to the stress concentration, this produced an initial crack, with a propagation highly dependent on the applied shear retention. With full shear retention, cracking even extended somewhat into the units.

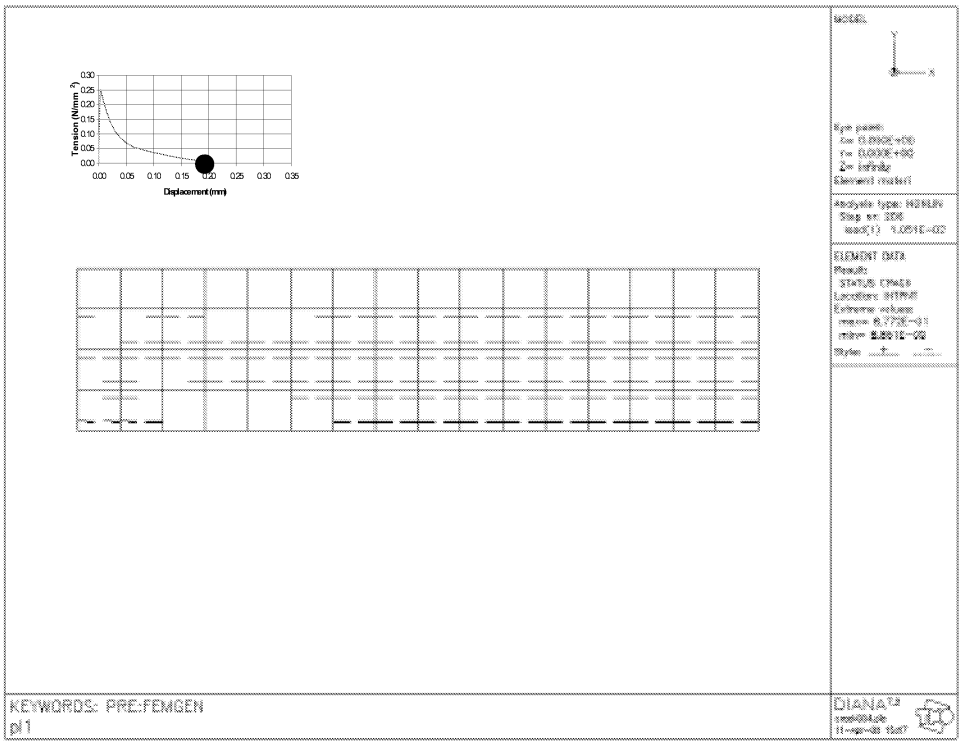

Figure 9. *Crack pattern at the end of analysis*

CONCLUSIONS

From the experiments, there are two observations particularly useful for evaluation of the numerical analyses: the cracking and the relationship between stress (loading) and deformation.

The analyses of units showed that cracking was initiated in the integration points nearest to the notch. The normal to the crack planes pointed towards the corner of the notch, which corresponds with the direction of the principal tensile stress in this area. With a linear softening diagram, as well as with the Hordijk formulation, the cracking propagated horizontally. Close to the centre of the specimen, crack branching occurred due to increasingly uniaxial stress distribution. After a fully developed crack pattern, however, the crack opening took place in the extension of the notch. This is in agreement with experimentally observed behaviour. It should be noticed that also in the experiments, frequently two cracks were initiated in the corner of the notches [4].

Concerning the stress/deformation relationship, the smeared crack models dependency of the crackband-width has been demonstrated. Provided a realistic crackband-width is used, both softening diagrams gave a fracture energy close to those which were measured in the experiments. The Hordijk softening diagram is however more in line with the mechanical behaviour of quasi-brittle materials like LECA, and the deformations were therefore also closer to the experimental results.

In the experiments with masonry specimens, the test results showed that complete fracture occurred in the interface between units and joint.

The nonlinear analysis with an ideal connection between units and joint, and with full shear retention, produced a complete horizontal fracture in the middle of the joint. This discrepancy between observed and numerical results indicates a higher stiffness and strength in the middle of a joint than in the interface area. In the analysis, average properties were used.

Due to the horizontal crack-band achieved in the analysis, which was in agreement with the anticipated crack-band width, the load-deformation relationship was very close to the measured one.

Seep and drying shrinkage along the surface of joints may produce stress-concentrations and hence initiate cracking in the interface between units and joint. This has been demonstrated by numerical analyses. However, both with full shear retention and almost no shear resistance in crack-planes, the crack propagation took place in the middle of the joint. Again, this is probably due to higher stiffness and strength in the middle of a joint than at the interface.

The analyses have shown that, even under uniaxial conditions, shear retention is an important parameter with respect to the development and propagation of cracks. With full shear retention, cracking even extended somewhat into the units. Taking into consideration that the stiffness and strength of the interface between unit and joint are comparable with the stiffness and strength of units, this could indicate that lightweight concrete masonry may be considered as homogeneous material. The implications of such an approximation need however to be quantified.

ACKNOWLEDGEMENTS

The present work was initiated by Oddvar Hyrve, Research Director in Norsk Leca AS. He soon involved the masonry guild at the Faculty and the Norwegian Masonry Centre, which has been an excellent forum for discussions about numerical analysis of masonry structures. Their funding of the present study is highly appreciated.

At the Peter van Musschenbroek Laboratory of TU-Eindhoven, a number of test-facilities for investigation of the mechanical behaviour of masonry have been developed over the years. This equipment, in combination with the extensive competence of the scientific staff at the Faculty of Architecture, made the experimental investigations possible.

REFERENCES

[1] *Diana, User's Manual release 7– Nonlinear Analysis*, TNO Building and Construction Research, 1998.

[2] Gylltoft, K.: *Fracture Mechanics Models for Fatigue in Concrete Structures*, Doctoral Thesis 1983:25D, University of Luleå, Division of Structural Engineering.

[3] Rots, J. G.: *Computational Modeling of Concrete Fracture*, Doctoral Thesis, Delft University of Technology, Civil Engineering Department, 1988.

[4] Kvande, T.: Deformation Controlled Tensile Tests on Masonry of LECA, Working report 6, October 1999.

[5] Hordijk, D. A.:Tensile and Tensile Fatigue Behaviour of Concrete; Experiments. Modelling and Analyses, Heron Vol. 37 No. 1, 1992.

[6] Høiseth, K. V.: Material Modelling of Lightweight Concrete Masonry Units (LECA) – Uniaxial Tension, R-15-99, NTNU, Dep of Struct Eng, 1999

[7] Høiseth, K. V.: Material Modelling of Lightweight Concrete Masonry (LECA) – Uniaxial Tension of Masonry, R-3-00, NTNU, Dep of Struct Eng, 2000

APPENDIX 7

Kvande. T.
Deformation Controlled Combined Compression and Shear Tests on LECA Masonry,
Report N 8330-7, Norwegian Building Research Institute, Trondheim 2001.

BYGGFORSK
Norwegian Building Research Institute

Head Office
Forskningsveien 3b
P.O.Box 123 Blindern
N-0314 OSLO
Tel. +47 22 96 55 55
Fax +47 22 69 94 38

Local Department
Høgskoleringen 7
N-7491 TRONDHEIM
Tel. +47 73 59 33 90
Fax +47 73 59 33 80

E-mail firmapost@byggforsk.no
Internet www.byggforsk.no
Registration No. NO 943 813 361 VAT

Clients
Mur-Sentret and
Department of Building and
Construction Engineering - NTNU

Client's addresses
Pb. 53 Blindern, 0313 Oslo
and
7491 Trondheim

Client's contact-persons
Geir Wold-Hansen og
Jan Vincent Thue

Project/archive no.	Date	Rev. date	No. of pages	Appendixes	Classification	Author(s)
N 8330-7	31.01.2001		26	1	Unrestricted	Tore Kvande

Project leader	Sign.	Responsible manager	Sign.	Quality assurance	Sign.
Tore Kvande		Terje Jacobsen		Karl Vincent Høiseth	

Assignment Report

Deformation controlled combined compression and shear tests on LECA Masonry

Summary

This report gives an overview of deformation-controlled combined compression and shear tests on masonry of Light Expanded Clay Aggregate (LECA) concrete blocks. The main purpose of the test was to establish the behaviour of bed joint in LECA masonry subjected to combined compression and shear stresses. The determined behaviour may be applied for numerical modelling of shear cracking of LECA masonry.

The tests are carried out in a combined testing arrangement developed at the Pieter van Musschenbroek Laboratory at Technische Universiteit Eindhoven, the Netherlands.

The results include mean values for shear strength, shear stiffness, mode II fracture energy and dry friction coefficient. The results support partly the validity of exponential cohesion-softening (Lourenço 1996) and dilatancy softening (Van der Pluijm 1999) of the bond interface to describe the post peak behaviour.

Bond shear strength of LECA masonry had a higher measurement than the tensile strength of block. Due to this, failure of LECA masonry more often appears as tensile failure of the block than shear bond failure.

This work has been a part of the dr.ing-project "Material Properties for Masonry of Light Expanded Clay Aggregate Concrete as a Constructive Material". The doctoral study has been funded by The Research Council of Norway and Norsk Leca (presently Optiroc). The study has been a part of the research program "Loadbearing Masonry 1997-2000" co-ordinated by Mur-Sentret. The current report is based on Working Report 7 of 20. September 1999.

Address of the building	Built (year)

Activity code	Keywords	Filename
3.4	Lettbetong, Styrke, Stivhet, Mørtel	N8330-7.doc

Contents

1. Introduction

This report gives an overview of deformation-controlled combined compression and shear tests on masonry of Light Expanded Clay Aggregate (LECA) concrete blocks. The main purpose of the test was to establish the behaviour of bed joint in LECA masonry subjected to combined compression and shear actions. The behaviour expressed should be applicable for numerical modelling of shear cracking of LECA masonry.

During his Ph.D-study, Van der Pluijm (1999) developed the test set-up used for the testing. The tests were carried out in the Pieter van Musschenbroek Laboratory at Technische Universiteit Eindhoven, TUE, during the period from Mars to Mai 1999. Martien Ceelen, TUE, and Tore Kvande, Norwegian University of Science and Technology - NTNU, have been responsible for the performance of the testing

A detailed summary of the test results is given in Kvande (2001-11).

2. Materials and specimens

The LECA blocks used in these tests were produced 17.08.98 at Norsk Leca's factory at Lillestrøm, Norway. Identification of the blocks is *Leca kompaktblokk 15 cm 3/770*. "3/770" indicates the quality of the concrete, telling about a compressive strength of about 3 N/mm² and a density of about 770 kg/m³. Material properties and material composition of these blocks are described of Kvande (2001-3).

For combined test of the masonry, test pieces measuring 69x100x205 mm were sawn from the LECA blocks. The strips were sawn in such a way that the original bond surfaces with the mortar were preserved. Before making the specimens, the test pieces were acclimatised by 20 °C and 60 % RH.

The test pieces were mortared together in couplets with a factory-made mortar "*Leca fasadepuss*" (LC 35/65/520), see Figure 1. 2.5 l water was added to 15 kg dry mortar. 20 specimens were made from each batch. In total 60 specimens were made. Because it was very important to obtain flat and parallel specimens, great pains were taken in the execution of the masonry work. After making the specimens, they were enclosed in plastic for four days and afterwards stored for a minimum period of 24 days by 20 °C and 60 % RH.

The specimen in Figure 1 was made with 30 mm notches in both long sides. The notches reduced the fracture area to 40x205 mm. Most of the specimens were tested with such notches cut in the interface between mortar and LECA block. The notches were made after hardening of the specimen.

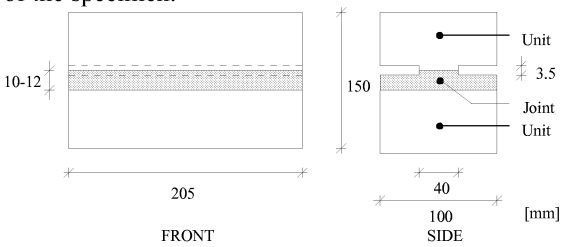

Figure 1:
Specimen for combined compressive and shear test of masonry.

3. Test arrangement

3.1 Deformation-controlled combined compression and shear tests

In Figure 2 and 3 the bi-axial test arrangement of the Pieter van Musschenbrock Laboratory is introduced. The main characteristic of the test arrangement is that the bed joint of a coupled specimen can be tested under a combined perpendicular load and parallel load. The test arrangement consists of two plates connected to separate parallelogram-mechanisms. The arrangement makes it possible to move both plates independently of each other. The coupled specimen is glued between the two plates as presented in Figure 3. The parallelogram connected to the upper plate allows the plate to move straight up or down without any rotation. The bottom plate is allowed to move similarly in the shear direction. To enlarge the stiffness of the test set-up, a large steel plate is connected on the front and the rear of the arrangement. By this arrangement the two steel plates, to which the specimen is glued, are kept parallel during the test. Moving of the bottom plate in the shear direction leads to pure shear action in the centre of the specimen as illustrated in Figure 2.

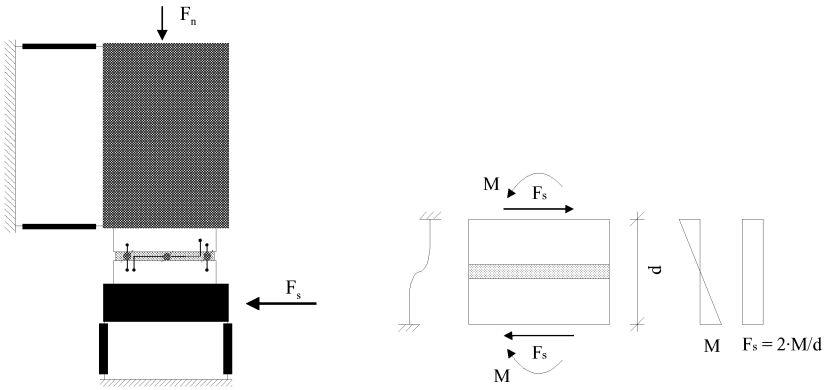

Figure 2:
Principal sketch of the bi-axial test arrangement and forces on specimen (Van der Pluijm 1998).

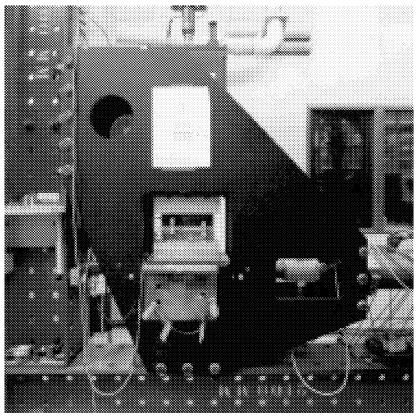

Figure 3:
Photo of bi-axial test arrangement. (Photo: Ben Elfrink, TUE)

In this test program the normal force, F_n, was kept constant while, in the meantime, the shear force, F_s, was controlled by the shear deformations. Linear Variable Differential Transducers, LVDTs, were used to control the increase of shear deformation. The LVDTs were glued to the specimen as seen in Figure 5a. In total four normal and two shear displacements were measured, because displacement measurements were carried out on the front and rear of the specimens. The gauge length of the LVDTs for normal displacements was 30 mm while the gauge length of the shear displacements was 100 mm.

For both the normal and the shear force, the spring force of the parallelograms has to be subtracted from the measured loads. Also the weight of the steel construction connected to the load cell have to be subtracted from the measured normal load. For a detailed description of the test set-up, the reader is referred to Van der Pluijm (1998).

3.2 Calculations

The main purpose of the bi-axial tests was to determine the behaviour of the bed joints in LECA masonry subjected to combine compressive and shear stresses. An idealised shear stress-deformation relationship obtained at a constant normal stress is given in Figure 4. To do numerical analysis of shear cracking of bed joint, the shear stress-deformation relationship and the normal displacement have to be known. The relationships may be expressed by the following quantities (Rots 1997, Van der Pluijm 1993):

- shear bond strength, τ_u
- friction at shear stress, τ_{fr}
- shear modulus, G
- mode II fracture energy, G_{fII}
- softening distance, v_{nonlin}
- dry friction coefficient, μ
- angle of dilatancy, ψ

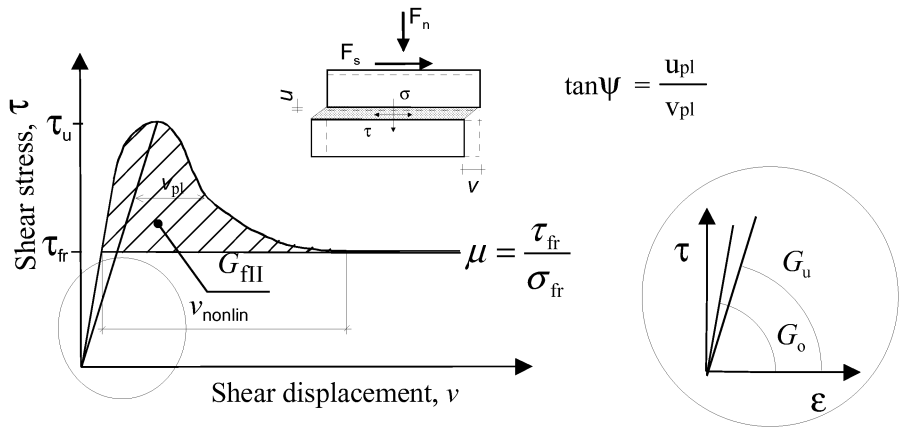

Figure 4:
Schematic diagram of a deformation, v, controlled shear test with analysed quantities.

Shear stress, τ, and normal stress, σ, are calculated by simply dividing the shear and normal force by the cross sectional area. The calculation of the shear modulus of the mortar joint, G^j, is based on Equation 1. The formula is deduced from Van der Pluijm (1999). The equation is based on the assumption that Poisson's ratios are equal for block and mortar.

$$G^j = \frac{t^j \cdot G^{j+u} \cdot G^u}{G^u\left(t^u + t^j\right) - G^{j+u} \cdot t^u} \qquad \text{Equation 1}$$

where:

G^j	is the shear modulus of the joint,
G^u	is the shear modulus of the block,
G^{j+u}	is the shear modulus of the specimen within the gauge length, and follows directly from the measurements,
t^j	is the thickness of the mortar joint,
t^u	is the sum of the thicknesses of the concrete block parts within the gauge length.

The shear modulus of the block is calculated from its modulus of elasticity by Equation 2. The calculation is based on E_o= 3000 N/mm² and Poisson's ratio 0.2.

$$G = \frac{E}{2(1+\nu)} \qquad \text{Equation 2}$$

where:

G	is the shear modulus,
E	is the modulus of elasticity,
ν	is the Poisson's ratio.

The surface area under the curve as marked in Figure 4 is defined as the mode II fracture energy G_{fII}. The fracture energy is the energy that is needed per unit area to create a shear crack (Rots 1997).

The dry friction coefficient, μ , is calculated by dividing the mean shear stress by the mean normal stress in the last twenty measurements in the horizontal part of the tail of the diagram presented in Figure 4.

$$\mu = \frac{\tau_{fr}}{\sigma_{fr}} \qquad \text{Equation 3}$$

where:

τ_{fr}	is the friction at shear stress.
σ_{fr}	is the normal stress when τ_{fr}.

The dilatancy angle, ψ, is defined by:

$$\tan\psi = \frac{u_{pl}}{v_{pl}} \qquad \text{Equation 4}$$

where:

v_{pl}	is the plastic shear displacement,
u_{pl}	is the plastic normal displacement.

4. Results

The first six tests were carried out on specimens without notches. All the specimens failed in the LECA block close to the steel plates. In Figure 5a a typical failure can be observed. Almost horizontal cracks can be observed both close to the upper and the lower steel plate. The cracks are observed easier after removing the specimen from the test set-up as viewed in Figure 5b. The test of the pictured specimen is carried out in combination with compression 0.06 N/mm².

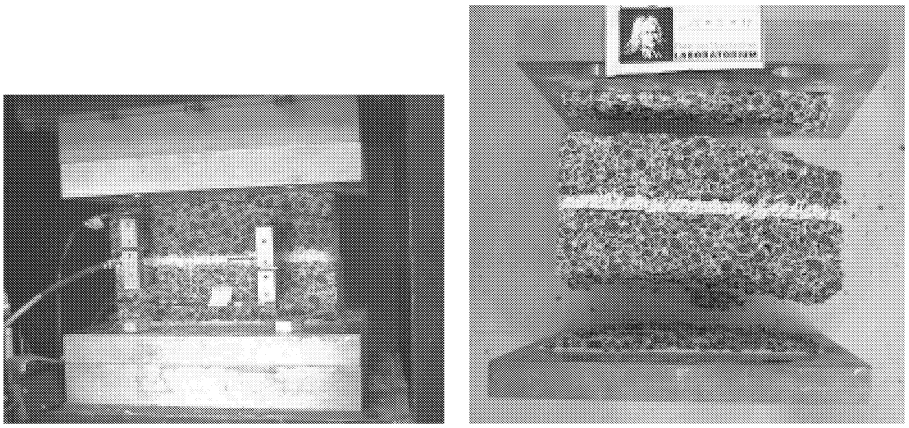

Figure 5:
a) Failure of specimen III-1 depicted in the test set-up. b) Specimen III-1 removed from the test set-up after failure.

Because the specimens without notches broke outside the LVDT, no representative values could be obtained from the tests. To obtrude the failure in the interface between mortar and LECA block 30 mm deep notches were made in both face sides of the specimen. The test results presented in this report are all obtained from specimen with such notches.

Because of unsatisfactory gluing of some of the specimens in the test set-up, eccentric loading has inadvertently been applied. Tests carried out in this manner have not been included in the presentations of the results. In total 37 deformation controlled bi-axial tests were carried out.

Due to the setting of the controller, a few of the tests were stopped too early in the descending branch to obtain a clear horizontal line at the end of the test (the friction level). Without reaching the horizontal part of the test, uncertainty arose in the calculation of mode II fraction energy, softening distance and friction coefficient. Presented mean values of these material properties in Table 1 include only values from tests where a horizontal line was obtained (see Appendix 1). For tests that failed before a horizontal line was obtained, only the shear bond strength and the shear modulus are included in the mean values in the table.

The collections of tests in Figure 6 to 8 are the result of all the tests used for calculation of mean values in Table 1. The developments of shear stress in the diagram were plotted dependent on shear displacement. Tests carried out at the same compression level are collected in separate figures. The influences of the compression level are shown more clearly when the graphs are collected in this manner, compared with a summary of all the tests in one figure.

Table 1:
Mean values obtained from the shear compression tests. The numbers in parenthesis are coefficient of variation, CV, in %.

Material property			Compression level, [N/mm²]		
			0.06	**0.15**	**0.23**
Shear bond strength	τ_u	[N/mm²]	0.88 (10)	0.93 (8)	0.97 (8)
Shear modulus	G_o^{j+u}	[N/mm²]	1300 (8)	1400 (17)	1300 (12)
	G_o^{j}	[N/mm²]	1400 (23)	1700 (44)	1400 (33)
	G_u^{j+u}	[N/mm²]	800 (31)	700 (18)	600 (29)
	G_u^{j}	[N/mm²]	500 (46)	400 (23)	400 (26)
Mode II fracture energy	G_{fII}	[N/mm]	0.091 (16)	0.126 (17)	0.122 (19)
Friction at shear stress	τ_{fr}	[N/mm²]	0.13 (37)	0.15 (6)	0.26 (10)
Normal stress when τ_{fr};	σ_{fr}	[N/mm²]	-0.10 (17)	-0.17 (4)	-0.24 (3)
Softening distance	v_{nonlin}	[mm]	0.331 (21)	0.461 (17)	0.406 (21)
Friction coefficient	μ	[-]	1.37 (27)	0.90 (5)	1.08 (12)
Angle of dilatancy	$\tan(\psi)$	[-]	0.87 (26)	0.60 (28)	0.45 (31)
Bond failure		[number]	6	2	5
Bond failure and tensile failure of block		[number]	2	2	4

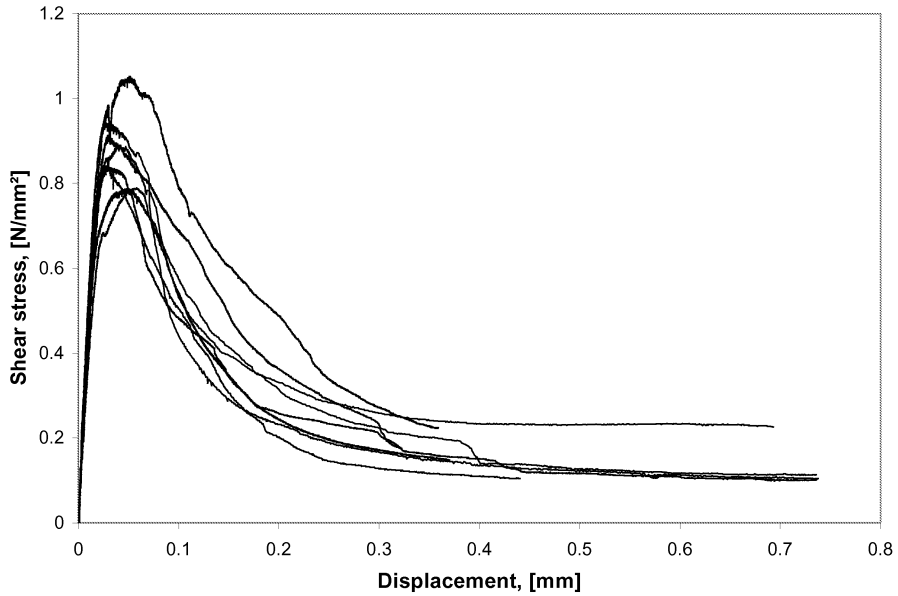

Figure 6:
Shear compression tests carried out with compression level 0.06 N/mm².

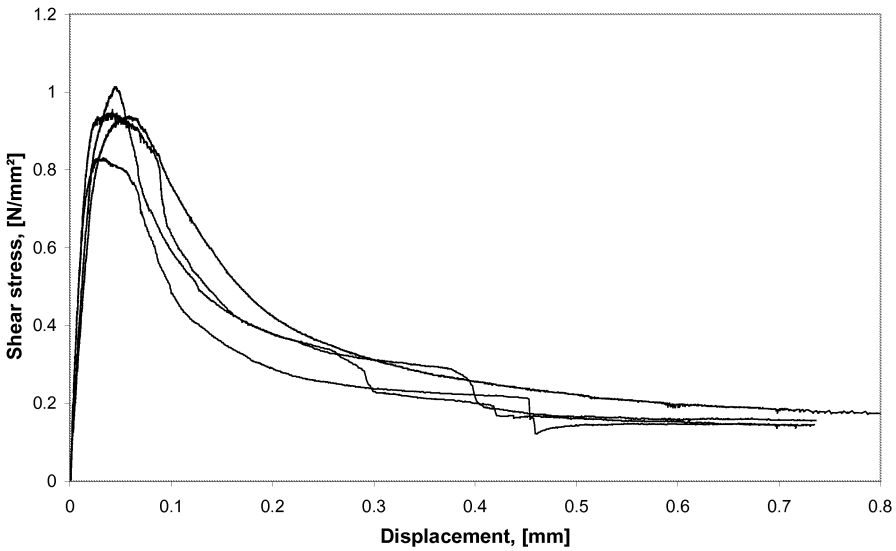

Figure 7:
Shear compression tests carried out with compression level 0.15 N/mm².

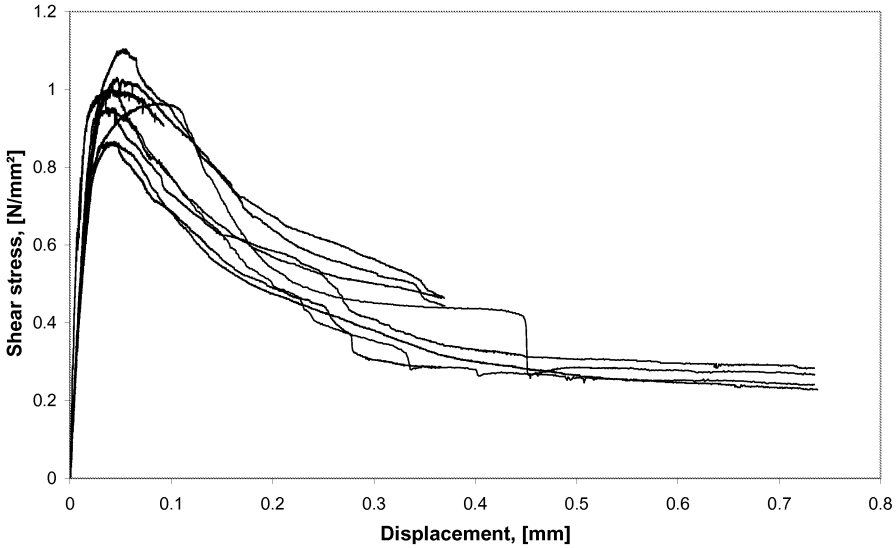

Figure 8:
Shear compression tests carried out with compression level 0.23 N/mm².

A typical example of the failure can be observed in Figure 9a. The failure appears in the interface between mortar and block as bond failure. Because of cavities in the bed face of the block, some of the failure also appears in the mortar. A principal sketch of the failure is presented in Figure 10a.

Another appearance failure is tensile failure of the blocks near their heads in combination with bond failure. A principal sketch of this type of failure is presented in Figure 10b). A

photo of such a failure can be seen in Figure 9b. A total of 13 specimens failed as in Figure 10a and 8 specimens as in Figure 10b.

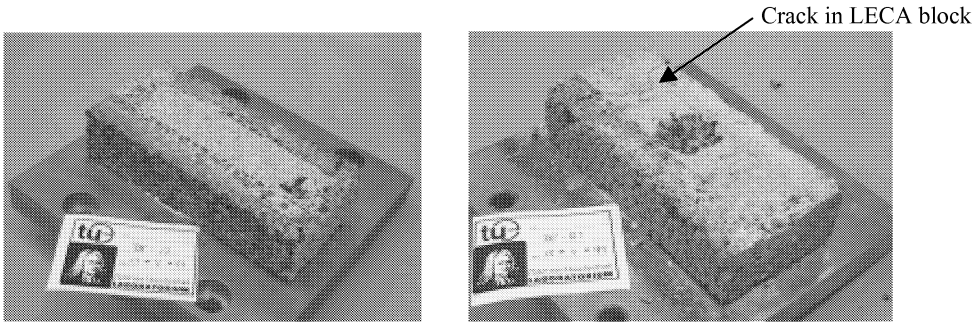

Figure 9:
a) Failure surface of specimen III-17. *b) Failure of specimen III-21.*

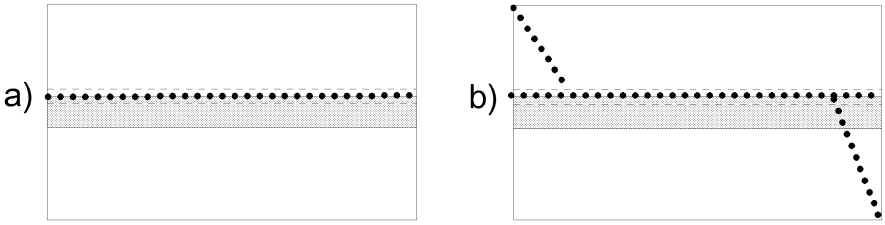

Figure 10:
Principal sketch of typical failures where a) represents bond failure and b) bond failure in combination with tensile failure of blocks near their heads.

The specimens were made from three different batches of mortar. Mean flexural- and compressive strength of the batches were measured to 3,2 N/mm² and 11,2 N/mm² respectively with coefficient of variation 7 % and 4 %. The mortar strengths were measured in accordance with prEN 1015-11.

5. Discussion

5.1 Control of the test set-up

When carrying out tests under combined compression and shear action, one of the biggest challenges is to control the test after the peak load. In order to control the test after the peak, it is necessary to establish test data such as mode II fracture energy and dilatancy behaviour. This is essential data for numerical analysis.

The bi-axial test arrangement at Pieter van Musschenbroek Laboratory is unique because of the possibilities it offers to control the test. By controlling the behaviour of the specimens in both normal and shear direction, the test arrangement makes it possible to control the tests beyond the maximum load. It is even possible to control the test up until the point where no other forces than pure dry friction force (in case of normal compression) remains active or a macro crack is formed.

As described earlier, the test arrangement consists of two plates, to which the specimen is glued, connected to separate parallelogram-mechanisms. The arrangement makes it possible to move both plates independently and parallel of each other. By keeping the steel plates parallel during the test, pure shear appears in the centre of the specimen.

The parallelogram mechanisms of the bi-axial test arrangement are based on the same system as the tension test arrangement. One of the uncertainties attached to the tensile test set-up was the stiffness of the horizontal plates in the parallelogram (Kvande 1999-6). To avoid the same uncertainties, the arms in the parallelogram in the bi-axial test arrangement are made of stiffer steel plates.

Another uncertainty attached to the tensile test-up was horizontal moving of the upper part of the specimen caused by vertical movement of the hollow section (see Figure 11). In the bi-axial test arrangement the effect will appear in both the shear and the normal direction. However, the LVDTs due to vertical and horizontal measurements of the specimens will measure the influence of those movements on the specimens.

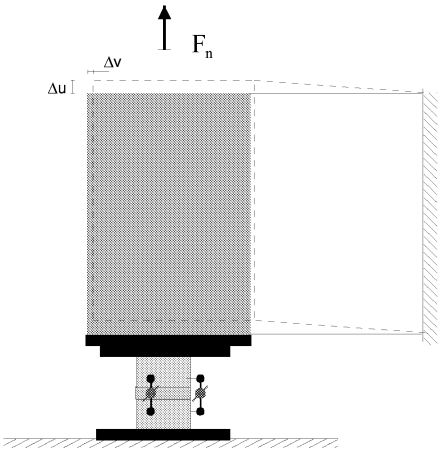

Figure 11:
"Unintended" horizontal displacement, Δv, because of vertical movement, Δu, of the parallelogram.

5.2 Carrying out the test program

In this test program no pure shear tests were carried out. This is due to the fact that introducing a pure shear stress distribution is nearly impossible (Hofmann et al. 1990). The test program started with test of specimens without notches. That was not a success. Failure appeared close to the steel plates, to which the specimens were glued. All specimens broke in the same way. In accordance with Figure 2 the highest bending moment appears close to the gluing. The specimen failed because the flexural strength of the masonry was exceeded and not because one exceeded the shear strength. To make it possible to obtain a failure in the interface between mortar and block, notches with depth 30 mm were made in each face side of the specimen.

Even with two 30 mm deep notches, one in each face side of the specimen, not all specimens failed as bond failure. Some failed as described in Figure 10b with a breakage of the edge of the top and bottom block as well as failure in the interface. The shear capacity of the interface is much higher than the tensile capacity of the specimen. In Kvande (2001-6) the tensile strength of the LECA block itself is measured to 0.5 N/mm². Breakage of the edges appears because of excess tensile capacity near the heads of the block.

The tests were controlled by the shear displacement of the specimen. Because of the need for high sensitivity of the controller, the sensitivity of the measurement in the shear direction was set to 0.35 mm/10 V. The measurement range in the normal direction was 1 mm/10 V. When controlling the test in this way, the shear displacement went out of range before reaching the friction level. Due to getting out of range, the test stopped by itself. Test III-15, -16, -18, -20 and -24 were stopped before the whole descending branch was obtained. To be able to reach the friction level, the measurement range in the shear direction was enlarged to 0.7 mm/10 V. Most of the tests in this report were carried out with the last assigned sensitivity.

The intention was to carry out the tests with a constant normal force. However, the normal stress increases slightly after reaching the peak shear stress (Kvande 1999-11). This is due to the normal displacement of the specimen. After reaching the peak shear stress further shear displacement caused an opening of the crack. Consequently, the upper LECA block was “pushed” up. Normal displacements up to 0.8 mm were recorded. The normal displacement of the specimen caused an increase of the spring force and a corresponding increase of the compressive force on the specimen. That happened because the measured force of the controller includes the pressure on the specimen, the weight of the steel construction connected to the load cell and the spring force. Both the spring-force of the parallelogram and the weight of the steel construction were subtracted from the measured load afterwards in the calculation of the test results. The test arrangement was not designed for such large normal displacement during the test.

Calculation of the friction level is based on the shear stress at the friction level and the normal stress when the friction level is reached. No other corrections due to the increased normal force have been made.

5.3 Shear stiffness

The shear stiffness of the joint was calculated in accordance with equation 1. The stiffness is obtained from both first linear parts from origin, G_o^j, and from secant at ultimate load, G_u^j. The stiffnesses were calculated to approximately 1500 and 400 N/mm² respectively. The shear stiffness seems to be scarcely affected by the level of the precompression.

5.4 Shear strength and τ -σ diagram

To be able to describe the shear bond strength dependent of normal stress, the Coulomb's friction failure criterion is commonly used as failure envelope in the compression part of the τ-σ diagram. The criterion is formulated by:

$$\tau_u = c_o - \tan\varphi \cdot \sigma \qquad \text{Equation 5}$$

where τ_u is the shear bond strength of test,
c_o is the cohesion or shear bond strength (τ when $\sigma = 0$),
φ is the angle of internal friction,
σ is the normal stress to the bed joint.

To obtain a failure envelope for LECA masonry, results from the shear compression tests and uni-axial tensile test (Kvande 1999-6) are used. All measurements obtained from the tests are plotted in the τ-σ stress plane with the vertical axis representing the shear stress and the horizontal axis representing the normal stress. The diagram is presented in Figure 12. From the diagram it can be seen that the largest scatter appears during tests with normal tension.

The failure envelope in the compression part of Figure 12 is obtained from the cohesion and the angle of internal friction as described with Equation 5. The cohesion and the angle of internal friction of the test series were determined in two ways. Firstly it was determined from the best-fit linear line from all the measurements. Alternatively it was expressed from the best-fit linear line obtained from the mean shear strength at each compression level. In both ways an initial cohesion of 0.85 N/mm² and internal friction of almost 30º ($\tan\varphi = 0.52$) were obtained.

In the tension part of the τ-σ stress plane, three alternative models for the interface behaviour are presented: a) Coulomb with a tension cut-off at the tensile bond strength, f_{tb}, (Lourenço et al. 1994), b) Parabolic tension cut-off (Rots1997) and c) Linear cut-off through c_o and f_{tb}, see Figure 12.

The parabolic tension cut-off can be expressed by the following principal formula (Rots 1997):

$$\sigma = \frac{1}{4 f_{tu} \tan^2\varphi}\tau^2 + f_t \qquad \text{Equation 6}$$

where σ is the normal stress,
f_{tu} is the (arbitrary) ultimate value of the tensile strength,
f_t is the residual value from the tensile strength during softening,
$\tan\varphi$ is the gradient of the tangent line when $f_t = f_{tu}$ and $\sigma = 0$.

Van der Pluijm (1998) concludes that the parabolic cut-off seems more suitable than the Coulomb with a tension cut-off. However, no test data is so far obtained for LECA masonry

in the tensile part of the τ-σ stress plane. A linear cut-off will, according to the test of Van der Pluijm (1998), be in the conservative area.

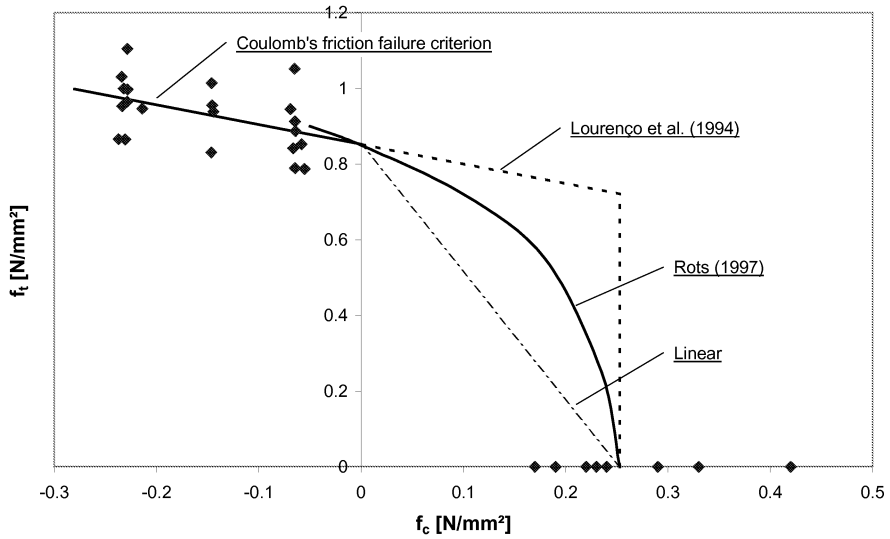

Figure 12:
Experimental data plotted in the τ-σ stress plane. Tensile data from Kvande (2001-6).

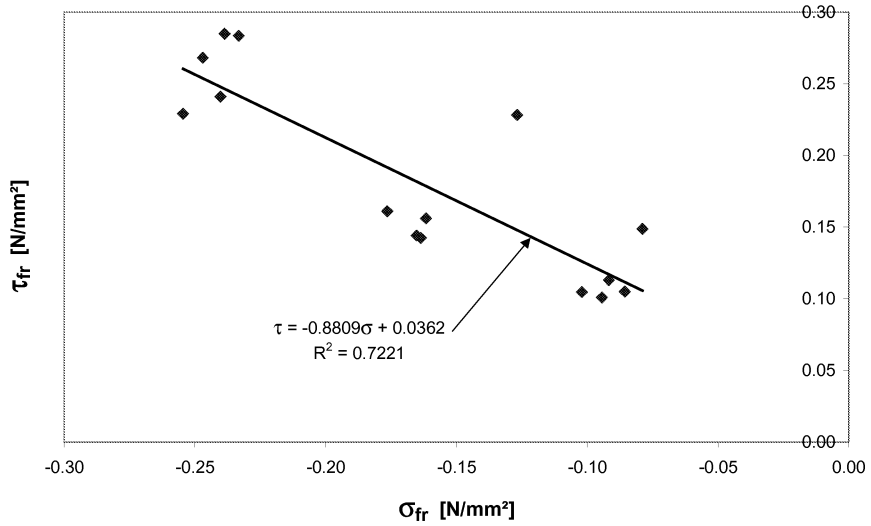

Figure 13:
Shear stress, τ_{fr}, at the horizontal part of the shear-displacement curve dependent on the corresponding compressive stress, σ_{fr}.

5.5 Dry friction coefficient

Dry friction coefficient, μ, is calculated from the shear and normal stress in the horizontal part of the shear-displacement curve. A definition of the friction coefficient is shown in Figure 4
By plotting shear and normal stress in the horizontal part of the curve of every test, it is possible to obtain an average dry friction coefficient from the test series. Such a plot is shown in Figure 13 with shear stress at the vertical axis and normal stress at the horizontal axis. With linear regression analyses an average dry friction coefficient of 0.88 is obtained. The formula is included in the diagram.

5.6 Mode II fracture energy

The mode II fracture energy for bed joint in LECA masonry was measured to 0.091, 0.125 and 0.122 N/mm at compression stress level 0.06, 0.15 and 0.23 N/mm² respectively. In Van der Pluijm (1999) an increase of mode II fracture energy with enlarged normal compression stress is indicated as a general tendency. The same tendency is hard to prove for LECA 3/770. To check if the type of failure has any effect on the measured fracture energy, a comparison of mode II fracture energy dependence of type of failure and normal stress was made (see Figure 17.). Clearly bond failure in combination with tensile failure of blocks near their heads, influences the amount of absorbed energy. Cracking of blocks probably makes the results more diffuse as indicated in (Van der Pluijm 1999). More results should be obtained to clarify this tendency. Meanwhile, data obtained only from tests with bond failure should be used. Mode II fracture energy calculated solely from tests with bond failure are 0.092, 0.137 and 0.138 N/mm at compression stress level 0.06, 0.15 and 0.23 N/mm² respectively.

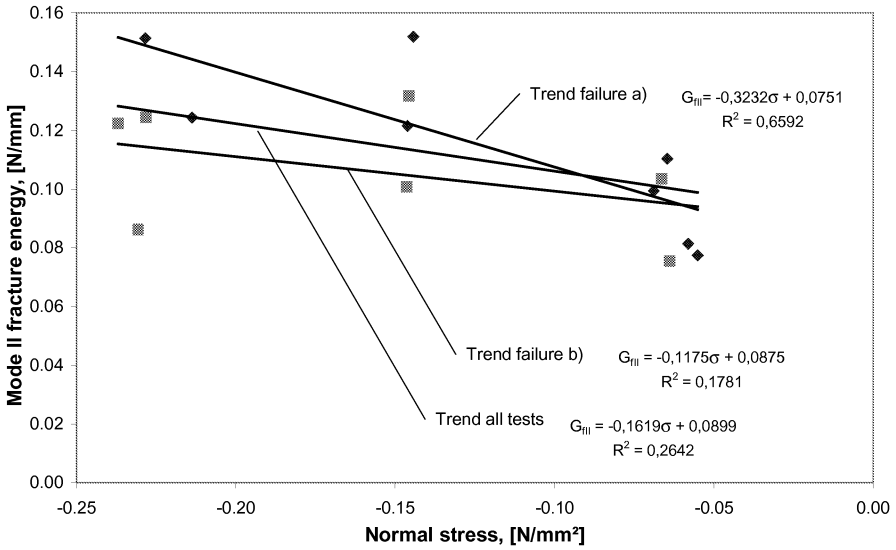

Figure 14:
Mode II fracture energy dependence of type of failure and normal stress.

5.7 Cohesion-softening

Comparisons of behaviour under shear and behaviour under tension show great similarity. The shear stress-deformation diagram differs from the tensile stress-deformation diagram mainly because of the tail that stabilises at a certain stress level. The similarity was a basis for both Lourenço (1996) and Van Zijl (1996) when modelling the descending branch. As a matter of form, both models are presented in the following sequence and compared with the test results. A similar comparison is to be found in (Van der Pluijm 1999).

The cohesion-softening of Lourenço (1996) expressed by using Coulombs friction failure criterion (Equation 5) with c_o replaced by the following equation:

$$c_r = c_o \cdot e^{-\frac{c_o}{G_{fII}} v_{pl}} \qquad \text{Equation 7}$$

where c_r is the residual cohesion,
c_o is the initial cohesion,
G_{fII} is the mode II fracture energy,
v_{pl} is the softening distance.

Van Zijl (1996) based his formula on the description of Hordijk and Reinhardt (1990) of the descending branch under tension. By changing the mode I parameters in corresponding mode II parameters Equation 8 appeared.

$$\frac{c_r}{c_o} = \left(1 + \left(c_1 \frac{v_{pl}}{v_{nonlin}}\right)^3\right) e^{-c_2 \frac{v_{pl}}{v_{nonlin}}} - \frac{v_{pl}}{v_{nonlin}}\left(1 + c_1^3\right) e^{-c_2} \qquad \text{Equation 8}$$

where: v_{nonlin} is the shear displacement over which the cohesion reduces to zero,
c_1 is dimensionless constant 3.0,
c_2 is dimensionless constant 6.93.

In accordance with Van der Pluijm (1999) a relationship exists between the mode II fracture energy, the initial cohesion and the distance over which the cohesion reduces to zero. Figure 15 shows this relationship. Here v_{nonlin} distance is plotted against G_{fII}/c_o for separate tests with bond failure (failure a) and bond failure in combination with tensile failure of block (failure b). Again the influence of the failure of the blocks is visible. The correlation coefficient of the linear trend for the two types of failure is much lower for tests with failure b. The linear trend should theoretically go through zero. The trend calculated from specimens with only bond failure is closest. Equation 9 expresses a linear regression line going through zero for specimens without tensile failure in the block.

$$v_{nonlin} = 2{,}9 \frac{G_{fII}}{c_o} \qquad \text{Equation 9}$$

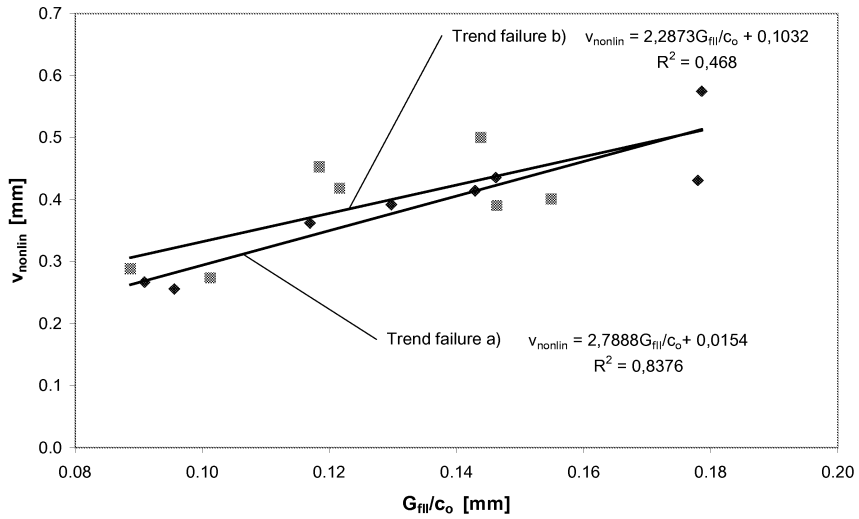

Figure 15:
Distance v_{nonlin} dependence of the mode II fracture energy/cohesion - ratio.

Using equation 9 in 8 it is possible to draw the cohesion softening for bed joint in LECA masonry in the same way as Van der Pluijm (1999). A control of Equation 7 and 8 is made in Figure 16 to 19 by including graphs from all test series with bond failure and long tails together with the theoretical equations. The figures show that the exponential softening (equation 7) matches best, especially in the first part of the descending branch. At the end of the descending branch none of the equations fit very well. This is du to the increase of τ_{fr} when normal stress increase is different from the increase of τ_u ($\Delta\tau_u = \tan\varphi \cdot \sigma$).

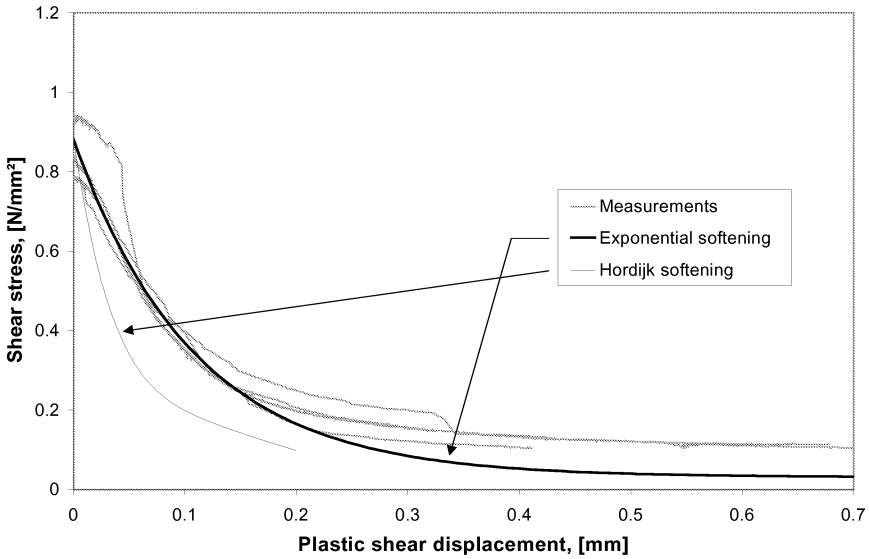

Figure 16:
Cohesion softening of shear test with compression 0.06 N/mm². Experimental data compared with theoretical line from Equation 7 (exponential softening) and 8 (Hordijk softening).

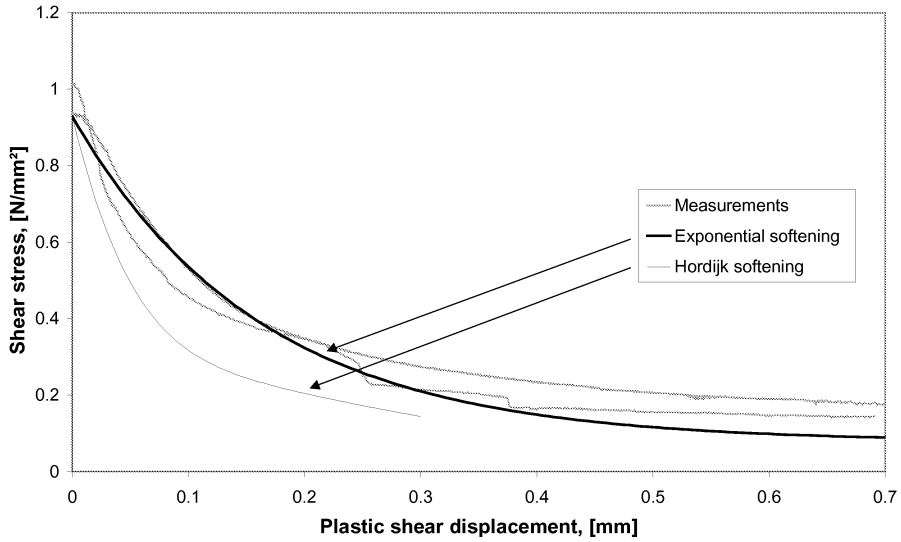

Figure 17:
Cohesion softening of shear test with compression 0.15 N/mm². Experimental data compared with theoretical line from Equation 7 (exponential softening) and 8 (Hordijk softening).

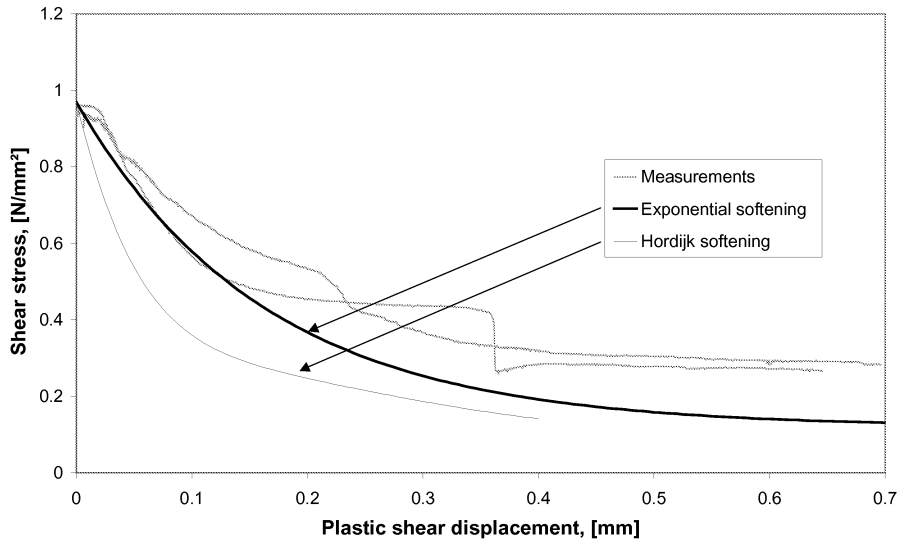

Figure 18:
Cohesion softening of shear test with compression 0.23 N/mm². Experimental data compared with theoretical line from Equation 7 (exponential softening) and 8 (Hordijk softening).

5.8 Dilatancy

The term dilatancy expresses the behaviour of the bed joint during softening. When a relative plastic shear deformation, v_{pl}, of a specimen takes place, a relative plastic transverse deformation, u_{pl}, also appears. The angle between the horizontal and the vertical displacement is of Rots (1997) referred to as the angle of dilatancy, ψ.

Rots (1997) and Lourenço (1996) both handle dilatancy as a constant during the development of shear failure. As a matter of fact this is not the situation. Van der Pluijm (1999) tries in his thesis to describe dilatancy with the following Equation 10:

$$\Delta \tan\psi = \tan\psi_o \left(2\left(\frac{v_{pl}}{r}\right)^{1,5} - 3\frac{v_{pl}}{r} + 1 \right) \qquad : v_{pl} \le r$$

$$\Delta \tan\psi = 0 \qquad : v_{pl} > r$$

Equation 10

where: $\Delta\tan\psi_o$ is the initial (maximum) value of the tangent of the dilatancy angle,
r is the roughness distance over which $\Delta\tan\psi$ reduces to zero.

Equation 10 is based on an assumption that the roughness of a crack surface does not influence the shear strength. It is also based on the discovery of Van der Pluijm (1999) that the compression level does not significantly influence the distance where $\Delta\tan\psi$ reduces to zero. For bed joint of LECA masonry 1,0 mm is chosen for r and $\tan\psi_o$ are 0.82, 0.75 and 0.59 for compression level 0.06, 0.15 and 0.23 N/mm² respectively. Figures 19 to 21 contain dilatancy expressed by $\Delta\tan\psi$ dependent of plastic shear displacement. Both measurement and theoretical approach are included in the figures. Only tests with bond failure are included in the comparison.

The measurements indicate a great variation of the dilatancy during the cohesion-softening. It is not easy to find a representative general formula. With precompression 0.06 N/mm² the theoretical curve seems to start a little to low. This is probably due to the fact that the starting point of the theoretical line is based on mean $\tan\psi_o$ from all tests with bond failure. Great uncertainties exist in the beginning of the curve because of the very small plastic deformation after the initial cracking. This makes it rather difficult to find the real starting point of the theoretical curve. However, the formula of Van der Pluijm (1999) fits reasonably well also for bed joint in LECA masonry and far better than a constant value as in (Rots 1997) and (Lourenço 1996).

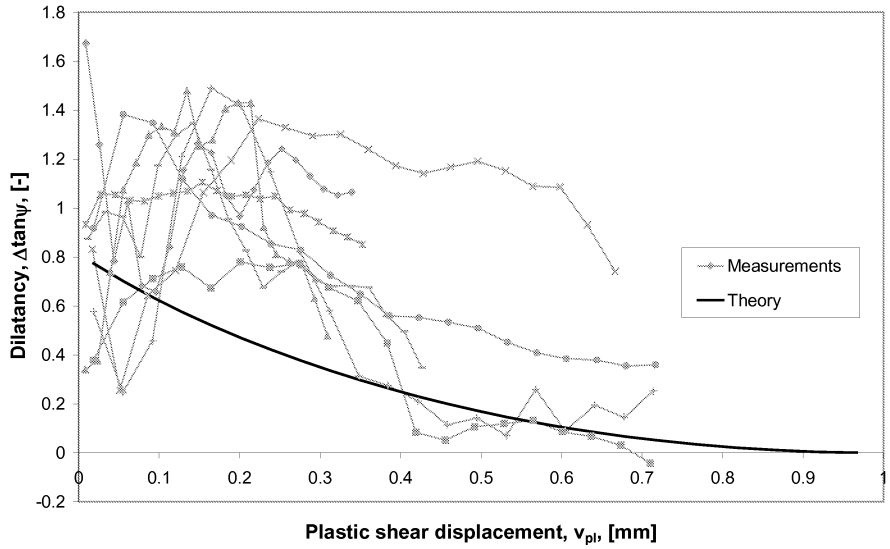

Figure 19:
Dilatancy expressed by $\Delta\tan\psi$ dependent on plastic shear displacement. Compression level 0.06 N/mm². Both measurement and theoretical approach are included in the diagram.

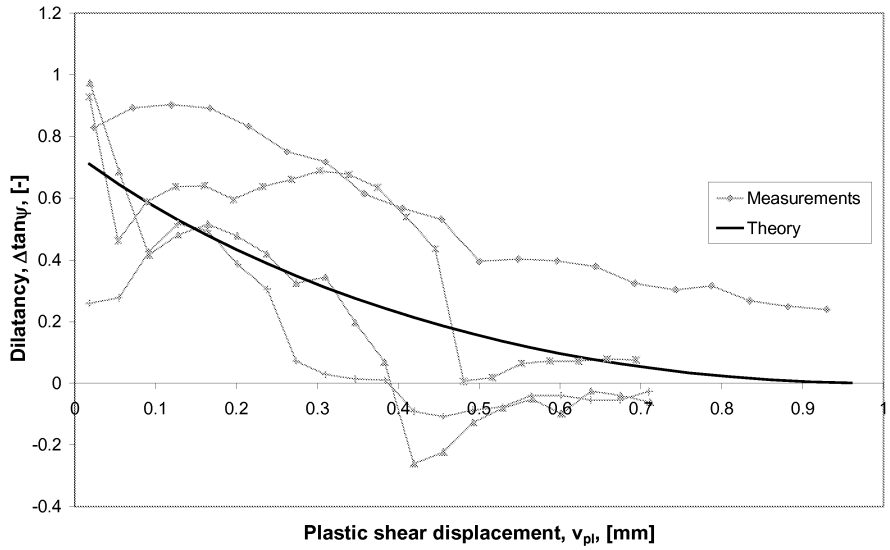

Figure 20:
Dilatancy expressed by $\Delta\tan\psi$ dependent on plastic shear displacement. Compression level 0.15 N/mm². Both measurement and theoretical approach are included in the diagram.

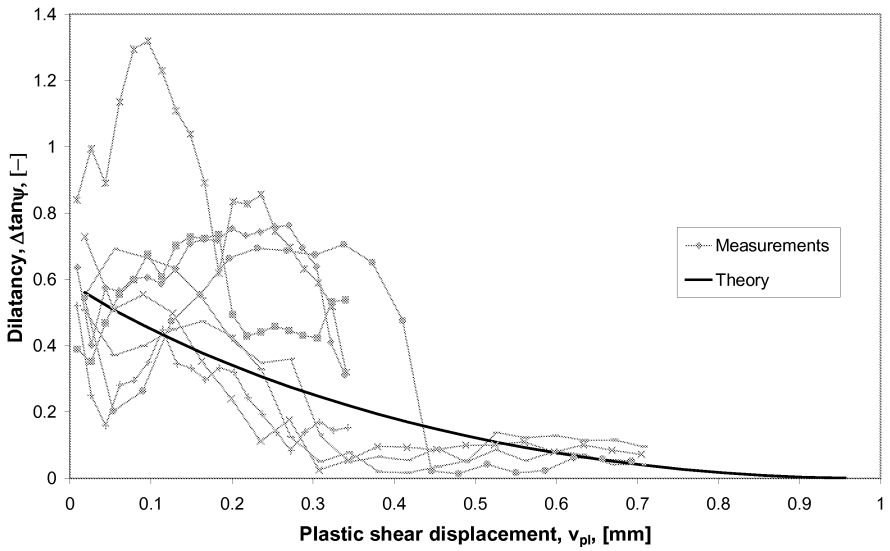

Figure 21:
Dilatancy expressed by $\Delta\tan\psi$ dependent on plastic shear displacement. Compression level 0.23 N/mm². Both measurement and theoretical approach are included in the diagram.

6. Conclusions

Parameters necessary in the finite-element methods program to describe the behaviour of bed joint in LECA masonry subjected to combined compression and shear action are determined during this test program. The results include mean values for shear strength, shear stiffness, mode II fracture energy and dry friction coefficient. The results support partly the validity of exponential cohesion-softening (Lourenço 1996) and dilatancy softening (Van der Pluijm 1999) of the bond interface to describe the post peak behaviour.

Bond shear strength of LECA masonry had a higher measurement than the tensile strength of block. Due to this, failure of LECA masonry more often appears as tensile failure of the block than shear bond failure.

7. References

Hordijk and Reinhardt (1990)
Hordijk, D.A and Reinhardt, H.W – *Testing and modelling of plain concrete under mode I loading in Micro Mechanics of failure of quasi brittle materials,* Elsevier Applied Science, pp. 559-568, ISBN 1-85166-511-0, 1990.

Hofmann et al. (1990)
Hofmann, P, Stöckl, S and Mainz, J – A Comparative Finite Element Evaluation of Mortar Joint Shear Tests, *Masonry International*, Vol. 3 No. 3, pp. 101-104, 1990.

Kvande (2001-3)
Kvande, T – *Råstoff og materialeigenskapar for lettklinkerbetongblokk-kvalitet 3/770 150x250x500 mm. Prøveuttak frå a.s Norsk Leca sitt fabrikkanlegg på Lillestrøm 17.08.98.* (Light Expanded Clay Aggregate (LECA) Concrete Blocks, Quality 3/770 150 x 250 x 500: Raw material and material properties). Report N 8330-3, Norwegian Building Research Institute, Trondheim 2001 (in Norwegian).

Kvande (2001-6)
Kvande, T – *Deformation controlled tensile tests on LECA masonry,* Report N 8330-6, Norwegian Building Research Institute, Trondheim 2001.

Kvande (2001-11)
Kvande, T – *Deformation controlled combined compression and shear tests on LECA masonry. Collection of results,* Report N 8330-11, Norwegian Building Research Institute, Trondheim 2001.

Lourenço et al. (1994)
Lourenço, P.B, Rots, J.G, Blaauwendraad, J. – Implementation of an interface cap model for the analysis of masonry structures, *Computational Modelling of Concrete Structures,* (Ed. Mang, H. *et al.*), Pineridge Press, Swansea, UK, pp. 123-134, 1994.

Lourenço, P.B (1996)
Lourenço, P.B – *Computational Strategies for Masonry Structures*. Dissertation, Delft University of Technology, Delft 1996.

Pluijm (1993)
Pluijm, R. van der – Shear behaviour of bed joints, *The 6th North American Masonry Conference*, Drexel University, Philadelphia, Pennsylvania, USA, pp. 125-136, 1993.

Pluijm (1998)
Pluijm, R. van der – *Overview of deformation controlled combined tensile and shear tests*. TUE/CCO/98.20, Faculty of Architecture, Building and Planning, Technische Universiteit Eindhoven, Eindhoven 1998.

Pluijm (1999)
Pluijm, R. van der. – *Out-of-Plane Bending of Masonry. Behaviour and strength.* Dissertation, Technische Universiteit Eindhoven, ISBN 90-6814-099-X, Eindhoven 1999.

prEN 1015-11
Draft European Standard prEN 1015-11:1995: *Method of test for mortar for masonry – Part 11: Determination of flexural and compressive strength of hardened mortar*, European Committee for Standardization CEN, Brussels 1995.

Rots (1997)
Rots, J.G (Editor) – *Structural Masonry. An Experimental/Numerical Basis for Practical Design Rules*. CUR, Balkema, ISBN 90 54-10-680-8, Rotterdam 1997.

Zijl (1996)
Zijl, G.P.A.G. van – *Shear transfer across bed joints in masonry: A numerical study*, Technical report 03.21.0.22.28, Delft University of Technology, Delft 1996.

Symbols

CV	coefficient of variation	[%]
E	modulus of elasticity	[N/mm²]
F_n	normal force	[N]
F_s	shear force	[N]
G	shear modulus G_o is calculated from best-fit true linear part from origin G_u is calculated from secant at ultimate load	[N/mm²]
G_{fI}	mode I fracture energy	[N/mm]
G_{fII}	mode II fracture energy	[N/mm]
c	cohesion or shear bond strength	[N/mm²]
c_o	initial cohesion	[N/mm²]
c_r	residual cohesion	[N/mm²]
f_c	compressive strength	[N/mm²]
f_{tb}	tensile bond strength	[N/mm²]
f_s	shear bond strength	[N/mm²]
f_{tu}	(arbitrary) ultimate value of the tensile strength	[N/mm²]
f_t	residual value from the tensile strength during softening	[N/mm²]
r	roughness distance over which $\Delta\tan\psi$ reduces to zero	[mm]
t	thickness	[mm]
u	normal deformation of specimen	[mm]
u_{pl}	plastic normal displacement	[mm]
v	shear deformation of specimen	[mm]
v_{pl}	plastic shear displacement	[mm]
v_{nonlin}	softening distance	[mm]
φ	angle of internal friction	[°]
μ	dry friction coefficient	[-]
σ	normal stress	[N/mm²]
σ_{fr}	normal stress when τ_{fr}	[N/mm²]
τ	shear stress	[N/mm²]
τ_u	shear bond strength	[N/mm²]
τ_{fr}	friction at shear stress	[N/mm²]
ν	Poisson's ratio	[-]
ψ	angle of dilatancy	[°]

Superscripts

u	of masonry unit
m	of mortar
j	of (mortar)joint
j+u	of joint + masonry unit within measuring length

Results from deformation controlled combined compressive and shear test of masonry

Test period: 15.03.99 - 03.05.99

E_o = 3000 N/mm² Poisson's ratio = 0,2

$\sigma \approx$ - 0.06 N/mm²

Spesimen	σ_u [N/mm²]	τ_u [N/mm²]	σ_{fr} [N/mm²]	τ_{fr} [N/mm²]	G_o^j [N/mm²]	G_o^{j+u} [N/mm²]	G_u^j [N/mm²]	G_u^{j+u} [N/mm²]	G_{fII} [N/mm]	v_{nonlin} [mm]	μ [-]	Failure	Comments
III-15	-0.065	1.052	-0.091	0.224	1242	1286	350	621	0.1180	0.2949	2.46	A	Test stopt to early
III-16	-0.065	0.913	-0.084	0.178	1263	1294	628	928	0.1001	0.2969	2.13	A	- " -
III-17	-0.055	0.787	-0.079	0.149	1337	1326	255	491	0.0773	0.2673	1.89	A	
III-23	-0.066	0.841	-0.094	0.101	1292	1301	708	968	0.1034	0.4185	1.07	B	
III-25	-0.058	0.852	-0.086	0.105	1337	1308	585	868	0.0813	0.2558	1.23	A	
III-33	-0.065	0.789	-0.092	0.113	1036	1179	200	406	0.1103	0.3921	1.23	A	
III-34	-0.064	0.887	-0.127	0.228	2102	1527	410	692	0.0754	0.2886	1.80	B	
III-35	-0.069	0.945	-0.102	0.105	1585	1412	839	1058	0.0994	0.3619	1.02	A	
Mean	***-0.06***	***0.88***	***-0.09***	***0.15***	***1399***	***1329***	***497***	***754***	***0.0957***	***0.3220***	***1.60***		
St.dev.	***0.00***	***0.09***	***0.01***	***0.05***	***321***	***102***	***227***	***237***	***0.0159***	***0.0606***	***0.54***		
CV, [%]	***7***	***10***	***16***	***36***	***23***	***8***	***46***	***31***	***17***	***19***	***34***		

$\sigma \approx$ - 0.15 N/mm²

Spesimen	σ_u [N/mm²]	τ_u [N/mm²]	σ_{fr} [N/mm²]	τ_{fr} [N/mm²]	G_o^j [N/mm²]	G_o^{j+u} [N/mm²]	G_u^j [N/mm²]	G_u^{j+u} [N/mm²]	G_{fII} [N/mm]	v_{nonlin} [mm]	μ [-]	Failure	Comments
III-26	-0.144	0.938	-0.177	0.161	926	1113	251	485	0.1518	0.5746	0.91	A	
III-27	-0.146	0.955	-0.162	0.156	2065	1546	401	682	0.1317	0.4005	0.96	B	
III-29	-0.146	0.831	-0.164	0.142	2508	1612	449	763	0.1007	0.4527	0.87	B	
III-30	-0.146	1.014	-0.165	0.144	1178	1247	407	689	0.1215	0.4141	0.87	A	
Mean	***-0.15***	***0.93***	***-0.17***	***0.15***	***1669***	***1379***	***377***	***655***	***0.1264***	***0.4605***	***0.90***		
St.dev.	***0.00***	***0.08***	***0.01***	***0.01***	***742***	***238***	***87***	***119***	***0.0213***	***0.0792***	***0.04***		
CV, [%]	***1***	***8***	***4***	***6***	***44***	***17***	***23***	***18***	***17***	***17***	***5***		

$\sigma \approx$ **- 0.23 N/mm²**

Spesimen	σ_u [N/mm²]	τ_u [N/mm²]	σ_{fr} [N/mm²]	τ_{fr} [N/mm²]	G_o^j [N/mm²]	G_o^{j+u} [N/mm²]	G_u^j [N/mm²]	G_u^{j+u} [N/mm²]	G_{fII} [N/mm]	v_{nonlin} [mm]	μ [-]	Failure	Comments
III-18	-0.229	1.104	-0.247	0.468	1844	1473	359	632	0.0960	0.3262	1.90	A	Test stopt to early
III-19	-0.232	1.000	-0.234	0.912	528	998	452	766	0.0043	0.0541	3.89	B	Failure to early
III-20	-0.234	1.030	-0.252	0.446	1206	1258	384	662	0.0924	0.3268	1.77	A	Test stopt to early
III-21	-0.231	0.865	-0.239	0.285	1783	1289	348	584	0.0861	0.2738	1.19	B	
III-22	-0.237	0.866	-0.255	0.229	1022	1185	334	600	0.1223	0.4999	0.90	B	
III-24	-0.233	0.953	-0.253	0.466	1512	1370	487	775	0.0589	0.3086	1.84	A	Test stopt to early
III-31	-0.214	0.946	-0.233	0.283	1819	1474	455	743	0.1243	0.4355	1.22	A	
III-32	-0.228	0.965	-0.247	0.268	1299	1300	154	325	0.1513	0.4311	1.09	A	
III-36	-0.228	0.997	-0.240	0.241	1945	1494	390	300	0.1244	0.3905	1.00	B	
Mean	***-0.23***	***0.97***	***-0.24***	***0.40***	***1440***	***1315***	***374***	***599***	***0.0956***	***0.3385***	***1.64***		
St.dev.	***0.01***	***0.08***	***0.01***	***0.22***	***470***	***161***	***98***	***177***	***0.0437***	***0.1289***	***0.92***		
CV, [%]	***3***	***8***	***3***	***54***	***33***	***12***	***26***	***29***	***46***	***38***	***56***		

APPENDIX 8

Kvande. T. and Høiseth, K.V.
Behaviour of LECA Masonry under Restrained Shrinkage.
Submitted for publications in Masonry International in January 2001.

Behaviour of LECA Masonry under Restrained Shrinkage

by

T. KVANDE[1] and K.V. HØISETH[2]

Abstract

The purpose of this investigation was to study the shrinkage behaviour of Light Expanded Clay Aggregate (LECA) masonry walls restrained to the foundation. To control the effect of shrinkage reinforcement, the investigation contained five restrained LECA walls with different amount of reinforcement. As reference, two walls resting on "ideal" sliding layers and three single LECA blocks were tested. Even though no cracking of LECA blocks were observed in the restrained specimens during the test period of 1½ year, the test results indicate that the amount and placement of the shrinkage reinforcement influence the magnitude of the horizontal shrinkage. The least horizontal shrinkage was obtained on the wall with most reinforcement ($A_s/A_M \approx 0.67$ ‰). The effect of the reinforcement seems, however, to be limited. There was no significant difference between vertical shrinkage of the restrained walls and the shrinkage of the other specimens. Design values for shrinkage may therefore be derived from tests of single untreated LECA blocks.

Introduction

Restrained shrinkage cracking of masonry is one of the major causes of damage to buildings [1,2]. Masonry made of Light Expanded Clay Aggregate (LECA) concrete blocks is no exception to this. Arriving from the production line, the moisture content of the LECA blocks is relatively high. Due to the relatively large shrinkage and the relatively low tensile strength, LECA masonry requires shorter distance between movement joints than traditional masonry of clay bricks [2]. Despite the fact that restrained shrinkage cracking is a problem in masonry, movement-joint design is to a large extent done by rules-of-thumb [3].

Traditionally, sliding layer is rarely used between the foundation and LECA masonry. The use of sliding layer is more common in connection with masonry of clay bricks. Normally, LECA masonry is built with a mortar layer between the foundation and the wall. This is somewhat surprising considering the higher coefficient of thermal expansion and the higher measure of shrinkage for LECA masonry than for brick masonry [4]. In Norway, LECA masonry is normally made without mortar in the perpend joints. The open (free) perpend joints contribute to limit the tensile capacity of the LECA masonry even more.

In this paper, the term shrinkage will be used to denote changes in length or strain due to loss of moisture in masonry units and mortar in the hardened state or after a certain initial hardening [5].

[1] Department of Building and Construction Engineering, Norwegian University of Science and Technology
[2] MARINTEK Department of Structural Engineering

Objective

The purpose of the investigation was to study the behaviour of LECA masonry subjected to restrained shrinkage. Of special interest is to study walls restrained to the foundation. This is due to the fact that LECA masonry very often is made without a sliding layer between the foundation and the masonry. The intention was to use the experimental results later on to evaluate the results of numerical analysis.

The test series comprised five restrained LECA walls. In order to study the effect of shrinkage reinforcement, the walls were built with different amount of shrinkage reinforcement. To evaluate the results of the restrained LECA walls, tests were also carried out on two walls which were built on "ideal" sliding layers and three single LECA blocks.

Test procedure

Norsk Leca manufactured the masonry units used in the test programme. Typical material properties of the tested blocks are given in Table 1 and [6]. After manufacturing, the blocks were enclosed in plastic for a period of four to five weeks before the walls were made.

Totally, seven walls were built on foundation of hollow steel members resting on a concrete floor. The walls were made in the basement of the laboratory at Department of Building and Construction Engineering at Norwegian University of Science and Technology (NTNU). Five of the walls were restrained to the steel members by epoxy adhesive in order to obtain a worst case (fixed) condition, see Figure 1. An "ideal" sliding layer, by means of steel rollers, was used for the two last walls, see Figure 2. Table 2 contains an overview of the characteristics of each wall. The mortar used in the test program was factory made.

Table 1:
Material characteristics of LECA blocks.

Material characteristics	Value
Dimension	147 x 249 x 499 mm³
Holes	None
Dry density	760 kg /m³
Initial moisture content	11 weight-%
Compressive strength	3.0 N/mm²
Tensile strength	0.5 N/mm²
Modulus of elasticity	3000 N/mm²
Poisson's ratio	0.2

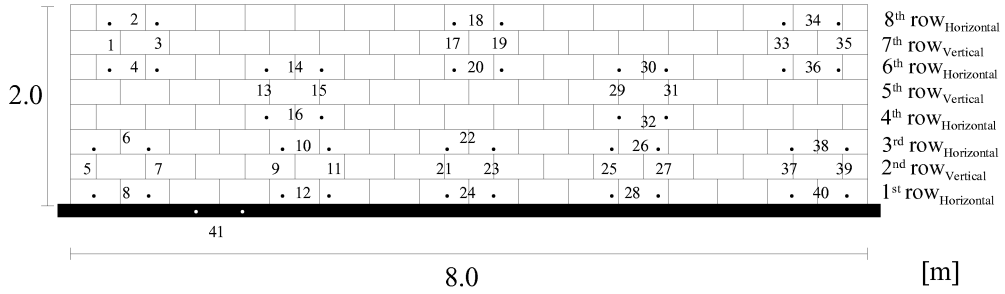

Figure 1:
LECA wall type I to V. The numbers identify the gauge locations. The gauge measurements are in the following presented as mean values according to the identification given to the right.

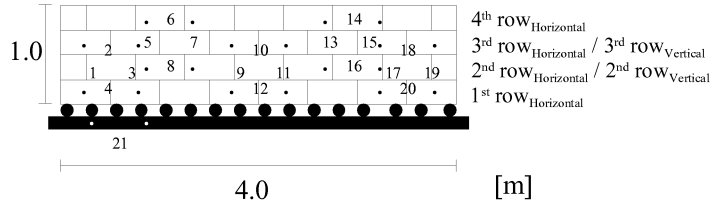

Figure 2:
LECA wall type VI to VII. The numbers identify the gauge locations. The gauge measurements are in the following presented as mean values according to the identification given to the right.

Table 2:
Characteristics of the tested LECA walls.

Wall	Dimension	Shrinkage reinforcement [1)]	Mortar [2)]	Boundary condition
I	2 x 8 m	None	1:1:7	Glued to the foundation
II	2 x 8 m	1 bar in every 4th bed joint => $A_s/A_M \approx 1.6 \cdot 10^{-4}$	1:1:7	Glued to the foundation
III	2 x 8 m	2 bars in every 4th bed joint => $A_s/A_M \approx 3.3 \cdot 10^{-4}$	1:1:7	Glued to the foundation
IV	2 x 8 m	1 bar in every 2nd bed joint => $A_s/A_M \approx 3.3 \cdot 10^{-4}$	1:1:7	Glued to the foundation
V	2 x 8 m	2 bars in every 2nd bed joint => $A_s/A_M \approx 6.7 \cdot 10^{-4}$	1:1:7	Glued to the foundation
VI	1 x 4 m	None	1:1:7	Made on steel rollers
VII	1 x 4 m	None	1:3	Made on steel rollers

1) Norsk Leca reinforcement 2 Ø 4, A_s= 25 mm², f_{tk} = 700 N/mm².
2) Volume lime:cement:aggregate or volume cement:aggregate

All walls were built by the same mason during a six days period mid-September 1998. The walls were made without mortar in the perpend joints, which is the most common way to produce LECA masonry. The mason made two walls during one day, plastering the walls the following day. The walls were plastered with a factory made mortar in order to visualise possible cracks during testing. The thickness of the plastering was 2-3 mm.

Each wall was enclosed in plastic for three days before the measurements were started. Gauge location pads were glued on one face of the walls (see Figure 1 and Figure 2). Even numbers denote a horizontal gauge length, while uneven numbers denote a vertical gauge length. The last number (41 for Walls I to V and 21 for Walls VI and VII) denotes horizontal gauge length on the steel foundation.

The faces of three single LECA blocks were plastered the same way as the walls. The sides of the blocks were not treated. Gauge location pads were glued on both faces of the blocks. Because the gauge length of 500 mm was larger than the LECA blocks, the location pads were glued diagonally on the faces of the blocks. The blocks were placed on steel rollers similarly to Walls VI and VII to avoid any obstruction.

The walls were made in a room with limited possibilities for control of the ambient climate. Season variations in the humidity and temperature in the room may therefore have influenced the behaviour of the walls. Relative humidity and temperature were recorded continuously during the test period.

The shrinkage of the walls was measured frequently during the test program with a Demec gauge (demountable mechanical gauge) with a gauge length of 500 ±2 mm. The shrinkage and the change of weight of the three single LECA blocks were also recorded. Because of the large number of gauge locations, it was impossible to do all the measurements during one day. Normally, the measurements were done within a period of three days. The shrinkage measurements of a wall was however always completed during one day. The development of crack pattern was recorded frequently during the test program by highlighting with ink on the plaster surface.

Results

Results given in this paper were obtained during the period mid-September 1998 to the end of April 2000. The tests are, however, not finished yet.

The relative humidity and the temperature in the test room varied during the test period. Lowest relative humidity and temperature were registered during winter-time, while the highest values were registered in the summer, see Figure 3. Because the temperature variations influence the recorded displacements, the drying shrinkage has been adjusted for deviation in temperature from the first measurement. The adjustments were done by using a coefficient of temperature expansion of 0.008 mm/(m°C) for the LECA masonry [7] and 0.011 mm/(m°C) for the steel foundation [8]. Due to a temperature range of about 10 °C, the temperature expansion was significant.

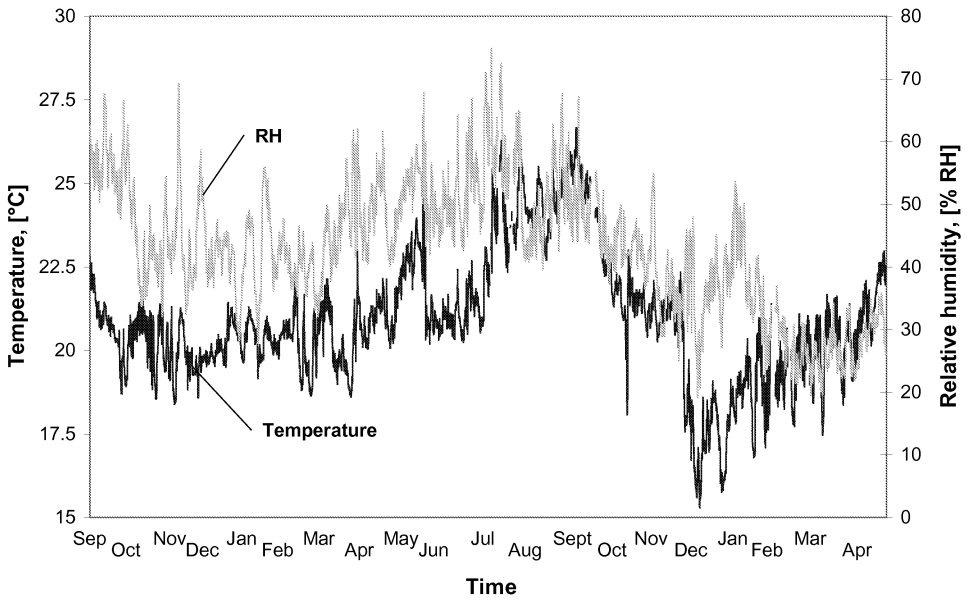

Figure 3:
Variation in ambient climate during the test period from mid-September 1998 to the end of April 2000.

In the following, a negative displacement represents a decreasing length (shrinkage).

Figure 4 shows the development of the shrinkage of the three single LECA blocks as mean values. The mean shrinkage at the end of the test period was measured to –0.62 mm/m with a coefficient of variation equal to 6 %. The figure also shows the change of weight of the blocks during the test relative to the weight at the beginning of the test. Because the test program has not been finished yet, the blocks have not been dried. The moisture content of the blocks during the test has consequently not been established yet.

No significant differences were recorded between the two walls on the steel rollers, Walls VI and VII, and the shrinkage of these two walls is presented as mean values. Shrinkage measurement carried out at the same distance from the foundation is presented as average values to illustrate the effect of the "free to move" condition in the horizontal direction, see Figure 5. Identification of gauge locations at the same distance from the foundation is given in Figure 2. The mean shrinkage of all gauge measurements at the end of the test period was –0.62 mm/m with a coefficient of variation equal to 3 %.

The shrinkage in the restrained walls is shown in Figure 6. In the Figure, the shrinkage values represents the mean values of the measurements in equal positions in Wall I to V. Shrinkage measurements done at equal distances from the foundation is also presented as mean values. Identification of gauge locations at the same distance from the foundation is given in Figure 1. The effect of the restraint appears only in the horizontal measurements. There is a clear trend that the shrinkage increases with the distance from the foundation. The horizontal shrinkage measured at the top of the walls and the vertical shrinkage measured at different positions from the foundation have approximately the same magnitude. The mean shrinkage in all measurements in the vertical direction at the end of the test period was –0.59 mm/m with a coefficient of variation equal to 4 %.

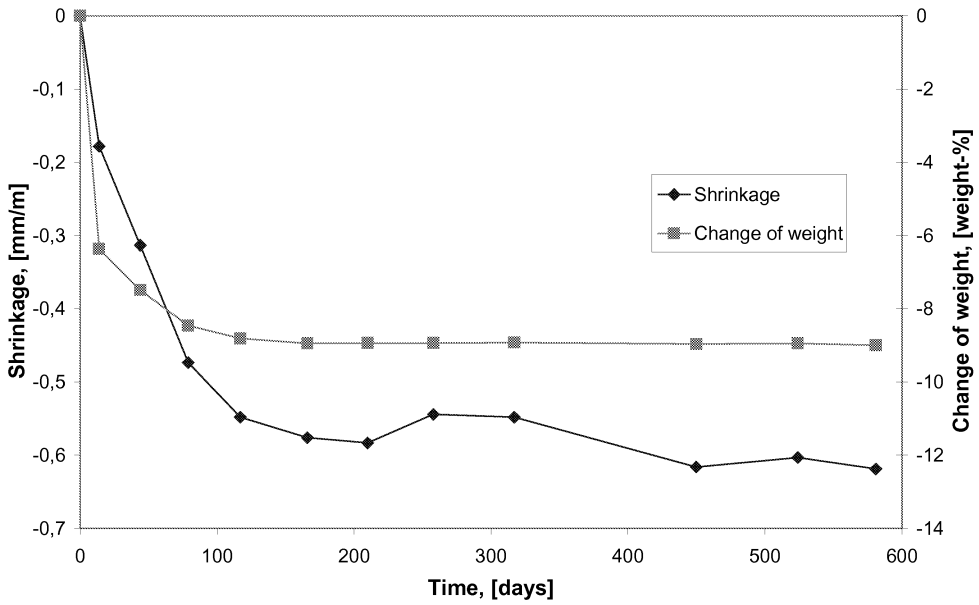

Figure 4:
Development of mean shrinkage and change of weight of the single LECA blocks during the test period from mid-September 1998 to the end of April 2000.

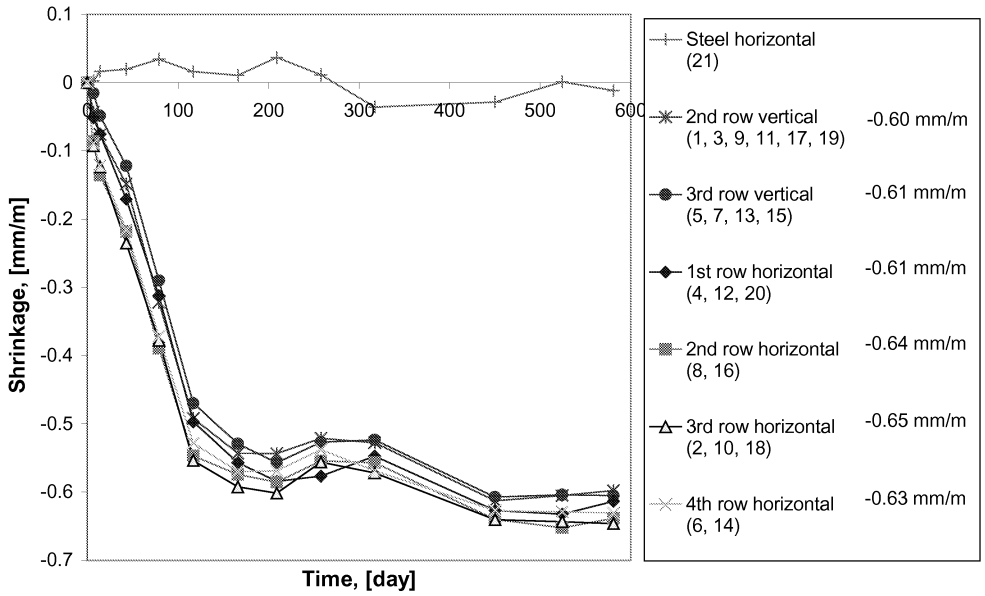

Figure 5:
Development of mean shrinkage for Walls VI and VII during the test period from mid-September 1998 to the end of April 2000. Shrinkage at the end of the test is given at the right side.

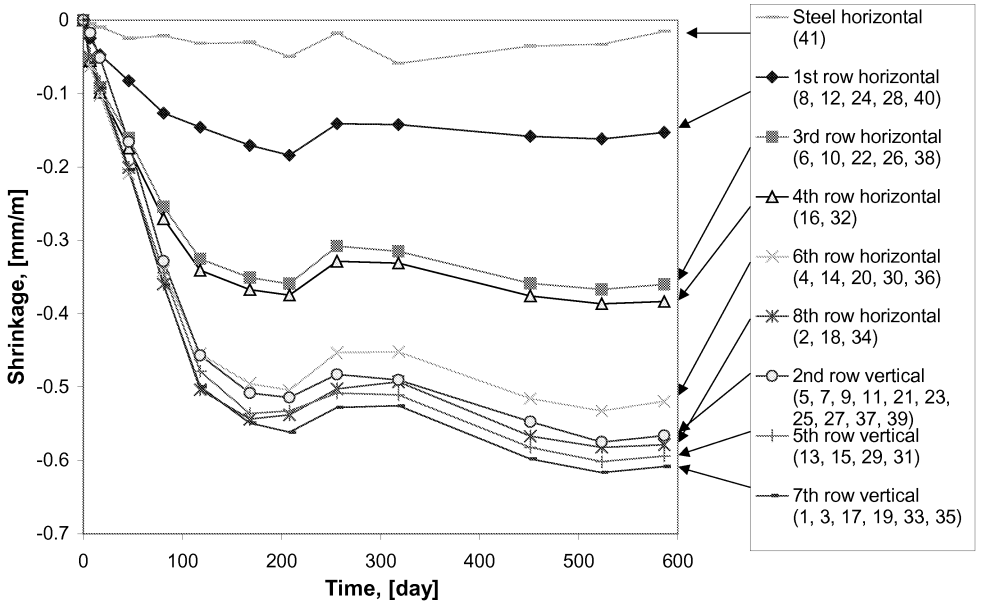

Figure 6:
Development of mean shrinkage for Walls I to V during the test period from mid-September 1998 to the end of April 2000.

Figure 7 shows the deformed shape of the restrained walls after the shrinkage period. While the vertical deformation was uniform, the horizontal deformation was dependent on the distance from the foundation. It should be noticed that the deformation is enlarged 100 times compared to the dimension of the walls.

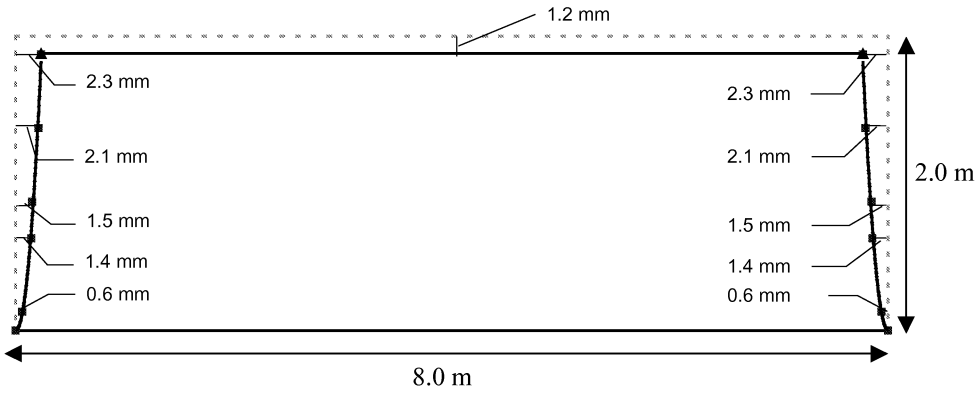

Figure 7:
Mean deformation of Walls I to V at the end of the test period. Horizontal deformation is given at the different position from the foundation, see Table 3.

Figure 6 and 7 shows the mean values of the measurements at the surface of Wall I to V. There were however some scatters in the readings. Table 3 and 4 shows the difference between Wall I to V. Table 3 shows the mean horizontal shrinkage at the end of the test at the different positions from the foundation according to Figure 1. Enclosed in the table are principal figures showing the cross section of each wall with amount and placing of

reinforcement as well as position of measurement. A similar presentation is made for the vertical shrinkage, see Table 4. It should be noticed that the thickness of the mortar joints in the figures is enlarged to show the location of reinforcement. The effect of the reinforcement may be illustrated by the coefficient of variation given in the tables, while the coefficient of variation is larger for the horizontal measurement than for the vertical ones. Except for the 1. row, the least horizontal shrinkage was recorded on the wall with most reinforcement (Wall V). Also for the vertical shrinkage a trend of increasing shrinkage with increasing distance from the foundation was registered, see Table 4. The trend is however hardly significant.

Table 3:
Mean horizontal shrinkage at the end of the test period for Wall I to V. Coefficient of variation is given for the mean of all walls. Location of reinforcement is given in the schematic cross section figure of each wall.

Position from the foundation	Shrinkage [mm/m]					Mean [mm/m]	CV [%]
	Wall I	Wall II	Wall III	Wall IV	Wall V	Walls I to V	
8th row	-0.57	-0.62	-0.60	-0.62	-0.49	-0.58	9
6th row	-0.56	-0.52	-0.54	-0.53	-0.45	-0.52	8
4th row	-0.40	-0.42	-0.42	-0.35	-0.34	-0.38	9
3rd row	-0.39	-0.38	-0.36	-0.33	-0.33	-0.36	8
1st row	-0.20	-0.15	-0.13	-0.15	-0.13	-0.15	18
Steel							

Table 4:
Mean vertical shrinkage at the end of the test period for Wall I to V. Coefficient of variation is given for the mean of all walls. Location of reinforcement is given in the schematic cross section figure of each wall.

Position from the foundation	Shrinkage [mm/m]					Mean [mm/m]	CV [%]
	Wall I	Wall II	Wall III	Wall IV	Wall V	Walls I to V	
7th row	-0.60	-0.58	-0.65	-0.62	-0.60	-0.61	4
5th row	-0.58	-0.58	-0.61	-0.60	-0.60	-0.59	3
2nd row	-0.55	-0.54	-0.56	-0.58	-0.60	-0.57	4
Steel							

No cracking of LECA blocks occurred during the test period. Only cracking of the plastering over the open perpend joints was observed. Approximately the same crack pattern was observed for all the restrained walls. Figure 8 shows the crack pattern of Wall V. The figure shows that most cracks developed close to the foundation and in the middle of the wall. The cracks were initiated in the first row. No cracks were visible in the unrestrained walls supported by steel rollers.

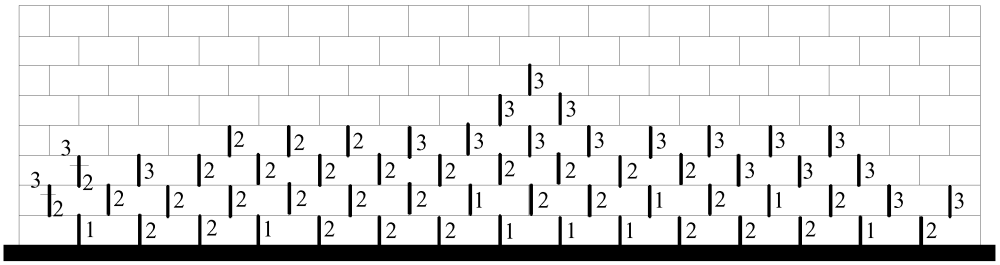

Figure 8:
Crack pattern of Wall V. Number 1 indicate cracks registered within October 1998, 2 within Mars 1999 and 3 within April 2000.

The 28-day's flexural and compressive strength according to [9] were 1.8 N/mm² and 6.6 N/mm², respectively, for the lime:cement-mortar and 3.8 N/mm² and 18.3 N/mm² for the cement-mortar.

Discussion

The current test program was aimed at studying the influence of ambient humidity on the shrinkage of LECA masonry and single LECA blocks. It has been shown that seasonal variations influenced the shrinkage. Due to a drier indoor climate, a larger shrinkage was recorded during the last winter of the test programme than during the first. Expansions were recorded during the more humid summer time. No significant differences were recorded between the shape of the diagrams neither the magnitude of the final shrinkage. Because the mortar joints, normally, represent less than 5 % by volume of the LECA masonry it has previously been shown that the contribution from the joints is insignificant on the shrinkage of the masonry [10]. This was also found in the present study, where no significant difference between the behaviour of Wall VI (made with a lime/cement-mortar) and Wall VII (made with a cement mortar) was measured. Given that the contribution from the mortar joints is small, Schubert [5] concludes that it is possible to determine shrinkage of masonry by testing of single masonry units. Schubert [5] also stresses the importance of sealing the masonry units according to their position in the masonry element. In this test programme, however, the insignificant difference between the behaviour of the separate LECA blocks and the LECA masonry indicate that no sealing is necessary for LECA blocks. The development of the shrinkage of the LECA masonry may consequently be obtained by testing single untreated LECA blocks.

The crack pattern presented in Figure 8 gives an impression of the tensile stresses in the wall. The crack pattern matches very well with the calculated principal tensile stresses in a similar masonry wall reported in [11].The highest tensile stress appeared close to the foundation and in the middle of the wall. Consequently, more shrinkage reinforcement should be required in the lower part of the wall than in the upper part.
The LECA blocks did not crack in any of the restrained walls, not even in the wall without reinforcement. It may therefore be difficult to judge the effect of the reinforcement. The results, however, show a larger coefficient of variation for the horizontal shrinkage than the vertical shrinkage, see Table 3 and 4, The smallest horizontal shrinkage was also found for the wall with most reinforcement. For Wall VI and VII, which were supported by sliding layers, about the same horizontal and vertical shrinkage should be expected in the masonry. The same vertical shrinkage of the restrained walls indicates further that there was no significant difference in the initial moisture content of the walls. It therefore seems to be the amount of reinforcement which causes the variations in the horizontal shrinkage.

Shrinkage reinforcement required by the Norwegian code [12] is given by A_s/A_M–ratio = 0.30 ‰, for indoor LECA masonry of the same quality as used in this test programme. For outdoor masonry without sliding layer at the bottom, the requirement is 0.60 ‰. The test results gave no clear trend regarding the amount/location of the reinforcement and the magnitude of shrinkage, even though the smallest horizontal shrinkage was obtained on Wall V with $A_s/A_M \approx 0.67$ ‰. It should, however, be noticed that cracking of the masonry (plaster) took place at the open perpend joints only, and the shrinkage reinforcement may therefore not have been fully activated. On the other hand, the crack pattern and crack width were strongly influenced by the distance between the open perpend joints. Consequently, due to the open perpend joints in Norwegian LECA masonry, the shrinkage reinforcement may be unnecessary in situations similar to those in this study.

Concluding remarks

In this test programme, the shrinkage behaviour of restrained and unrestrained LECA masonry as well as single LECA blocks have been observed over a period of 1½ year. The results indicate that determination of shrinkage of LECA masonry may be derived from tests of single untreated LECA blocks. Even though no cracking of LECA blocks were observed during the test period, the test results indicate that the amount and location of the shrinkage reinforcement influence the magnitude of the horizontal shrinkage. The effect of the reinforcement seems, however, to be limited. Consequently, the amount of shrinkage reinforcement required today [12] may be of limited significance for prevention of restrained-shrinkage cracking of LECA masonry.

The present investigation forms a basis for evaluating the results from numerical analysis. Further investigations of shrinkage of LECA masonry should include walls with restrained shrinkage cracking. Both experimental testing and numerical analysis should be performed to give reliable guidelines for the amount and location of shrinkage reinforcement and the design of movement joints.

Acknowledgements

The authors gratefully acknowledge the financial support of The Research Council of Norway and Norsk Leca. Thanks are also due to Noralf Bakken for his help in carrying out the experiments, and Lars Myhre for his many important corrections.

Symbols

A_M	area of masonry	[mm²]
A_s	area of reinforcement	[mm²]
$Ø$	diameter of reinforcement	[mm]
f_{tk}	characteristic tensile strength of reinforcing steel	[N/mm²]

Reference

1. Jong, P. de – Bouwschade ter lering (I) (Lessons from damage in building industry (I)), *Cement*, No. 2, pp. 26-28, 1992 (in Dutch).

2. Madsø, F.E. – Bevegelser og bevegelsesfuger i murverk. Del 1 (Movement and Movement Joints in Masonry. Part 1), *Mur*, No. 2, pp. 27-30, 1997 (in Norwegian).

3. Ibrahim, K.S and Suter, G.T. – Contribution to the rational determination of movement joint spacing in concrete masonry walls. 6th *North American Masonry Conference,* (Editors: Hahmid, A.A. and Harris, H. G.), Drexel University, Philadelphia, pp. 491-503, 1993.

4. European Prestandard ENV 1996-1-1:1995. Eurocode 6: *Design of masonry structures. Part 1-1: General rules for buildings – Rules for reinforced and unreinforced masonry*, European Committee for Standardization CEN, Brussels 1995.

5. Schubert, P. – Test methods for the determination of creep and shrinkage in masonry, *10th International Brick and Block Masonry Conference*, Masonry Council of Canada, The University of Calgary, Calgary, pp. 777-786, 1994.

6. Kvande, T. – *Råstoff og materialeigenskapar for lettklinkerbetongblokk-kvalitet 3/770 150x250x500 mm. Prøveuttak frå a.s Norsk Leca sitt fabrikkanlegg på Lillestrøm 17.08.98.* (Light Expanded Clay Aggregate (LECA) Concrete Units, Quality 3/770 150 x 250 x 500: Raw material and material properties). Report N 8330-3, Norwegian Building Research Institute, Trondheim 2001 (in Norwegian).

7. Leca anvisning 1.000: *Leca murverk prosjektering* (Design of LECA masonry), as Norsk Leca, Oslo 1995 (in Norwegian).

8. NBI 571.403: *Metaller i bygningsbruk. Typer og egeskaper* (Metal used in buildings. Types and properties), Norwegian Building Research Institute, Oslo 1986 (in Norwegian).

9. Draft European Standard prEN 1015-11: *Method of test for mortar for masonry - Part 11: Determination of flexural and compressive strength of hardened mortar*, CEN, Brussels 1995.

10. Kvande, T. – *Determination of creep and shrinkage in LECA masonry.* Report N 8330-9, Norwegian Building Research Institute, Trondheim 2001.

11. Rots, J.G (Editor) – *Structural Masonry. An Experimental/Numerical Basis for Practical Design Rules*. CUR, Balkema, ISBN 90 54-10-680-8, Rotterdam 1997.

12. *Bransjenorm, Veiledning til ENV 1996-1-1:1995, Prosjektering av murverk. Beregning og dimensjonering* (Draft National Application Document for ENV 1996-1-1:1995) Arbeidsdokument pr. 2000.01.19, Utarbeidet av Mur-Sentret, Oslo 2000 (in Norwegian).